



INSTITUTO
UNIVERSITÁRIO
DE LISBOA

Emotion Recognition and β -Band Analysis based on Simulated Flights

Válber César Cavalcanti Roza

PhD in Information Science and Technology

Supervisor:

Dr. Octavian Adrian Postolache, Full Professor,
ISCTE – Instituto Universitário de Lisboa

April, 2024



TECNOLOGIAS
E ARQUITETURA

Department of Information Science and Technology

Emotion Recognition and β -Band Analysis based on Simulated Flights

Válber César Cavalcanti Roza

PhD in Information Science and Technology

Jury:

Prof. Dr. João Carlo Ferreira, Assistant Professor (with Aggregation) (President)

ISCTE – Instituto Universitário de Lisboa

Prof. Dr. Nuno Guimarães, Full Professor,
ISCTE – Instituto Universitário de Lisboa

Prof. Dr. Rui Neves Madeira, Assistant Professor,
IPS – Instituto Politécnico de Setúbal

Prof. Dr. Prof. Dr. Francisco Martin, Full Professor,
Universidad de Oviedo

Prof. Dr. Octavian Adrian Postolache, Full Professor,
ISCTE – Instituto Universitário de Lisboa

April, 2024

I would like to dedicate all my effort, all my work, to Jesus Christ, my savior.

Acknowledgement

I would like to thank to God, to Jesus Christ who stood me up when I felt disappointed. Besides I would thank to my dear Professor and adviser, Octavian Postolache who believed me and guided me in doing this project, providing me invaluable advices and helping me in difficult periods. His motivation and help, contributed tremendously to the successful completion of present work.

I'd like also, to thank my mother Miriam, father Zé Wilson (in memory), my grandmother Letícia Higino (in memory), my wife and daughter, all family and friends around the world for their support. Without that support, I couldn't have succeeded in completing this project.

At last but not in least, I'd like to thank everyone who helped and motivated me to work on this project such as, experiments' volunteers, professors of UFRN and ISCTE-IUL, secretaries and assistants of the PhD Department of ISCTE-IUL and IT-IUL.

Abstract

Several safety-related improvements are applied every year to try to minimize the number of civil aviation accidents. Fortunately, these improvements work well, reducing the number of accident occurrences. However, while the number of accidents due to mechanical failures has decreased, the number of accidents due to human errors seems to grow. Based on that and to try to minimize these unwanted situations, the present work developed a sensing architecture and a set of experiments bringing two different solutions focused on the pilot of the aircraft through of simulated flights and volunteers having different expertise on flight procedures. The flight simulations were executed by the Microsoft Flight Simulator–Steam Edition (FSX-SE). The two proposed solutions are based on: emotion recognition and β -band analysis of pilots' brain in flight. Volunteers was invited to acted like pilots in simulated flights along seven flight moments: takeoff, climb, cruise flight, descent, approach, final approach and landing. Regarding to β -band analysis, Electroencephalography (EEG) was considered and also several spectrogram and statistical measurements of each volunteer were carried out. The results of this analysis shown that the takeoff, approach and landing corresponded to the highest brain signal amplitudes, i.e., close to 37.06%–67.33% higher than the brain activity of other flight tasks. When some accidents were about to occur, the amplitudes of the brain activities were similar to those of the final approach task. Considered the volunteers' expertise and their confidence on the proposed flight simulation, it shown that the highest brain amplitudes and oscillations observed of more experienced and confident volunteers were on average close to 68.44% less, compared to less experienced and less confident volunteers in the same tasks. Moreover, in general, more experienced and confident volunteers, presented different patterns of brain activities compared to volunteers with less expertise or less familiarity with flight simulations and/or electronic games. Regarding to emotion recognition, the present work shown that it is possible to recognize emotions of different pilots in flight, combining their actual and previous emotions felt in flight. Three biosignals were considered: Galvanic Skin Response (GSR), cardiac system based on Heart Rate (HR) through PPG sensor, and EEG. The reference to produce the emotion recognition model was based on the intensities of emotions detected of the volunteers' faces by the software Face Reader. These biosignals were used to extract the emotions patterns along the flights. Five main emotions were considered: happy, sad, angry, surprise and scared. The emotion recognition was based on Deep Neural Networks (DNN) techniques. The Root Mean Squared Error (RMSE) and Mean Absolute Error (MAE) were the main methods used to measure the quality of the multi-outputted regression models. The tests

of the produced multi-output models shown that the lowest recognition errors were reached when all biosignals were considered or when the GSR datasets were omitted of the model training . It also showed that the emotion surprised was the easiest to recognize, having a mean RMSE of 0.13 and mean MAE of 0.01; while the emotion sad was the hardest to recognize, having a mean RMSE of 0.82 and mean MAE of 0.08. When only the major emotion values along the time were considered, the mean of the best classification accuracies was close of 76.42%.

Resumo

Várias melhorias são aplicadas todos os anos para minimizarem o número de acidentes na aviação civil. Felizmente, estas melhorias têm funcionado bem, reduzindo a quantidade de ocorrências de acidentes. No entanto, enquanto o número de acidentes aéreos causados por falhas mecânicas tem diminuído, o número de acidentes causados por falhas humanas parece ter aumentado. Baseado nisso e para tentar minimizar tais indesejadas situações, o presente trabalho desenvolveu uma arquitetura sensorial e um conjunto de experimentos, trazendo duas diferentes perspectivas focadas no piloto da aeronave através de voos simulados e voluntários possuindo diferentes níveis de conhecimento em procedimentos de voo simulado. Os voos simulados foram executados com o software Flight Simulator–Steam Edition (FSX-SE). As duas soluções propostas são baseadas em: reconhecimento de emoções e análises de ondas beta dos cérebros dos pilotos em voo. Os voluntários do experimento, foram convidados a atuaram como pilotos nos voos simulados ao longo de sete momentos ou tarefas de voo, definidas como: decolagem, subida, voo de cruzeiro, descida, aproximação, aproximação final e pouso. Sobre as análises das ondas beta, dados de Eletroencefalografia (EEG) foram considerados e também diversos espectrogramas e medições estatísticas para cada voluntário foram executadas. Os resultados desta análise mostraram que as tarefas de decolagem, aproximação e pouso, corresponderam aos momentos com sinais cerebrais de maiores amplitudes sendo, 37.06%–67.33% maiores que as atividades cerebrais das demais tarefas. Quando algum acidente estava prestes a acontecer, as amplitudes cerebrais foram similares a tarefa de aproximação final. Considerando a experiência e autoconfiança dos voluntários em executar os voos simulados propostos, isto mostrou que as mais altas amplitudes cerebrais observadas em voluntários mais experientes e confiantes foram em média 68.44% menor, comparadas a voluntários menos experientes e menos confiantes para executas as mesmas tarefas. Além disso, em geral, voluntários mais experientes e confiantes no experimento, apresentaram diferentes padrões de atividades cerebrais comparadas a voluntários menos experientes ou com menor familiaridade com simuladores de voo e/ou jogos eletrônicos. Sobre o reconhecimento de emoções, o presente trabalho mostrou que é possível reconhecer emoções de diferentes pilotos em voo, combinando suas emoções sentidas durante o voo e anteriormente. Para isso, três biosinais foram considerados, EEG, Resistência Galvânica da Pele (RGP) e um sistema cardíaco baseado em Ritmo Cardíaco (RC). A referência para produzir o modelo de reconhecimento de emoções, foi baseada nas intensidades de emoções detectadas das faces dos voluntários pelo software Face Reader. Todos os biosinais foram usados para

extrair padrões de emoções ao longo dos voos. Cinco emoções principais foram consideradas: alegria, tristeza, raiva, surpresa e medo. O reconhecimento das emoções foi baseado em técnicas de Redes Neurais Artificiais Profundas (RNAP). O Erro Quadrático Médio (EQM) e o Erro Médio Absoluto (EMA) foram os métodos principais usados para medir a qualidade dos múltiplos modelos de regressão criados. Os testes dos múltiplos modelos criados mostraram que os menores erros de reconhecimento de emoções foram alcançados quando todos os biosinais foram considerados ou quando os dados de RGP foram omitidos do processo de treinamento. Também mostrou que a emoção surpresa foi a mais fácil de reconhecer, tendo o EQM de 0.13 e EMA médio de 0.01; enquanto que a emoção tristeza foi a mais difícil de ser reconhecida, apresentando um EQM de 0.82 e EMA médio de 0.08. Quando apenas as emoções faciais com maiores intensidades ao longo do tempo foram consideradas, a média das melhores classificações foi de aproximadamente 76.42%.

List of Figures

1.1 Boeing statistical summary about fatal accident rate per million departures between 1959 through 2022 (Boeing, 2023).	3
1.2 Work scope diagram – practical contribution regarding to the on-flight phase.	7
1.3 Circumplex model of emotion-related categories (Plutchik and Kellerman, 2013).	11
2.1 General architecture of a FER system.	16
2.2 General architecture of a speech-based system to recognize emotions.	18
2.3 General architecture of a biosignal-based system to recognize emotions.	20
2.4 Comparison between the number of selected publications (2015 to 2019).	22
2.5 Venn diagram over the most common techniques used to recognize emotions based on face, speech and biosignal (2015 to 2019).	27
2.6 Recognition techniques found on emotion-related researches (2015 to 2019).	28
3.1 Diagram with some examples of application based on the developed multimodal system proposed in this work.	30
3.2 Execution steps of the proposed multimodal sensing system.	31
3.3 Setups of the PoCs. First PoC approach using pilot and co-pilots (right); second PoC using only a pilot and supervisor as co-pilot (left).	33
3.4 Flight simulation experiment during the second PoC using previous setup, a small environment and basic volunteer screen.	34
3.5 Airplane Extra 300S used during the training.	35
3.6 Setup used on the main experiment.	37
3.7 Experiment environment. Volunteer side (left); supervisor side (right).	38
3.8 Experiment checklists executed by the supervisor.	40
3.9 Airplane Cessna 172SP used during the main experiment.	41
3.10 Flight route (red line) of the experiment (Lisbon to Alverca).	41
3.11 Lateral view of the proposed flight task chart, route and tasks.	42
3.12 EEG’s accelerometer output of the double head shaking movement.	44
3.13 Electrodes placement. EEG and HR, placed on the scalp and ear (left); and GSR, placed on the indicator and middle fingers (right).	45

3.14	Emosense RT software, to acquire HR and GSR data (top) and Enobio-N8 to acquire EEG data (bottom).	47
3.15	EEG raw (noisy) 8 channels dataset referent to CR1 experiment.	48
3.16	Acquisition devices: Enobio-N8 (left); Shimmer GSR (middle-left); Shimmer for ECG/HR (middle-right) and MedLab P100 (right).	49
3.17	Face Reader software used to detect emotions from face.	50
3.18	Face recording of some volunteers during experiment.	51
3.19	Questionnaire with 22 emotions, used before and after the experiment.	52
3.20	Emotions selected on questionnaires and the resumed emotions.	53
3.21	Distribution of fatal accidents by civil aviation (Boeing report) and general accidents (proposed experiment) (adapted from Boeing, 2017).	55
3.22	Raw datasets correlation, based on HR and GSR input data.	58
3.23	Raw datasets correlation, based on HR and GSR input data.	59
3.24	Classes of emotions detected by Face Reader software for each flight dataset.	60
4.1	Reference line function and modes along any dataset preprocessing.	62
4.2	GFFM on abrupt signal correction. Gravity force functions in shared mode (top); gravity force application (middle); final data (bottom).	62
4.3	Gravity force functions and modes along any dataset preprocessing.	63
4.4	GFFM test using a dataset with 150 samples. Reference line on static mode based on median, and gravity force function as independent mode, linear and coefficients $g_t=1.0$ and $g_b=0.7$.	64
4.5	GFFM test using a dataset with 150 samples. Reference line on static mode based on mean, and gravity force function as shared mode, linear and coefficients $g_t=0.8$ and $g_b=1.0$.	64
4.6	GFFM test using a dataset with 1000 samples. Reference line on static mode based on mean, and gravity force function as shared mode, linear and coefficients $g_t=0.9$ and $g_b=1.0$.	65
4.7	GFFM test using a dataset with 2000 samples. Reference line on static mode based on min-max, and gravity force function as shared mode, linear and coefficients $g_t=0.9$ and $g_b=1.0$.	65
4.8	GSR dataset correction referent to the flight dataset CL3.	67
4.9	GSR dataset correction referent to the flight dataset RC1 and RC3.	68
4.10	GSR dataset correction referent to the flight datasets GC1 and LS2.	69
4.11	GSR dataset correction referent to the flight datasets VC1 and CLX.	70
4.12	HR dataset correction referent to the flight datasets CL3 and VC1.	71
4.13	HR dataset correction referent to the flight datasets RC1 and GC3.	72

4.14	Outliers detected in some dataset.	73
4.15	Raw face emotion dataset with smoothing and resampling.	76
4.16	A set of raw HR and GSR data with N=10e+3 samples) preprocessing result. Raw dataset before preprocessing (left); raw dataset after (right).	77
5.1	Detailed stages from recorded data until feature extraction.	79
5.2	Result of the drift removal from a raw EEG dataset having $t = 9.78$ min.	80
5.3	Filtering output over EEG data regarding to β -band.	82
5.4	Some dataset spectrograms, showing the flight parts with high amplitude.	83
5.5	Processed EEG (8 channels) dataset referent to CR1 experiment.	84
6.1	Feature extraction and sampling demonstration using the feature μ for all detected emotions from the face.	85
6.2	Wavelet shifts along of a sine wave with different frequencies, where $a_i \neq a_j$ and $b_i \neq b_j$.	88
6.3	Peaks detections and counting over 3600 samples (DS-RC1).	89
6.4	Poincaré plot demonstration over the flight dataset RC2.	89
6.5	Poincaré plot for raw dataset and processed dataset (CL3).	90
6.6	Poincaré plots for raw datasets and processed datasets (RC1 to GC1).	91
6.7	Poincaré plots for raw datasets and processed datasets (GC3 to VC1).	92
6.8	Poincaré plots for raw datasets and processed datasets (VC2 to CLX).	93
6.9	Columns centering over feature vectors, before (left) and after (right).	94
6.10	Scatter plot for some extracted features.	95
7.1	Perceptron model.	98
7.2	Learning rate $\eta(n)$ analysis by test errors $\varepsilon(n)$ for each iteration n from RC1 to CL3 (left); learning rate by correct matches (right).	100
7.3	Descend errors and divergence descend close to 1,100 iterations.	101
7.4	Cross validation applied to test the models. It trains using volunteers datasets, to detect emotions of one single volunteer k .	102
7.5	ANN using RTOR methodology over the output neurons $y_{1 \rightarrow n}$.	102
7.6	RTOR being applied on a neuron output. Note the corrected output y_k^* (blue) and the raw output y_k having outliers (green).	103
8.1	Spectrogram of the flight dataset RC1-frontal left lobe (Fp1). (a) Processed 12-40Hz data; (b) Raw data spectrogram; (c) Spectrogram of the processed 12-40Hz data; (d) Processed data on delimited Y-axis; (e) Grayscale spectrogram with tasks delimitation.	106

8.2 Spectrogram of the flight dataset RC1 - temporal right lobe (T8).	107
8.3 Mean values of spectrogram magnitudes of the flight dataset RC1 - temporal left and right lobes (T7 and T8).	107
8.4 Spectrogram of the flight dataset CR1-frontal left lobe (F3). (a) Processed 12-40Hz data; (b) Spectrogram of the processed 12-40Hz data; (c) Grayscale spectrogram with tasks delimitation; (d) Mean values of spectrogram energies.	108
8.5 Spectrogram of the flight dataset CR3-temporal left lobe (T7). (a) Processed 12-40Hz data; (b) Spectrogram of the processed 12-40Hz data; (c) Grayscale spectrogram with tasks delimitation; (d) Mean values of spectrogram energies.	109
8.6 Mean values of spectrogram magnitudes of the flight dataset CR1 and LS2 - frontal left lobe (F3).	110
8.7 Normalized mean values of the brain activities for all datasets and the volunteers' expertise (left lobe).	111
8.8 Normalized mean values of the brain activities for all datasets and the volunteers' expertise (right lobe).	112
8.9 Normalized mean values of brain activities for all datasets over each task according to volunteers' expertise.	112
8.10 Mean values of brain magnitudes by tasks, of the flight dataset CR1 - frontal left lobe (Fp1), considering a total of 13 volunteers' datasets.	113
8.11 Mean of magnitudes by tasks, of the flight dataset CR1 - frontal left lobe (Fp1).	114
9.1 Preprocessing executed before the processing, feature extraction and tests.	124
9.2 Processing executed before the feature extraction.	124
9.3 Errors results (RMSE+MAE) from tests 3 to 6 (with feature extraction).	127
9.4 Errors results (RMSE) comparison from tests 3 to 34 (with feature extraction).	128
9.5 Errors results (MAE) comparison from tests 3 to 34 (with feature extraction).	129
9.6 Errors results comparison between RMSE and MAE from tests 1 to 34 (with feature extraction).	130
9.7 Major emotion accuracies from the tests 3 to 6 (with feature extraction).	131
9.8 All major emotion accuracies from the tests 1 to 34. All accuracies (left); mean of all accuracies (right).	132
9.9 Traditional learning versus deep learning (DP). Improvement applied in this work, regarding to the major value emotions when applying the traditional learning and deep learning (no feature extraction).	133
A.1 Flow diagram of the pictures selection process from the IAPS dataset.	178
A.2 Electrode positions for EEG (up); main and auxiliary electrodes for emotion detection (up-right); ECG, GSR and SpO2 (bottom).	178

A.3	ANN result comparison and ANN squared errors during the training.	179
A.4	ANN outputs during the training.	179
A.5	Smart phone application screens: questionnaire and the main screen.	180
A.6	Publication regarding to the emotional relation between city places and citizens' emotions (Roza and Postolache, 2016).	181
A.7	Publication regarding to the design of a multimodal interface based on emotion (Roza and Postolache, 2017).	182
A.8	Publication regarding to the design of an ANN to detect arrhythmias from ECG data (Roza, Almeida, and Postolache, 2017).	183
A.9	Publication regarding to the design of a multimodal architecture based on emotion and flight simulator (Roza and Postolache, 2018).	184
A.10	Publication regarding to the performance analysis of ANN and SVM on arrhythmia identification (Roza et al., 2018).	185
A.11	Publication regarding to the emotional assessment on simulated flight experiments (Roza et al., 2019).	186
A.12	Publication regarding to the multisensing approach to identify emotions based on simulated flight experiments (Roza and Postolache, 2019).	187
A.13	Publication regarding to the β -band analysis (Roza and Postolache, 2021).	188
A.14	Publication regarding to the inverse kinematic applied to orthosis walking tests (Roza et al., 2017).	189
A.15	Publication regarding to the development of a multisensing platform to give support to children with cerebral palsy (Roza, Souza, and Postolache, 2017).	190
A.16	Publication regarding to the improvement of a probabilistic method over path planning tasks (L. Bruno P. Nascimento et al., 2018).	191
B.1	Mean of magnitudes by tasks and lobes, of the flight dataset CL3 (beginner level volunteer).	194
B.2	Mean of magnitudes by tasks and lobes, of the flight dataset CR1 (beginner level volunteer).	195
B.3	Mean of magnitudes by tasks and lobes, of the flight dataset CR3 (beginner level volunteer).	196
B.4	Mean of magnitudes by tasks and lobes, of the flight dataset GC3 (mid-level volunteer).	197
B.5	Mean of magnitudes by tasks and lobes, of the flight dataset LS1 (mid-level volunteer).	198
B.6	Mean of magnitudes by tasks and lobes, of the flight dataset VC1 (experienced level volunteer).	199
		xiii

B.7	Mean of magnitudes by tasks and lobes, of the flight dataset VC2 (experienced level volunteer).	200
C.1	Configuration panel.	201
C.2	Three main panel: RT acquisition panel, aviation experiment panel and electrodes setup panel.	202
C.3	Log storage and nomenclature.	203
C.4	Emosense Offline software.	203

List of Tables

1.1 Some accidents on commercial aviation, caused mainly by human failure. The victims situation was defined as fatal (F) and injured (I).	4
2.1 Some techniques regarding to face emotion recognition since 2015.	22
2.2 Some techniques regarding to speech based on emotion recognition since 2015.	23
2.3 Some techniques regarding to biosignal based on emotion recognition since 2015.	26
3.1 Resources applied on each PoC and in the main experiment.	39
3.2 Pilot and co-pilot checklists used during the main flight simulations.	43
3.3 Devices and its application in the main experiment.	49
3.4 Dataset description according to the flight experiment tasks.	54
3.5 Raw valid dataset description according to number of samples and time.	56
3.6 Reduced datasets according to amount of samples, emotions and time.	57
4.1 Corrections of abrupt data changes using ACCM, over the experiment datasets RC1 to CL3.	67
4.2 Outliers detection and removal using Z-Score and modified Z-Score.	73
6.1 Extracted features for HR, GSR, EEG and Face datasets.	86
8.1 μ_0 , σ_0 and σ_0^2 of β -band, 31-39Hz and 40Hz of the flight dataset CR1 (beginner level volunteer).	115
8.2 μ_0 , σ_0 and σ_0^2 of β -band, 31-39Hz and 40Hz of the flight dataset RC1 (mid-level volunteer).	115
8.3 μ_0 , σ_0 and σ_0^2 of β -band, 31-39Hz and 40Hz of the flight dataset RC2 (mid-level volunteer).	116
8.4 μ_0 , σ_0 and σ_0^2 of β -band, 31-39Hz and 40Hz of the flight dataset RC3 (mid-level volunteer).	116
8.5 μ_0 , σ_0 and σ_0^2 of β -band, 31-39Hz and 40Hz of the flight dataset GC1 (mid-level volunteer).	117
8.6 μ_0 , σ_0 and σ_0^2 of β -band, 31-39Hz and 40Hz of the flight dataset GC3 (mid-level volunteer).	117
8.7 μ_0 , σ_0 and σ_0^2 of β -band, 31-39Hz and 40Hz of the flight dataset LS1 (mid-level volunteer).	118

8.8 μ_0 , σ_0 and σ_0^2 of β -band, 31-39Hz and 40Hz of the flight dataset LS2 (mid-level volunteer).	118
8.9 μ_0 , σ_0 and σ_0^2 of β -band, 31-39Hz and 40Hz of the flight dataset VC1 (experienced level volunteer).	119
8.10 μ_0 , σ_0 and σ_0^2 of β -band, 31-39Hz and 40Hz of the flight dataset VC2 (experienced level volunteer).	119
8.11 μ_0 , σ_0 and σ_0^2 of β -band, 31-39Hz and 40Hz of the flight dataset CR3 (beginner level volunteer).	120
8.12 μ_0 , σ_0 and σ_0^2 of β -band, 31-39Hz and 40Hz of the flight dataset CLX (beginner level volunteer).	120
8.13 μ_0 , σ_0 and σ_0^2 of β -band, 31-39Hz and 40Hz of the flight dataset CL3 (beginner level volunteer).	121
9.1 Description of each execution test according to preprocessing, processing and feature extraction.	125
9.2 Description of each execution test according to preprocessing, processing and feature selection.	126
9.3 Emotion recognition results tests 1 and 2. ANN with 6×10^3 train epochs and raw data (no features).	135
9.4 Emotion recognition results tests 3 and 4. ANN with 6×10^3 train epochs and input data with feature extraction.	136
9.5 Emotion recognition results tests 5 and 6. ANN with 6×10^3 train epochs and input data with feature extraction.	137
9.6 Emotion recognition results tests 7 and 8. ANN with 6×10^3 train epochs and input data with feature extraction.	138
9.7 Emotion recognition results tests 9 and 10. ANN with 6×10^3 train epochs and input data with feature extraction.	139
9.8 Emotion recognition results tests 11 and 12. ANN with 6×10^3 train epochs and input data with feature extraction.	140
9.9 Emotion recognition results tests 13 and 14. ANN with 6×10^3 train epochs and input data with feature extraction.	141
9.10 Emotion recognition results tests 15 and 16. ANN with 6×10^3 train epochs and input data with feature extraction.	142
9.11 Emotion recognition results tests 17 and 18. ANN with 6×10^3 train epochs and input data with feature extraction.	143
9.12 Emotion recognition results tests 19 and 20. ANN with 6×10^3 train epochs and input data with feature extraction.	144

9.13	Emotion recognition results tests 21 and 22. ANN with 6×10^3 train epochs and input data with feature extraction.	145
9.14	Emotion recognition results tests 23 and 24. ANN with 6×10^3 train epochs and input data with feature extraction.	146
9.15	Emotion recognition results tests 25 and 26. ANN with 6×10^3 train epochs and input data with feature extraction.	147
9.16	Emotion recognition results tests 27 and 28. ANN with 6×10^3 train epochs and input data with feature extraction.	148
9.17	Emotion recognition results tests 29 and 30. ANN with 6×10^3 train epochs and input data with feature extraction.	149
9.18	Emotion recognition results tests 31 and 32. ANN with 6×10^3 train epochs and input data with feature extraction.	150
9.19	Emotion recognition results tests 33 and 34. ANN with 6×10^3 train epochs and input data with feature extraction.	151
A.1	Publications developed during the studies of the present PhD.	177

Outline

Acknowledgement	iii
Abstract	v
Resumo	vii
List of Figures	ix
List of Tables	xv
Chapter 1. Introduction	1
1.1. Main Motivation and Practical Contribution	2
1.1.1. Human Factors and Aviation Accidents	4
1.1.2. Looking for Real Pilots' Feedback Regarding to the Research Application	5
1.1.3. Contribution	7
1.2. Challenges	8
1.3. Going Deep on Emotion Researches	9
1.4. Thesis Content	12
Chapter 2. Literature Review – Techniques on Emotion Sensing and Recognition	15
2.0.1. Emotion Recognition Techniques based on Facial Expressions	16
2.0.2. Emotion Recognition Techniques based on Human Speech	17
2.0.3. Emotion Recognition Techniques based on Physiological Parameters	19
2.0.4. Techniques Comparisons	21
2.0.5. Recognition Techniques Comparisons	27
Chapter 3. Multimodal Sensing System and Data Acquisition	29
3.1. Multimodal Architecture Description	30
3.2. Proof of Concept (PoC) of the Experiment	32
3.3. Training Flight - Cognition versus Emotion	34
3.3.1. Cognitive Reappraisal and Acceptance	35
3.4. Main Flight Experiment	36
3.4.1. Computers Configuration	39
3.4.2. Execution Checklist - Listing the Steps of the Experiment	39
3.4.3. Execution of the Simulated Flight	41
3.4.4. Flight Plan - Route of the Simulation	41
3.4.5. Tasks of the Experiment	42
3.4.6. Volunteers and Flight Checklists	42
	xix

3.4.7.	Head Shaking Indicator - Beginning and End of Experiment	43
3.4.8.	Physiological Sensing	44
3.4.9.	Facial Emotion Sensing	50
3.4.10.	Emotion Questionnaires	50
3.4.11.	Flight Analysis	54
3.4.12.	Dataset Description	55
Chapter 4. Data Preprocessing		61
4.1.	Gravity Force-Fit Method (GFFM) - First Detrend	61
4.2.	Abrupt Change Correction Method (ACCM)	66
4.2.1.	Abrupt Change Correction for GSR Data	67
4.2.2.	Abrupt Change Correction for HR Data	71
4.3.	Outliers Detection and Correction	73
4.3.1.	Z-Score	74
4.3.2.	Modified Z-Score	74
4.4.	Data Normalization	75
4.5.	Face Dataset - Smoothing Abrupt Oscillations	75
4.6.	Preprocessing Output	77
Chapter 5. Data Processing		79
5.1.	Drift Removal	79
5.2.	Auto Regressive Exogenous - Motion Artefact Removal	80
5.3.	Filtering - Bandpass and Lowpass Combination	81
5.3.1.	Spectrogram View	82
5.4.	Discrete Fourier Transform Analysis	83
Chapter 6. Feature Extraction		85
6.1.	Features Description	86
6.1.1.	Mean Features (FEAT_MN)	86
6.1.2.	Median Features - Correcting Mean's Discrepancies (FEAT_MD)	86
6.1.3.	Standard Deviation and Variance Features (FEAT_STD, FEAT_VAR)	87
6.1.4.	Continuous Entropy Features (FEAT_ENT)	87
6.1.5.	Wavelets Features (FEAT_WAC, FEAT_WDC)	87
6.1.6.	Peaks Counting Features (FEAT_PEK)	88
6.1.7.	Poincaré Plots Features (FEAT_SD1, FEAT_SD2, FEAT_SCT, FEAT_SAR)	89
6.1.8.	Sample Absolute Interval Range Features (FEAT_RNG)	93
6.2.	Singular Value Decomposition - Features Selection	94
6.3.	Features Columns Centering	94
6.4.	Features Correlation	95
6.4.1.	Pearson Correlation Coefficient - Evaluating the Features Correlations	95
Chapter 7. Emotion Recognition		97
7.1.	Artificial Neural Network	97

7.1.1.	McCulloch-Pitts Neuron Model	97
7.1.2.	ANN Development and Modeling	98
7.1.3.	Learning Rate Analysis	99
7.1.4.	Finding an Optimal Hidden Neurons	100
7.1.5.	Finding an Optimal Train Iterations	101
7.2.	Cross Validation - Testing Recognition Models	101
7.3.	Realtime Outliers Removal - RTOR	102
7.4.	Evaluation Metrics for Emotion Output - Regression Models	103
7.4.1.	Mean Absolute Relative Difference (MARD)	103
7.4.2.	R-Squared Value (R^2)	103
7.4.3.	Root Mean Squared Error (RMSE)	104
7.4.4.	Mean Absolute Error (MAE)	104
Chapter 8.	Result on β -Band Analysis from Simulated Flight Experiments	105
8.1.	β -Band Spectrogram Analysis	105
8.1.1.	Situations of Imminent Accident or Loss of Control	108
8.1.2.	Volunteer's Expertise and Brain Activity	110
8.2.	β -Band Analysis for Flight Tasks	113
Chapter 9.	Result Analysis on Emotion Recognition	123
9.1.	What Has Been Done So Far	123
9.2.	Description of the Recognition Tests	125
9.2.1.	Emotion Recognition Tests based on Raw Data - Test 1 and Test 2	126
9.2.2.	Emotion Recognition Tests based on Feature Extraction - Test 3 to 34	126
9.3.	Emotion Recognition Analysis	127
9.3.1.	Improvements Coming from the Feature Extraction	129
9.3.2.	Considering the Higher Emotion Intensities	130
9.3.3.	Results Improvements	132
Chapter 10.	Findings, Limitations and Conclusions	153
10.1.	Findings	153
10.2.	Limitations	154
10.3.	Final Remarks and Future Works	154
References		157
Appendix A.	Publications	177
A.1.	Experiment with Pictures and Emotions	178
A.2.	Speech Emotion Recognition	179
A.3.	Emotion in Smart City	180
A.4.	Main Publications	181
A.5.	Publications out of Main Work Context (Parallel Publications)	189
Appendix B.	Additional Plots of each Volunteer	193
		xxi

Appendix C. Emosense Software - User Manual	201
C.1. Emosense Realtime/Online	201
C.1.1. Log File Nomenclature	202
C.2. Emosense Offline	203

CHAPTER 1

Introduction

Going deep in the daily researches about emotions, it was noticed that in fact, each emotion is a complex explosion of “selfish” sensations, which each sensation goes in its own way and sometimes it blocks and interferes with other sensations.

Its complexity and inseparability between all emotions are somehow, the reason that only one measurement channel is not sufficient to fully identify it. Since emotions are present at every moment, researchers should be able to understand its aspects and responses, especially because in everyday life the people suffer with emotion-related problems such as: stress and emotional disturbance affecting their actions, humor, work, well-being, family and general relationship that can also cause mental health disturbance (Quah, 2018; Hagen, Knizek, and Hjelmeland, 2017), low immunity and malignant diseases such as cancers and others irreversible damages (Alberdi, Aztiria, and Basarab, 2016; Elefteriou and Campbell, 2015).

Emotion is an important part of the human behavior and it is organized on two primary categories – conscious and unconscious. Conscious emotion relates the emotional response based on some cognitive processes; and the unconscious emotion that is based on the autonomic process from nervous system (Barrett, 2006; Poels and Dewitte, 2006). Based on that, several researches shown that the interactions with different environments (Lim, 2016), pleasant places (Thompson et al., 2012), hazards situations or by the judgment that it require (Breakwell, 2014), memory bias and societal influences (Poels and Dewitte, 2006) are some situations that can determine and influence the emotional state of an individual. Spontaneous positive feedback obtained when walking in green city’s places establishing a visual contact with nature (Thompson et al., 2012; Grinde and Patil, 2009a), listening some music (Thomas et al., 2013), meditation (Tang, Tang, and Posner, 2016) and affective cognition (Misky, 2006; Ong, Zaki, and Goodman, 2015) are some of external factors that can also induce or optimize some emotional states. It is important to also note the use of music and meditation to induce good feelings or relaxing moments.

Besides that, the emotion is led by the brain and it is the result of chemical processes that bring together several internal (biological) and external factors to produce an output or response which it reflects as an emotional state (Misky, 2006). Additionally, this response is perceived as being felt in the body (Barret, Lewis, and Haviland-Jones, 2016) and sometimes it reflects some physiological changes in our human body (Roberson et al., 2018) or psychophysiological modes that themselves track and steer the redirection of physiological and psychological resources to adapt behaviour (Critchley and Garfinkel, 2017).

Sometimes the emotion arouses from biological resources while it suppress other e.g., in the anger emotion, that it seems that the body arouse resources that increase the muscles' power to run or fight ¹, while it inhibits the resource of planning and prudence, replacing cautiousness with aggressiveness and the sympathy for hostility (Misky, 2006). In particular, the primary emotion anger plays a fundamental role in the human life such as, fear and trust, that are directly related to protection, defense and maintenance of life.

Regarding to the emotion analysis, several methods and techniques can be applied to improve the health and emotion recognition through the use of a couple of hardware devices and software such as: in multisensing systems (Roza and Postolache, 2017), Artificial Intelligence (AI), robotics (Chepin et al., 2016) and Internet of Things (IoT) (Postolache, 2017), for instance. We can also present the advances in biomedical signal and image processing, linking the emotions' treatments to several techniques such as the relationship between electrophysiological signals i.e., Electrocardiogram (ECG), Electrocardiogram (EMG), Electroencephalogram (EEG) and functional image processing and their derived interactions (Rajeswari and Jagannath, 2017).

This work uses a multimodal approach ² based on a set of these technologies, concepts and a practical methodology architecture to recognize emotions, through the signal acquisition, processing, feature extraction and recognition techniques, which it can be also applied to several workplaces e.g., administrative sectors (Mishra et al., 2011), aviation (Roza and Postolache, 2018), smart vehicles (Okegbile et al., 2019) and in urban areas (Roza and Postolache, 2016).

1.1. Main Motivation and Practical Contribution

Nowadays, aviation accidents continue to occur and together with these undesirable situations, comes several improvements on aviation safety. Despite being in a COVID-19 pandemic situation, it was possible to note important improvements as presented in April 2022, by the International Air Transport Association (IATA). It revealed that in 2021, there were 26 accidents versus 35 in 2020, where the number of fatalities declined from 132 in 2020 to 121 in 2020. Part of these substantial reduction was due to the COVID-19 pandemic since that just over 25 million flights were operated in 2021, an increase of 16% compared to 2020, but 55% below than 2019 (IATA, 2022).

Before the pandemic context, these improvements also happened. In April 2020, the IATA presented a safety report revealing the accident rates along 2019 and shows all reached improvements compared to 2014-2018. In 2019, were a total of 53 accidents, which 8 of them were fatal, having 240 deaths. In 2018, were a total of 62 accidents, which 11 were fatal, having 523 deaths. Looking for the period 2018-2014, were an average of 63.2 accidents, 8.2 fatal, having 303.4 deaths per year (IATA, 2020). It represents a reduction of 9 accidents (3 fatal), compared to 2018, and a reduction of 283 deaths. Also

¹It is also known as fight or flight, it is a physiological reaction that occurs in response to a perceived attack, harmful event or threat to survival.

²Sometimes it is called multisensing or multimodal sensing system, which it consists of a system that uses several input modes to return a resultant output.

in 2017, the Boeing Aerospace Company presented a statistical summary (Boeing, 2017), about commercial jet airplane accidents confirmed to worldwide operations since 1959 till 2016. It considered airplanes that are heavier than 60,000 pounds maximum gross weight, showing a very clear statistical analysis of accidents, which it was possible to note the impressive evolution of aviation safety along the past years. In addition, according to the last Boeing’s report (Boeing, 2023), the rates of fatal accidents as well as hull losses are steadily decreasing over time.

As well as the Boeing, the International Civil Aviation Organization (ICAO) also presented a similar report considering the period between 2008 to 2018. It shown the same evolution of aviation safety along this period (ICAO, 2017). Fortunately, the aviation has been safer year by year, reaching lower levels of accidents, considering fatalities with hull losses or not. However, there aren’t reasons to forget these risks, because there are another problems to solve along the next years that is, the analysis of physio-psychological burden (Suzuki et al., 2017) and behaviour from the aircrew inside of a real flight activity (IATA, 2016), which it surely can result on a mitigation of accidents by human failures.

Analyzing several accident reports from the last 15 years, it shown that the main causes of these accidents, were the human factors and their respective physiological aspects (ANAC, 2019; IATA, 2016; Ancel and Shih, 2012). Based on that, it is possible to note that the aviation safety is facing a new age of accident factors, i.e. the age of aviation accidents caused by human failure, what it motivate us to find new solutions to minimize these undesirable occurrences. The lack of a proper attention on these aspects, can result on irreversible problems, e.g. serious injuries and fatal accidents. Stress, drugs, fatigue, high workload, lack of pilot skills during an unexpected event and emotional disorders (Bendak and Rashid, 2020; Kandra, Škultéty, and Mesárošová, 2019; McKay and Groff, 2016) can optimize the occurrence of accidents. Same reasoning can be applied to the people of the airport ground staff, air traffic controls, among others. Figure 1.1, shows the progress of accidents rate on commercial aviation since 1959 up to 2022.

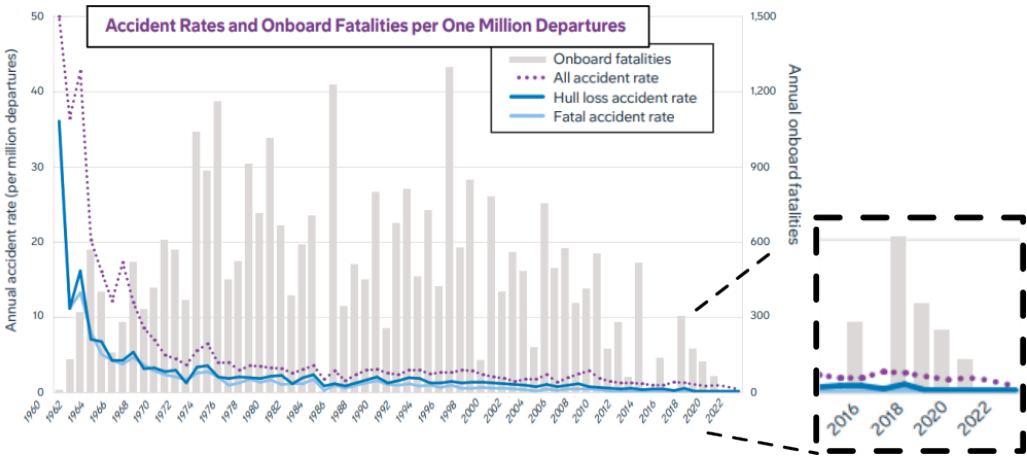


FIGURE 1.1. Boeing statistical summary about fatal accident rate per million departures between 1959 through 2022 (Boeing, 2023).

1.1.1. Human Factors and Aviation Accidents

Table 1.1, presents some accidents on commercial aviation, which the final reports indicated the main causes as human factors.

Table 1.1: Some accidents on commercial aviation, caused mainly by human failure. The victims situation was defined as fatal (F) and injured (I).

Company	Depart/Arrival	Year	Victims	Main Cause/Probable Cause
China Eastern Airlines	China/ China	2022	132 (F)	◇ No final report was presented yet. But according to US NTSB, the analysis suggests someone in the cockpit intentionally downed the plane.
Pakistan International Airlines	Pakistan/ Pakistan	2020	97 (F) 2 (I)	◇ Crashed on go around (under investigation). First information indicate human failure, probably due the lack of attention of the pilots.
Pegasus Airlines	Turkey/ Turkey	2020	3/179 (F/I)	◇ Runway overrun during landing (under investigation).
Ethiopian AL	Ethiopian/ Kenyan	2019	157 (F)	◇ Incorrect MCAS operation/conflict.
Aeroflot	Russia/ Russia	2019	41 (F)	◇ Incorrect approach, landing weight and landing (bounced landing).
Lion Air	Indonesia/ Indonesia	2018	189 (F)	◇ Incorrect MCAS operation/conflict.
Cubana de Aviación	Cuba/Cuba	2018	112 (F)	◇ Wrong aircraft weight setup and uncorrect takeoff.
Fly Dubai	UAE/Russia	2016	62 (F)	◇ Incorrect landing.
German Wings	Spain/Germany	2015	150 (F)	◇ co-pilot suicide.
Malaysia AL	Malaysia/China	2014	239 (F)	◇ Probable co-pilot suicide.
Lion Air	Indonesia/Indonesia	2013	46 (I)	◇ Crashed into water in final approach. Pilot under the influence of drugs.
**demo flight **	Indonesia/ Indonesia	2012	45 (F)	◇ Controlled flight into terrain.
Air France	Brazil/ France	2009	228 (F)	◇ Lost of control after wrong procedures in flight.
Turkish Airlines	Turkey/ Netherlands	2008	9 (F)	◇ Stall close to the landing. The crew noticed the problem too late.
TAM L. Aéreas	Brazil/Brazil	2007	199 (F)	◇ Incorrect landing (wrong reverse setup).

Gol L. Aéreas	Brazil/Brazil	2006	154 (F)	◇ Partial collision with another aircraft (TCAS ³ off). Failure of the air traffic control.
Bashkirian Airlines	Russia/ Spain	2002	71 (F)	◇ In-flight collision mainly due the air traffic control failure.
Air Transat	Canada/ Portugal	2001	18 (I)	◇ Fuel starvation and the bad crew execution of fuel control in flight.
American Airlines	USA/ USA	2001	265 (F)	◇ Incorrect co-pilot procedures during takeoff under strong turbulence produced by another aircraft.
Aero México	Mexico/ USA	1986	64+3 (F)	◇ In-flight collision with another aircraft (Piper PA-28-181 Archer). Second aircraft did not contact the tower to change course, intercepting the route of the other aircraft.

1.1.2. Looking for Real Pilots' Feedback Regarding to the Research Application

During the development of this work, some meetings were held with real pilots⁴ of some air companies and military air force from Brazil and Portugal. It were important to obtain some practical and realistic feedback from professional pilots regarding to the proposed work in a practical and real situation.

Several feedback were also acquired regarding to the proposed work methodology, which all contacted pilots really agreed with the need of these researches on real aviation. When the possibility of real application were presented, some of them agreed and others were afraid to, for several reasons as presented below.

"I have more than 20 years as civil pilot and surely it will bring more problems than benefits to us, because the pilots maybe will be afraid to reveal your own emotional condition before each flight!" (Civil aviation pilot, 2018)

"Pilots like to fly and if the companies start to prohibit us to fly due our majority emotional state, it will not be good!" (Civil aviation pilot, 2018)

"I recognize how important your researches are but, I think that for aviation context it will not worth. Why you don't try to apply it on car contexts?!" (Civil aviation pilot, 2018)

Other feedback were also obtained, where they presented real situations that occurred in their work, revealing to us the need for a deeper emotional analysis of the pilots during training and flight activities.

³A Traffic Collision Avoidance System (TCAS) or traffic alert and collision avoidance system.

⁴In this work section, the pilot and co-pilot will be referred as pilot or simply, aircrew.

"Really interesting this approach! We can use it to try to measure our emotional stability during our first flight just after the end of vacation, that is when we are very excited to fly again!" (Military pilot – Air Force, 2015)

"Interesting work! It can be useful to us. Keep me in touch." (Military pilot – Air Force, 2018)

"Nowadays, we don't have how to measure the level of nervousness of our cadets, or even if they were really confident at each flight exercise. This proposed work, can be useful to us." (Military pilot – Air Force, 2020)

"Surely it will be useful to our pilots along the training because it can show us if our pilots are confident enough along the flight missions." (Military pilot – Air Force, 2021)

When they was argued about the huge amount of system compensation that the modern aircraft have (e.g. fly-by-wire, self navigation, instrument landing system and other automatic flight controls) to make the pilots' work easier during a flight, they said:

"Today, I understand our work more as a system operator then indeed, an aircraft pilot!" (Civil aviation pilot, 2018)

When was presented other probable perspective, regarding to the devices to be used to store their biosignals in real time and how much time it will sometimes be necessary to a probably device set-up, dataset storage and calibration just before and/or after each flight, they said:

"I think that sometimes to arrive a little bit early to the airline company, only to collect my biosignals will increase our stress!" (Civil aviation pilot, 2018)

They also presented a probable feedback from the airline companies regarding to future practical applications.

"Nowadays, it is almost impossible to be applied on any airline company, because it will be expensive for them to implement it!" (Civil aviation pilot, 2018)

In 2016, a Portuguese flight school was contacted to try to apply the proposed work there, together with their students and flight simulator but unhappiness it wasn't possible. For our request they said:

"Sorry, but we can not execute these experiments with our students because it will produce a lot of instabilities in their training!" (Flight school Directory – Portugal, 2016)

In 2015, talking about aviation with a military pilot, he said about his returns to the flight activities after days of vacation:

"That day, I was very excited to fly again after my vacation. Due to that, I couldn't sleep before that day!" (Military pilot – Air Force, 2015)

These feedback are important to motivate us to go deeper in these researches, because it give us professional perspective regarding to the demand of the development of the proposed work.

1.1.3. Contribution

The main contribution of the present work is to study the complex hazards and to improve the physiological data analysis of the pilots also looking for their emotional responses before, during and after the flights and than, to give support on aviation accidents avoidance, caused by human failures. With these data, it is possible to create a multisensing integrated dataset, to build a generalist and also particular pilot dataset profile based on the emotional and β -band responses along the flight activities. In a further developments, the integrated multisensing dataset can also includes physiological data from three different phases: before, during and after the flight, as shown in Figure 1.2.

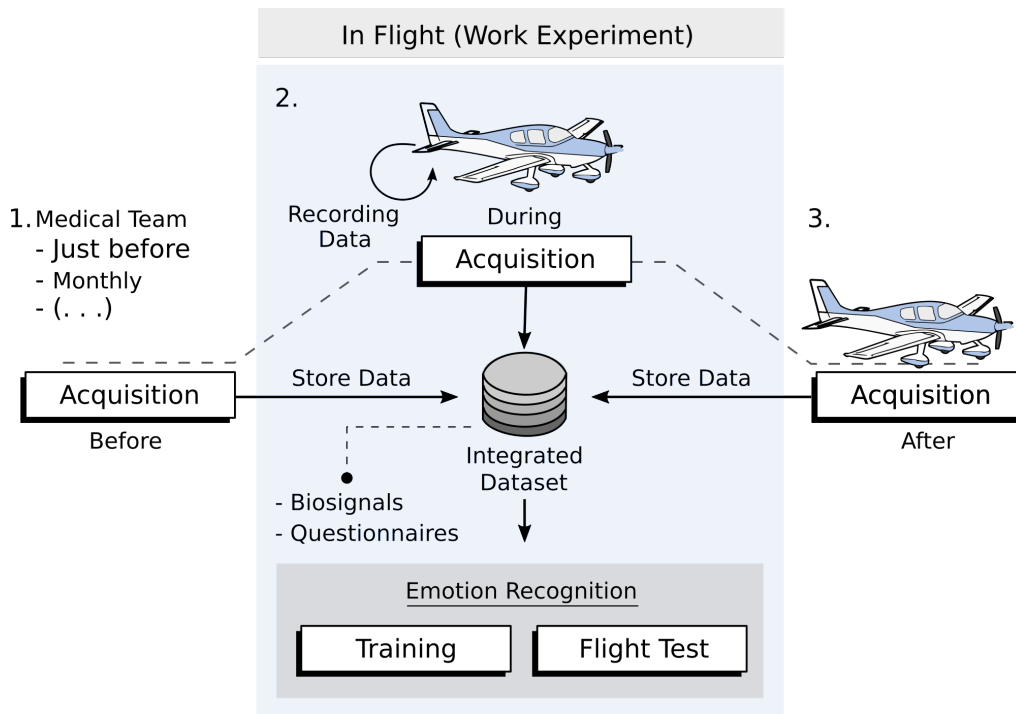


FIGURE 1.2. Work scope diagram – practical contribution regarding to the on-flight phase.

Therefore, this work presents a practical contribution regarding to the on-flight phase, including the data acquisition, processing, storage and recognition on offline mode.

Some main questions and answers are presented below, about the proposed dataset, system outputs and the data acquisition in real context.

1.1.3.1. *Using the Produced Dataset* This work considers that all acquired and processed data from the flight experiments, represent a sample about what can happen in a real flight context. In real application, the dataset must to be defined on two different types: generalist dataset, having data from all pilots, considering the similarity of emotional patterns between them; and the particular dataset, which it brings information of each

pilot. Both dataset must share information to produce high generalism on the emotion recognition process based on deep learning and data mining techniques. It must be the best way to produce a better engine of emotion recognition, not missing the particular patterns of each pilot nor their general aspects either. However, since the present work focused on the generalist dataset, the training, testing and validation were executed over some sets of the same dataset.

1.1.3.2. *System Outputs on Real Application* In the context of emotion recognition, the proposed system must to return intensities of emotions (i.e. 5 different emotions in this case) based on EEG, HR and GSR techniques. In a practical real life context, once obtained the dataset, the chosen learning method⁵ trains over this dataset, being able to be used before, during or after every flight.

In a practical context and inside the context of aviation, an airline company can use the proposed system to know which emotions the pilots are feeling before, during or after a flight. This way, the company must to use the proposed system and put some skin surface electrodes on the pilots' body to acquire their biological data (in this case, without facial information because now, the recognition model was already developed after the model training). These acquired data must to be stored and analyzed offline. At the end, the system must return e.g. a report, presenting the recognized emotions that probably were felt by the pilot along the time.

These outputs can be used by the flight supervisor or medical team to carry out the necessary actions to improve the flight safety and avoid future accident. In case of the pilot presents some critical emotions when it are not compatible with some flight phase, the system should alert about it. In addition, to reach good results, the system must present high accuracies which it can be improved with the time and more good data of other experiments.

1.1.3.3. *Real Pilots and Electrodes Application during a Real Flight* To recognize emotions based on biosignals, some electrodes must to be used. The pilot comfort should also be considered in real life and for this reason, a possible approach can be through the use of smart wearable textiles.

Emotion recognition based on face, should only be used if the system needs more data to improve the learning process otherwise, once we have the learning method already trained, only bio acquisition based on electrodes is necessary to recognize new emotions.

1.2. Challenges

A multisensing architecture aims to do multi-data acquisition in a synchronized way to keep the minimum of data coherence along the time for each event. It should to return data according to the computed inputs.

During the development of this work, a couple of challenger situations happened, as presented below:

⁵The chosen learning method is the technique used to recognize emotions based on the acquired dataset. It is presented in detail later.

- Impossibility to execute experiments with real pilots on a real aviation context e.g., flight school;
- The choice of an environment to execute the experiments;
- No major support from airline companies;
- The choice of the psychological data acquisition inside the experiment context;
- Short time to develop a device that execute this data acquisition together with some wearable technologies e.g., t-shirt;
- The non-existence of a software that do the synchronized data acquisition, processing and recognition;
- Functional integration between several electrodes, acquisition software and the face recognition software;
- High noise acquired during each experiment.

These main challengers were solved using flight simulator. The real pilots were replaced by voluntaries i.e., beginner volunteers of flight simulator; the environment of experiment was adapted on laboratory. The psychological support was mainly introduced through questionnaires. Due to the short time to develop very complex devices and wearable, it were replaced by a couple of commercial sensors. To figure out the work requirements about the data acquisition, processing and emotion recognition in a multimodal way, three proprietary software prototypes were developed: EmoSense - Real Time (ES-RT) for real time multi-acquisition, EmoSense - Processing (ES-P) for offline data processing, and EmoSense - Machine Learning (ES-ML) for emotion recognition based on deep learning.

Several software and sensors were used together; three execution checklists (defining the correct execution step) were developed to give support to the correct execution and synchronization of the system. It were executed before, during and after each flight experiment.

A set of other methods were also used and developed to remove or attenuate the noises of the data, mainly due to motion artifacts.

1.3. Going Deep on Emotion Researches

Since the 18th century the researchers try to find out a reliable approach to know what indeed happens behind the feelings and emotions.

William James, said that observing the body expressions caused by some emotional stimuli, they appear to prove that there are pleasures and pains inherent in certain forms of nerve-action wherever that action occurs (James, 1884). Other authors based on the definition of the autonomic, sympathetic, parasympathetic and enteric nervous systems, executed the initial researches to understand how different emotional states are represented within the brain and how it are expressed in different patterns of activities (Langley, 1898; Cannon, 1927).

According to Paul Ekman, one of the main references on emotion and facial expressions, in recent years the field of emotion researches has grown enormously as well as the number of scientists involved in (Ekman, 2016). It probably gave support to nowadays,

to say that these first authors were correct in their suspicions about emotions. A couple of analysis proved that emotions are completely linked to the Autonomic Nervous System (ANS) and it play a critical role in the human bio-regulation, survival, social inclusion and human relationship (Preckel, Kanske, and Singer, 2018; Clark et al., 2016; Damásio, 2001). Physiologically, the emotion and the ANS share similar temporal features, which the ANS responses can change during an emotion state (Barret, Lewis, and Haviland-Jones, 2016). These responses are inconstant and short-term event that come from chemical processes that join several biological (internal) and external factors to produce an output reflected as an emotional state (Misky, 2006). The emotion can also be understood as a mental state or feeling that can also occurs in spontaneous manner, reflecting the physiological changes in the human body which it is leaded by the brain (Roberson et al., 2018). These external and spontaneous factors can induce or optimize some emotions (e.g. positive feedback) resulting in several situations as e.g., motivations (Berridge, 2018), good feelings when listening an appraisal music (Cespedes-Guevara and Eerola, 2018; Reybrouck, Eerola, and Podlipniak, 2018; Thomas et al., 2013), when walking in green places of a city, establishing a visual contact with nature (Riaz, Gregor, and Lin, 2018; Thompson et al., 2012; Grinde and Patil, 2009b); meditating (Beblo et al., 2018; Tang, Tang, and Posner, 2016), or even when executing an affective cognition tasks (Petrovica, Anohina-Naumeca, and Ekenel, 2017; Ong, Zaki, and Goodman, 2015; Misky, 2006). It is important to note that is also possible to induce emotions e.g., when the person choices to listen some songs, looking for good feelings or relaxing moments. Music (Sánchez-Porras and Rodrigo, 2017), smell (Soto-Vásquez and Alvarado-García, 2017), food (Lagast et al., 2017; Randler et al., 2017) and meditation (Soto-Vásquez and Alvarado-García, 2017) are some interesting examples that show that our emotional states can also be induced by our wishes (Preckel, Kanske, and Singer, 2018).

These emotional responses to several inputs can certainly justify its inconstancy about each event along the time. In addition, the emotion regulation can also be affected by some body impairments such as, depression (Sanchez et al., 2017), drugs abuse (Clark et al., 2016), intellectual disability (Pereira and Faria, 2015), nervous anorexia (Kolar et al., 2017), stress (Alberdi, Aztiria, and Basarab, 2016), schizophrenia and brain's damages, representing specific deficits or part of a more general cognitive dysfunction inside of the social information processing as for instance in the recognition of facial emotions and identity (Yang et al., 2018; Barkhof et al., 2015).

Robert Plutchik, considered that there are eight primary emotions related to improve the animal and human survival process. He identified these emotions as: anger, fear, sadness, disgust, surprise, anticipation, trust and joy (Plutchik, 1980). Although, due to the complex mechanism of the brain having its several inputs, outputs and reactions, there isn't a precise answer for that question.

Figure 1.3, shows the circumplex model developed by Robert Plutchik and Kellerman to clearly describe the observed emotion-related categories (Plutchik and Kellerman, 2013).

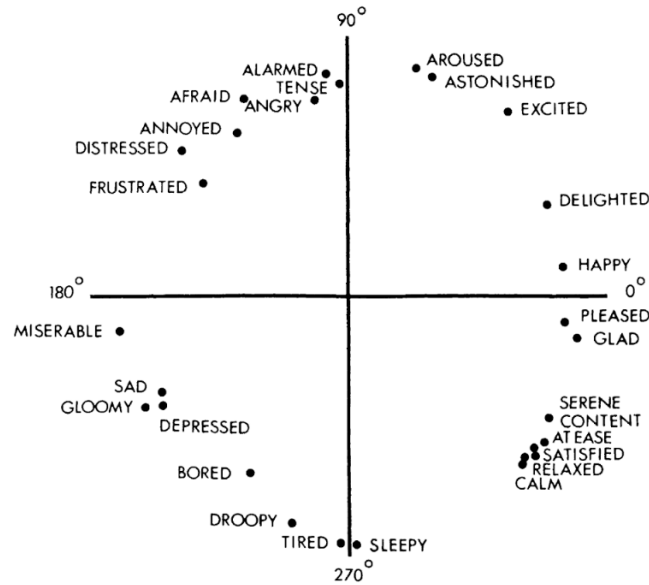


FIGURE 1.3. Circumplex model of emotion-related categories (Plutchik and Kellerman, 2013).

Computationally, a couple of researches also tried to answer this question using the emotion processing and recognition methods (sometimes called of automatic emotion processing and classification). These studies are getting space in academic fields, developing several applications and techniques to try to understand and accurately classify or recognize the human’s emotional states. A huge set of algorithms and methods are frequently developed to try to recognize emotions automatically and then, apply it in different contexts. There are a massive amount of researches and datasets that lead with emotions as such as the methods to evaluate it. Signal processing, feature extraction techniques, artificial intelligence, data mining and statistical learning are some examples that comply the role in the processing, analysis and recognition of emotions’ patterns.

In details, the automatic emotion classification, identification or recognition, is a complex and important task that also can be used to improve the health and the life’s quality as presented in this work, which the emotion recognition techniques are applied to find a manner to recognize and measure emotions using several approaches. These approaches and techniques can be used based on: Gaussian process regressions and Mel-Frequency Cepstrum Coefficients (MFCC) (Fukuyama and Goto, 2016); fuzzy logic (Salankar et al., 2017; Qamar and Ahmad, 2015; Matiko, Beeby, and Tudor, 2014); analysis of the potential of physiological signals for emotion recognition using the extended linear discriminant analysis (pLDA) to extract features (Kim and André, 2008); cross-correlation (Roza and Postolache, 2016); Artificial Neural Networks (ANN) (Roza and Postolache,

2017); wavelets (Al-Fahoum and A Al-Fraihat, 2014); Hilbert-Huang transform (Agrafioti, Hatzinakos, and Anderson, 2012), among others.

There are different ways to start a research based on emotions recognition: analyzing and acquiring physiological data (i.e. biosignals), using basically a set of dry or wet electrodes in a non-intrusive and non-invasive manner (Sun et al., 2017; Joutsen et al., 2018; Roza and Postolache, 2016); analyzing psychological questionnaires and picture presentation to trigger and detect different emotions (Xu et al., 2017; Reis, Arriaga, and Postolache, 2015); analyzing facial expression using computer vision techniques (Tarnowski et al., 2017; Li et al., 2017; Gunes and Hung, 2016); analyzing suicide notes (O’Dea et al., 2015; Desmet and Hoste, 2013), and other textual analysis based in lexical means in communication (Kima, and Sumner, 2017); analyzing the body expressions during emotional triggers (Rajhans et al., 2016); and analyzing and acquiring human speech data (Franti et al., 2017; Wen et al., 2017a; Sánchez-Gutiérrez et al., 2014).

The based-emotions researches and its effects or mechanisms may be used for several purposes. Some of these purposes are based on researches and applications including subjective and objective analysis such as: tests of emotional influence through behavioral mechanisms (Roberson et al., 2018); analysis of product-evoked emotions (Silva et al., 2017) to give support in health care based on smart city context and concepts of IoT (Postolache, 2017; Patsakis et al., 2014); detection of the relation between emotions and the regulation of lifestyle behavior (Isasi, Ostrovsky, and Wills, 2013); analysis of suicides notes to avoid recurrent occurrences (Desmet and Hoste, 2013); analysis of its positives effects in individuals when they are in green and natural city’s places (Thompson et al., 2012); developments of tools of meaning detection of language to understand, recognize emotions (Ezhilarasi and Minu, 2012); and also by developing of interfaces to detect emotions from facial expressions to helps anxious individuals (Heuer et al., 2010).

1.4. Thesis Content

This thesis is organized in such way to propose a clear and easy understanding regarding to the main steps developed in this work. Each method and techniques were applied to reach the emotion recognition which it were set in details, chapter by chapter, as briefly presented below.

Chapter 3, outlines the developed multimodal sensing system and data acquisition, presenting the sensors and acquisition processes; Chapter 4, outlines the preprocessing techniques to be executed before the phases: processing, features extraction and recognition process; Chapter 5, outlines the data processing and the techniques applied on this task; Chapter 6, outlines the feature extraction and detailed descriptions of the used techniques for that; Chapter 7, outlines the emotion recognition methodology and application; Chapter 8, outlines the result analysis regarding to the β -Band spectrogram; Chapter 9, outlines the result analysis regarding to the emotion recognition process; Chapter 10,

outlines all findings conclusions and limitations; Appendix A, outlines all produced publications along the present work and Appendix B, outlines additional plots referent to the brain data of all volunteers.

CHAPTER 2

Literature Review – Techniques on Emotion Sensing and Recognition

Several examples on literature has appeared to reveal the importance of the multimodal sensing systems to recognize emotions: emotion recognition through the presentation of several pictures and use of several biosignals (Roza and Postolache, 2017); identification of cognitive states of aircraft pilots while they are using flight simulators (Wang et al., 2020; Harrivel and Pope, 2017); harmonization of robotic devices and emotion states as frustration and boredom (C.Rodriguez-Guerrero et al., 2017); development a multimodal dataset to improve the emotion analysis, where the physiological responses to both visual and audiovisual stimuli are recorded (Conneau et al., 2017); multimodal sensing with support of cross-correlation method to identify emotions (Roza and Postolache, 2016); use of two different physiological signals to identify emotions (Alhouseini et al., 2016); and multimodal system to exam of the usefulness of physiological measurements in a bio-cooperative feedback loop to adjusts the difficulty of an upper extremity rehabilitation task (Novak et al., 2011).

These multimodal sensing systems are usually based on a couple of techniques and exam types such as: Heart Rate Variability (HRV) (Mather and Thayer, 2018; Haiblum-Itskovitch, Czamanski-Cohen, and Galili, 2018); Electrocardiography (ECG) analysis (Roza, Almeida, and Postolache, 2017; J., Murugappan M, and S., 2013; Shalin and Vanitha, 2013; Agrafioti, Hatzinakos, and Anderson, 2012); Electroencephalography (EEG) (Roza and Postolache, 2017; Voznenko et al., 2016; Othman et al., 2013) analysis; salivary cortisol analysis (Thompson et al., 2012); Galvanic Skin Response (GSR) (Sierra, 2011). Generally, to acquire the biosignals are used a set of electrodes on a non-intrusive and non-invasive manner (Roza and Postolache, 2016; Vojtech et al., 2013) through the use of: psychological questionnaires, using emotion valence and picture/video presentation (Reis, Arriaga, and Postolache, 2015; al., 2005; Pereira and Faria, 2015); facial expression recognition using computer vision (Gunes and Hung, 2016); speech communication (Wu, Falk, and Chan, 2011), using speech analysis; analysis of suicide notes (Desmet and Hoste, 2013), and other textual analysis based on lexical means in communication (Zaśko-Zielińska and Piasecki, 2015).

Regarding to the recognition system architecture, it is possible to affirm that emotions can't be recognized accurately using only one metric such as Heart Rate (HRV), for instance. Previous researches shown that in fact, the HRV could reflect the human emotion only in emotional situations that are relatively strong or intense, what is not applicable nor

feasible either to daily applications (Choi et al., 2017). If the system intends to recognize emotions accurately, fatally the usage of multimodal sensing is the main requirement.

In the following sections, a state of the art is presented based on emotion analysis and recognition. Multimodal systems relying on face, speech and physiological sensing were considered, which the researches based on face and physiological sensing are the main trunk of this work.

2.0.1. Emotion Recognition Techniques based on Facial Expressions

Facial Emotion Recognition (FER) is a powerful and very important research topic in the fields of computer vision and artificial intelligence. It can be applied to give support to the health, security, robotics, among others. Some of these automatic facial emotion recognition are based on the researches of Paul Ekman and Friesen (Ekman and Friesen, 1978), whom they defined the Facial Coding System (FACS), which it is a system based on facial muscle changes. The FACS is being very useful to characterize facial actions to express individual and involuntary emotions reactions.

In this scope, according to Paul Ekman, it is sufficient to note that there is consistent evidence across investigators, of an universal facial expressions for at least five emotions; he also putted in discussion if there are more emotions that have universal facial expressions (Ekman, 1992). It is also valid to consider that not necessary, the facial expression and what it signified is socially learned as culturally variable (Ekman, 1999). Figure 2.1, shows the general architecture of a FER system for mainly all supervised learning process.

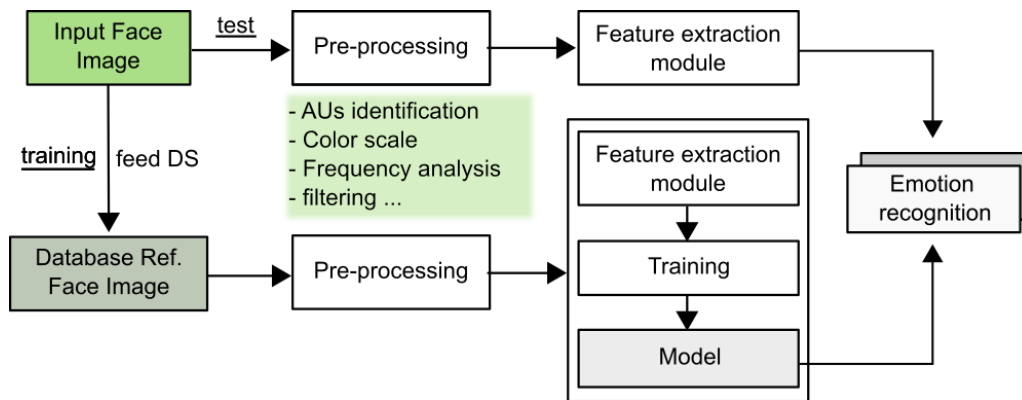


FIGURE 2.1. General architecture of a FER system.

On this context, Barros et al., proposed a neurocomputational model that learns to attend to emotional expressions and to modulate emotion recognition (Barros et al., 2017). Chenchah and Lachiri, examined an assessment of emotion error rate using classical descriptors (MFCC and PLP) and new type of speech features considered as more robust to noise and reverberation distortions also using various Signal-to-Noise Ratio (SNR) levels (Chenchah and Lachiri, 2017). De et al., presented a human facial expression and emotion recognition system using eigenface approach and Hue-Saturation-Value (HSV) color model to detect on offline mode the human face in an image (De, Saha, and Pal, 2015). Jain et al., proposed a network architecture based on convolution layers followed by Recurrent

Neural Network (RNN) to design a combined model to extract the relations within facial images (Jain et al., 2018). Kayaa et al., describes a multimodal approach for video-based emotion recognition in the wild, using summarizing functional of complementary visual descriptors for video modeling (Kayaa, Gürpınar, and Salah, 2017). Khalfallah and Ben Hadj Slama, presented a web-based intelligent tutoring system called Remote Laboratory (RL), that it is a computer-based learning environment that allows students from anywhere to access and perform experiments on real laboratory equipment based on Internet (Khalfallah and Slama, 2015). Krithika and Lakshmi, developed a system to recognize emotions based on the movements of the head and eyes, captured from a recording using a video camera (Krithika and G.G., 2016). Lopes et al., proposed a simple solution for facial expression recognition that uses a combination of Convolutional Neural Network (CNN) and specific image pre-processing steps (Lopes et al., 2017).

Mao et al., proposed a real-time emotion recognition approach based on both 2D and 3D facial expression features captured by Kinect sensors (Mao et al., 2015). Martinez, proposed a model that predicts emotions and the existence of a large number of previously unknown facial expressions, including compound emotions, affect attributes and mental states that are regularly used by people (Martinez, 2017). Matlovic et al., focused on two approaches to identify emotions such as, namely emotions detection using facial expressions recognition and electroencephalography (EEG) (Matlovic et al., 2016). Mayya et al., proposed a novel method for automatically recognize facial expressions using Deep Convolutional Neural Network (DCNN) features (Mayya, Pai, and Pai, 2016). Patwardhan, developed a multimodal system to detect emotions based on audio-visual continuous data (Patwardhan, 2017). Subhashinia and Niveditha, developed a C# application to analyzing and detection of the employees' emotions for amelioration of organizations, using facial images and Bézier Curves (BC) (Subhashinia and Niveditha, 2015). Tarnowski et al., developed a system to identify emotions based on facial expressions using three-dimensional face model (Tarnowski et al., 2017).

2.0.2. Emotion Recognition Techniques based on Human Speech

Emotion recognition based on speech analysis, represents a complex problem inside of signal processing, including a couple of features mainly based on frequency analysis e.g. filter-banks and wavelets. To try to solve this complex goal, several researches presented feasible solutions. The emotion recognition tasks through human speech data can be understood basically, as shown in Figure 2.2.

Abdelwahab and Busso, present a solution to address the problem of low performance of speech emotion classifiers by combining Active Learning (AL) and supervised Domain Adaptation (DA) using an elegant approach for Support Vector Machine (SVM) (Abdelwahab and Busso, 2017). Alonso et al., developed a system to recognize emotional intensity from speech using a few feature set obtained from a temporal segmentation of the speech signal of different language like German, English and Polish (Alonso et al., 2015). Bahreini et al., present the voice emotion recognition part of the Framework for

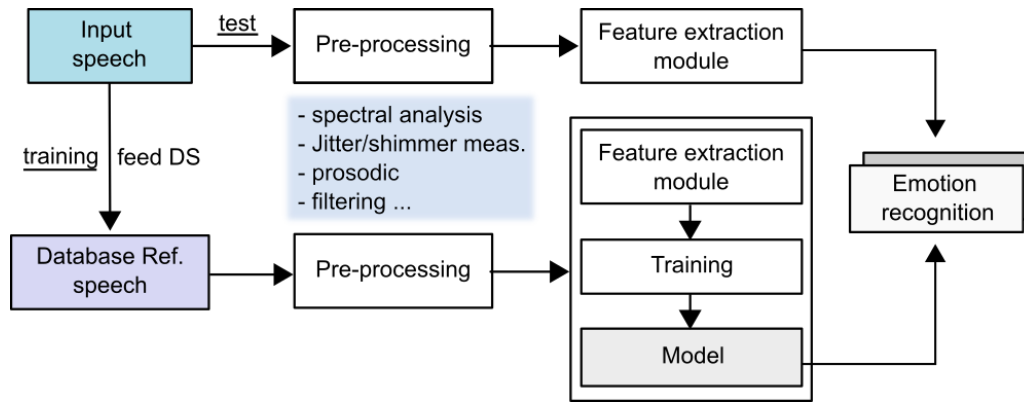


FIGURE 2.2. General architecture of a speech-based system to recognize emotions.

Improving Learning Through Webcams And Microphones (FILTWAM) for real-time emotion recognition on affective e-learning settings (Bahreini, Nadolski, and Westera, 2016). Bertero and Fung, developed a real-time Convolutional Neural Network (CNN) model for speech emotion detection, also providing an in-depth model visualization and analysis (Bertero and Fung, 2017). Brester et al., propose an evolutionary feature selection technique based on two-criterion optimization model to give support to emotion recognition task (Brester et al., 2016). Cao et al., presented a ranking approach for emotion recognition which naturally incorporates information about the general expressibility of several speaker (Cao, Verma, and Nenkova, 2015). Davletcharova et al., conducted an experimental study on recognizing emotions from human speech, considering the emotions neutral, anger, joy and sadness, using several recognition methods (Davletcharova et al., 2015). Deb and Dandapat, explored the effect of breathiness component on speech under stress inside of the speech emotion analysis (Deb and Dandapat, 2015). Fayek et al., developed a frame-based formulation to speech emotion recognition that relies on minimal speech processing and end-to-end deep learning to empirically explore feed-forward and Recurrent Neural Network (RNN) architectures and their variants (Fayek, Lech, and Cavedon, 2017). Goran and Negoescu, presented a framework to improve the class quality and the student memorization in the school, using emotional constraints by speech, face and texts (Goran and Negoescu, 2015). Lanjewar et al., developed a speech emotion recognition system based on spectral components of Mel Frequency Cepstrum Coefficients (MFCC), wavelets features of speech and pitch of vowel traces (Lanjewar, Mathurkar, and Patel, 2015). Mannepalli et al., developed an adaptive fractional Deep Belief Network (DBN) and several spectral features to recognize different emotions from speech (Mannepalli, Sastry, and Suman, 2017). Motamed et al., developed an optimized model based on limbic system of mammalian brain for speech emotion recognition on dynamic situations like the brain's emotional networks (Motamed, Setayeshi, and Rabiee, 2017).

Muthusamy et al., presented a new feature enhancement to improve the discriminatory power of the features extracted from speech and glottal signals (Muthusamy, Polat, and Yaacob, 2015a). They also presented a novel Particle Swarm Optimization system

based Clustering (PSOC) and Wrapper based Particle Swarm Optimization (WPSO) to enhance the discerning ability of the features and to select the discriminating features respectively (Muthusamy, Polat, and Yaacob, 2015b). Ozseven, presented a new feature selection methods to increase the emotional recognition success and to reduce the processing workload with these fewer features (Ozseven, 2019). Shahin and Ba-Hutair, present a solution to speech emotion recognition using the second-order Circular Suprasegmental Hidden Markov Models (CSPHMM2s) as the classifiers (Shahin and Ba-Hutair, 2015). Shukla et al., presents a novel subspace projection approach for analysis of speech signal under stressed condition (Shukla, Dandapat, and Prasanna, 2016). Sun et al., presents a novel Weighted Spectral Features (WSF) based on local *Hu* moments to improve the speech emotion recognition (Sun, Wen, and Wang, 2015). Szaszak et al., developed an information analysis technique, called Weighted Correlation based Atom Decomposition (WCAD) to execute the speech synthesis inside the context of stress detection that can also be applied to some emotion status (Szászák, Tundik, and Gerazov, 2018). Trigeorgis et al., proposed a solution to the problem of context-aware emotional relevant feature extraction, by combining Convolutional Neural Networks (CNNs) with Long short-term memory (LSTM) networks in order to automatically learn the best representation of the speech signal (Trigeorgis et al., 2016).

Yogesh et al., presented a new set of features and feature enhancement techniques, e.g. Generalized Regression Neural Network (GRNN), to recognize emotion and stress from speech signals (Yogesh et al., 2017b). Yogesh et al., also developed a speech emotion and stress recognition system, by identifying speakers' emotion from their voices, using higher order spectral and selection algorithm features (Yogesh et al., 2017a). Wang et al., developed a new Fourier parameter model using the perceptual content of voice quality and the first- and second-order differences for speaker-independent speech emotion recognition (Wang et al., 2015). Wen et al., present an ensemble of random Deep Belief Networks (DBN) method for speech emotion recognition (Wen et al., 2017b). Xue et al., propose a rule-based voice conversion system for emotion which it is capable of converting neutral speech to emotional speech using dimensional space (arousal and valence) to control the degree of emotion on a continuous scale (Xue, Hamada, and Akagi, 2018). Zha et al., apply Multiple Kernel Learning (MKL) algorithm to recognize the spontaneous speech emotion (Zha et al., 2016).

2.0.3. Emotion Recognition Techniques based on Physiological Parameters

Emotion recognition using physiological sensing (biosignal) is the main contribution of this work. In general, the emotion recognition systems using biosignal are mainly based on multimodal sensing.

Various researches shown that an emotion recognition system using only a single-mode channel of biosignal does not worth for several emotional situations. This way, to increase the range of the emotion analysis, the proposed work decided to use a multimodal or a more complex approach. Figure 2.3, shows a general architecture of a supervised system

to recognize emotions from biosignals data. It starts on input data; during the training phase, input data are stored in some dataset to be processed further. After the processing, several features are extracted from these data to train and produce a model to recognize emotions automatically. In the test, no models are created but the features of the input data are applied over the produced model of the training phase.

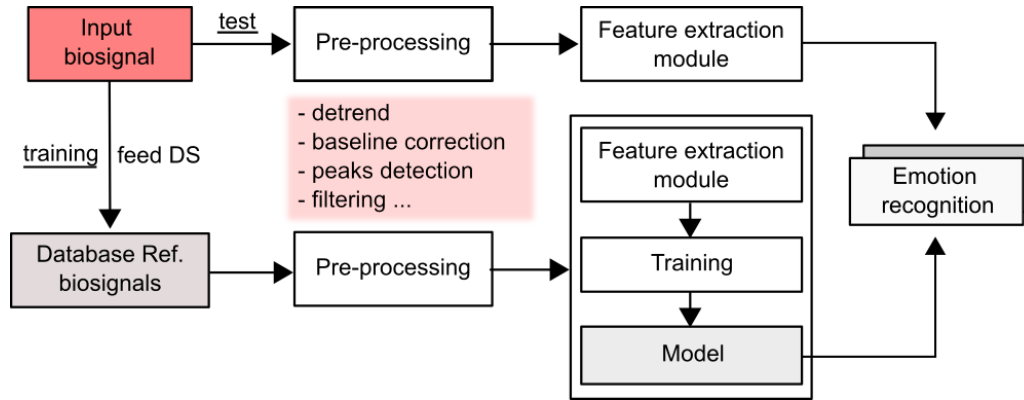


FIGURE 2.3. General architecture of a biosignal-based system to recognize emotions.

Alhouseini et al., presented an analysis of emotional properties based on two physiological signals such as, ECG and EEG (Alhouseini et al., 2016). Bozhkov et al., proposed an unified system for efficient discrimination of positive and negative emotions in a group of 26 volunteers based on EEG signals (Bozhkov et al., 2015). Capuano et al., used the Friedman test to verify whether the work on exposure and emotional identification influences help to decrease the levels of anxiety and depression (Capuano et al., 2017). Cruz et al., presented an automatic recognizer of the facial expression around the eyes and forehead based on Electrooculography (EOG) signals, giving support to emotion recognition task (Cruz et al., 2015). Goshvarpour et al. (2017), used GSR and ECG data to develop a study to examine the effectiveness of Matching Pursuit (MP) algorithm in emotion recognition, using mainly Principal Component Analysis (PCA) to reduce the features dimensionality and Probabilistic Neural Network (PNN) as the recognition technique (Goshvarpour, Abbasi, and Goshvarpour, 2017). He et al., presented an emotion recognition system based on physiological signals using ECG and respiration (RSP) signals, recorded simultaneously by a physiological monitoring device based on wearable sensors (He, Yao, and Ye, 2017). Kaur et al., proposed a methodology and also performed an analysis about the impact of positive and negative emotions using SVM and Radial Basis Function (RBF) as the recognition methods (Kaur, Singh, and Roy, 2018). Kumar et al., executed derived features based on bi-spectral analysis for quantification of emotions using a valence-arousal emotion model to get a way of gaining phase information by detecting phase relationships between frequency components and characterization of the non-Gaussian information from EEG signals (Kumar, Khaund, and Hazarika, 2016). Lan et al., proposed a novel real-time subject-dependent algorithm using Stability Intra-class Correlation Coefficient (ICC) with the most stable features that give a better accuracy

than other available algorithms when it is crucial to have only one training session (Lan et al., 2016). Lahane and Sangaiah, presented a new approach to emotion recognition based on EEG and classification method using Artificial Neural Networks (ANN) with features analysis based on Kernel Density Estimation (KDE) (Lahane and Sangaiah, 2015). Petrovica et al., presented an analysis of emotion recognition techniques used on existing systems to enhance ongoing research on the improvement of tutoring adaptation (Petrovica, Anohina-Naumeca, and Ekenel, 2017). Reis et al., developed an application that stores several physiological signals based on HR, ECG, SpO2 and GSR, which it were acquired while the volunteers watched advertisements about smoking campaigns (Reis, Arriaga, and Postolache, 2015).

Roza and Postolache, executed experiments based on flight simulator to developed a multimodal sensing architecture to recognize emotions using three different techniques for biosignal acquisitions (Roza et al., 2019; Roza and Postolache, 2018). Roza and Postolache, also developed a multimodal sensing system to identify emotions using different acquisition techniques, based on image presentation methodology (Roza and Postolache, 2017). Roza et al., developed an emotion recognition system based on cross-correlation and the Flowsense database (Roza and Postolache, 2016). Shin et al., proposed a real-time user interface with emotion recognition that depends on the need for skill development to support a change in the interface paradigm to one that is more human centered (Shin, Shin, and Shin, 2017). Yin et al., developed a solution to recognize emotions through physiological sensing using a Multiple-fusion-layer based on Ensemble classifier of Stacked Autoencoder (MESAE) (Yin et al., 2017b). Yin et al., proposed an ensemble deep learning framework by integrating multiple stacked auto-encoder with parsimonious structure to reduce the model complexity and improve the recognition accuracy using physiological feature abstractions (Yin et al., 2017a).

2.0.4. Techniques Comparisons

Figure 2.4, shows some main publications referred in this work, published between 2015 and 2019, inside of the context of emotion recognition using facial, speech and physiological sensing technologies.

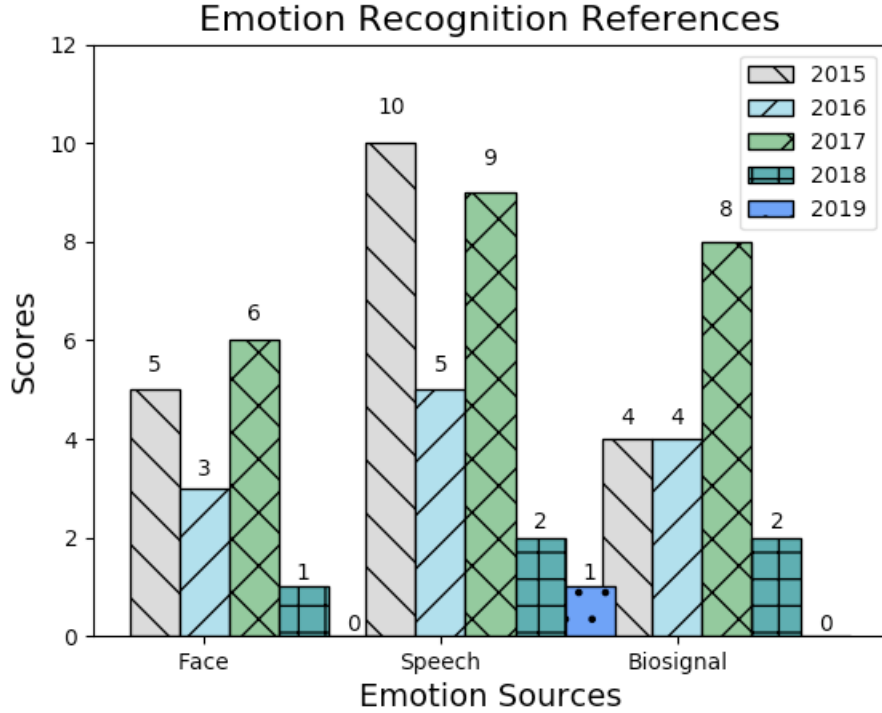


FIGURE 2.4. Comparison between the number of selected publications (2015 to 2019).

Tables 2.1 to 2.3, show a more detailed information of each research, previously presented in this work.

Table 2.1: Some techniques regarding to face emotion recognition since 2015.

Reference	Source	Techniques	Major Contribution
Jain et al.	Facial	CNN, RNN	◊ Development an DNN architecture combining CNN and RNN to better recognize emotion patterns within facial images.
Barros et al.	Facial	CNN	◊ Development of a neuro-computational model that learns to attend to emotional expressions and to modulate emotion recognition.
Kayaa, Gürpınarb, and Salah	Facial	CNN, ELM, PLS	◊ Description of a multimodal approach for video-based emotion recognition in the wild.
Lopes et al.	Facial	CNN	◊ Simple methodology to identify emotions using images of faces as references.
Martinez	Facial	AUs	◊ Development of a model based on face expression recognition to predict emotion, valence, arousal and specific combination of facial muscle movements.

Patwardhan	Facial, Speech	SVM	◇ Development of a multimodal system to detect emotions from audio and video data.
Tarnowski et al.	Facial	ANN, KNN	◇ Development of a system to identify emotion based on facial expressions.
Matlovic et al.	Facial, Biosignal	SVM	◇ Use of two approaches to identify emotions based on emotions detection using facial expressions recognition and EEG signals.
Mayya, Pai, and Pai	Facial	Deep CNN	◇ Development of a novel method for automatically recognizing facial expressions using Deep Convolutional Neural Network.
Krithika and G.G.	Facial	Viola jones, LBP, Ada Boost, ANN	◇ Development of a system that can identify and monitor emotions of the student in an e-learning environment and provide a real-time feedback mechanism to enhance the e-learning aids.
De, Saha, and Pal	Facial	ED, Eigen- faces	◇ Development of a human facial expression and emotion recognition system modeled using eigenface approach and Hue-Saturation-Value (HSV) color model.
Mao et al.	Facial	SVM	◇ Development of a real-time emotion recognition approach based on both 2D and 3D facial expression features.
Khalfallah and Slama	Facial	> 70 Small classifiers	◇ Web-based tutoring system to allows students to access and perform experiments on real laboratory equipment via Internet.
Goran and Negoescu	Facial, Speech	Memorization level (ML)	◇ Measure the acquisition level and the efficiency in the memorization of several lessons presented in the school.
Subhashinia and Niveditha	Facial	BC	◇ Detection of employee's emotion for amelioration of organizations.

Table 2.2: Some techniques regarding to speech based on emotion recognition since 2015.

Reference	Source	Techniques	Major Contribution
Ozseven	Speech	SVM, ANN, k-NN	◇ Proposed a new statistical feature selection method based on the changes in emotions on acoustic features.

Szaszák, Tundik, and Gerazov	Speech	HMM, WCAD	◊ Developed a prosodic stress detection system for fixed stress languages.
Xue, Hamada, and Akagi	Speech	Fujisaki F0 model, target prediction model	◊ Proposes an inverse three-layered model with acoustic features as output at the top layer, semantic primitives at the middle layer and emotion dimension as input at the bottom layer.
Abdelwahab and Busso	Speech	SVM	◊ Development of a solution to address the low performance of speech emotion classification.
Bertero and Fung	Speech	CNN	◊ Development of a real-time Convolutional Neural Network model for speech emotion detection.
Chenchah and Lachiri	Speech	HMM	◊ Analysis of an assessment of emotion error rate using MFCC and PLP, and a new type of speech features.
Fayek, Lech, and Cavedon	Speech	Deep ANN	◊ Development of a speech emotion recognition system to explore feed-forward and recurrent neural networks.
Mannepalli, Sastry, and Suman	Speech	Adaptive Fractional DBN	◊ Development of an adaptive fractional deep belief networks to recognize different emotion from speech.
Motamed, Setayeshi, and Rabiee	Speech	ANN, ANFIS	◊ Development of a model based on the limbic system in order to obtain a desirable learning model for speech emotion recognition.
Yogesh et al.	Speech	ELM	◊ Development of a speech emotion/stress recognition system using spectral features.
Yogesh et al.	Speech	ELM Kernel, KNN, PNN, GRNN	◊ Presents a new set of features and feature enhancement techniques to support the emotion and stress recognition.
Wen et al.	Speech	Random DBN	◊ Development of an new approach of random deep belief networks method for speech emotion recognition.
Bahreini, Nadolski, and Westera	Speech	SVM	◊ Shows a valid use of computer microphone data for real-time and adequate interpretation of vocal intonations.
Brester et al.	Speech	SVM, ANN, Logit	◊ Design of a parallel multicriteria heuristic procedure based on an island model.

Shukla, Dandapat, and Prasanna	Speech	HMM	<ul style="list-style-type: none"> ◇ Development of a novel subspace projection approach for analysis of speech signal.
Trigeorgis et al.	Speech	CNN, LSTM	<ul style="list-style-type: none"> ◇ Solution to the problem of "context-aware" emotional relevant feature extraction.
Zha et al.	Speech	MKL	<ul style="list-style-type: none"> ◇ Application of Multiple Kernel Learning (MKL) to recognize the spontaneous speech emotion.
Alonso et al.	Speech	SVM	<ul style="list-style-type: none"> ◇ Development of a system to recognize emotion from speech using different languages like German, English and Polish.
Cao, Verma, and Nenkova	Speech	SVM	<ul style="list-style-type: none"> ◇ Introduced a novel ranking models for emotion recognition.
Davletcharova et al.	Speech	NB, RBF, Ada boost, Lazy IB1	<ul style="list-style-type: none"> ◇ Study aimed at exploring dependencies the nature of utterance have with the human emotional state.
Deb and Dandapat	Speech	HMM	<ul style="list-style-type: none"> ◇ Evaluation of the performance of breathiness features for classification of speech under stress.
Lanjewar, Mathurkar, and Patel	Speech	GMM, KNN	<ul style="list-style-type: none"> ◇ Development of system to detect emotions from speech.
Muthusamy, Polat, and Yaacob	Speech	GMM	<ul style="list-style-type: none"> ◇ Improvement of emotion recognition task from speech using Gaussian Mixture Model and Extreme Learning Machine.
Muthusamy, Polat, and Yaacob	Speech	ELM	<ul style="list-style-type: none"> ◇ Development of a particle swarm optimization model to enhance the emotion speech recognition.
Shahin and Ba-Hutair	Speech	HMM	<ul style="list-style-type: none"> ◇ Enhancement of talking condition recognition in stressful and emotional talking environments.
Sun, Wen, and Wang	Speech	SVM	<ul style="list-style-type: none"> ◇ Shows that the Hu WSF can be computed from local regions of a spectrogram using Hu moments.
Wang et al.	Speech	SVM	<ul style="list-style-type: none"> ◇ Development of a new Fourier parameter model for speaker-independent speech emotion recognition.

Table 2.3: Some techniques regarding to biosignal based on emotion recognition since 2015.

Reference	Source	Techniques	Major Contribution
Kaur, Singh, and Roy	Biosignal	SVM, RBF	◊ Performed an analyze about the impact of positive and negative emotions using electroencephalogram.
Roza and Postolache	Biosignal	ANN	◊ Developed of a multimodal architecture to acquire and recognize emotions based on flight simulation tasks.
Capuano et al.	Biosignal	Friedman Test (FT)	◊ Verification whether work on exposure and emotional identification influences the decreased level of anxiety and depression.
Goshvarpour, Abbasi, and Goshvarpour	Biosignal	PNN	◊ Developed a study to examine the effectiveness of Matching Pursuit (MP) algorithm in emotion recognition.
He, Yao, and Ye	Biosignal	SVM	◊ Development of an emotion recognition system based on ECG and respiration (RSP) signals using wearable sensors.
Shin, Shin, and Shin	Biosignal	ANN, SVM, BN	◊ Provides services to meet the need to recognize emotions when using contents.
Yin et al.	Biosignal	MESAE	◊ Presentation of a classifier to reduce the model complexity and improve the accuracy for emotion recognition.
Yin et al.	Biosignal	MESAE	◊ Development of a solution to identify emotions using physiological sensing based on MESAE.
Roza and Postolache	Biosignal	ANN, SVM	◊ Development of a multimodal system to identify emotions by the use of several techniques of biosignals acquisition.
Petrovica, Anohina-Naumeca, and Ekenel	Biosignal	ANN, NB, Logit, LR, SVM, KNN, DT	Analysis of the emotion recognition techniques used in existing systems.
Alhouseini et al.	Biosignal	ANN	◊ Considers two physiological signals and shows the analysis of its emotional properties.
Kumar, Khaund, and Hazarika	Biosignal	ANN, SVM, RBF	◊ Execution of bispectral analysis to offers a way to obtain other important information from the analyzed biosignal.

Lan et al.	Biosignal	ICC	◇ Proposed and tested a novel real-time subject-dependent algorithm with stable features to have only one training session for the user.
Roza and Postolache	Biosignal	SCC	◇ Emotion classification using biosignals from Flowsense dataset.
Bozhkov et al.	Biosignal	ANN, Logit, LDA, KNN, NB, SVM, DT	◇ Development of an unified system for efficient discrimination of positive and negative emotions.
Cruz et al.	Biosignal	Multiclass LDA	◇ Development of an automatic recognizer of the facial expression based on EOG to to give support to emotion recognition.
Lahane and Sangaiah	Biosignal	ANN	◇ Development of a new approach to emotion recognition based on EEG.
Reis, Arriaga, and Postolache	Biosignal	Questionn., ANOVA	◇ Application to store several physiological signals.

2.0.5. Recognition Techniques Comparisons

By observing the techniques used in these researches to recognize emotional patterns, some of them were applied on more than one perspectives e.g., ANN, SVM, KNN, CNN, HMM, ELM, PNN, RBF, NB, Ada boost, ML and Logit, as shown in Figure 2.5.

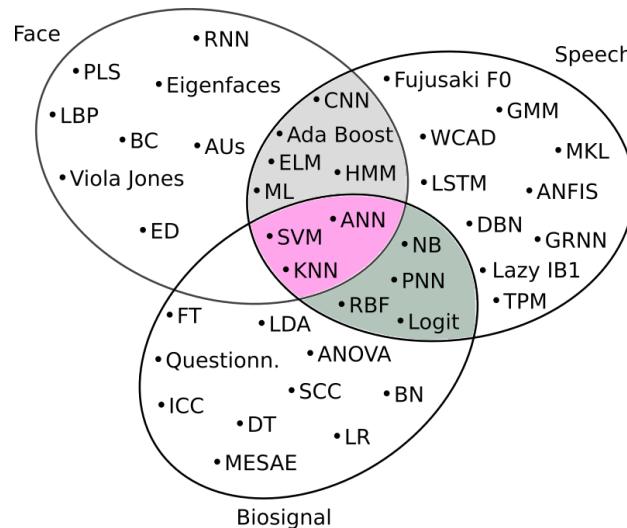


FIGURE 2.5. Venn diagram over the most common techniques used to recognize emotions based on face, speech and biosignal (2015 to 2019).

Recognition techniques based on the neural networks class were majority in emotion recognition context, e.g, RNN, CNN, ANN, RBF, PNN and GRNN. The second more used was SVM, as shown in Figure 2.6.

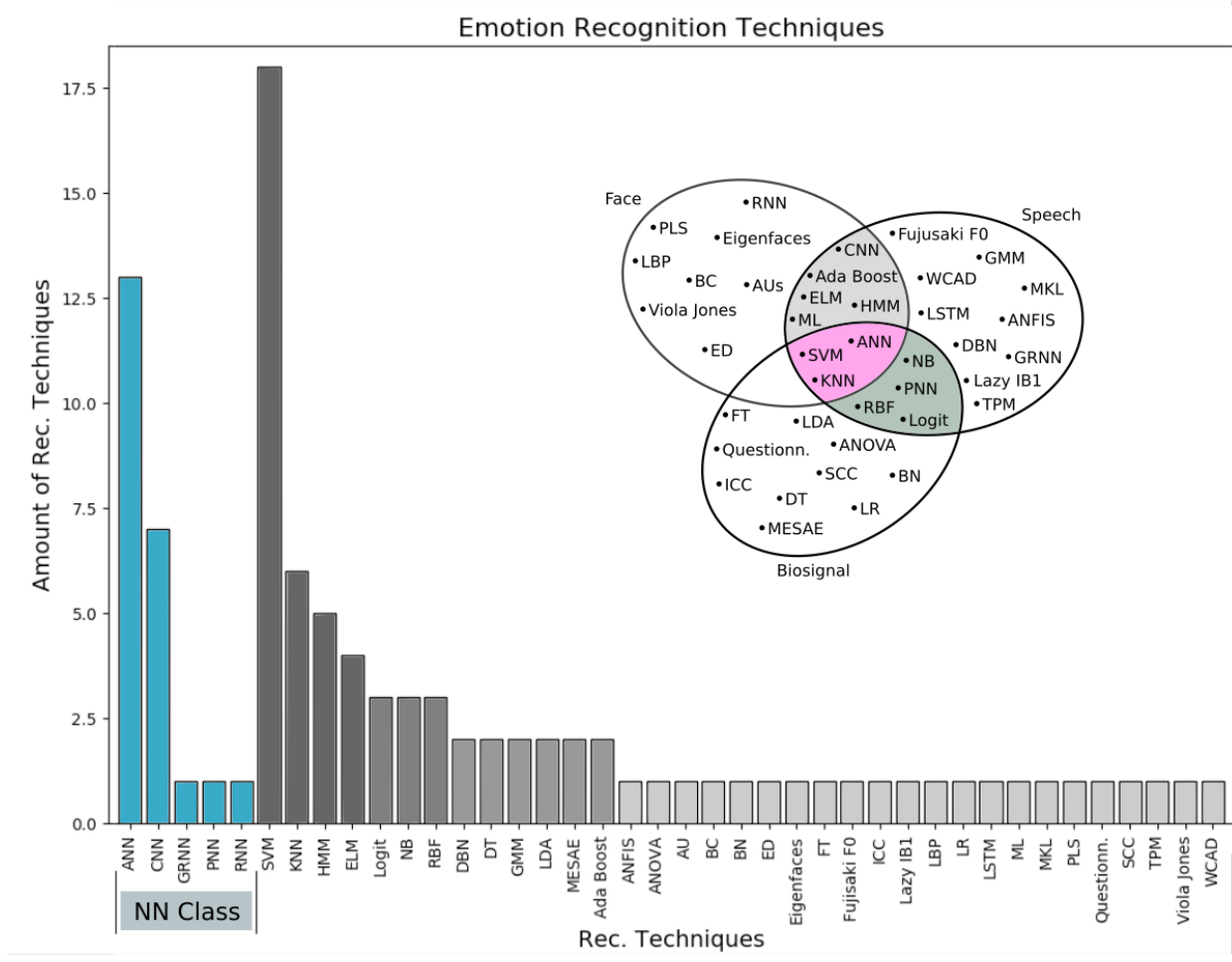


FIGURE 2.6. Recognition techniques found on emotion-related researches (2015 to 2019).

The present state of the art was fundamental to define the best recognition technique to be used in this work and which tools or sensing techniques to apply.

Multimodal Sensing System and Data Acquisition

Multimodal sensing approach is not a new architecture or new method to support a recognition system, but it is a more robust and powerful approach to be applied in situations in which a low amount of channel (inputs) are not sufficient to reach a good recognition accuracy along the time. It is based on several channels that come mainly from different sources of data, resulting on related outputs. It is sometimes challenging for researchers due the time analysis and multi sampling rate synchronization. For some researches contexts like, emotion recognition based on biosignals for instance, it is not recommended to use only one type of biosignal e.g. heart rate variability, to accurately detect emotions, because it can reflect emotions only in strong or intense emotional situations (Choi et al., 2017). According to some studies, when an extended number of biosignals are considered, better results can be reached.

These multisensing approaches can also be found in another applications as for instance: on dynamic system and nanostructures (Adhikari and Khodaparast, 2021); on aviation context, using flight simulations (Roza and Postolache, 2019; Roza et al., 2019; Roza and Postolache, 2018); temperature measurement on chemistry (Chi et al., 2019); using summarizing functional of complementary visual descriptors, for video modeling (Kayaa, Gürpınar, and Salah, 2017); on identification of cognitive states of aircraft pilots, while they are using flight simulators (Harrivel and Pope, 2017); and to exam of the usefulness of psychophysiological measurements in a bio-cooperative feedback loop to adjust the difficulty of an upper extremity rehabilitation task (Novak et al., 2011).

The complexity of the present research requires the use of a multimodal sensing system to give support to the emotion recognition process in a general perspective. In this work, the aviation context was used to execute the experiments and validate the research results. A set of acquisition and recognition techniques were used. The chosen biosignal acquisition techniques were based on: Electroencephalography (EEG); Heart Rate (HR) through PPG sensor and Galvanic Skin Response (GSR). It were also considered the data acquisition based on face recordings and questionnaires, which this last acted as a personal emotion report, directly answered by each volunteer. After the data acquisition and storage, the further steps were data preprocessing, processing, features extraction and emotion recognition.

The experimental context is based on aviation but the designed methodology, used techniques and reached results, can also be applied on other researches contexts e.g. smartcity, biophilia, automobilism or even, administrative works. Applying it on smartcity context, an emotion regulation strategy can be used to improve the tourism in city's places (Roza

and Postolache, 2016); on biophilia context, it can be powerful to relate emotions with green places, using different strategies to improve the development of green places and also collaborating with some smartcity concepts; if considering the automobilism, it can be extremely useful to monitor the drivers' emotional state along a travel or delivery task (Benoit et al., 2006); finally, when considering the administrative works, it researches and multimodal sensing system can be useful to analyze not only emotions but also the well being, life quality, stresses levels at work and satisfaction or happiness levels along the work period (Mishra et al., 2011). In the aviation context, this research brings a contribution, ensuring an emotion regulation and/or monitoring of each pilot to give support in the avoidance of aviation accidents caused by human failures (Roza et al., 2019), for instance.

Figure 3.1, shows a set of contexts that can be applied inside of the present work methodology of data acquisition, analysis and recognition.

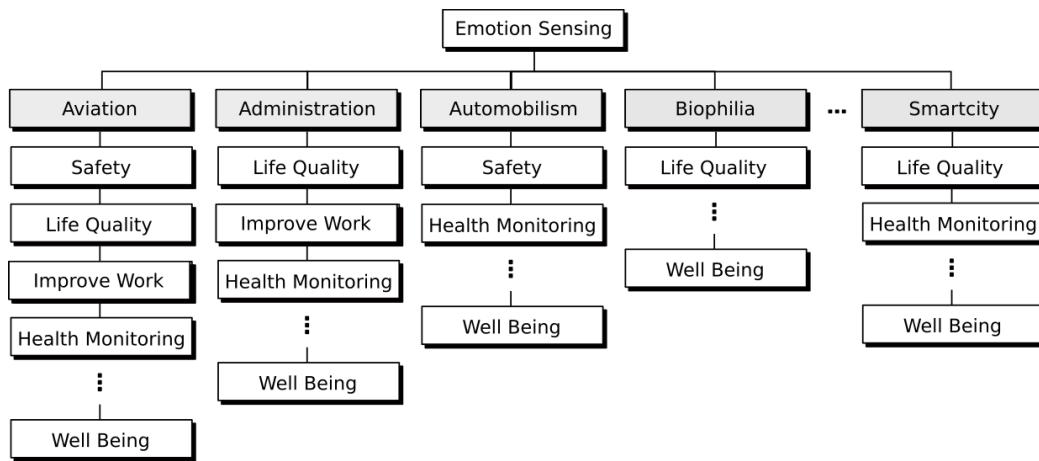


FIGURE 3.1. Diagram with some examples of application based on the developed multimodal system proposed in this work.

Between 2016 and 2018, a couple of other experiments were developed inside of the scope of physiological signals (biosignals), signal processing and emotion recognition, which it were important to give support to the final multimodal system presented here.

3.1. Multimodal Architecture Description

Each multimodal sensing system can presents different execution procedure. In this present work, several steps were considered since the environment setup until the final emotion recognition. All experiments were executed in late afternoon and night due to be a calm and noiseless time in the laboratory. The experiment's supervisor closed all communication with the volunteer during the simulated flight. Figure 3.2, presents the general steps of execution.

The environment setup was designed to keep the repeatability and minimum error propagation along the experiment. It includes: environment illumination, keeping similar light intensities for all volunteers in experiment; noise control, to avoid noises as much as possible during the experiments; simulation screen configuration (i.e. bright, contrast,

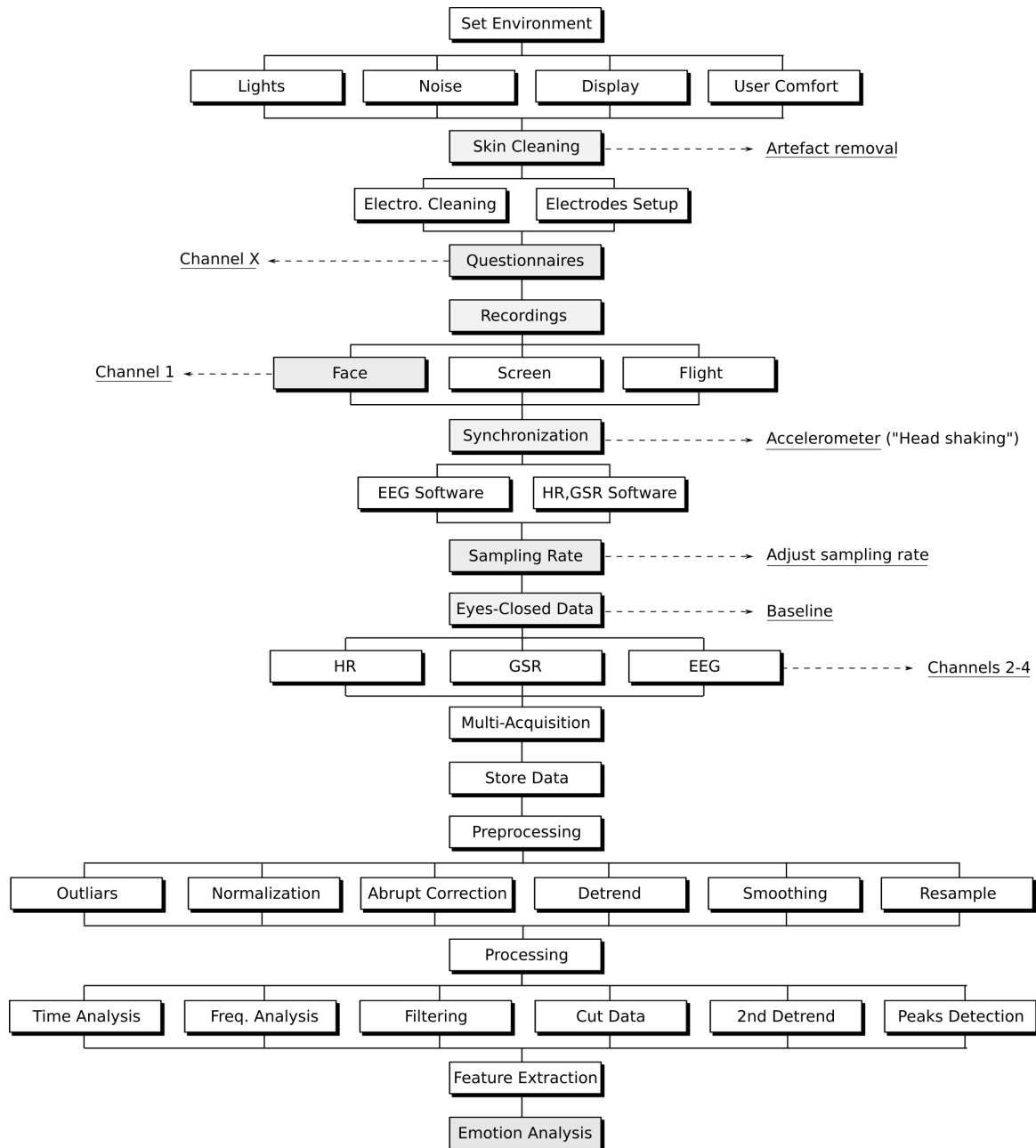


FIGURE 3.2. Execution steps of the proposed multimodal sensing system.

resolution, etc) and size were the same for all experiments. The volunteer comfort is other important behaviour to be considered in the present multimodal experiment due the number of sensors on the volunteer's body. Furthermore, good chairs, properly table with ideal high, among other factors. The volunteers' feedback about the their own comfort, before the experiment begin was also considered.

The next steps is based on electrodes procedures such as, electrodes setup and cleaning. This work also considers an auxiliary channel of data acquisition based on questionnaires, represented in the diagram with the label channel X. It is useful to understand, based on volunteers' feedback, the emotional state of each one before, during and after the flight experiment.

The volunteers' face recordings were used to represent the emotions references (target) along the experiments. These references leaded the emotion recognition process, outputting emotion intensities to be used on the training phase.

This work used two different software to execute the physiological data acquisition: Neuroelectrics Instrument Controller (NIC) software for EEG, and the EmoSense - Real Time (ES-RT) software to acquire HR from PPG, and GSR data. The software synchronization was mainly based on sampling rate and accelerometer parameters.

Environment setup, skin cleaning and data synchronization are important behaviours that must be executed to avoid bad raw biosignal acquisition on multisensing context. All these previous behaviours can not worth enough, if no baseline technique be applied just before the data acquisition. Without this baseline, the beginning of the experiment can brings a high level of data uncertainties and a couple of data artifacts due to several reasons, e.g. distractions (visual mainly), loss of attention, abrupt body movements and so on. In this work, the baseline was based on the eyes-closed data acquisition with 30 to 60 seconds of duration. It is useful to normalize the physiological parameters before the experiment begins. Just after the baseline time ends, the system begins to recording the facial expression, HR from PPG, GSR and EEG data. All these data are acquired at same time. The questionnaires' answers were recorded before, during and after each experiment. With exception of questionnaires, all those acquired data are raw and need a such couple of the preprocessing before to go forward. It was based on outliers detection and removal, normalization, abrupt data correction, data smoothing and trend corrections (detrend).

The preprocessing represents a complex phase of this work from where it is possible to extract good data features and emotion recognition. In the processing phase, some mistakes from previous phases can also be fixed, as such as the data optimization. Time and frequency analysis, filtering, data resampling, peak detection, among other things can be executed. With all these data treatment and processing, it is much simpler to extract features since these features were already well defined according to input data. Once the feature extraction has done, it is possible to execute the emotion recognition.

In the emotion recognition process, the data shape must be well defined and organized in a such way to produce coherent results. Since was chosen a supervised learning technique to recognize emotions, the set of emotions intensities and classes must to be minimally coherent to produce good training results and then, good new data recognition on test and validation.

3.2. Proof of Concept (PoC) of the Experiment

A Proof of Concept (PoC) is an execution of a certain methodology or idea, in order to demonstrate its feasibility, complexity level and coherence. It can also represents a prototype to verify if some concept or theory has practical potential. It is usually simpler than a final concept, system or architecture. Although it be simpler, its outputs can determine if the proposed methodology or idea should go further or not.

This work executed two different PoCs, on which the idea of the proposed multimodal sensing system was tested. Each PoC included at most three flight simulations (for each volunteer) and several emotional events analysis. Previous studies shown that there is a direct and critical relation between the risk work and emotional events (Breakwell, 2014) and the results of the PoCs were important to show emotional stimuli along the simulated flights.

Figure 3.3, shows two different approaches of the PoCs proposed in this work, based on the multimodal architecture presented above. On the first PoC (right setup), the simulation was executed with two volunteers as flight pilots and one experiment supervisor. The HR, EEG, SpO2 and GSR, were considered in this first PoC. Three people were involved on: the volunteer acting like a pilot, that was responsible by joystick commands (using the left or right hand) and some keyboard commands as landing gear up and down; the second volunteer acting like co-pilot, that was responsible by the "80 knots" speed call-out, flaps controls and to inform to the first volunteer about the flight tasks checklists along the simulation (i.e. alert of before flight, takeoff, navigation, approach, landing and after flight); and the supervisor, that only inform the beginning and the end of a flight, keeping in silence with the volunteers along the flight. Additionally, in the first approach, were also considered the face recording, three points HR electrodes (left and right wrists and one ankle), flight plan/checklist, headset (to avoid noise from external environment) and questionnaires. The experiment execution wasn't based on execution checklist, which sometimes the execution sequence was impaired several times due that. No data processing and emotion recognition were executed in this first approach. Only the aircraft Extra 300S was used.

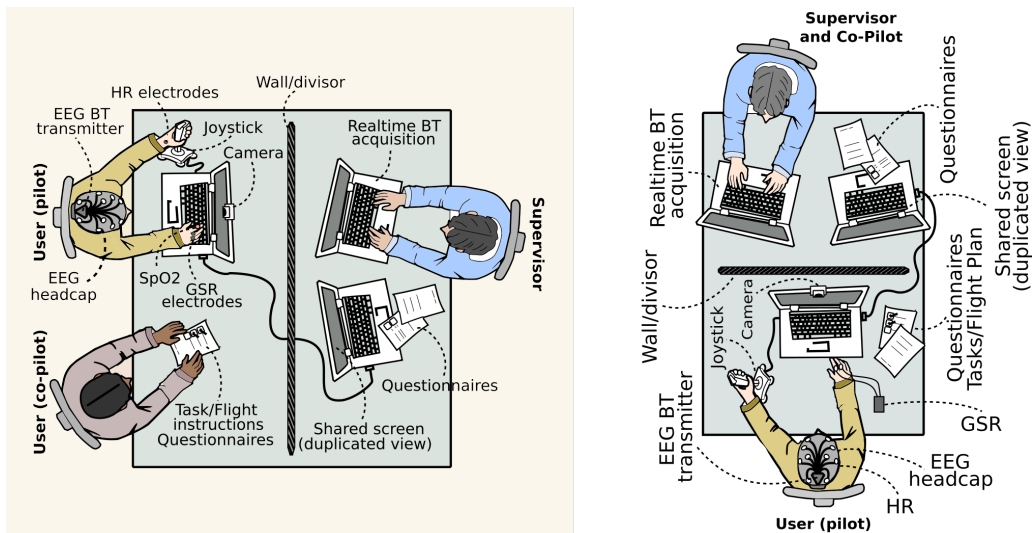


FIGURE 3.3. Setups of the PoCs. First PoC approach using pilot and co-pilots (right); second PoC using only a pilot and supervisor as co-pilot (left).

Several improvements of the first PoC, were applied in the second PoC (left setup) and in the main experiment, such as: HR sensor was changed from wrists (with high motion artifacts) to earlobe, using a single earclip based on Photoplethysmogram (PPG)

¹; Pulse Oximetry (SpO₂)² wasn't used on the second PoC nor in the main experiment either because it presented constant values along the experiments, close to 99%; only one volunteer was considered during this PoC, reducing the complexity of the execution; the supervisor kept the previous functions and also absorbed the co-pilot tasks from the prior PoC; processing and basic emotion recognition were executed based on HR and GSR only. The hand with GSR electrodes was kept moveless along the experiment. Along the execution of both PoCs, presented a lot of motion artifacts mainly, due to mainly the not well defined execution checklist with precise tasks to do by the supervisor. A execution checklist was only used on the main experiment. The aircrafts Extra 300S and Cessna 172SP were used respectively to, training flight and main flight.

The PoCs execution and its outputs shown that is possible to apply the proposed multimodal sensing system architecture to support the emotion recognition along simulated flight experiments. The first data processing and statistical analysis revealed different emotional states along each flight. Figure 3.4, shows two different executions of the second PoC.

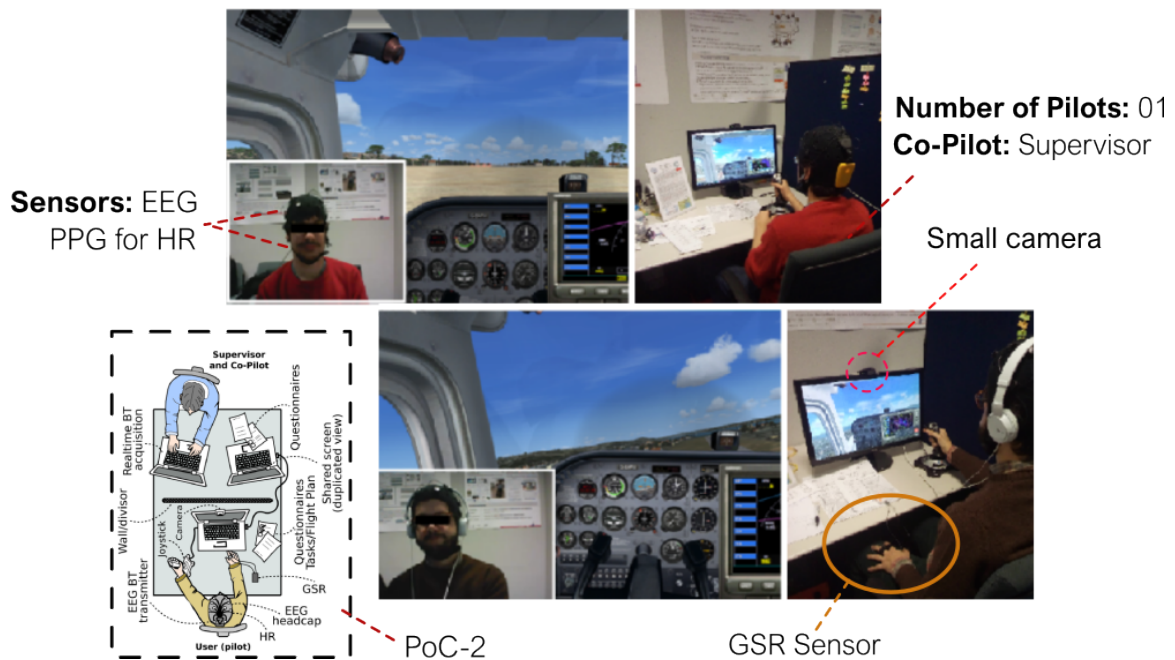


FIGURE 3.4. Flight simulation experiment during the second PoC using previous setup, a small environment and basic volunteer screen.

3.3. Training Flight - Cognition versus Emotion

The training flight prepares the volunteers to the main flight experiment. It was simpler than the main experiment, including some basic flight procedures to help the volunteer to be more familiar with the simulation behaviours and controls. The training was based on: the flight maneuvers, GPS use, airplane controls in the air, takeoff, climb, navigation

¹Photoplethysmogram (PPG) is an optically obtained plethysmogram used to detect several skin phenomena.

²Pulse Oximetry (SpO₂) is a technique to measures the arterial blood oxygen saturation and pulse rate.

(cruise route), descent, approach, final approach and landing. Other maneuvers such as, pitch, roll and flight in route (stabilized flight). Speed and altitudes controls were up to the volunteer (i.e. free flight).

The Microsoft Flight Simulator - Steam Edition (FSX-SE)³ was used during all flight experiments. The default airplane was the Extra 300S—Patty Wagstaff was used in the training, as shown in Figure 3.5.



FIGURE 3.5. Airplane Extra 300S used during the training.

The training was used to observe and attenuate the cognition effects on the volunteers in flight.

Several studies show the close relationship between cognition and emotion (Perlovsky, 2020; Ekman, 1999). According to Forgas, in general, the affect is another aspect that can influence the kind of information, processing strategies that people adopt; in the same way the affect can also reduces or even eliminates such common judgmental mistakes (as the fundamental attribution error) by triggering more harmonious and externally oriented thinking (Forgas, 2008). On the same context, Berle and Moulds, said that prevailing cognitive-behavioural models of mental disorders give passing regarding to the possibility that the relationship between cognition and emotions may be bidirectional or that emotional states may influence cognitive content and processes (Berle and Moulds, 2013).

Breakwell, said that in hazard situations, the cognition process can be affected by emotional situations switching drastically a normal to tragic situation (Breakwell, 2014). For this reason, the training flight proposed in this work was used as an important resource to make the volunteer more self confidence with the flight procedures and commands, reducing the cognition effects on emotional events and vice versa (strategy based on cognitive reappraisal) (Dixon et al., 2020). In another words, the training flight was an useful tool for emotion regulation strategy in order to change naturally their emotion levels while they try to flight regularly (McRae, 2016).

3.3.1. Cognitive Reappraisal and Acceptance

Cognitive reappraisal and acceptance are two emotion regulation strategies. Both are associated with beneficial psychological health outcomes over time (Troy et al., 2018)

³FSX-SE download link: <https://store.steampowered.com/app/FSX-SE>.

by the deliberate control of attention to minimize excessive emotional reactivity (Dixon et al., 2020).

Cognitive reappraisal, is a primary form of cognitive change, using cognitive skills (e.g. challenging interpretations, perspective-taking, reframing the meaning of situations) and linguistic processes to reframe or reinterpret the meaning of a stimulus or situation in order to up- or down-regulate the emotions (Goldin, Jazaieri, and Gross, 2014). It Reappraisal can modify emotional reactions to stressful, anxiety-provoking situations and can lead to psychological flexibility and emotional well-being (Gross and Thompson, 2007). Troy et al., also shown several studies that are consistent in highlighting the positive effects of reappraisal on long-term outcomes that relate to psychological health and well-being (Troy et al., 2018).

Acceptance, is a component of mindfulness practice, which it has demonstrated efficacy in reducing social anxiety severity. Unlike reappraisal, which it focuses on changing the content of one's thoughts and feelings, acceptance involves changing how one relates to his or her thoughts and feelings (Troy et al., 2018). Acceptance also involves an active willingness to fully experience thoughts, emotions and sensations in an open and nonjudgmental manner as they change from moment to moment, without attempting to change or avoid them (Dixon et al., 2020).

3.4. Main Flight Experiment

This work was based on a set of flight simulations to understand and analyze the biosignals and the resulted emotional responses of the volunteers during the simulated flights. These volunteers acted like pilots in flight which they were trained to execute some simulated flights. They are not real aircraft pilots. The motivations and contributions regarding to context of these experiments, are explained in details in Section 1.1–Main Motivation and Practical Contribution.

To execute these flights, the Microsoft Flight Simulator–Steam Edition (FSX-SE) (Steam and Microsoft, 2006) was used, adding some auxiliary add-ons based on turbulence and terrain, to produce more realism during the flight Steam and Microsoft, 2006. The environment setup from the main experiment, was the result of two initial proof of concepts (POCs) (Section 3.2). Several improvements from those PoCs were applied and are shown in the final setup (Figure 3.6).

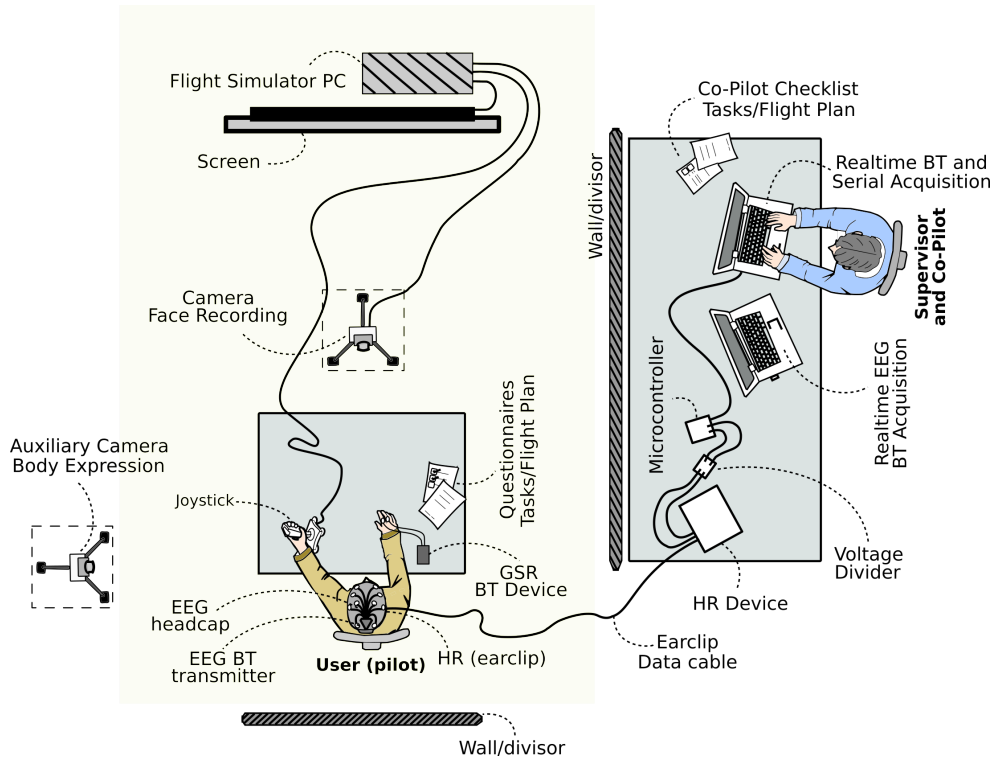


FIGURE 3.6. Setup used on the main experiment.

Several improvements were applied in the final setup: a large screen to improve the immersive experience during the simulation, maintaining an average distance of 1.70 to 1.90 meters of the volunteer; a computer to run the flight simulator and to record facial emotions; the volunteer must use only the joystick during the experimental flight and only one hand to control the aircraft; the GSR electrodes were placed on the free hand i.e., without movements to avoid motion artifacts; a microcontroller was used to acquire the HR data from the HR device (e.g. Arduino board); the supervisor used two different softwares, one to receive HR and GSR data from Bluetooth communication, and another to receive the Bluetooth data from EEG device; also a video camera was used to record the volunteers' body gestures.

During the experiment, the volunteers (acting like pilots in command) had no contact with the supervisor. The supervisor only communicated with the volunteers before and after each simulation. Was also recommended to the volunteers, to avoid to talk and to move the hand having the GSR electrodes, because it can produce additional noises and motion artifacts.

Figure 3.7, shows the real environment used in the main simulation. The position of desk table, small camera and the screen, were kept the same during all experiments. Different from the solution presented on PoCs, which the supervisor had a replicated screen to see the volunteers actions, in the main experiment, the supervisor watched in real time the simulated flights, as shown in Figure 3.7-right.

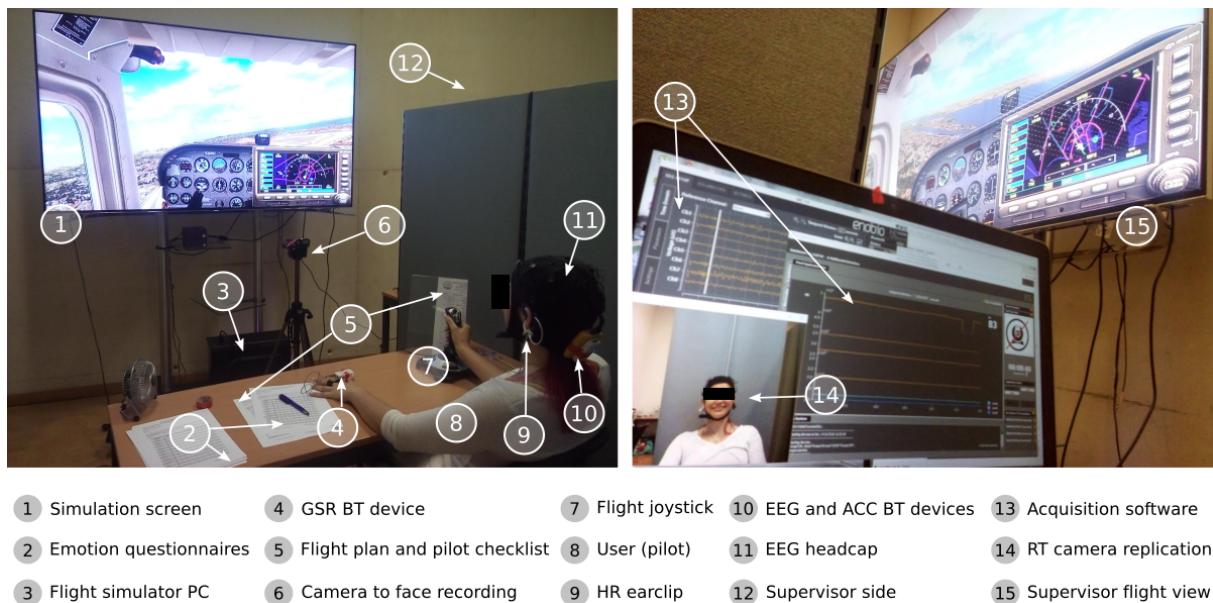


FIGURE 3.7. Experiment environment. Volunteer side (left); supervisor side (right).

Additional volunteer (acting like a co-pilot), wasn't considered in the main experiment due to some reasons: difficulties to find more people (pilot and co-pilot) for each experiment; time to train both volunteers for different tasks along the experiment; each volunteer should have double time of experiment because generally, the volunteer (co-pilot) also wished to simulate as a pilot. Other improvement is the use of a single HR electrode which presented less motion artefact along the experiment; the double back pat on volunteer's back (executed by the supervisor during all PoCs to give instructions and to get instantaneous volunteer feedback about the his feelings) was removed because the volunteers in experiment, reported that it took too much loss of attention to answer this requested questions during the flights; the headset was removed from the volunteer (pilot) because during the experiment the supervisor executes some instructions by call-outs. Other additional input data such as the volunteer's voice, wasn't considered on main experiment.

Considering the practical context and the complexity of the proposed experiment, i.e. aviation based on flight simulations and multimodal sensing, two different experiments were executed: a flight training (presented before) and executed before the main flight; and the main flight experiment presented in this section. Moreover, to avoid mistakes of experiment execution, an execution checklist was developed to aim the supervisor to correctly accomplish the several steps regarding to the proposed multimodal sensing system.

Table 3.1, presents the main resources applied for each case i.e., first and second PoC and main experiment. It shows the improvements of each PoC until the main experiment.

TABLE 3.1. Resources applied on each PoC and in the main experiment.

Resource (Biosignal)	PoC 1				PoC 2				Main Experiment			
	HR	GSR	EEG	Face	HR	GSR	EEG	Face	HR	GSR	EEG	Face
Acquisition	×	×	×	×	×	×	×	×	×	×	×	×
Preprocessing	×	×	×	×	×	×	×	×	×	×	×	×
Processing	×	×	—	×	×	×	—	×	×	×	×	×
Recognition	—	—	—	—	×	×	—	×	×	×	×	×
Resource	PoC 1				PoC 2				Main Experiment			
Camera (Face)			×				×				×	
Head Shaking			×				×				×	
Questionnaire			×				×				×	
Flight Plan/Route			×				×				×	
Flight Checklist			×				×				×	
Training Flight			×				×				×	
Eyes-Closed Baseline			×				×				×	
Headset			×				×				—	
Double "Back Pat"			×				×				—	
Aircraft Extra 300S			×				×				—	
Aircraft Cessna 172SP			—				×				×	
GSR Hand (Fixed)			—				—				×	
Execution Checklist			—				—				×	
Supervisor Call-outs			—				—				×	
Large Screen			—				—				×	
Immersive View			—				—				×	
Camera (Body)			—				—				×	
HR Earclip			—				×				×	
HR 3xElectrodes			×				—				—	
Co-Pilot (New Volunteer)			×				—				—	
SpO2 (fingerclip)			×				—				—	
Voice Recorder			×				×				—	

3.4.1. Computers Configuration

Three different computers were used in this work for different purposes. The acquisition and the EmoSense software development were executed by the computer having the configuration: Hewlett Packard (HP), processor with 2.2 GHz Intel Core i7 (7th Gen), memory with 16 GB having 1600 MHz DDR3 and Intel HD Graphics board 6000 having 1,536 MB.

The raw data preprocessing, processing, feature extraction and emotion recognition were executed in a computer having the characteristics: MacBook Air, processor with 2.2 GHz Intel Core i7, memory with 8 GB having 1600 MHz DDR3 and Intel HD Graphics board 6000 having 1,536 MB. The flight simulator and the face recordings were executed in a computer having: ASUS, processor with 3.2 GHz Intel Core i7 (8th Gen), memory 16 GB having Intel HD Graphics board 6000 having 1,536 MB.

3.4.2. Execution Checklist - Listing the Steps of the Experiment

Execution checklists were designed to the supervisor and it were fundamental to give support to the to all steps necessary to execute correctly the experiment. It presents

a couple of sequential and direct actions since the environment setup until the end of experiment.

Were developed there different execution checklists, inspired on the real aviation procedure checklists (Figure 3.8): Before Execution Checklist (BEC), Just Before Execution Checklist (JBEC) and Execution Checklist (EC).

BEFORE EXECUTION CHECK (BEC)		
1	Initial Adjustments	Connect Webcam
2		Pre-Start Software to Record Face and Flight (Ex. OBS Software)
3		Pre-Start Flight Simulator (FS)
4		Adjust FS Time and Season
5		Adjust FS Airports/Route
6		Adjust FS Joystick
7		Adjust TV Configuration
8		Adjust Light Environment
9		Adjust Webcam position
10		Adjust PC Experiment (pre-start ENOBIO and EmoSense)
11		Participant Read Term of Experiment
12		Start Instructions of the Experiment (Leaded by the Supervisor)
13		Participant Clean Hands (GSR Electrodes) and Part of Ear (HR Electrodes)
14		Participant Sit on the Chair (Confortable Way)
1	Electrodes Placement	Set EEG Electrodes
2		Set HR Electrodes
3		Set GSR Electrodes
1	HR	Start MEDLab Device for HR Acquisition
2		Check Arduino Connection for HR Acquisition
JUST BEFORE EXECUTION CHECK (JBEC)		
1	Device Connections and Questionnaire	Connect to ENOBIO bluetooth module using ENOBIO Software
2		Connect to Shimmer Modules and Serial Port using EmoSense Software
3		Set ENOBIO Software to BETA Band Acquisition
4		Change the FileName of the File's Experiment on ENOBIO Software
5		Execute the Test Acquisition from EmoSense Software
6		Fill Initial Emotion Questionnaire
7		START Flight Simulator and Face Recording
EXECUTION CHECK (EC)		
1	Neutral Baseline	Marker 1: Shake Participant Head Twice to Front and Back
2		Participant Close Eyes During 30 seconds or 1 minute (Supervisor inform to stop)
3		Participant Open Eyes During 30 seconds or 1 minute (Supervisor inform to stop)
4		Marker 2: Shake Participant Head Twice to Front and Back
1	FLIGHT	Start Flight
2		Finish Flight (With Accident or Not)
3		Marker 3: Shake Participant Head Twice to Front and Back

FIGURE 3.8. Experiment checklists executed by the supervisor.

3.4.3. Execution of the Simulated Flight

This work analyzed emotions of 8 volunteers (N=8) of flight simulator, during the execution of 7 different tasks while they fly based on basic concepts of Visual Flight Rules (VFR) through the air traffic rules and procedures applicable to air traffic in Lisbon FIR and Santa Maria Oceanic FIR, conform with Annex 2 and 11 to the Convention on International Civil Aviation (ICAO, 2005).

All experiments and training were executed under Visual Meteorological Condition (VMC) and minimum navigation altitude of 1,800ft (feet MSL). For each volunteer, a maximum of 3 flights were executed. The used airplane for this main experiment was the default aircraft model Cessna 172SP Skyhawk, as shown in Figure 3.9.



FIGURE 3.9. Airplane Cessna 172SP used during the main experiment.

3.4.4. Flight Plan - Route of the Simulation

The flight route used in this experiment have almost 8.4nm (Nautical Miles) of distance from Lisbon International Airport (ICAO LPPT/374ft/THD ELEV 378ft MSL) to Alverca (ICAO LPAR/11ft/THD ELEV 15ft MSL), intercepting the waypoints WP1 (HDG 063°), WP2 (HDG 036°) and WP3 (HDG 039°). Takeoff was planned to departure from runway 03 (HDG 026°) and landing on runway 04 (HDG 039°), as shown in Figure 3.10.

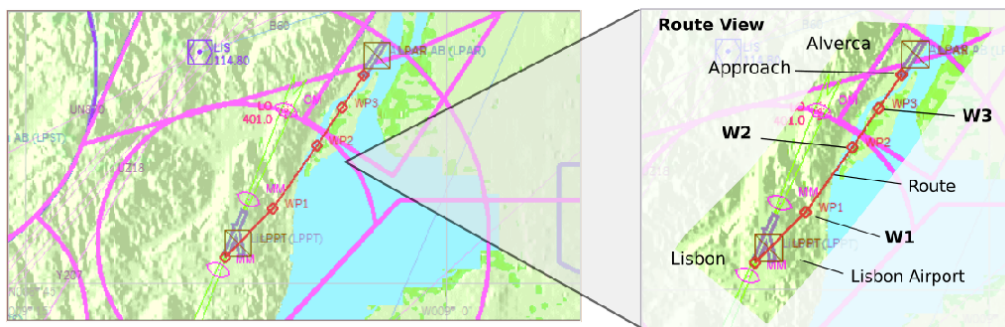


FIGURE 3.10. Flight route (red line) of the experiment (Lisbon to Alverca).

The supervisor explained each task of the simulated flight to the volunteers; also shown the ideal air speed (for takeoff, climb, approaches and landing), flight direction (flight head) and altitudes. Other complex tasks such as, the air charts, fuel mixtures,

VOR/ILS navigation, flaps set up, real checklists, Automatic Terminal Information Service (ATIS) reports, technical communications or another technical airplane operation were not considered. If any complex action was required in flight, the supervisor executed.

3.4.5. Tasks of the Experiment

Since this work tries to aim some problems of the real aviation, it considered to use main real flight phases such as: takeoff (Task 1), climb (Task 2), navigation/cruise route (Task 3), descent (Task 4), initial approach (Task 5), final approach (Task 6) and landing (Task 7), as shown in Figure 3.11.

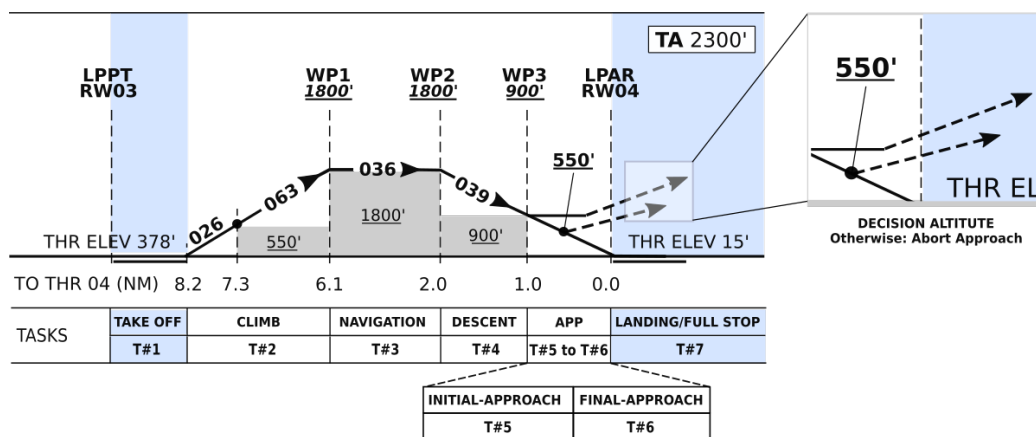


FIGURE 3.11. Lateral view of the proposed flight task chart, route and tasks.

It were also recommended by the supervisor to keep a maximum flight altitude in route of 2,300 feet and an average final approach altitude of 550 feet to avoid accidents during the landing task. If it is not possible to maintain 550 feet at final approach, the volunteer was advised to abort the landing task, climb the aircraft, turn to the left side of Alverca Airport (i.e. runway 04) and initiate the final approach again.

Each volunteer had a maximum time of 10 minutes to execute these tasks, otherwise the supervisor stops the simulation and stores the simulation data as valid to analysis. Some volunteers did not completed all the tasks due some accidents along the simulated flight.

3.4.6. Volunteers and Flight Checklists

The experiment considers two different volunteers: the first pilot or pilot in command (PIC), and the co-pilot or second in command (SIC). Each one using a set of well defined tasks along the simulated flight. In the main experiment, the co-pilot actions (executed by a second volunteer in the first PoC) were replaced to be executed by the supervisor.

The pilot and co-pilot tasks are guided by two different checklists. These checklists informed to both what to do during each step of the flight, as presented in Table 3.2. The different colors on it, inform to the aircrew the importance of each procedure in flight: green color, means not critical procedure; purple means, not critical but mandatory;

and red color means, that this procedure is critical, mandatory and must be executed immediately to avoid accident.

TABLE 3.2. Pilot and co-pilot checklists used during the main flight simulations.

Tasks	Pilot Checklist		Co-Pilot Checklist	
	Procedure	Value	Procedure	Value
T1	Throttle	Full	–	–
	Wait For	80KIAS	Alert	80KIAS "Call-out"
T2	Climb	550ft	Alert	Climb
	Roll	Right for 10s	Alert	Roll Time
	Climb	1,800ft	Alert	Climb
	Intercept	WP1	Alert	Intercept
T3	Throttle	70%	Alert	Throttle
	Check	Route	Check	Route
	Intercept	WP2	Alert	Intercept
	Throttle	10%	Alert	Throttle
	Wait	5s	Alert	Wait
T4	Descent	900ft	Alert	Descent
	Intercept	WP3	Alert	Intercept
T5	Descent	550ft	Alert	Descent
	Throttle	40-65KIAS	Flaps	Set Full
	Pitch	15°	–	–
	Descent	250ft	Alert	Descent
T6	Descent	15ft	Alert	Descent
T7	Touch	–	–	–
	Throttle	0KIAS	Flaps	Set 0°
	Full Stop	–	–	–

The tasks of the co-pilot were executed by the experiment supervisor. The checklists as such as the route, are based on a real flight procedure. However, the flight scenario, physics of the environment and flight model, not presented a full realism due the beginner level of the involved volunteers.

3.4.7. Head Shaking Indicator - Beginning and End of Experiment

The head shaking indicator was the strategy used to synchronize the real-time EEG sensing acquisition with the other data having different sampling rate. The head shaking methodology was inspired by standard procedures of real military pilots, in which they quickly shake their heads to indicate the beginning or the synchronization of some flight procedures, for instance, synchronized takeoff and maneuvers (Figure 3.12).

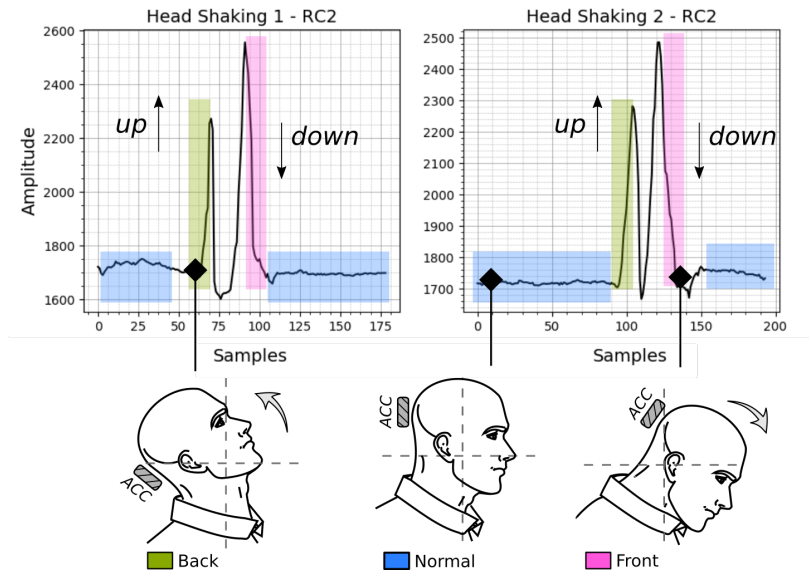


FIGURE 3.12. EEG's accelerometer output of the double head shaking movement.

The EEG and GSR devices used in this work have also embedded accelerometers, which they were used to capture the head shaking (placed on the head back) of the volunteers during the flight. The head shaking represents a signal like a wave mark used in the further data split process. It was used in four different moments of the experiment: double head shaking to indicate the beginning of the eyes-closed baseline; double head shaking to indicate the end of this baseline; double head shaking to indicate the beginning of the flight (i.e., takeoff); and double head shaking to indicate the end of the flight experiment.

3.4.8. Physiological Sensing

The proposed multimodal sensing system, considered three physiological sensing: cardiac system based on Heart Rate (HR), Galvanic Skin Response (GSR) and Electroencephalography (EEG). To acquire these sensing, 11 Ag/AgCl dry electrodes and one earclip were used: 8 electrodes placed on the scalp (EEG), 1 placed on the earlobe (EEG reference), 1 placed on earlobe (HR) and two on the hand of the volunteer (GSR).

The GSR signal is based on Electrodermal Activity (EDA) and refers to the electrical resistance between two sensors, when a very weak current occurs passed between them. It is typically acquired from the hands or fingers (Goshvarpour, Abbasi, and Goshvarpour, 2017). In this work, it was acquired by the Shimmer3-GSR+ unit, which can measure activity, emotional engagement and psychological arousal in lab scenarios and in remote capture scenarios that are set outside of the lab. Was recommended that these electrodes kept immobile during the experiment to avoid an additional motion artifacts in GSR data.

Emotional and cognitive responses, can also affect the brain functioning, producing several stimuli. The usage of flight simulation shows to be a powerful tool to produce these brain stimulations in different flight moments.

The brain activities were acquired by the device Neuroelectrics Enobio-N8, which it had 8 channels, Bluetooth communication and a sampling rate of 500 samples per second. Some studies claim that it is difficult to find the specific region of scalp where the brain activity is sufficiently high to detect emotional states (Murugappan, Nagarajan, and Yaacob, 2011; Min, Chung, and Min, 2005); however, if one intendeds to detect emotional responses, it is recommended to use the prefrontal cortex or frontal lobe (located near the front of the head) because it be more involved with cognition and decision making of emotional responses (Umeda and Satoshi, 2013; Rosso et al., 2004).

The 10–20 system or International 10–20 system was the method used to describe and apply the location of scalp electrodes. This way, to better detect emotion, alertness situations and cognition artifacts of the scalp, the electrodes were placed on that recommended areas (Kucikienė and Praninskienė, 2018; Umeda and Satoshi, 2013; Rosso et al., 2004), some of which were also used by Harrivel and Pope (Wang et al., 2020; Harrivel and Pope, 2017) in other simulated flight experiments: Fp1 (channel 1), F3 (channel 2), C3 (channel 3), T7 (channel 4), Fp2 (channel 5), F4 (channel 6), C4 (channel 7) and T8 (channel 8). The EEG reference electrode (EEGR) was placed on the volunteers’ earlobes (Othman et al., 2013; Murugappan, Nagarajan, and Yaacob, 2011). Furthermore, according to Min et al. (2005), most of the meaningful information about emotional changes are found in the frequency below 30Hz (Min, Chung, and Min, 2005). It frequency aimed our choice to use the beta rhythms (or band) in this experiment (Othman et al., 2013; Murugappan, Nagarajan, and Yaacob, 2011).

Figure 3.13, shows the positions of each electrode, used during the experiment. Note the usage of electrodes on frontal cortex to acquire EEG data, due its close relation to the emotional events.

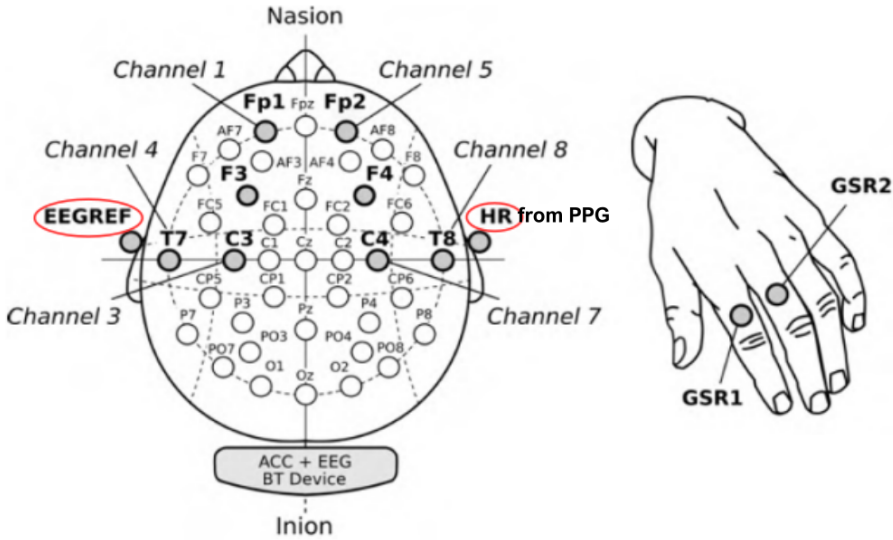


FIGURE 3.13. Electrodes placement. EEG and HR, placed on the scalp and ear (left); and GSR, placed on the indicator and middle fingers (right).

3.4.8.1. *The Beta Rhythms* The beta rhythms (beta band) are expressed by distinct peaks on the spectrograms and may be found in various locations of the cortex in normal conditions. According to Kropotov (Kropotov, 2009), the beta band is more often found in the frontal or central areas when compared to posterior regions of the brain cortex, showing a frequency around 13 Hz. It is conventionally divided into the following sub-bands: low beta (from 13 to 20 Hz), high beta (from 21 to 30 Hz) and gamma activity (from 31 Hz and higher). He also says that there is a special beta frequency activity at 40 Hz. For this reason, the present work considered the beta band analysis from 12 to 30 Hz and 40 Hz. Unfortunately, from analyzing only 40 Hz, it is hard to conclude relevant results; thus, it was decided to also consider a small part of gamma band, i.e., 31 to 40 Hz (Kropotov, 2009), to produce continuous plots from 12 to 40 Hz.

The most prominent hypotheses suggest that the beta band indicates ongoing sensorimotor integration (Khanna and Carmena, 2017), being more related to awareness and concentration contexts. In the beta state, our brain easily does the analysis and preparation of the information and generates solutions and new ideas. Furthermore, it is very beneficial for work productivity, studying for exams or other activities that require high concentration and alertness, as is reported in (Khanna and Carmena, 2017; Woaswi et al., 2016).

At least two distinct beta rhythms can be found: the beta rhythms located over the sensorimotor strip (primary motor cortex)—the Rolandic beta rhythms, and the beta rhythms located more frontally—frontal beta rhythms (Kropotov, 2009; Ritter, Moosmann, and Villringer, 2009).

In this work, the Rolandic or pericentral beta rhythms were also considered. The selected beta rhythm is modulated during various motor and cognitive tasks (Harrivel and Pope, 2017; Wang et al., 2020), being observed as a spontaneous activity during eyes-open and eyes-closed conditions in healthy subjects over the areas C3, Cz and C4. The close relation of the prefrontal cortex and beta rhythm, with the emotion artifacts and the cognitive tasks, makes these brain outputs an important data to be used in this work as well (Umeda and Satoshi, 2013; Rosso et al., 2004).

3.4.8.2. *Acquisition Software* To store in real time, all raw data acquired by each device, two software were considered in the experiment: the Enobio-N8, and the Emosense (ES-RT). This last, was entirely developed in this work on Python 3.5. The first software was used to acquire EEG data, and second one to acquire HR and GSR data.

Figure 3.14, shows both real time software used on acquisition and storage of all data of the main experiment.

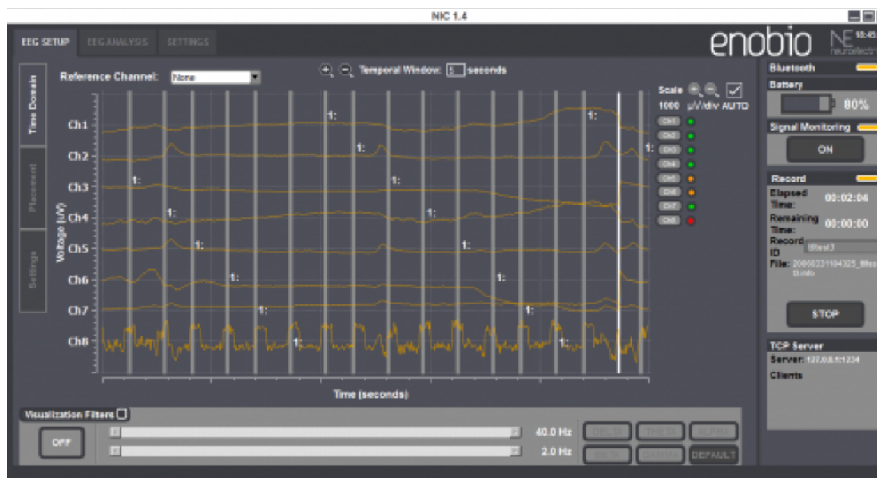


FIGURE 3.14. Emosense RT software, to acquire HR and GSR data (top) and Enobio-N8 to acquire EEG data (bottom).

Figure 3.15, shows an example of EEG 8-channels raw data, acquired and stored by the Enobio-N8 software.

There, are possible to see the raw data with several motion artifacts, eyes movements artifacts and other additional noises. Some of these noises and artifacts were removed using several techniques presented in details further.

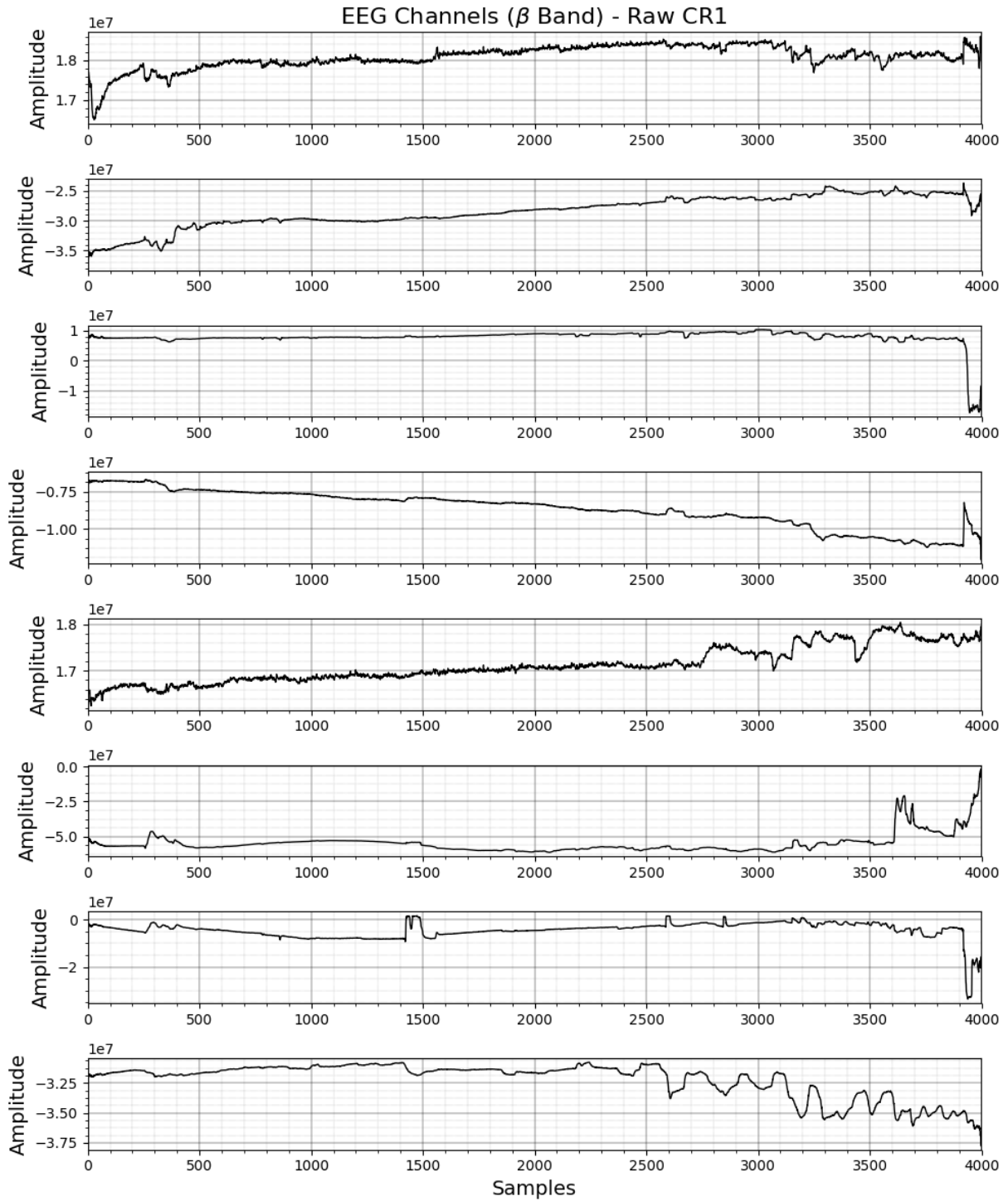


FIGURE 3.15. EEG raw (noisy) 8 channels dataset referent to CR1 experiment.

3.4.8.3. *Acquisition Devices* The multimodal biosignal acquisition was based on Heart Rate (HR), Galvanic Skin Response (GSR) and Electroencephalography (EEG). The emotion monitoring system includes a set of smart sensors such as: two shimmer3-GSR+, one Medlab-Pearl100, and one Enobio-N8, as presented in Table 3.3.

TABLE 3.3. Devices and its application in the main experiment.

Device	Electrodes	Accelerometer	Application	Where?
Shimmer3-GSR+	2 Dry	–	GSR BT data	Hand (fingers)
MedLab-Pearl100	1 PPG/Earclip	–	HR data	Earlobe
Enobio-N8 Headcap	8 Dry + 1 REF	–	EEG BT data	Head (scalp)
Shimmer3-GSR+	–	Applied	Head shaking	Head (back)
Enobio-N8 Acc	–	Applied	Head shaking	Head (back)

A total of two Shimmer3-GSR+ units were the devices used to acquire the GSR data and to act as an auxiliary head shaking indicator, using its embedded accelerometer. It includes: 1 channel GSR (Analog); the measurement range: 10k and 4.7M Ω (.2 μ S - 100 μ S); frequency range: DC-15.9Hz; input protection RF/EMI filtering, current limiting; auxiliary input: 2 channel analog/I2C; digital input: via 3.5mm; 24MHz MSP430 CPU with a precision clock subsystem; 10 DoF inertial sensing via accelerometer integrated, gyroscope, magnetometer and altimeter; low power consumption, light weight and small form factor; also perform the analog to digital conversion and readily connects via Bluetooth or local storage via micro SD card. Furthermore, it is also a highly configurable which can be used in a variety of data capture scenarios (Shimmer3, 2017).

Figure 3.16, shows the devices applied in this work to acquire all physiological data and head movements.

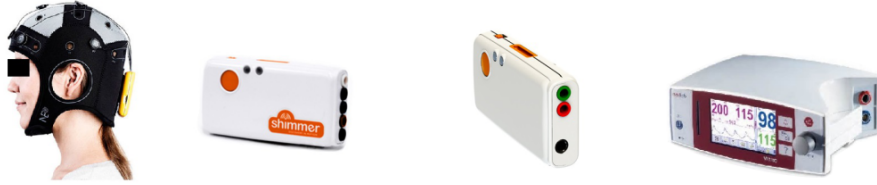


FIGURE 3.16. Acquisition devices: Enobio-N8 (left); Shimmer GSR (middle-left); Shimmer for ECG/HR (middle-right) and MedLab P100 (right).

The HR data was acquired by the Medlab-Pearl100 device. It is considered an excellent artefact suppression device due to PEARL-technology and includes: a compact, portable and attractive design; crisp, easily readable TFT colour display; reliably measures SpO₂; pulse rate, and pulse strength; integrated 100h trend memory; integrated context sensitive help system; intuitive, multi-language user interface; works on mains and from integrated battery; full alarm system with adjustable alarm limits; usable from neonates to adults (Medlab, 2017).

To acquire the EEG data, the Enobio-N8 Toolkit was used. It is a wearable toolkit with a wireless electrophysiology sensor system for the recording of EEG. Using the Neuroelectrics headcap toolkit (having several dry and wet electrodes), the Enobio-N8 is ideal for out-of-the-lab applications. It comes integrated with an intuitive, powerful user

interface for easy configuration, recording and visualization of 24 bit EEG data at 500 sampling rate, including spectrogram and 3D visualization in real time of spectral features. It is ready for research or clinical use. In addition to EEG, triaxial accelerometer data is automatically collected. You can also use a microSD card to save data offline in Holter mode; and as like as Shimmer device, it can use Bluetooth to transmit real time data too (Quesada Tabares et al., 2017).

3.4.9. Facial Emotion Sensing

During the experiment, the face of the volunteers and the flights actions along the experiments, were recorded and its outputs were processed after the experiment. Two software were used to record different data: the OBS-Studio, to record the flight and volunteer's face at the same time in a synchronized manner; and the Face Reader software, used to recognize the emotions based on the face recording (Figure 3.17).

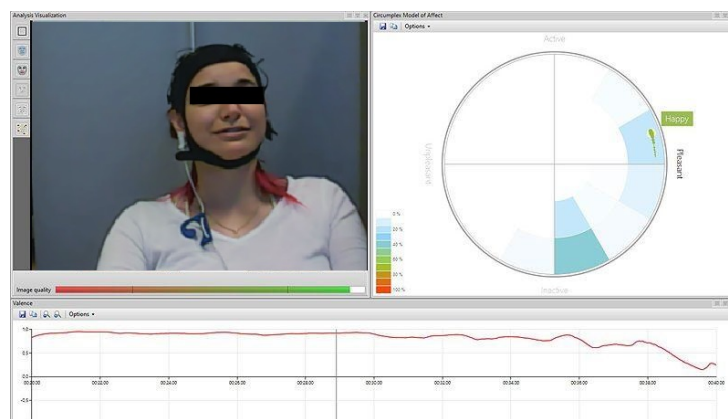


FIGURE 3.17. Face Reader software used to detect emotions from face.

Figure 3.18, shows different face expressions from 3 females and 5 males volunteers along of some proposed simulated flights. The Face Reader software, considers 7 emotions: neutral, happy, sad, angry, surprised, scared and disgust. Although, the neutral and disgust emotions were omitted from analysis due to the low importance in these experiments.

3.4.10. Emotion Questionnaires

Questionnaires are another important tools used to acquire emotional data before and after all experiments. Several studies also use questionnaires to give support to the volunteers' feedback, based on what they are feeling in such moment (Roza and Postolache, 2017; Xu et al., 2017; Reis, Arriaga, and Postolache, 2015).

To comply these requirements, a standard questionnaire was adopted, having 22 emotions descriptors and its measurements based on the standard study presented by Jones et al., which they used it for sport context, being easily adapted to the present work (Jones et al., 2005). These questionnaires responses represent a subjective data that can be used to try to match with the detected facial emotion at the end of experiment. Each



FIGURE 3.18. Face recording of some volunteers during experiment.

volunteer must to execute at most three flights, having to answer one questionnaire for each different moment, as defined below:

- Before the first flight (QB1);
- After first (A1) flight/Before second (B2) flight (QA1B2);
- After second (A2) flight/Before third (B3) flight (QA2B3);
- After third flight (QA3).

Figure 3.19, presents the emotion questionnaire filled by each volunteer during the phases of the main experiment. A set of four questionnaires were considered, having 22 different emotions description each one, which it were rated between 0 (not at all) to 4 (extremely) in different moments of the experiment (flight sequence).

The field Participant Code, represents the individual volunteer code for each experiment; Flight Phase, represents the flight moment of questionnaire: Before, if the flight sequence is 1 (before first flight); During if the flight sequence is more than 1 and less or equal to 3; After, if already executed the last flight of experiment; and Sequence, represents the flight repetition order, because each volunteer can flight more than one time.

Experiment: PhD Experiment - Flight Simulator x Emotions
Participant Code: FSP _____
Phase: Before | During | After
Sequence: 1 | 2 | 3 | 4 | 5 |
Date: ____/____/____

Table below presents a list of words which describe a range of feelings that participants may experience. Please read each one carefully and indicate on the scale next to each item how you feel *right now, at this moment*, in relation to each phase of the experiment.

Important: There are no right or wrong answers. Do not spend too much time on any one item, but choose the answer which best describes your feelings right now in relation to the experiment.

Feelings		Not at all	A little	Moderately	Quite a bit	Extremely
1	Uneasy	0	1	2	3	4
2	Upset	0	1	2	3	4
3	Exhilarated	0	1	2	3	4
4	Irritated	0	1	2	3	4
5	Pleased	0	1	2	3	4
6	Tense	0	1	2	3	4
7	Sad	0	1	2	3	4
8	Excited	0	1	2	3	4
9	Furious	0	1	2	3	4
10	Joyful	0	1	2	3	4
11	Nervous	0	1	2	3	4
12	Unhappy	0	1	2	3	4
13	Enthusiastic	0	1	2	3	4
14	Annoyed	0	1	2	3	4
15	Cheerful	0	1	2	3	4
16	Apprehensive	0	1	2	3	4
17	Disappointed	0	1	2	3	4
18	Energetic	0	1	2	3	4
19	Angry	0	1	2	3	4
20	Happy	0	1	2	3	4
21	Anxious	0	1	2	3	4
22	Dejected	0	1	2	3	4

FIGURE 3.19. Questionnaire with 22 emotions, used before and after the experiment.

3.4.10.1. *Analyzing the Questionnaires Responses* All emotions presented on proposed questionnaires, were conceptually resumed to five emotions classes as described by Jones et al. (Jones et al., 2005): anxiety, dejection, excitement, anger and happiness. These resumed emotions were obtained from the previous 22 emotions, as shown below.

- Anxiety: uneasy (E01), tense (E06), nervous (E11), apprehensive (E16), anxious (E21);

- Dejection: upset (E02), sad (E07), unhappy (E12), disappointed (E17), dejected (E22);
- Excitement: exhilarated (E03), excited (E08), enthusiastic (E13), energetic (E18);
- Anger: irritated (E04), furious (E09), annoyed (E14), angry (E19);
- Happiness: pleased (E05), joyful (E10), cheerful (E15), happy (E20).

The results of these questionnaires, are shown in Figure 3.20. It is possible to note that during the experiment, since first questionnaire (QB1) to the last questionnaire (QA3), the volunteers confirmed to feel several emotions more characterized as, anxiety, excitement and happiness, which they kept having high intensities along the experiments. The anger and dejection, were other resumed emotions that the volunteers said to feel too, but in less intensities.

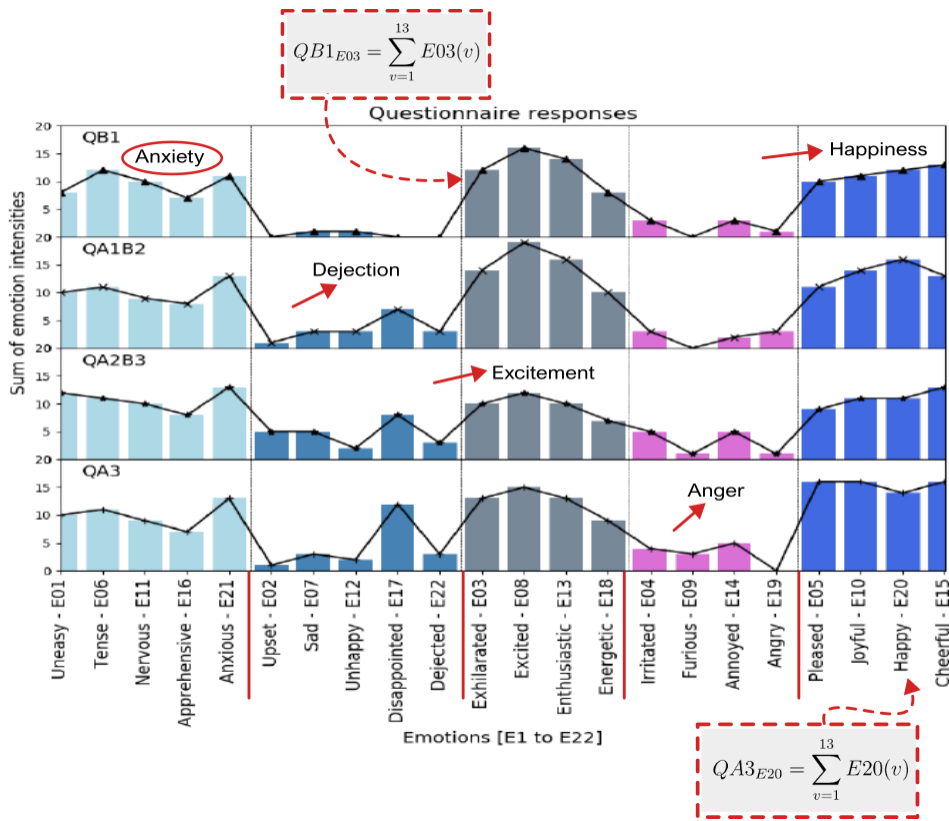


FIGURE 3.20. Emotions selected on questionnaires and the resumed emotions.

When the volunteers chose to flight more than once, it was possible to see a small anxiety attenuation along the flights, probably characterized by the learning process (tasks and flight controls) experienced by the volunteers. The intensities of dejection increased along the flights, which disappointed (E17) presented the higher values, because it reflected the amount of air crashes (accidents) along the simulated flights (see Section 3.4.12). The intensities of anger also increased along the experiment, due probably by the same reason of dejection. These both emotions were not strongly characterized in this work but between them, the resumed emotion dejection was more notable, due the situation of frustration after the occurrences of accidents.

3.4.11. Flight Analysis

The practical results of 21 flights are presented in Table 3.4. In 21 flights executed, 62% of them presented general accidents; all flight tasks were accomplished in 38% of the flights i.e., landing successfully; 19% crashed during the climb task, including 14.2% due to stall occurrences and 4.8% due to direct collision occurrences; 9% crashed at final approach task; and 33.3% crashed at landing. The landing tasks were classified as abrupt landing (A-Landing), less smooth landing (LS-Landing) and smooth landing (S-Landing). Regarding the volunteers' gender, 52.3% (11 out of 21) of the flights were executed by male volunteers and 47.7% by female volunteers. The latter reported having no experience with flight simulation and rarely had contact with electronic games. It is likely that these reasons were why the landing tasks were successfully concluded only by male volunteers.

TABLE 3.4. Dataset description according to the flight experiment tasks.

Dataset	Simulation/Flight Tasks							Result	Gender
	Task 1	T2	T3	T4	T5	T6	T7		
DS:RC1	×	×	×	×	×	×	—	Crash (collision)	Male
DS:RC2	×	×	×	×	×	×	—	Crash (collision)	Male
DS:RC3	×	×	×	×	×	×	×	A Landing	Male
DS:GC1	×	×	×	×	×	×	×	S-Landing	Male
DS:GC3	×	×	×	×	×	×	×	S-Landing	Male
DS:LS1	×	×	×	×	×	—	—	Crash (collision)	Male
DS:LS2	×	×	×	×	×	×	×	LS-Landing	Male
DS:VC1	×	×	×	×	×	×	×	S-Landing	Male
DS:VC2	×	×	×	×	×	×	×	S-Landing	Male
DS:CR1	×	×	×	×	×	×	—	Crash (collision)	Female
DS:CR3	×	—	—	—	—	—	—	Crash (stall)	Female
DS:CLX	×	—	—	—	—	—	—	Crash (collision)	Female
DS:CL3	×	×	×	×	×	×	—	Crash (collision)	Female
Dataset	** Invalid Flight Datasets **							Result	Gender
	Task 1	T2	T3	T4	T5	T6	T7		
DS:CL1	×	×	×	×	×	×	—	Crash (collision)	Female
DS:CL2	×	—	—	—	—	—	—	Crash (stall)	Female
DS:CR2	×	×	×	×	×	—	—	Crash (collision)	Female
DS:JO1	×	×	×	×	×	×	×	LS-Landing	Male
DS:GC2	×	×	×	×	×	×	×	S-Landing	Male
DS:RN1	×	×	×	×	×	×	—	Crash (collision)	Female
DS:RN2	×	—	—	—	—	—	—	Crash (stall)	Female
DS:RN3	×	×	×	×	×	×	—	Crash (collision)	Female

It is also important to consider that of the eight volunteers, one volunteer (male), reported to be an advanced user on flight simulation, i.e., 12.5% of them; four other volunteers (male) were considered to have a mid-level in flight simulation but an experienced level in electronic games, i.e., 50.0% of them. The remaining three volunteers (female) were reported to be beginner level on all these approaches. The volunteers were between 21 and 40 years old.

Figure 3.21 shows a comparison between the accidents or crashes occurrences during the simulated flights experiment ($N_{accid}=13$) and the accident report of the Boeing Aerospace Company (statistics from 1959 to 2016) (Boeing, 2017).

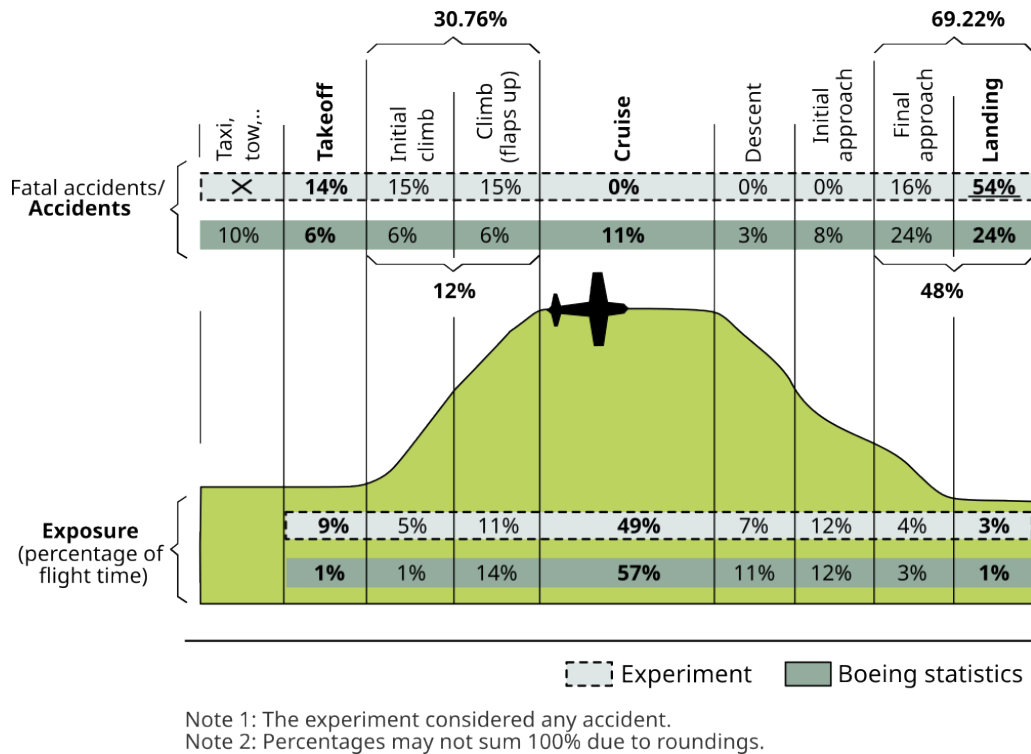


FIGURE 3.21. Distribution of fatal accidents by civil aviation (Boeing report) and general accidents (proposed experiment) (adapted from Boeing, 2017).

The percentage of accidents in the present experiment is based on a total of 13 accidents over 21 flights. The landing task presented the higher accident rate, having 7 occurrences out of 13, i.e., 53.84%. Final approach presented 2 occurrences of accidents out of 13, i.e., 15.38%. On the climb task, it were 4 out of 13, i.e., 30.76%. It is also possible to see that the present experiment shown a similar proportional occurrence if compared with real data reported by the Boeing Aerospace Company (Boeing, 2023; Boeing, 2017).

3.4.12. Dataset Description

In this work, a total of 21 multisensing datasets were acquired, which it came from 21 simulated flights obtained of 8 volunteers ($N_{vol}=8$), where each volunteer executed at most 3 flights. Between these flight datasets, 13 of them were valid to be analyzed and 8 were invalid due to several reasons such as: bad electrode connections, error in BT communication, wrong video frame rate and so on.

These datasets include, the emotion questionnaires, face recordings, HR, GSR and EEG data. The dataset names are a sequence of two letters and one number, to indicate

the volunteer’s name and the flight sequence of such volunteer, respectively (Roza and Postolache, 2018; Roza et al., 2019; Roza and Postolache, 2019).

3.4.12.1. *Dataset Resampling* The dataset synchronization was applied over all multisensing datasets. Originally, the obtained raw datasets presented different sampling rates and it was considered to equalize it before the analysis: 22,237 samples of the face dataset (5 S/s–samples per second or Hz), 44,237 samples of each HR and GSR dataset (sampling rate of 10 Hz) and $2,157,087 \times 8$ –channels (or 17,256,696 total samples) of the EEG dataset (sampling rate of 500 Hz), presenting a total of 17,367,407 multisensing samples to be processed and analyzed.

To optimize these raw datasets and then to save processing time and complexity, they were reduced to a common sampling rate of 10 Hz, presenting a final length of 44,237 samples for each data channel, i.e., 44,237 reduced samples for Face, HR and GSR and $44,237 \times 8$ –channels for EEG. It represents a total multisensing sample of $44,237 \times 11$ –channels (Face, HR, GSR and EEG), or a total of 486,607 reduced samples, that represents a total reduction of 97.19% samples to be processed. These sampling rate changes presented some loss of information being mostly corrected by the data processing.

Table 3.5, presents the raw datasets description with its individual number of samples, time and sampling rates between 5 and 500 Hz.

TABLE 3.5. Raw valid dataset description according to number of samples and time.

Dataset (Raw)	Face (5Hz) Samples	HR (10Hz) Samples	GSR (10Hz) Samples	EEG (500Hz) $\times 8$ Ch Samples	Time (s)	T (min)
DS:RC1	1,877	3,671	3,671	190,000	373.80	6.23
DS:RC2	1,880	4,247	4,247	188,510	375.00	6.25
DS:RC3	1,784	3,981	3,981	178,498	355.80	5.93
DS:GC1	1,881	4,081	4,081	188,600	375.60	6.26
DS:GC3	1,842	4,255	4,255	184,600	366.60	6.11
DS:LS1	2,271	5,558	5,558	220,000	453.00	7.55
DS:LS2	2,043	4,096	4,096	198,500	405.60	6.76
DS:VC1	1,790	2,611	2,611	179,500	357.00	5.95
DS:VC2	1,831	2,042	2,042	183,400	366.00	6.10
DS:CR1	1,946	3,998	3,998	95,500	387.60	6.46
DS:CR3	165	457	457	16,879	31.80	0.53
DS:CLX	237	518	518	18,000	45.60	0.76
DS:CL3	2,690	4,722	4,722	215,100	537.60	8.96
Total:	22,237	44,237	44,237	2,157,087	4,431	73.85

Table 3.6, presents in details each reduced dataset already smoothed and resampled to have 10S/s. The emotions surprised and scared presented the higher values of occurrences along the flight datasets (or simulated flights) varying between 26.12% and 72.0%, and between 19.98% and 38.34% respectively.

These emotion classes are the outputs of the Face Reader software, which it sometimes matched wrongly some emotions, mismatching the surprised emotion as angry, for

TABLE 3.6. Reduced datasets according to amount of samples, emotions and time.

Dataset	Higher Emotions/Classes Percentages			Samples	T(s)
DS:RC1	Happy 816 (22.22%) Surprised 999 (27.21%)	Sad 341 (9.28%) Scared 1,058 (28.82%)	Angry 457 (12.44%)	3,671	373.80
DS:RC2	Happy 1,023 (24.08%) Surprised 1,179 (27.76%)	Sad 477 (11.23%) Scared 1,111 (26.15%)	Angry 457 (10.76%)	4,247	375.00
DS:RC3	Happy 907 (22.78%) Surprised 1,040 (26.12%)	Sad 466 (11.70%) Scared 1,111 (27.90%)	Angry 457 (11.47%)	3,981	355.80
DS:GC1	Happy 907 (22.22%) Surprised 1140 (27.93%)	Sad 466 (11.41%) Scared 1,111 (27.22%)	Angry 457 (11.19%)	4,081	375.60
DS:GC3	Happy 1,031 (24.23%) Surprised 1,179 (27.70%)	Sad 477 (11.21%) Scared 1,111 (26.11%)	Angry 457 (10.74%)	4,255	366.60
DS:LS1	Happy 1,364 (24.54%) Surprised 1,479 (26.61%)	Sad 1,113 (20.02%) Scared 1,111 (19.98%)	Angry 491 (8.83%)	5,558	453.00
DS:LS2	Happy 907 (22.14%) Surprised 1,155 (28.19%)	Sad 466 (11.37%) Scared 1,111 (27.12%)	Angry 457 (11.15%)	4,096	405.60
DS:VC1	Happy 751 (28.76%) Surprised 796 (30.48%)	Sad 108 (4.13%) Scared 956 (36.61%)	Angry 0 (0.00%)	2,611	357.00
DS:VC2	Happy 355 (17.38%) Surprised 796 (38.34%)	Sad 108 (5.28%) Scared 783 (38.34%)	Angry 0 (0.00%)	2,042	366.00
DS:CR1	Happy 907 (22.68%) Surprised 1,057 (26.43%)	Sad 466 (11.65%) Scared 1,111 (27.78%)	Angry 457 (11.43%)	3,998	387.60
DS:CR3	Happy 0 (0.00%) Surprised 312 (68.27%)	Sad 0 (0.00%) Scared 145 (31.72%)	Angry 0 (0.00%)	457	31.80
DS:CLX	Happy 0 (0.00%) Surprised 373 (72.00%)	Sad 0 (0.00%) Scared 145 (27.99%)	Angry 0 (0.00%)	518	45.60
DS:CL3	Happy 1364 (28.88%) Surprised 1,239 (26.23%)	Sad 517 (10.94%) Scared 1,111 (23.52%)	Angry 491 (10.39%)	4,722	537.60
Dataset	** Invalid Flight Datasets **				
DS:CL1	Head shaking marker executed incorrectly.				
DS:CL2	No video emotion recognition executed.				
DS:CR2	No GSR data acquired. GSR electrodes/BT not connected correctly.				
DS:JO1	No EEG data acquired. EEG BT module not connected correctly.				
DS:GC2	No GSR data acquired. GSR electrodes/BT not connected correctly.				
DS:RN1	Wrong/too low video FPS to face recording analysis.				
DS:RN2	Wrong/too low video FPS to face recording analysis.				
DS:RN3	Wrong/too low video FPS to face recording analysis.				

instance. Despite these mismatches, the recognition process gone further and kept its training also in these probably wrong detected emotion classes.

Figures 3.22 and 3.23, show 12 datasets (out of 13), correlating it based on HR and GSR inputs data executed before the preprocessing. These raw correlations aren't based on extracted features, because at this point, no features and processing were executed yet. This certainly justify the high cluster overlapping. The emotion classes of each flight dataset are also presented in a bar plot, as shown in Figure 3.24.

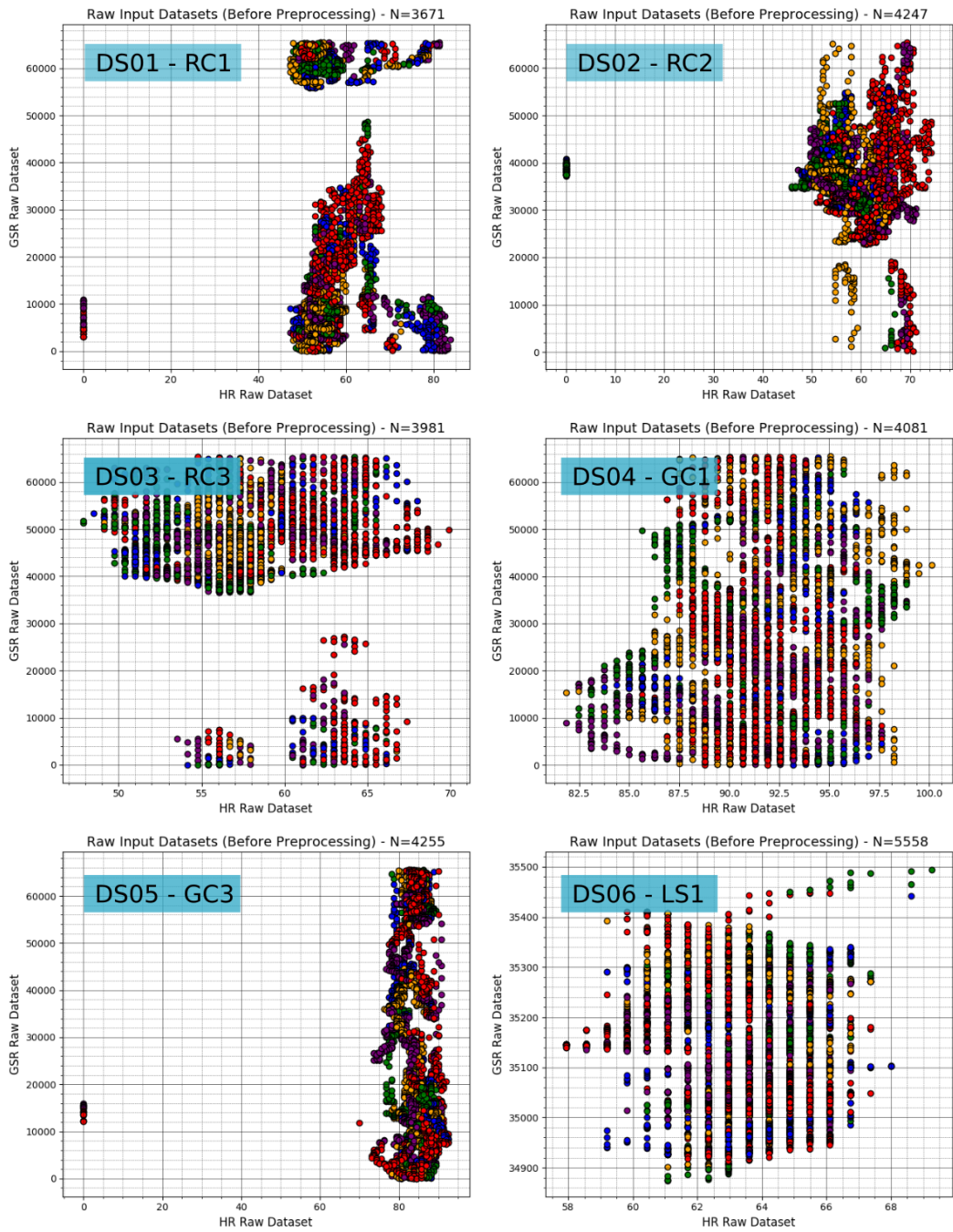


FIGURE 3.22. Raw datasets correlation, based on HR and GSR input data.

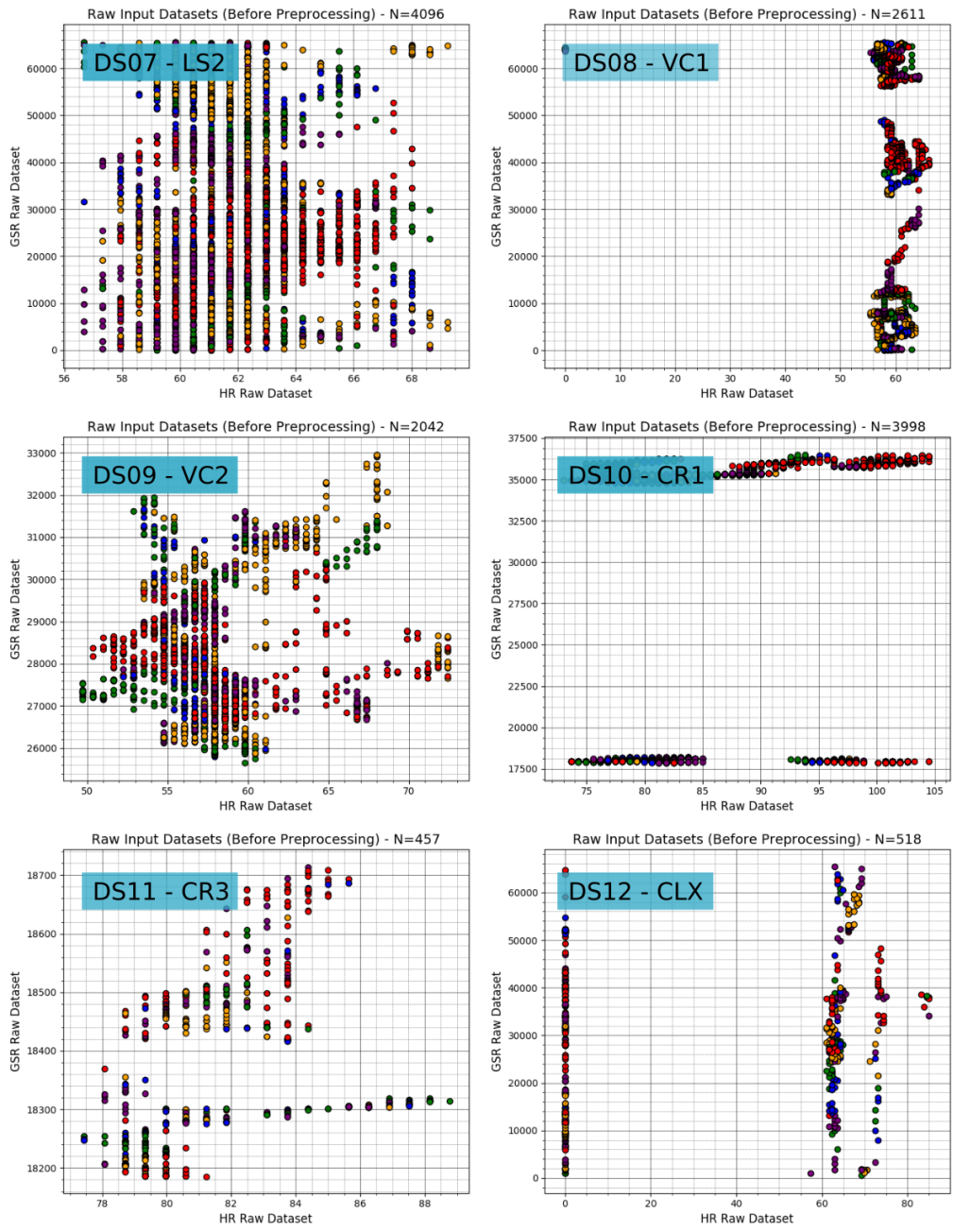


FIGURE 3.23. Raw datasets correlation, based on HR and GSR input data.

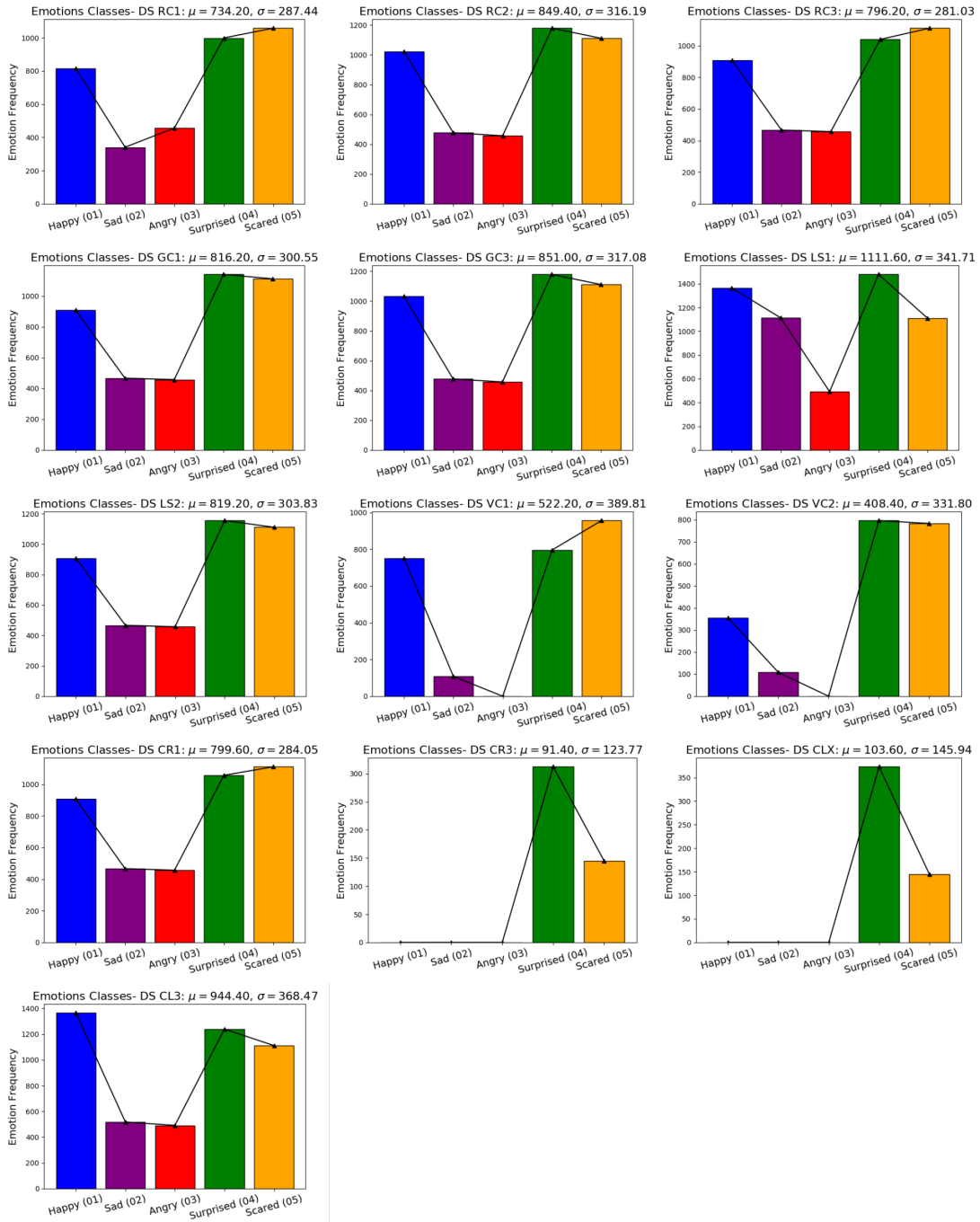


FIGURE 3.24. Classes of emotions detected by Face Reader software for each flight dataset.

Data Preprocessing

Preprocessing is the first treatment over the acquired datasets; such procedure is extremely important to prepare the data to the next steps of analysis e.g., processing, feature extraction and emotion recognition.

In resume, the preprocessing stage prepares the datasets in a way that makes the applied analysis more efficient. It also reformats the raw data into a format that can be manipulated by any programming language (Hafen et al., 2014). It can include: normalization, smoothing, outliers removal, detrends, abrupt signal correction, baseline corrections and others particular preprocessing. Preprocessing is also used to give support to the data meaning along the recognition process, avoiding that wrong information can be used as regular input.

This section, presents some preprocessing techniques and some results achieved over all acquired data, i.e. Face, GSR, HR and EEG; also it presents two new approaches: one to remove abrupt signal changes and another to detrend signals, which this last were mainly applied on EEG data.

4.1. Gravity Force-Fit Method (GFFM) - First Detrend

This innovative and iterative method called Gravity Force-Fit Method (GFFM), was created in this work to execute smooth, correct abrupt data changes, detrend and correct fluctuations in some raw data along the time. It was mainly applied to execute the first detrend over the EEG raw dataset. Since GSR and HR data presents a natural trends that can not be changed, no detrend was applied for them, otherwise it will produces mistakes on its analysis and feature extraction.

The GFFM methodology is based on a reference line, representing the ground reference where the “gravity forces” ($g_{t/b}$) pushes the data to fit to such reference. The $g_{t/b}$, is a function that can acts in two independent data segments along the y-axis called, the top-space and the bottom-space. The top-space segment includes all data values above the reference line, and the bottom-space includes all data values that are below the reference line. Such gravity function can also be shared between both segments.

The reference line, can be computed on static or dynamic mode. If the reference line is on static mode, it must to be computed only once for all data values; otherwise, if is using on dynamic mode, the reference line must to be computed again for each iteration until some stop condition. Regarding to the number of reference lines to be used along the time, it can be: single i.e., only one reference line for both space segments and iteration; or segmented i.e., more than one reference line along all data. In the segmented method,

each reference line have top-space and bottom-space. Regarding to the segment line, it can be computed based on e.g., min-max function, mean, median, among others functions. Figure 4.1, shows the reference line modes and how its function can be selected based on the dataset in use.

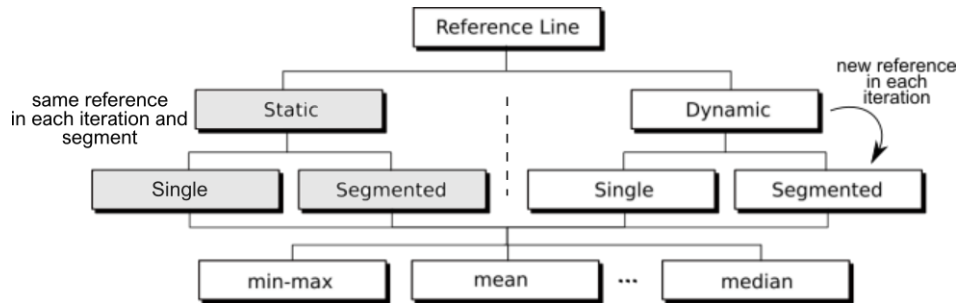


FIGURE 4.1. Reference line function and modes along any dataset preprocessing.

Figure 4.2, shows schematically many possible types of gravity force functions, static or dynamic reference line; also how GFFM can be used to correct abrupt signal changes.

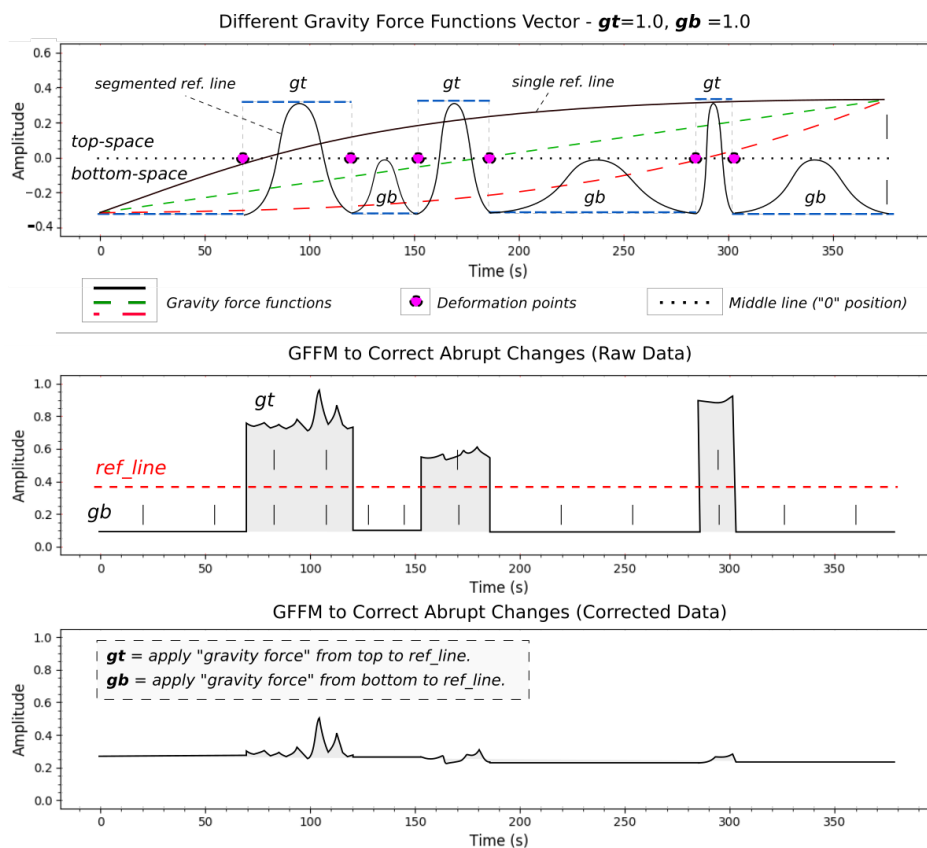


FIGURE 4.2. GFFM on abrupt signal correction. Gravity force functions in shared mode (top); gravity force application (middle); final data (bottom).

The coefficient g_t , represents the gravity force coefficient applied on the top-space, pushing down the signal to fit the reference line; g_b , represents the gravity force applied on

the bottom-space pushing up the signal to fit the reference line. The type of gravity force values can also be based on several functions e.g., constant function, linear, quadratic, exponential, logarithmic, among others as shown in Figure 4.3.

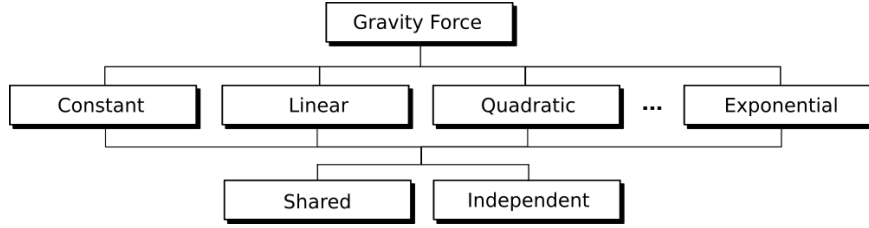


FIGURE 4.3. Gravity force functions and modes along any dataset preprocessing.

The reference line functions are different from gravity force functions. Without the reference line, the gravity force can't be applied because no ground reference exists.

It is recommended that the gravity force for each segment, must to be defined between $[0, 1]$, to fit the data to the reference line, as described in Algorithm 1.

Algorithm 1 GFFM core algorithm using static and single reference line.

```

len_data ← len(data)
bias ← 10e - 10
if rf_mode =: "static" then
  ref_line ← 0
  if rf_range =: "minmax" then
    ref_line ← (max(data) - min(data))/2
  else
    ref_line ← mean(data)
  end if
end if
[gt, gb] ← get_gravity_vec(data, ref_line, g_func)
i ← 0
while i > len_data do
  if data[i] < ref_line then
    new_data[i] ← data[i] + (ref_line * gb[i] + bias)
  else
    new_data[i] ← data[i] - (ref_line * gt[i] + bias)
  end if
end while
i ← i + 1

```

To validate the proposed GFFM, several random trended data were applied having different number of samples, comparing GFFM results with the traditional detrend method. Different GFFM configurations were used in this validation, and also several gravity force coefficients, reference line modes and gravity force functions. The results shown that GFFM indeed detrended

the signal in an iterative manner, which the data were smoothly detrend when g_t and g_b were less than 1. Otherwise, to totally fit the data to reference line, g_t and g_b must be 1.

Some differences can be seen among GFFM and traditional detrend method. While the traditional method uses a trend line as reference, the GFFM uses an idea of ground line as reference to apply “forces” to fit the data, as shown in the trended random data (Figures 4.4 to 4.7).

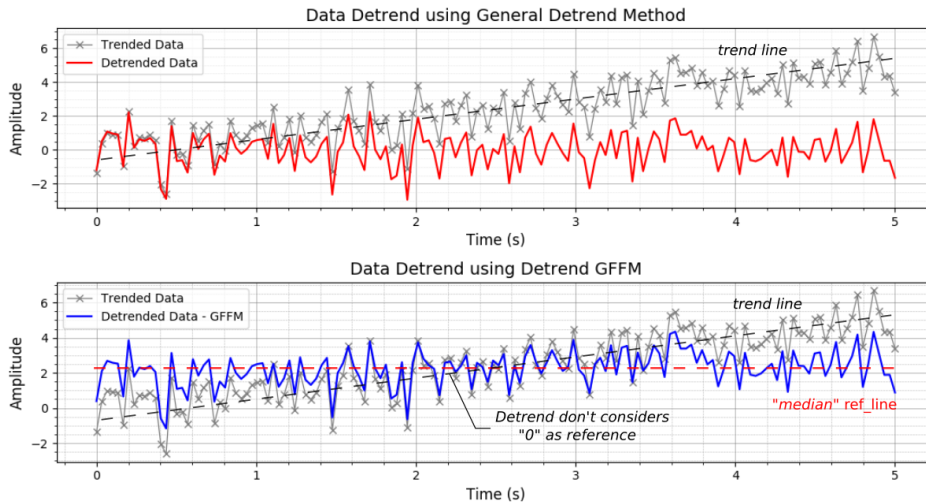


FIGURE 4.4. GFFM test using a dataset with 150 samples. Reference line on static mode based on median, and gravity force function as independent mode, linear and coefficients $g_t=1.0$ and $g_b=0.7$.

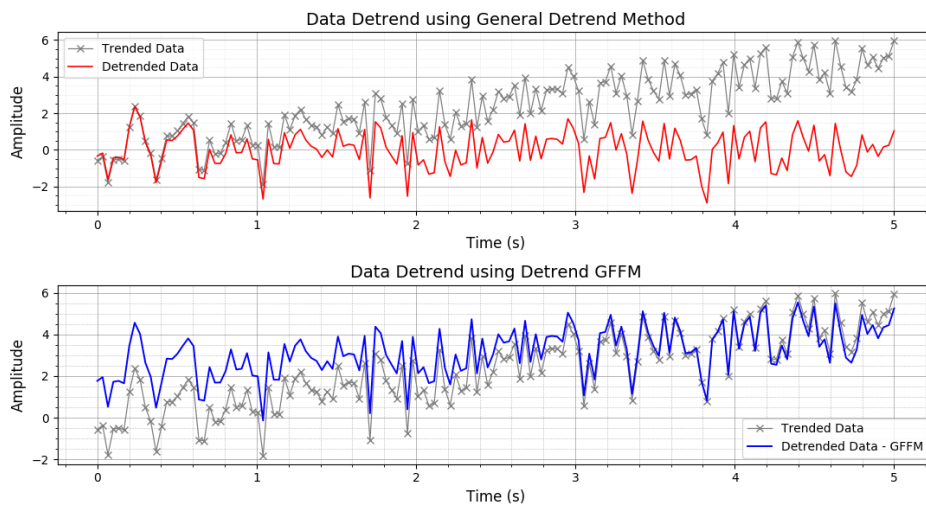


FIGURE 4.5. GFFM test using a dataset with 150 samples. Reference line on static mode based on mean, and gravity force function as shared mode, linear and coefficients $g_t=0.8$ and $g_b=1.0$.

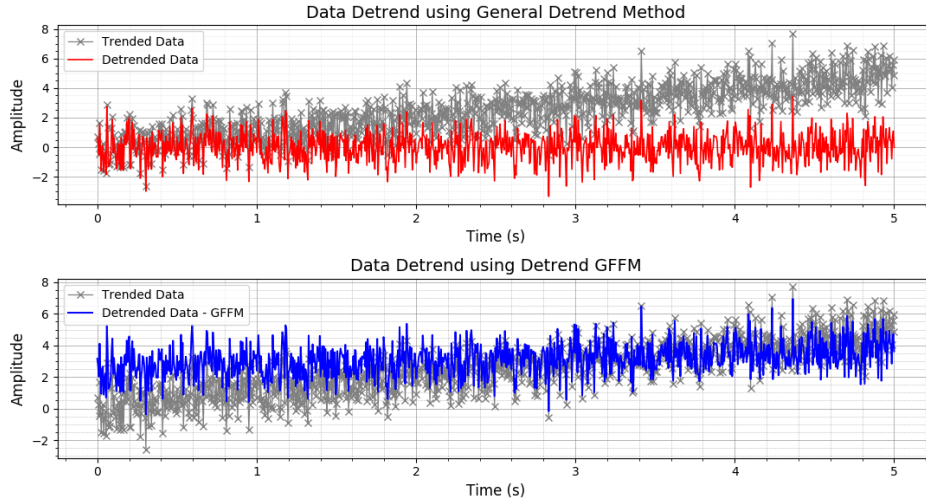


FIGURE 4.6. GFFM test using a dataset with 1000 samples. Reference line on static mode based on mean, and gravity force function as shared mode, linear and coefficients $g_t=0.9$ and $g_b=1.0$.

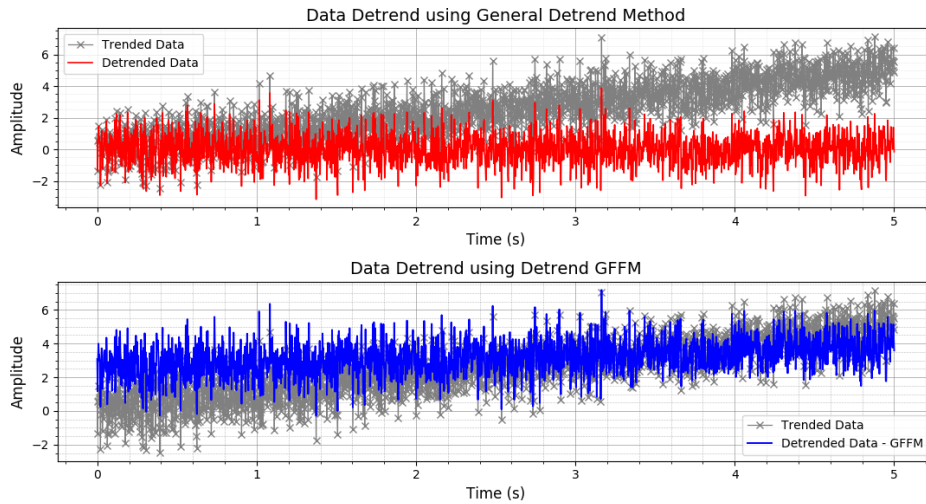


FIGURE 4.7. GFFM test using a dataset with 2000 samples. Reference line on static mode based on min-max, and gravity force function as shared mode, linear and coefficients $g_t=0.9$ and $g_b=1.0$.

High gravity force means that more data will fit to reference line. If the data presents a linear trend and the applied gravity force g_t is smaller than g_b for instance, the data in bottom-space will be more fitted to reference line and vice-versa. This method presents advantages and disadvantages. Regarding to the advantages of the GFFM, we can consider:

- Smooth and controlled detrends;
- Independent vertical spaces of detrend (top or bottom);
- Same detrend methods can be applied in any trend type, i.e. linear and polynomial;
- Detrend result looks more realistic keeping a controlled data fluctuations;
- Detrend results are kept in an average place of the raw data amplitude (not zero reference).

Regarding to the disadvantages of the GFFM, we can consider:

- Gravity forces values close to maximum, may damage some parts of the resulted data;
- For data with low trends, GFFM can smoothly damage some parts of the resulted data;
- Not always a better detrend is based on $g_t = g_b$, sometimes it should be tested before.

4.2. Abrupt Change Correction Method (ACCM)

The present method was initially developed to correct some abrupt changes in the data over time on the GSR and HR data. Noises and abrupt changes along the time, badly affect whole processing sequence. To correct it, a new approach called Abrupt Change Correction Method (ACCM) was developed in this work.

The ACCM algorithm uses a threshold between 0 and 1. For normalized data, the best threshold was 0.2. It means that, if the difference between consecutive data values is higher than 0.2, probably we are facing an abrupt data variation and it should be corrected. These problems were corrected keeping the correct data content along the time, using the Algorithm 2.

Algorithm 2 ACCM core algorithm.

```

data ← norm(data)
len_data ← len(data)
d ← diff(data[1:], data[:-1])
threshold ← 0.2
mag ← abs(d) >= threshold
edges ← nonzero(mag)
len_edges ← len(edges)
k ← 0
while k > len_edges do
  d_edges ← edges[k]
  j ← d_edges
  while j < len_data do
    if d[d_edges - 1] >= threshold then
      data[j] ← data[j] - d[d_edges - 1]
    end if
    if d[d_edges - 1] <= -threshold then
      data[j] ← data[j] + abs(d[d_edges - 1])
    end if
    j ← j + 1
  end while
  k ← k + 1
end while

```

The abrupt changes on GSR data, were mainly caused by motion artifacts and by the sensor default configuration, where it decreased abruptly the GSR data values after it reach the maximum y-axis. On HR data, it were cause by the earclip disconnections along the experiment. On EEG data, it were caused by motion artifacts (Table 4.1).

Table 4.1: Corrections of abrupt data changes using ACCM, over the experiment datasets RC1 to CL3.

Dataset	RC1	RC2	RC3	GC1	GC3	LS2	VC1	CR1	CLX	CL3
HR	×	×	×	×	×	×	×	×	×	×
GSR	×	×	—	—	×	—	×	—	—	×
EEG	—	×	×	—	—	—	—	×	×	—
** Corrections applied on Datasets **										
ACCM	>10	4	>10	>10	>10	>10	7	10	>10	>10

4.2.1. Abrupt Change Correction for GSR Data

Figures 4.8 to 4.11, show the data abrupt changes over the GSR datasets. These datasets were previously normalized and corrected along the time (in seconds).

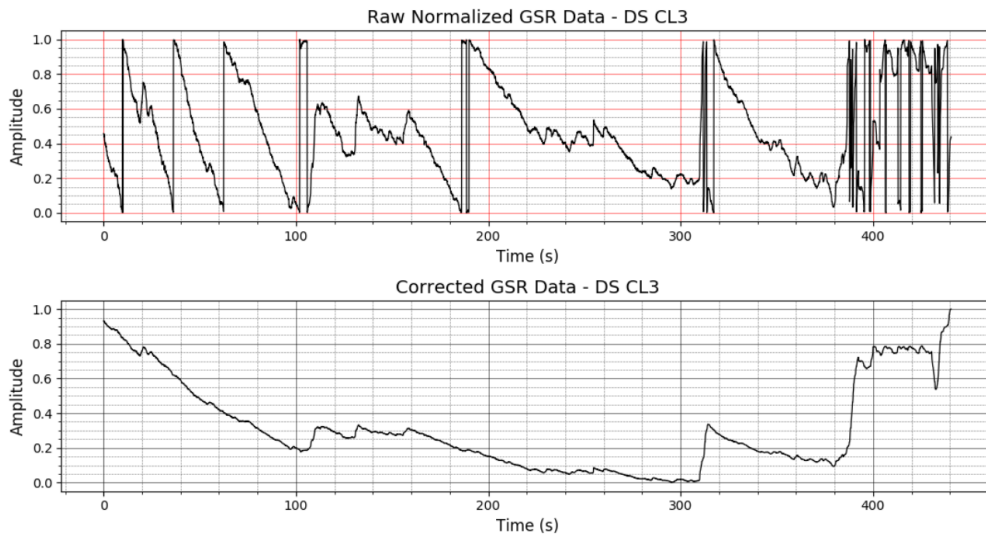


FIGURE 4.8. GSR dataset correction referent to the flight dataset CL3.

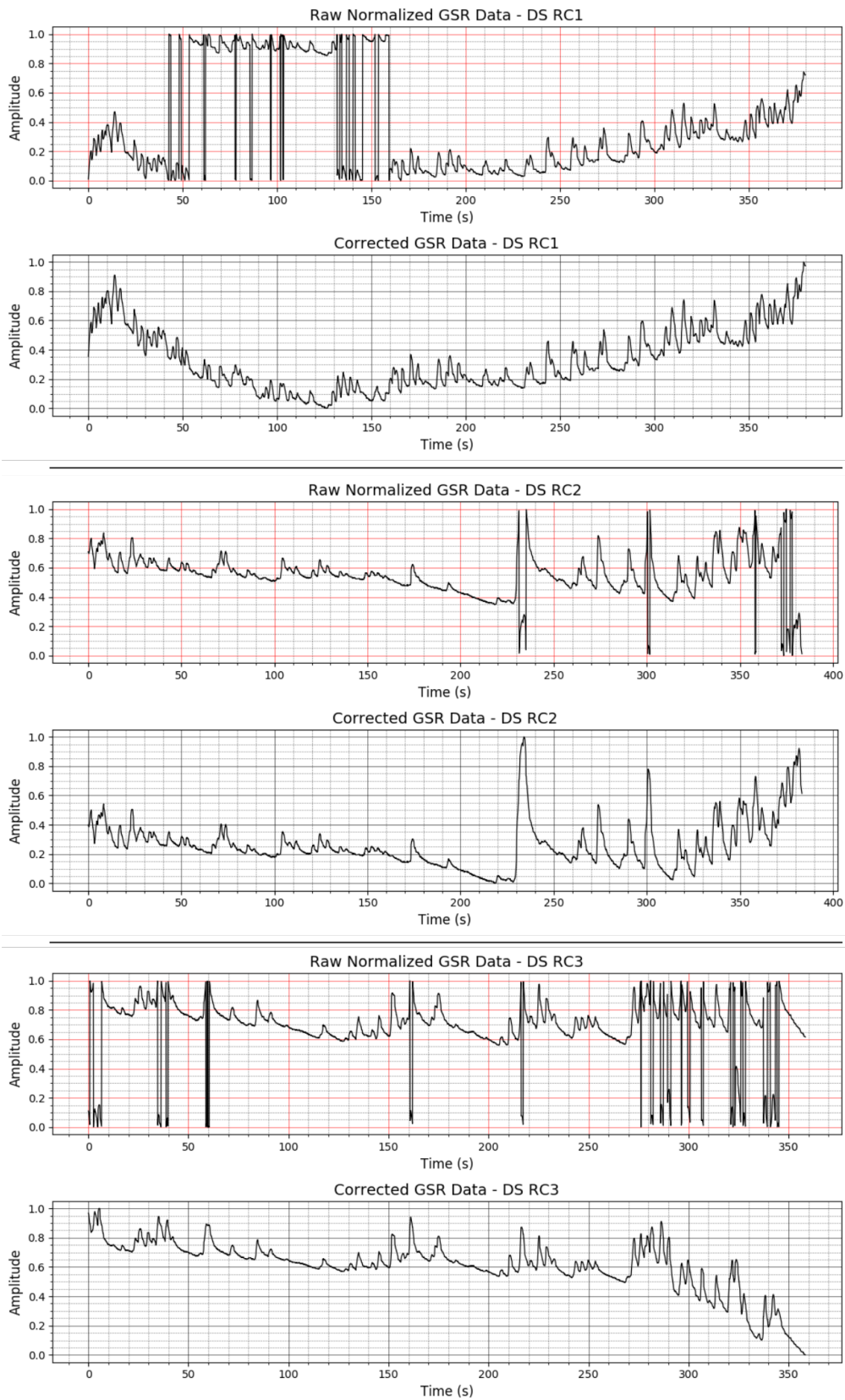


FIGURE 4.9. GSR dataset correction referent to the flight dataset RC1 and RC3.

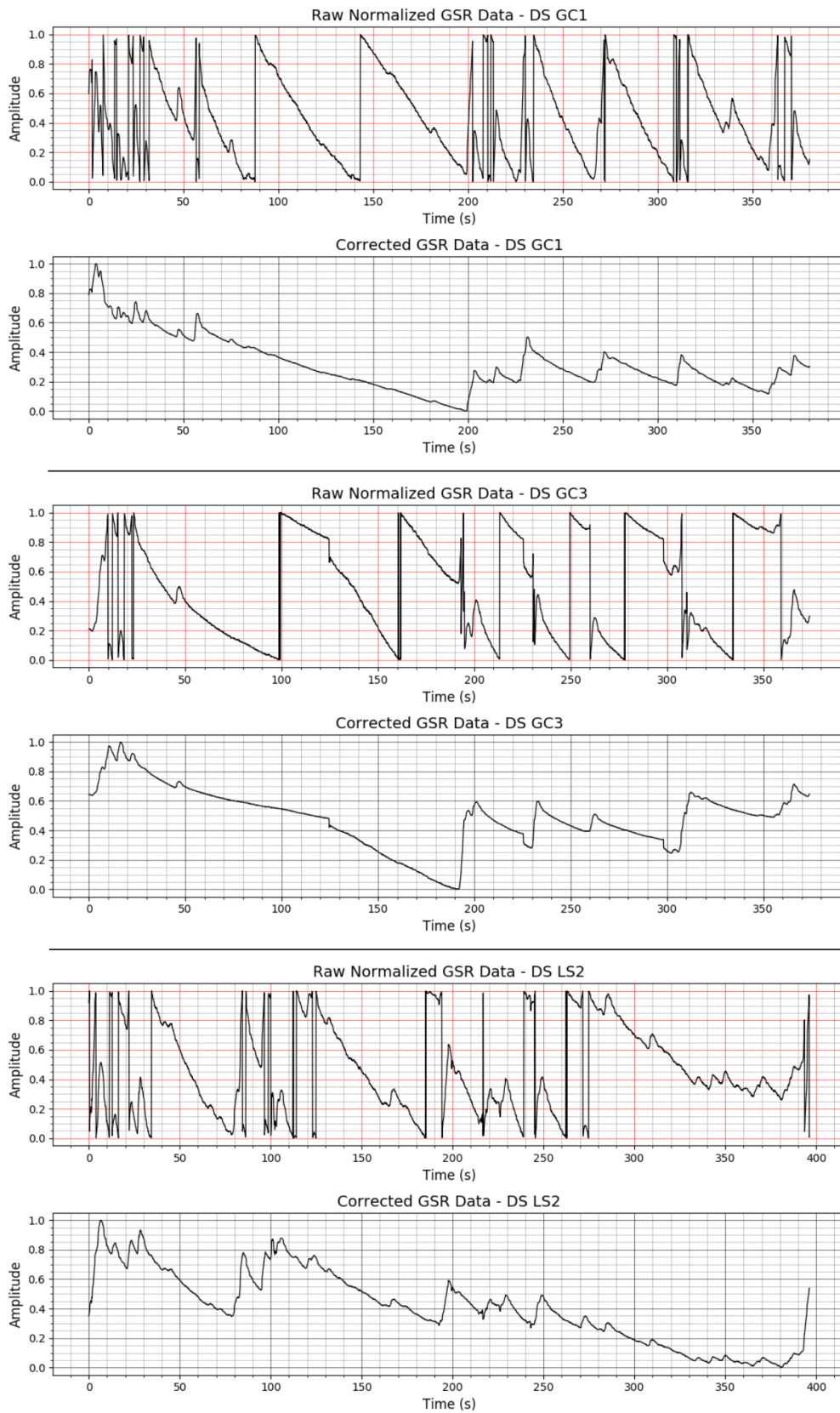


FIGURE 4.10. GSR dataset correction referent to the flight datasets GC1 and LS2.

4.2.2. Abrupt Change Correction for HR Data

Some corrections were also applied on HR dataset along the experiments, as shown in Figures 4.12 and 4.13. The HR abrupt changes were caused by the ear-clip disconnection. When the ear-clip disconnected, the experiment's supervisor put it back in place, immediately.

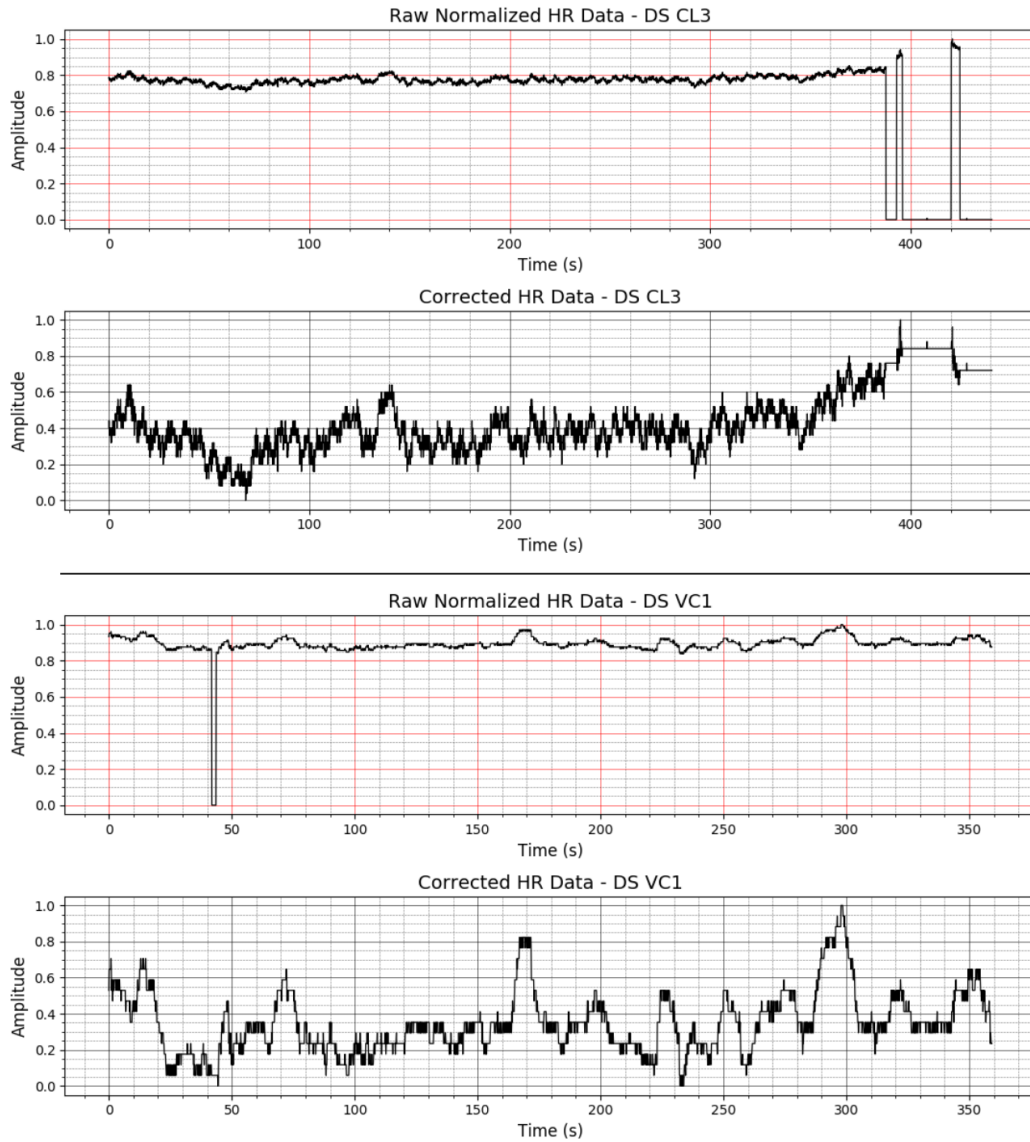


FIGURE 4.12. HR dataset correction referent to the flight datasets CL3 and VC1.

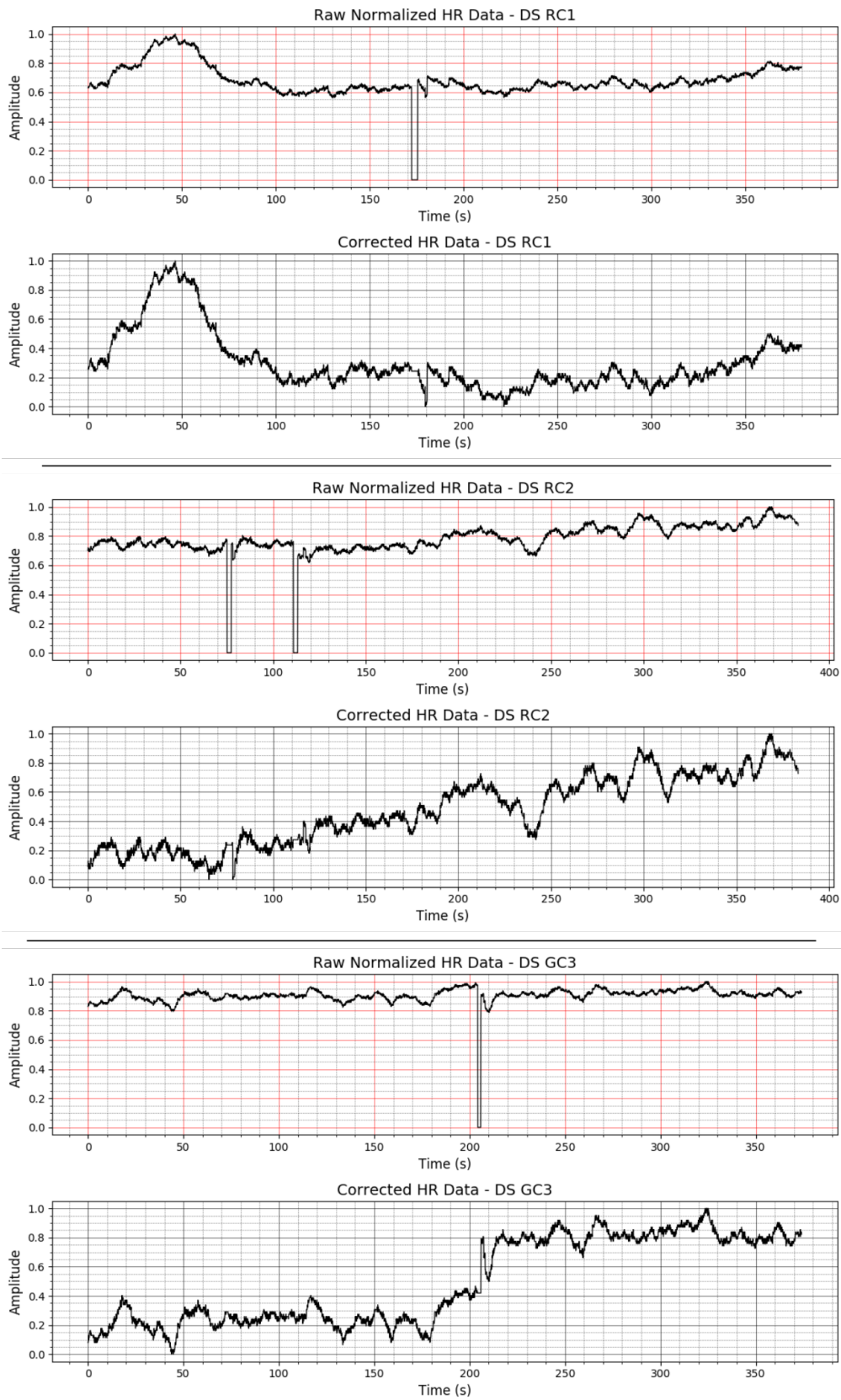


FIGURE 4.13. HR dataset correction referent to the flight datasets RC1 and GC3.

4.3. Outliers Detection and Correction

Other best practice to process the data before the emotion recognition is to identify the data outliers, which it can interfere on the final result.

An outlier is a value whose value is markedly different from the other values in the dataset (Figure 4.14). To partially solve this problem, there are a couple of methods used to detect possible outliers. Once detected the outliers, it can be removed or normalized according to the dataset values. In this work, the outliers detection method was also used to remove or normalize some signal spikes that arose from the processing phase.

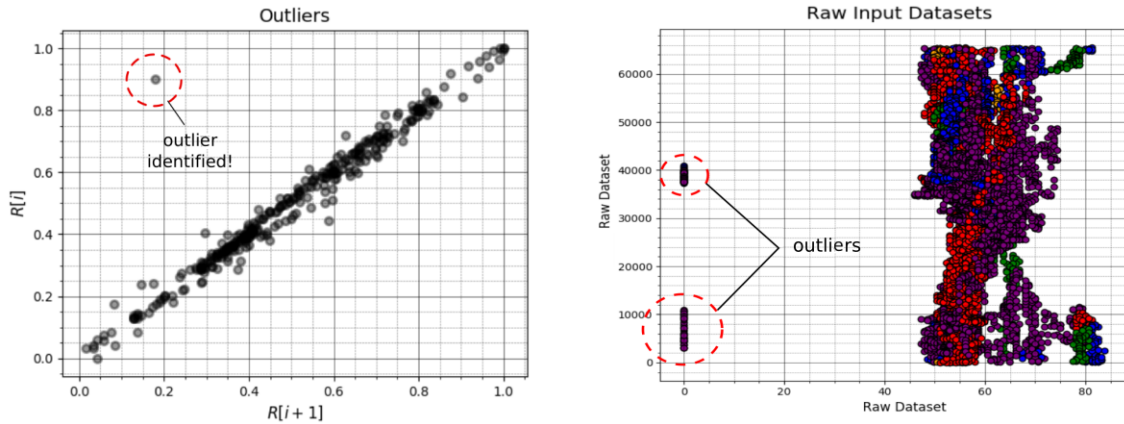


FIGURE 4.14. Outliers detected in some dataset.

The Z-Score and modified Z-Score are some methods that can be used to detect outliers. Table 4.2, presents the detected and removed outliers for all datasets. These methods were applied during the preprocessing and processing.

Table 4.2: Outliers detection and removal using Z-Score and modified Z-Score.

Outlier Method	ACCM	Normalization	Detected	Corrected
Z-Score	—	—	947(2.05%)	0%
Z-Score	—	Applied	947(2.05%)	0%
Z-Score	Applied	—	947(2.05%)	553(1.20%)
Z-Score	Applied	Applied	947(2.05%)	553(1.20%)
Modified Z-Score	—	—	3256(7.06%)	0%
Modified Z-Score	—	Applied	3256(7.06%)	0%
Modified Z-Score	Applied	—	3256(7.06%)	777(1.69%)
Modified Z-Score	Applied	Applied	3256(7.06%)	777(1.69%)

According to previous table, ACCM is also useful to remove outliers as consequence from the abrupt change data corrections along the dataset. It is also possible to see that the modified Z-Score detected different number of outliers. Both methods were tested and the best result was applied.

4.3.1. Z-Score

This method is used to detect outliers on a dataset. It presents low sensibility to detect outliers on small datasets. To compute the Z-score on each observation inside any dataset, the Equation 4.1 is used:

$$Z(n) = \frac{y(n) - \bar{y}}{std(y)} \quad (4.1)$$

The \bar{y} and $std(y)$ denote the sample mean and sample standard deviation, respectively. In another words, the data is computed in units of how many standard deviations it is from the mean. This method considers to use a threshold greater or lower than 3.0 to indicate potential outliers. It was also considered a constant values called *batch*, to define the number of previous samples to consider in the case of outlier correction or removal process (Algorithm 3).

Algorithm 3 Z-Score core algorithm detection and correction.

```

len_data ← len(data)
batch ← 10
i ← 0
while i < len_data do
  z[i] ← (data[i] − mean(data))/std(data)
  if z[i] < −3.0 ∨ z[i] > 3.0 then
    outlier ← TRUE
    if i > batch then
      z[i] ← median(data[(i − batch) : i])
    else
      z[i] ← median(data[0 : i])
    end if
  else
    outlier ← FALSE
  end if
  i ← i + 1
end while

```

4.3.2. Modified Z-Score

The modified Z-Score is an improvement of Z-Score based on the mean of absolute deviation and a constant. Compared with the Z-Score, the modified Z-Score is much more sensible to detect outliers on small datasets (Equation 4.2).

$$MZ(n) = \frac{0.6745 \times (y(n) - \tilde{y})}{MAD} \quad (4.2)$$

The Median Absolute Deviation (MAD) is defined by Equation 4.3. It is recommended to use a threshold greater or lower than 3.5 to better detect potential outliers. The \tilde{y} and $|y|$, define the median of the data and the absolute value of y , respectively.

$$MAD = median(|y(n) - \tilde{y}|) \quad (4.3)$$

The outliers were corrected based also on modified Z-Score (Algorithm 4). Like in Z-Score method, the batch size constant was also considered to correct the outliers.

Algorithm 4 Modified Z-Score core algorithm detection and correction.

```

len_data ← len(data)
MAD ← abs(data[:] - median(data))
const ← 0.6745
batch ← 10
i ← 0
while i < len_data do
  mz[i] ← const * (data[i] - median(data))/MAD
  if mz[i] < -3.5 ∨ mz[i] > 3.5 then
    outlier ← TRUE
    if i > batch then
      mz[i] ← median(data[(i - batch) : i])
    else
      mz[i] ← median(data[0 : i])
    end if
  else
    outlier ← FALSE
  end if
  i ← i + 1
end while

```

4.4. Data Normalization

The acquired data were normalized between 0 and 1. Normalization means to scale the data in identical level or power level. Equation 6.12, presents the normalization used in this work, which n represents each index from input vector.

$$y(n) = \frac{y(n) - \min(y)}{\max(y) - \min(y)} \quad (4.4)$$

4.5. Face Dataset - Smoothing Abrupt Oscillations

The dataset produced by the Face Reader software, was used as the dataset reference i.e., the target or desired output on the emotion recognition process. It presented a lot of abrupt and non natural variation of emotion intensities along the time, bringing also several mismatches e.g., sometimes recognizing scared emotions as disgusting or surprise. Some of these mismatches, were the major reason of errors on the developed emotion recognition. To minimize these effects, the modified Z-Score was used together with a third-order smooth filtering, varying the window length between 120 and 151 samples.

Figure 4.15, shows the application of modified Z-Score and Savitzky-Golay filter over the raw facial emotion dataset, also shows the emotion discretization between 1 and 5: 1-happy, 2-sad, 3-angry, 4-surprised and 5-scared.

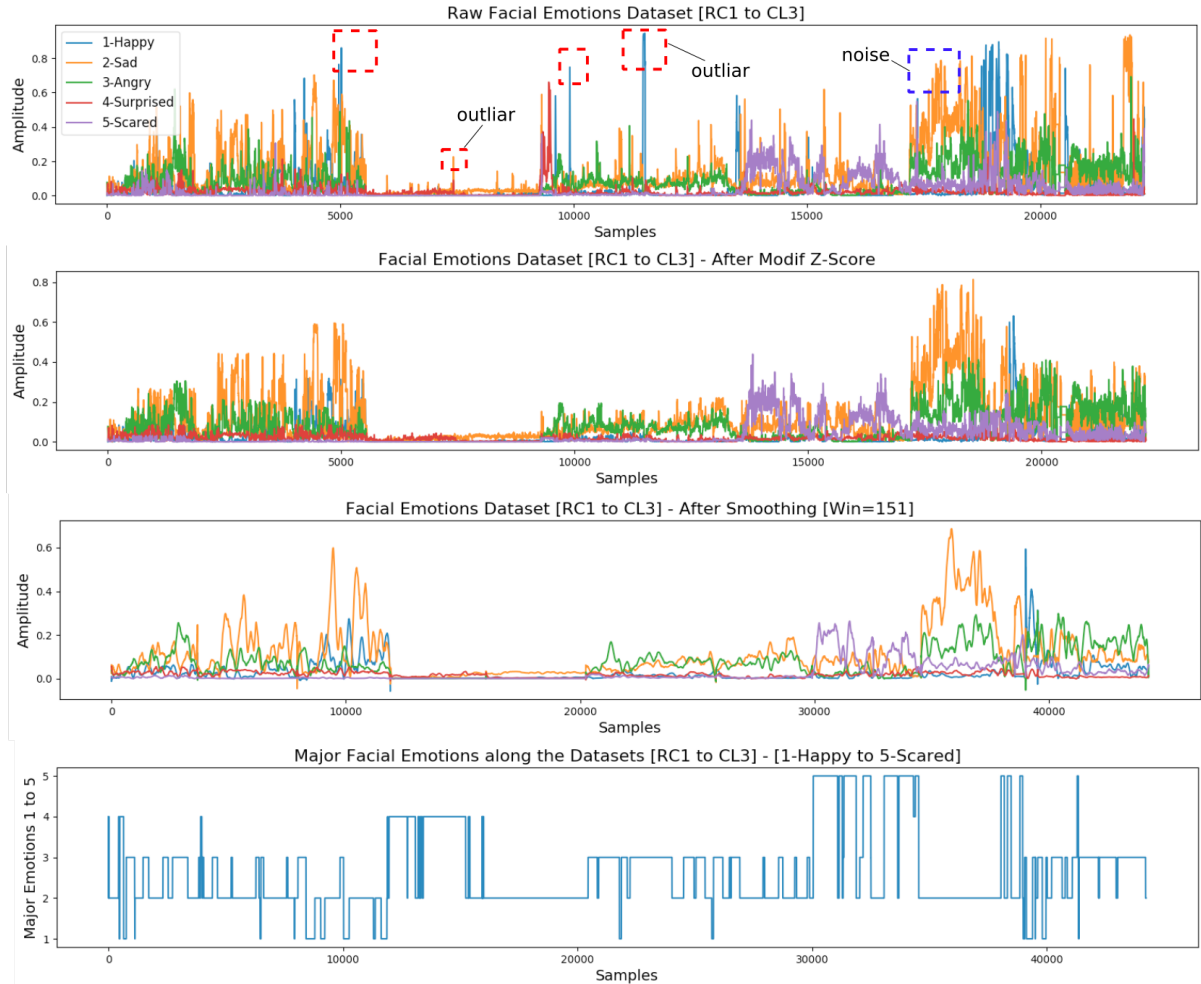


FIGURE 4.15. Raw face emotion dataset with smoothing and resampling.

The smoothing method applied on the facial emotion dataset, was based on Savitzky-Golay filter, to eliminate possible noises in the data by smoothing them using the least-squares polynomials (Savitzky and Golay, 1964).

The emotion discretization along the each sample (Figure 4.15-bottom), was based on Algorithm 5, where it defines the higher emotion intensity (or predominant instantaneous emotion) among all five different emotions by time; it can also be faced like the answer for the question, “which emotion presents the higher intensity now?”. This discretization is useful to predict the major (higher) emotion intensities along each sample time, returning a single output between 1 and 5.

Algorithm 5 Emotion discretization between 1 (happy) and 5 (scared).

```

len_face ← len(face_data)
num_emotions ← 5
emotion_classes ← []
i ← 0
while i < len_face do
    emo_tmp ← [face_data[i,0 : num_emotions]]
    max_emotion_index ← get_index(max(emo_tmp))
    emotion_classes[i] ← max_emotion_index
    i ← i + 1
end while

```

4.6. Preprocessing Output

At the end of the preprocessing steps presented before (i.e. abrupt changes corrections, normalization, smoothing and outliers detections) the data are ready to be processed and to extract its features. The data correlation will be improved after the data further processing.

Figure 4.16, shows a direct data correlation $N \times N$ before and after the preprocessing steps in a portion of the raw HR and GSR datasets ($N=10,000$ in a total of 44,237 samples).

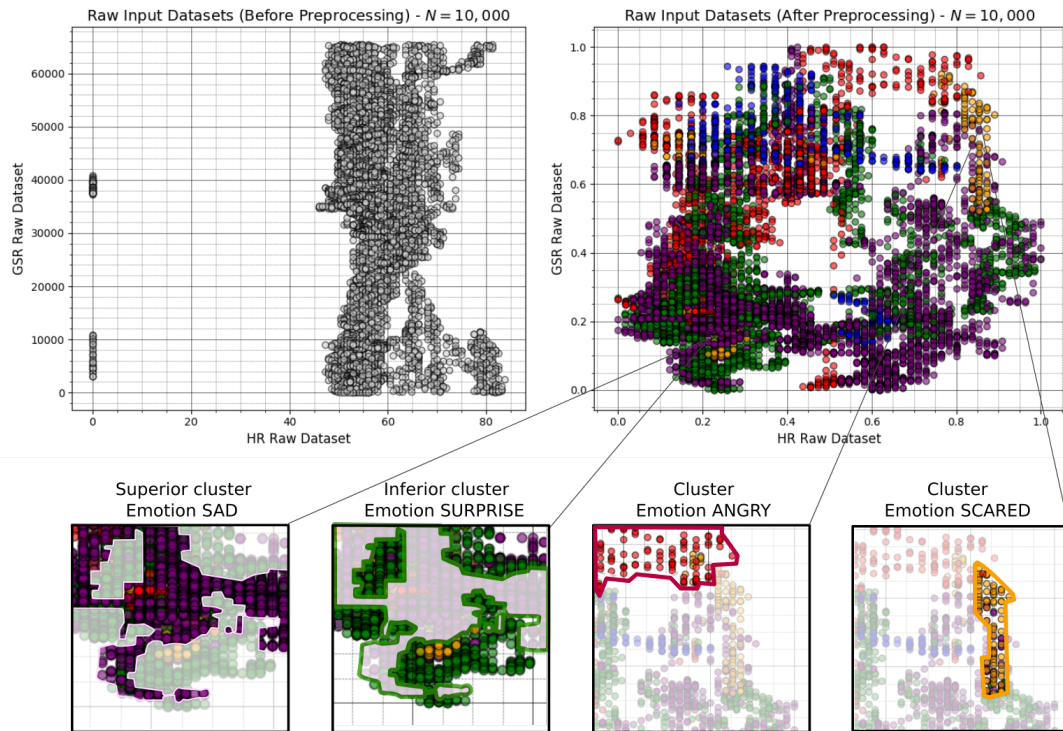


FIGURE 4.16. A set of raw HR and GSR data with $N=10e+3$ samples) preprocessing result. Raw dataset before preprocessing (left); raw dataset after (right).

All 5 colors in the Figure 4.16-right, represent the 5 emotions based on facial emotion recognition software. This also shows that after the preprocessing, it is possible to organize the

dataset in such a way that it is already easy to visualize several clusters based on facial emotions even they are overlapping clusters.

In this chapter were presented all raw data preprocessing under the facial, HR, GSR and EEG datasets, that it is important to be used in the next steps of this work.

CHAPTER 5

Data Processing

The dataset processing transforms the raw data into a data format that can be manipulated by any programming language, being possible to achieve good analysis accuracy (Hafen et al., 2014). In the present work, it includes: abrupt changes correction, outliers removal, signal detrend, signal analysis in time and frequency, peaks processing and analysis, data splitting, bandpass and lowpass filtering, as shown in Figure 5.1.

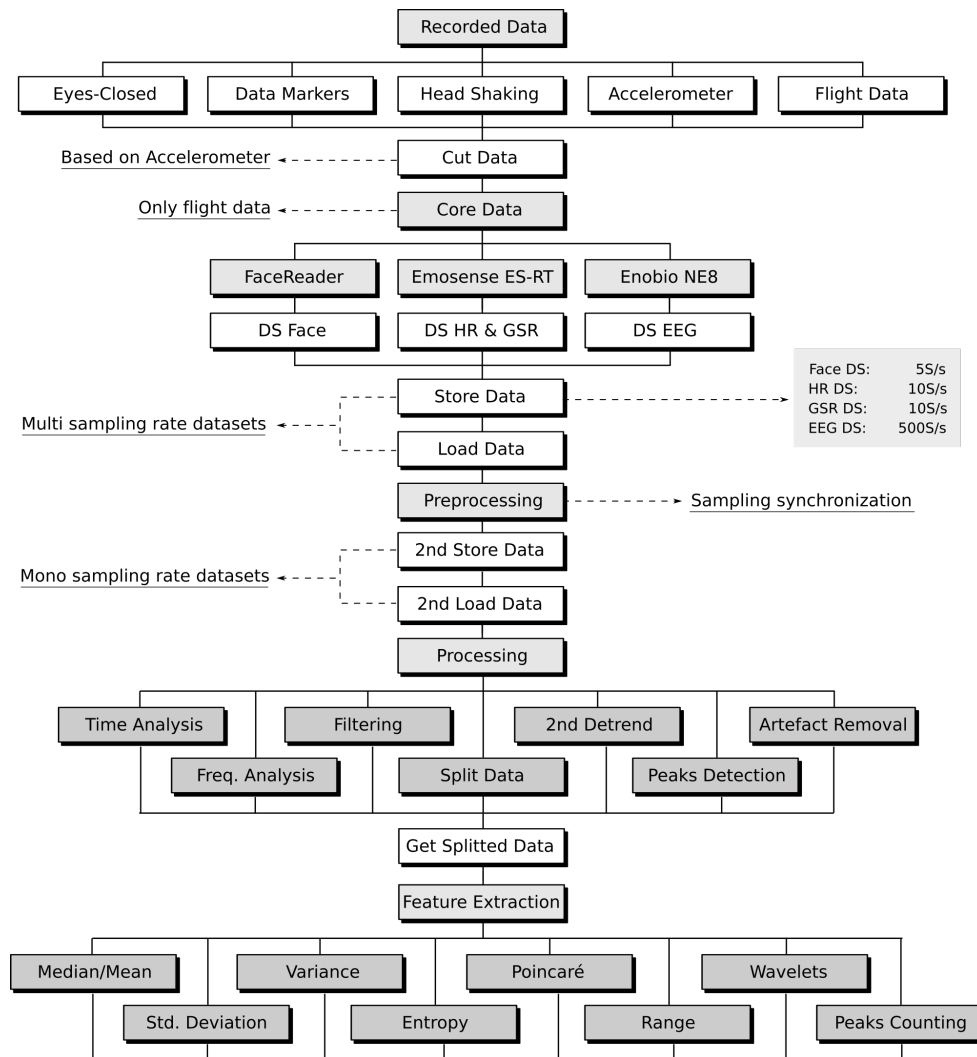


FIGURE 5.1. Detailed stages from recorded data until feature extraction.

5.1. Drift Removal

The second signal detrend applied to all input data $x(n)$, is also called as drift removal. This process is extremely important to improve the quality of data that will be used to perform

emotion recognition. Researches try to reduce the effect of these drifts along the time, through the use of different methods and applications as for instance, to compare the efficiency of some drift removal methods based on ECG (Lenis et al., 2017) or to measure human gait with wearable sensors (Takeda et al., 2014).

In this work, the small recursive filter dc-blocker was applied to execute the second drift removal. It is an efficient tool because conserves the main characteristics of each peak and remove the dc-component ¹ of a signal circulating in a delay-line loop (Julius, 2008). This recursive filter is specified by the difference equation below,

$$y(x) = x(n) - x(n - 1) + Ry(n - 1), \quad (5.1)$$

where R represents a parameter that normally vary between 0.9 and 1. The digital filters are often implemented by converting the transfer function to a linear constant-coefficient difference equation through the Z-transform, as presented by Equation 5.2.

$$H(z) = \frac{1 - z^{-1}}{1 - Rz^{-1}} \quad (5.2)$$

Figure 5.2, shows a raw EEG signal before and after the application of the dc-blocker, keeping all peaks characteristics and relative amplitudes.

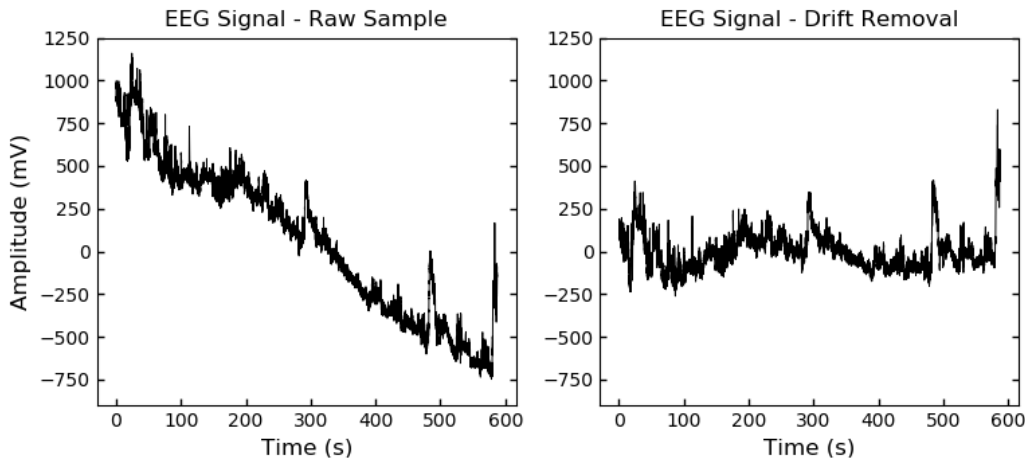


FIGURE 5.2. Result of the drift removal from a raw EEG dataset having $t = 9.78$ min.

5.2. Auto Regressive Exogenous - Motion Artefact Removal

The Auto Regressive Exogenous (ARX) method was used to estimate the accelerometer artifacts, inside a of several raw data (artefact estimation). It is part of the motion artefact removal acquired along the experiments and was applied mainly on EEG datasets (Siddiquee et al., 2018).

To estimate the accelerometer values along the time, we define the true data (i.e. clean, without noise) as $s(n)$, which it was corrupted by the motion artifacts $w(n)$; using these two parameters, the corrupted data for each data point n , can be defined by,

¹The *dc* component, also called average value, represents a constant voltage that shifts the signal up or down along the y-axis, e.g., considering the signal $x(t) = A + B\sin(2\pi)$, the term A represents the *dc*-component.

$$x(n) = s(n) + w(n). \quad (5.3)$$

The data coming from each device, are represented by $x(n)$, where it includes the true data and the artifacts. It is not possible to extract clearly the artefact to remove it although, it can be estimated. The artefact estimation can be represented by $\hat{w}(k)$, as presented below.

$$\hat{w}(k) = \left(\sum_{i=1}^{NA} a_i x(k-i) \right) + \left(\sum_{j=0}^{NB} b_j^T u(k-j) \right) \quad (5.4)$$

The $1 \times L$ model vector coefficients a and b can be defined by, $a = [a_1, a_2, \dots, a_{NA}]$ and $b = [b_1, b_2, \dots, b_{NB}]$ for $1 \times L$ input model vector $u = [u(k), u(k-1), \dots, u(k-NB)]$ representing the 3D-accelerometer values $u[k] = [A_x(k), A_y(k), A_z(k)]$. Thus, expanding the previous Equation, we will have,

$$\hat{w}(k) = a_1(k-1) + \dots + a_{NA}x(k-NA) + b_0^T u(k) + b_1^T u(k-1) + \dots + b_{NB}^T u(k-NB). \quad (5.5)$$

Equations 5.6 to 5.7, can be used to find the models coefficients, where $e(n)$ represents the instantaneous error between the model and the system input, and $J(a, b)$ represents the Jacobian matrix applied to the model coefficients.

$$e(k) = x(k) - \hat{w}(k) \quad (5.6)$$

$$J(a, b) = \sum_{k=1}^N (x(k) - \hat{w}(k)) \quad (5.7)$$

Once determined the $1 \times L$ vector a_1, a_2, \dots, a_{NA} and the $L \times 1$ vector $b_0^T, b_1^T, \dots, b_{NB}^T$, the artefact estimation can be found $\hat{w}(n)$, the true data $\hat{s}(n)$ can also be estimated as defined below.

$$\hat{s}(n) = x(n) - \hat{w}(n) \quad (5.8)$$

The Signal to Noise Ratio (SNR) defined by Equation 5.9, was used to control the best model estimation, where: σ_x^2 , $\sigma_{e_{Aft}}^2$ and $\sigma_{e_{Bef}}^2$ represent respectively, the variance of the data with motion artefact input ($x(n)$), the variance of the data after ($\hat{s}(n)$) and before ($\hat{w}(n)$) the artefact removal (Siddiquee et al., 2018).

$$\Delta SNR = 10 \log_{10} \left(\frac{\sigma_x^2}{\sigma_{e_{Aft}}^2} \right) - 10 \log_{10} \left(\frac{\sigma_x^2}{\sigma_{e_{Bef}}^2} \right) \quad (5.9)$$

5.3. Filtering - Bandpass and Lowpass Combination

The filtering was applied to consider only the β -band on these experiments, regarding to EEG data. The classical IIR digital filters Butterworth, were used in this work.

The frequency range between 12 to 40Hz was considered using a bandpass Butterworth filter (BPF) to guarantee a minimum β -band noises; furthermore, a lowpass Butterworth filter filter (LPF), having cutoff frequency of 40Hz, was also applied, to improve the prior filtering effect not increasing its order (Figure 5.3).

The filtering also removed the highest electrooculogram (EOG) artifacts. These EOG artifacts are one of the main noises over the EEG data and must be avoided. It were caused by the eyes globe movements along the experiments, since that the EOG frequencies are mainly between 0.5 to 12Hz.

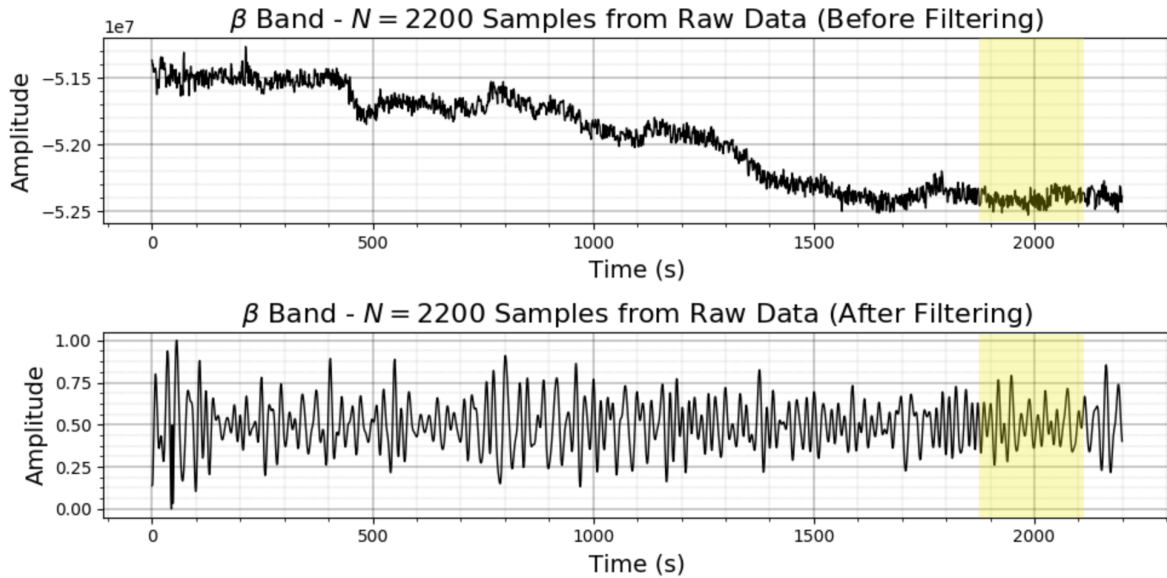


FIGURE 5.3. Filtering output over EEG data regarding to β -band.

5.3.1. Spectrogram View

Spectrograms can be used to visualize the change of a nonstationary frequency of a data over time. The spectrogram enable us to see the frequency energies or magnitudes along the time, based on consecutive Fourier transforms over different datasets and EEG channels, as shown in Figure 5.4.

Since the beta band (Umeda and Satoshi, 2013) is more related to cognition processes, it is possible to visualize the flight moments where it demanded more cognitive resource of each volunteer. These moments are takeoff (Task 1) and landing (Task 7), where it were indeed critical for all volunteers. The spectrogram shown that in general, the EEG amplitudes of all datasets along the Task 3, were less if compared with the amplitudes referent to takeoff and landing.

Figure 5.5, shows an example of EEG 8-channels after the filtering and processing. At this point, eyes motion artefact and other movement artifacts were removed. To compare the results from these processing, the Chapter 2 presents the same CR1 dataset in raw, without processing. Still in these processed EEG, it is possible to see the high data oscillation, mainly during the takeoff (Task 1), final approach (Task 6) and landing (Task 7).

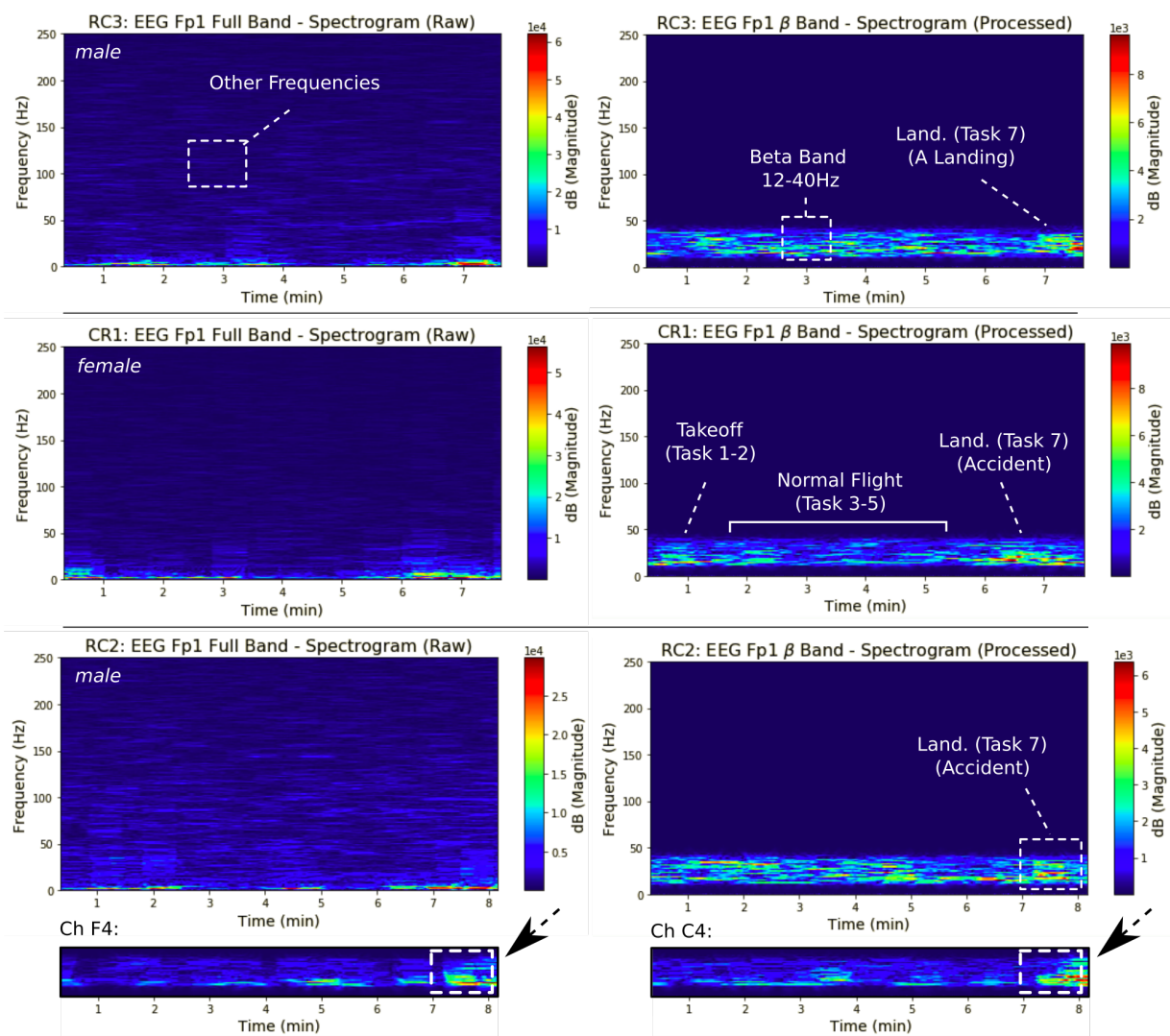


FIGURE 5.4. Some dataset spectrograms, showing the flight parts with high amplitude.

5.4. Discrete Fourier Transform Analysis

The Discrete Fourier Transform (DFT) plays a central role in this work, since most of the processing is based on that. It is also used to visualize the effect of the filtering process. The DFT transforms the data of the space of time, to space of frequency, defined by direct transform as defined in Equation 5.10. In another words, it is represented as linear combinations of bounded exponential through the Fourier transform (Oppenheim and Verghese, 2015). The application of the DFT to spectral analysis will be shown further.

$$x[n] = \sum_{k=0}^{N-1} X[k]e^{j(2\pi/N)kn} \quad (5.10)$$

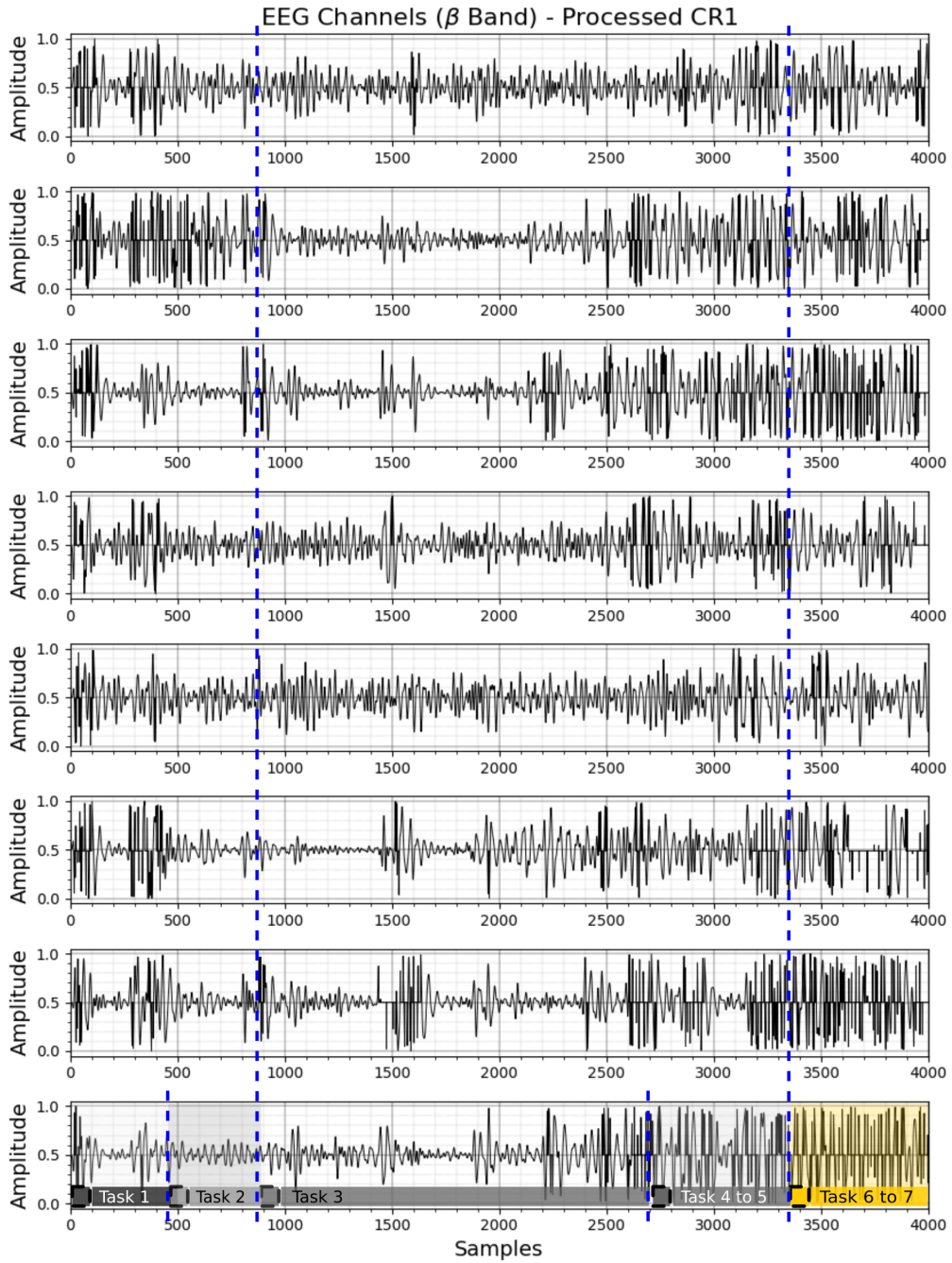


FIGURE 5.5. Processed EEG (8 channels) dataset referent to CR1 experiment.

Feature Extraction

Feature extraction, is the last step before the emotion recognition and it can be applied over time and frequency contexts. It is very important in the pattern identification, classification, modeling and general automatic recognition. Feature extraction is also fundamental to minimize the loss of important information embedded in some data and to optimize a dataset bringing a more clear information to recognize any pattern or cluster (Al-Fahoum and A Al-Fraihat, 2014). The considered feature extraction methods are adapted to the processed data, according to the physiological data, e.g. HR, GSR and EEG.

Figure 6.1, shows how the feature extraction works for each dataset along the time. For each part of a data (Δs) along the time, several features were extracted e.g., mean, standard deviation and so on. The features that were extracted of the emotions output dataset (happy, sad, angry, surprise and scared), were related with the same time interval of the features that are extracted of the biosignal dataset (HR, GSR and EEG1-8).

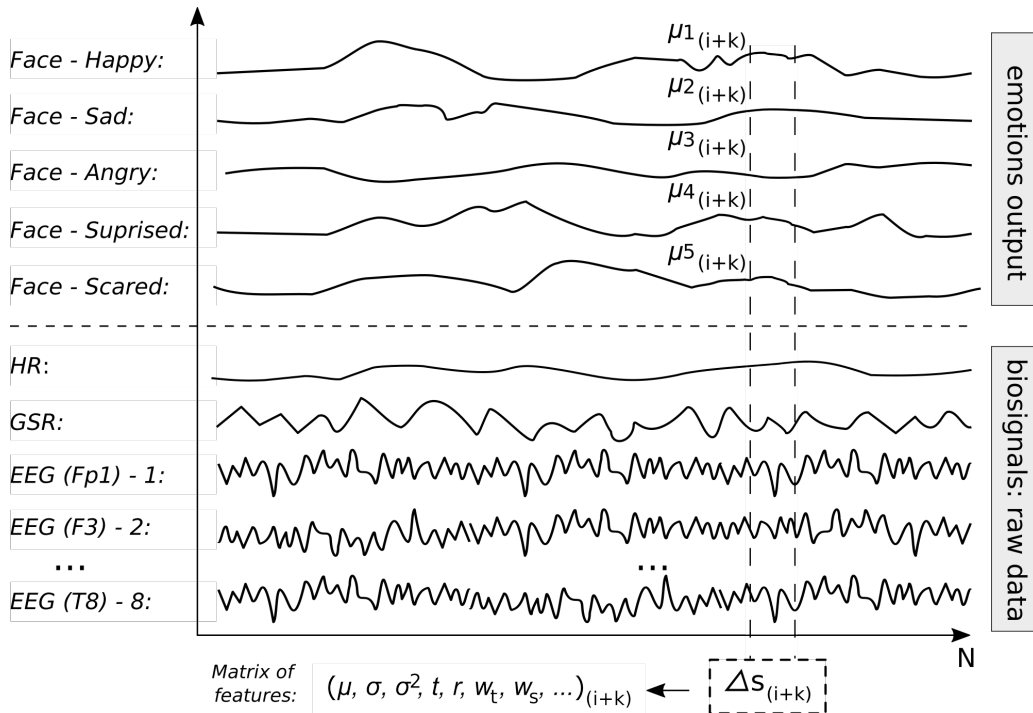


FIGURE 6.1. Feature extraction and sampling demonstration using the feature μ for all detected emotions from the face.

A fixed number of samples are selected by time and the features are extracted from it. The number of samples to select i.e., the window length to extract features, is up to the problem and data in case. For instance, for HR data, it is recommended a time window of at least five seconds of samples and so on.

6.1. Features Description

A total of 15 different features were extracted. Each feature was chosen according to each dataset characteristics as presented in Table 6.1, which it describes all extracted features as such as the correspondent datasets. Features based on wavelets were also applied over EEG dataset.

TABLE 6.1. Extracted features for HR, GSR, EEG and Face datasets.

Extracted Features	Feature Description	Applied to Dataset
FEAT_MN	◇ Mean of a sample.	HR, GSR, EEG, Face
FEAT_MD	◇ Middle value of a sample (median).	HR, GSR, EEG, Face
FEAT_STD	◇ Standard deviation (σ) of a sample.	HR, GSR, EEG
FEAT_VAR	◇ Variance (σ^2) of a sample.	HR, GSR, EEG
FEAT_ENT	◇ Measure the samples' entropy i.e., irregularities.	HR, GSR, EEG
FEAT_RNG	◇ Absolute range ($max - min$) value of a sample.	HR, GSR, EEG
FEAT_RMS	◇ Root mean squared of a sample.	HR, GSR, EEG
FEAT_PEK	◇ Measure the amount of peaks into a sample.	GSR
FEAT_WAC	◇ Mean of the wavelet (Symlets) approximation coeff.	EEG
FEAT_WDC	◇ Mean of the wavelet (Symlets) detailed coeff.	EEG
FEAT_SD1	◇ Short-term HR variability.	HR
FEAT_SD2	◇ Long-term HR variability.	HR
FEAT_SCT	◇ Vector norm from the Poincaré plot centroid.	HR
FEAT_SAR	◇ Ellipse area based on $SD1$ and $SD2$.	HR

Regarding to GSR datasets, it was important to understand its data profile and behaviour to properly relate it to the number of peaks (peak frequency) along the time/events; for this reason, one feature that relates peaks by time, was applied. Other peculiarities are also found over the HR datasets as for instance, the HR variabilities during several emotional events along time. This HR dynamic fluctuation, were mainly represented by three features. Furthermore, other statistical features were also applied over all datasets, considering several sample lengths.

Despite the extracted features, not all of them were used at same time, due it can provoke recognition ambiguities and regression problems. To solve that, some techniques were applied to select the best features, by correlating or removing them from some datasets.

6.1.1. Mean Features (FEAT_MN)

The mean value was applied over the HR, GSR, EEG and face datasets. It is represented by the sample vector $x = [x_1, x_2, \dots, x_n]$ as defined below, which the \bar{x} is the mean value of the sample.

$$\bar{x} = \frac{1}{N} \sum_{n=1}^N x_i = \left(\frac{x_1 + x_2 + \dots + x_n}{N} \right) \quad (6.1)$$

6.1.2. Median Features - Correcting Mean's Discrepancies (FEAT_MD)

The arithmetic feature median, is sometimes also applied as a feature from HR and GSR data instead of the mean. It because, the median works better when the dataset presents some high

spikes, which it cause wrong increase of the data mean value. In this case, the median (\tilde{x}) is more realistic, taking the middle value of this data already ordered (Devore, 2000).

Equation 6.2 must to be used if the sampled data have an odd number of items, or Equation 6.3, otherwise. In both cases of median \tilde{x} , the data vector x must be first sorted in ascending or descending order.

$$\tilde{x}_{odd} = x\left(\frac{n+1}{2}\right)item \quad (6.2)$$

$$\tilde{x}_{even} = \frac{x\left(\frac{n}{2}\right) + x\left(\frac{n}{2}+1\right)}{2}item \quad (6.3)$$

6.1.3. Standard Deviation and Variance Features (FEAT_STD, FEAT_VAR)

The standard deviation and variance, were also applied over the HR, GSR and EEG datasets. It are represented by, σ and σ^2 respectively, as defined by Equations below.

$$\sigma = \sqrt{\frac{\sum_{n=1}^N (x(n) - \bar{x})^2}{N}}, \quad \sigma^2 = \frac{\sum_{n=1}^N (x(n) - \bar{x})^2}{N} \quad (6.4)$$

6.1.4. Continuous Entropy Features (FEAT_ENT)

The continuous entropy or differential entropy, is another feature used in this work. It is a concept in data theory to represents the measurement of the average rate of a random variable; it is also understood as a method to measure the quality or classes¹ diversity of such dataset. On continuous probability distributions, it is based on the expansion from Shannon entropy concept, defined by Equation 6.5,

$$h(X) = - \int_0^{N(S)} f(x) \log f(x) dx, \quad (6.5)$$

where X represents a random variable, defined by a probability density function of a subset S . The discrete approximation of $h(X)$, can be defined as below.

$$h(X) = -\Delta x \sum_0^{N(S)} f(x) \log f(x) \quad (6.6)$$

6.1.5. Wavelets Features (FEAT_WAC, FEAT_WDC)

The wavelet analysis plays an important role as part of the feature extraction methods. It allows us to analyze time and frequency contents of signals simultaneously and with high data resolution. When it is applied over a continuous data, it is called of Continuous Wavelet Transform (CWT), and over a discrete data is Discrete Wavelet Transform (DWT) (Mallat, 2009). It lies on the concept of mother wavelet (MWT), which it is a function used to decompose and describe the analyzed data. The Symlets ('sym7') was the MWT used, due its high similarities and compatibilities with the EEG data in all scalp regions (Equation 6.7) (Al-Qazzaz et al., 2015).

¹In data mining or artificial intelligence, the class represents the type of an instance from a dataset or the target into the classification problem.

$$CWT(a, b) = \int_{-\infty}^{+\infty} x(t)\psi_{a,b}^*(t)dt, \quad (6.7)$$

where $x(t)$ represents the unprocessed signal, a is the dilation, and b is the translation factor. Furthermore, as shown previously, the CWT method includes a complex conjugate term denoted by $\psi_{a,b}^*$, where $\psi(t)$ is the mother wavelet (Al-Fahoum and A Al-Fraihat, 2014) (Equation 6.8).

$$\psi_{a,b}(t) = \frac{1}{\sqrt{|a|}}\psi\left(\frac{t-b}{a}\right). \quad (6.8)$$

Figure 6.2, shows the practical approach of wavelets, which it works basically, fixing a function called mother wavelet, decomposing the signal $x(t)$, into a shifted and scaled versions of this function, allowing to precisely distinguish local characteristics of the signals.

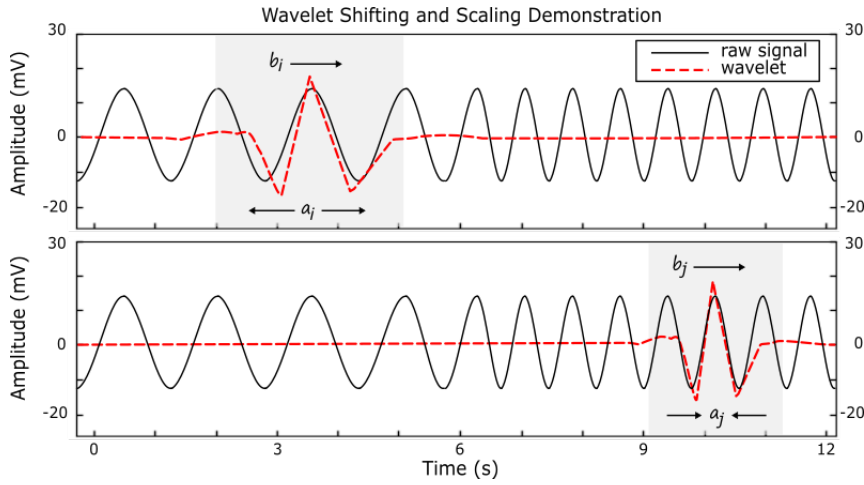


FIGURE 6.2. Wavelet shifts along of a sine wave with different frequencies, where $a_i \neq a_j$ and $b_i \neq b_j$.

6.1.6. Peaks Counting Features (FEAT_PEK)

Peaks detections and counting were applied over the GSR dataset. It is a important features to characterize the GSR data. Before detect the peaks position, the data was normalized and detrended, to equalize the peaks amplitude along the time. After that, the peaks detection was applied. Once the peak positions were detected, the final procedure was apply it over the original GSR data.

The result of this method, is shown in Figure 6.3 below, which refers to 3,600 samples from dataset RC1, after the detrend and normalization (top plot), returning to original shape (bottom plot).

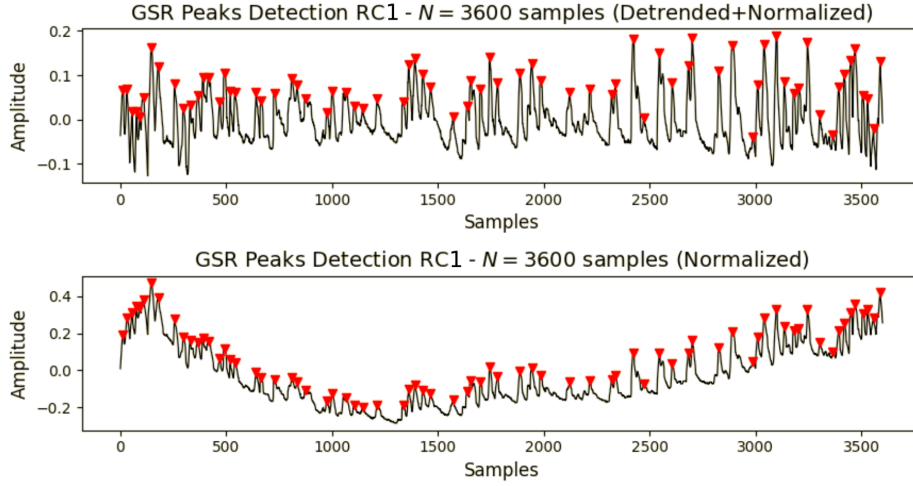


FIGURE 6.3. Peaks detections and counting over 3600 samples (DS-RC1).

Its detection was based on topographic prominence method, which is a useful concept to maintain a good peak choice, discarding the noisy peaks. In addition, it refers to the minimum point height, necessary to descend to get from the peak to any other higher surface.

6.1.7. Poincaré Plots Features (FEAT_SD1, FEAT_SD2, FEAT_SCT, FEAT_SAR)

The Poincaré plots of RR intervals is one of the methods used in Heart Rate Variability (HRV) analysis. It returns a useful visual map (or cloud), which is capable to summarize the dynamics of an entire RR time series regarding to actual and next one values. It is also a quantitative method to give information over the long- and short-term HRV (Golinska, 2013; Piskorski and Guzik, 2007).

This method is represented by Poincaré *descriptors*, $SD1$ and $SD2$, which are used to quantify geometrically the produced cloud. It is given in terms of the variance of each RR_i and RR_{i+1} pairs. The i refers to the i th RR value, as shown in Figure 6.4.

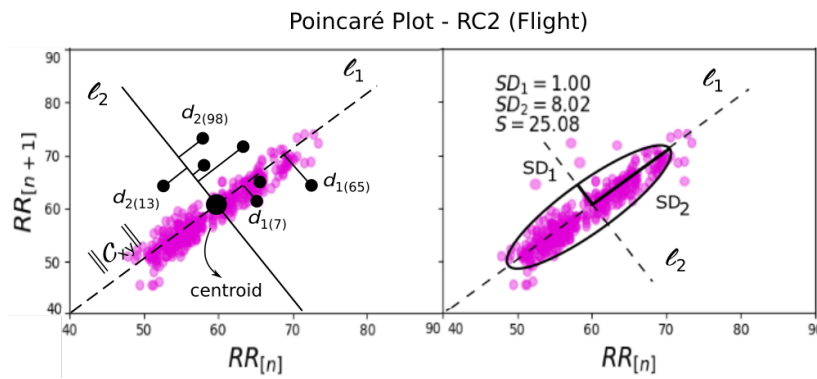


FIGURE 6.4. Poincaré plot demonstration over the flight dataset RC2.

Mathematically, let the HRV be defined by the vector $RR = [RR_1, RR_2, \dots, RR_{n+1}]$ and the position-correlated vectors x and y , as defined below (Tayel and AlSaba, 2015; Piskorski and Guzik, 2007),

$$x = [x_1, x_2, \dots, x_n] \equiv [RR_1, RR_2, \dots, RR_n], \quad (6.9)$$

$$y = [y_2, x_3, \dots, y_{n+1}] \equiv [RR_2, RR_3, \dots, RR_{n+1}]. \quad (6.10)$$

For a regular Poincaré plot, the centroid vector $C_{xy} = [x_c, y_c]$ of its cloud representation, is define by,

$$x_c = \frac{1}{n} \sum_{i=1}^n x_i, y_c = \frac{1}{n} \sum_{i=1}^n y_i. \quad (6.11)$$

To compute the numerical representation of the centroid, the *vector norm* is applied using the Equation 6.12.

$$\|C_{xy}\| = \sqrt{x_c^2 + y_c^2} \quad (6.12)$$

To compute the *descriptors* (short-term variability) $SD1$ and $SD2$ of a standard Poincaré plot, the distances d_1 and d_2 of any i th RR from the centroid *interceptors* l_1 and l_2 respectively are defined as,

$$d_{1i} = \frac{|(x_i - x_c) - (y_i - y_c)|}{\sqrt{2}}, d_{2i} = \frac{|(x_i - x_c) + (y_i - y_c)|}{\sqrt{2}}. \quad (6.13)$$

Considering those prior algebraic definitions for a standard cloud, it is possible to compute the $SD1$ and $SD2$.

$$SD1_c = \sqrt{\frac{1}{n} \sum_{i=1}^n d_{1i}^2}, SD2_c = \sqrt{\frac{1}{n} \sum_{i=1}^n d_{2i}^2} \quad (6.14)$$

The area covered by the resulted ellipse, was also used as a feature for HR dataset, and it can be determined as below.

$$SA = \pi \cdot SD1 \cdot SD2 \quad (6.15)$$

The results over the Poincaré plots for all datasets (raw and processed datasets) used in this work, are shown in Figures 6.5 to 6.8.

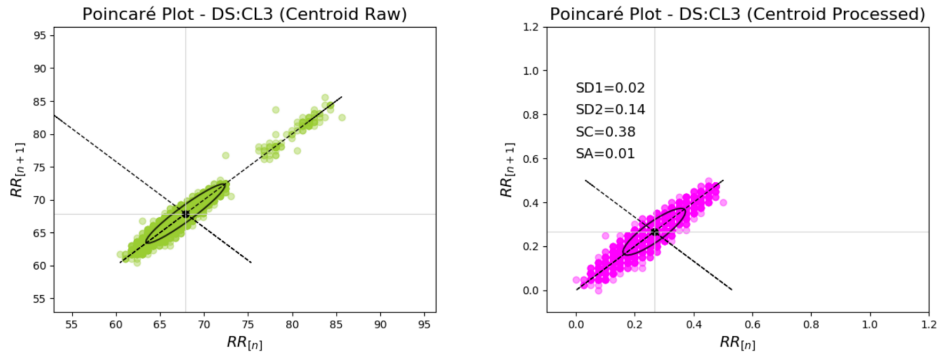


FIGURE 6.5. Poincaré plot for raw dataset and processed dataset (CL3).

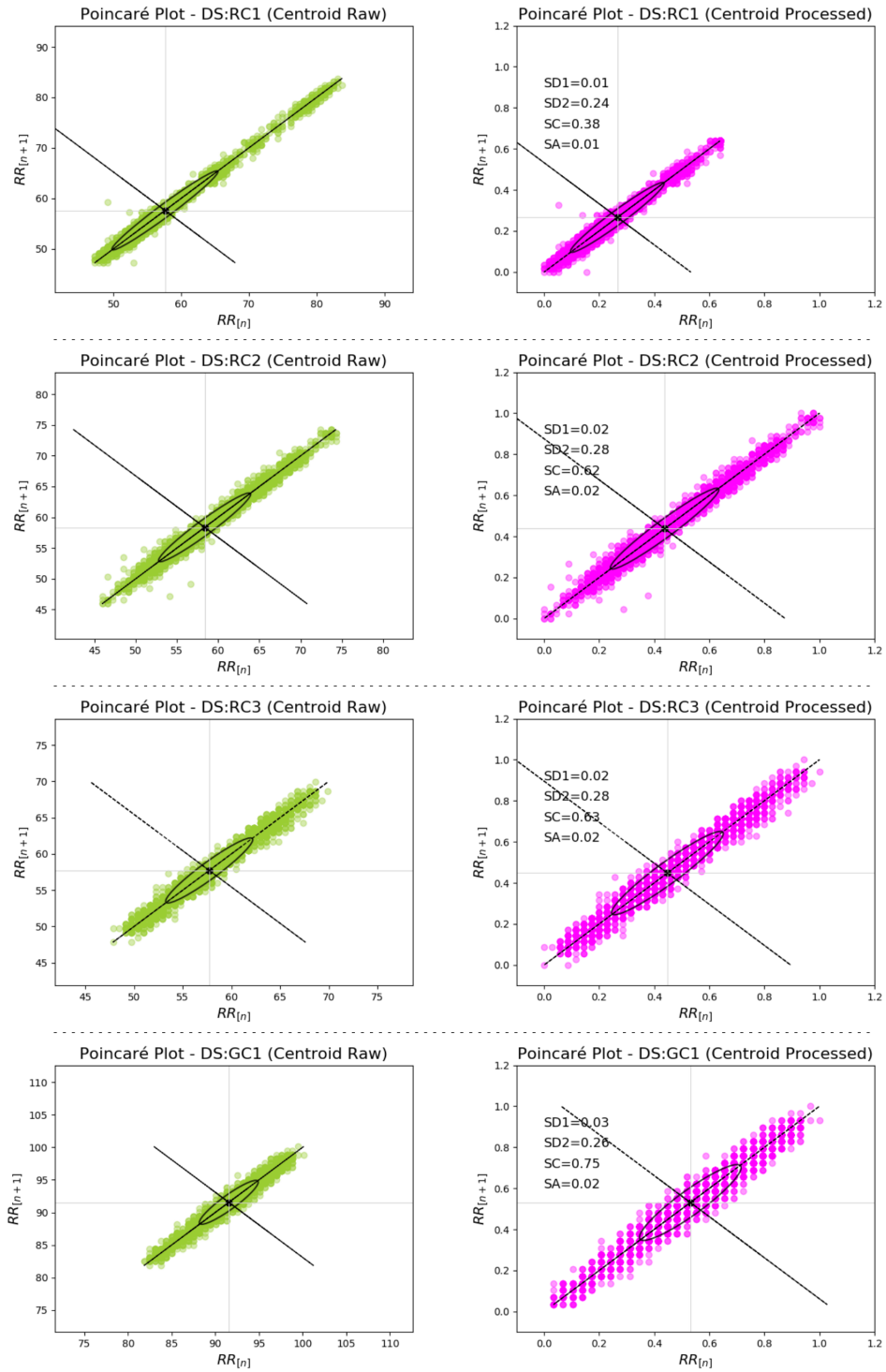


FIGURE 6.6. Poincaré plots for raw datasets and processed datasets (RC1 to GC1).

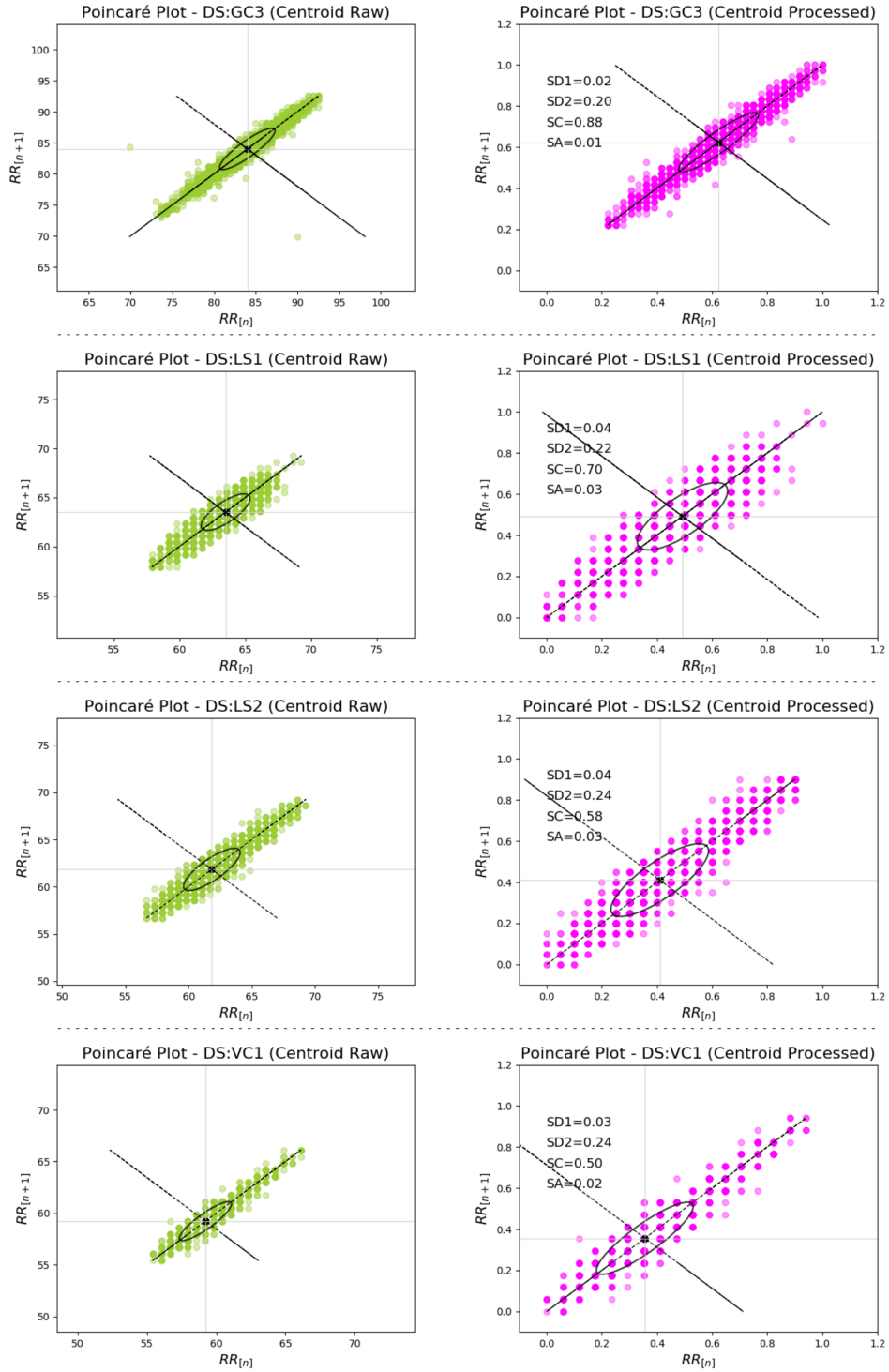


FIGURE 6.7. Poincaré plots for raw datasets and processed datasets (GC3 to VC1).

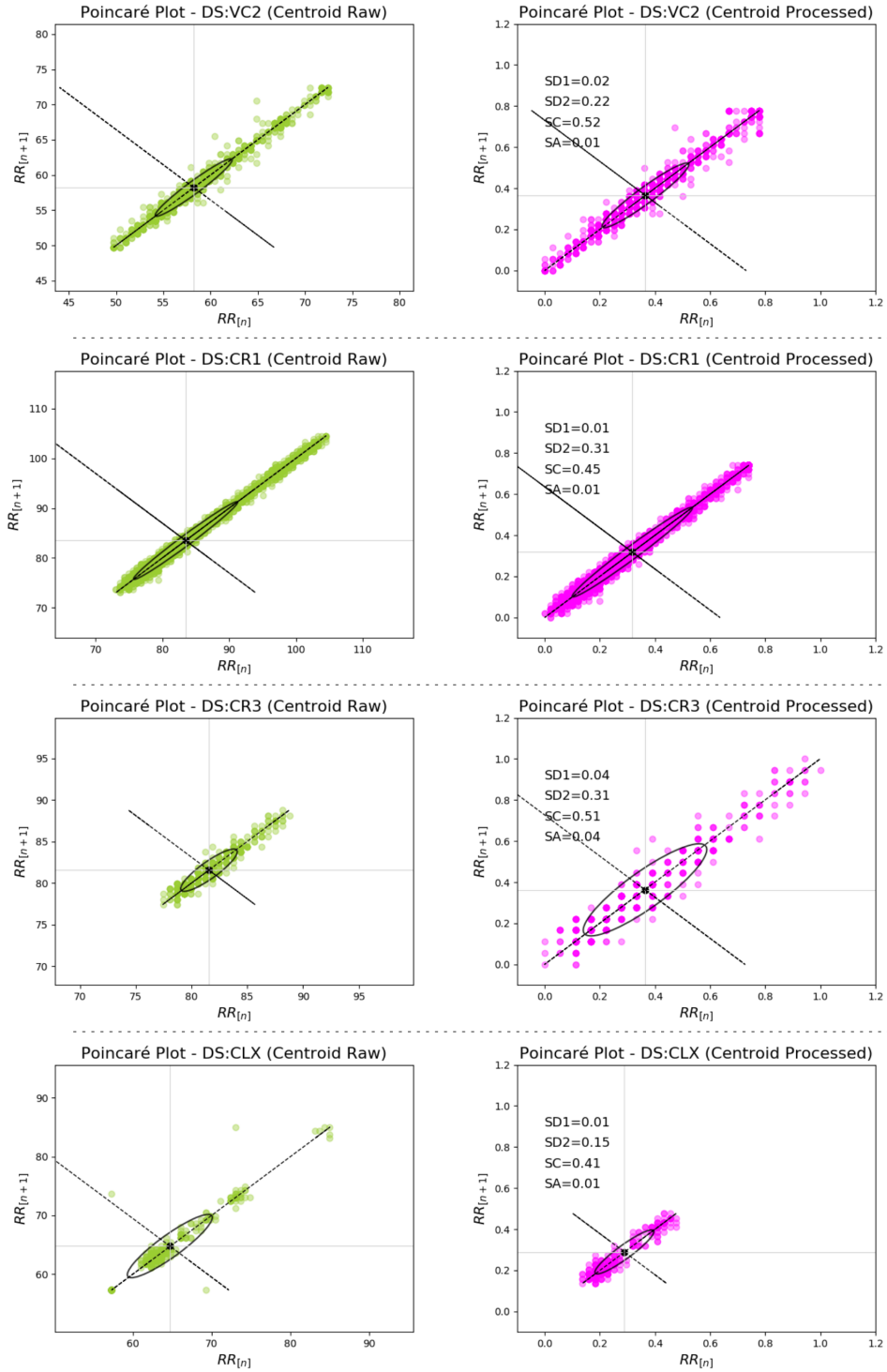


FIGURE 6.8. Poincaré plots for raw datasets and processed datasets (VC2 to CLX).

6.1.8. Sample Absolute Interval Range Features (FEAT_RNG)

The range of a sample was also used as a feature. It is defined as the absolute difference between the values referent to the last $f(t)$ and the first position $f(t - \Delta t)$ of a sample in time, as shown in Equation 6.16, which Δt represents the interval length to displace the interval from the actual position t .

$$R(t) = |f(t) - f(t - \Delta t)| \quad (6.16)$$

6.2. Singular Value Decomposition - Features Selection

Since the features were extracted, some of them can be useless in the recognition process due its low representativity. To select the best set of them, the features must to have its dimensionality reduced. Thus, the Singular Value Decomposition (SVD) was used, executing a matrix decomposition or matrix factorization of the input matrix (extracted features). It is based on eigenvalues, applied to a bidimensional $m \times n$ matrix A .

Mathematically, this method factorizes a matrix into a product of matrices, as shown in Equation 6.17.

$$A = UDV^*, \quad (6.17)$$

where D is a nonnegative diagonal matrix, having the singular values of A ; U and V are matrices that satisfy the condition $U^*U = I$ and $V^*V = I$. The resultant matrix of this decomposition, is the new input matrix applied into the recognition process.

6.3. Features Columns Centering

After apply a matrix decomposition, a mean centering or also called column/block centering was computed. It is important to normalize the input vector for each data, in the same space of reference to have zero expectation by each measurement i.e., must be centered as shown in Figure 6.9.

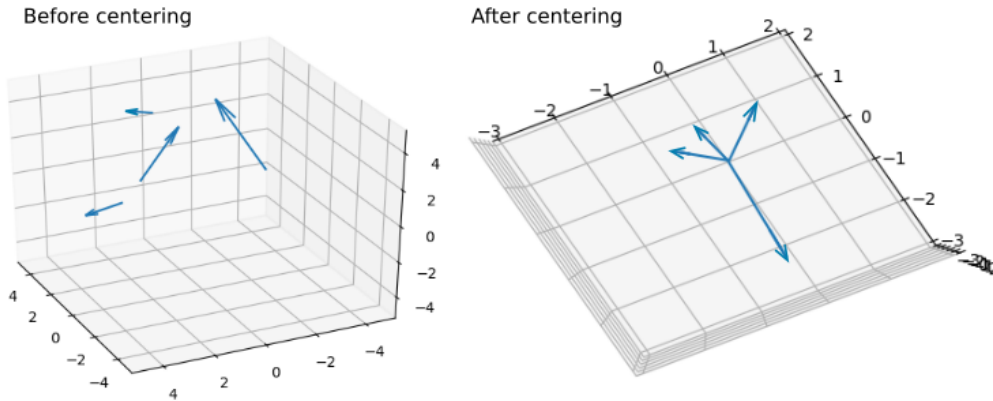


FIGURE 6.9. Columns centering over feature vectors, before (left) and after (right).

Equation 6.18 below, shows how to apply it for each data column, which C_A represents the centered columns and μ_A represents the mean of each column vectors or columns from dataset A .

$$C_A(n) = \sum_{n=1}^N (A(n) - \mu_A) \quad (6.18)$$

6.4. Features Correlation

Several statistical parameters are used to analyze the extracted features such as: point estimation, probability density function and Pearson Correlation Coefficient (PCC).

To not interfere negatively on the final result, some features were not used. In this work, the features means and medians were strongly correlated, motivating us to use only one of them, as shown in Figure 6.10.

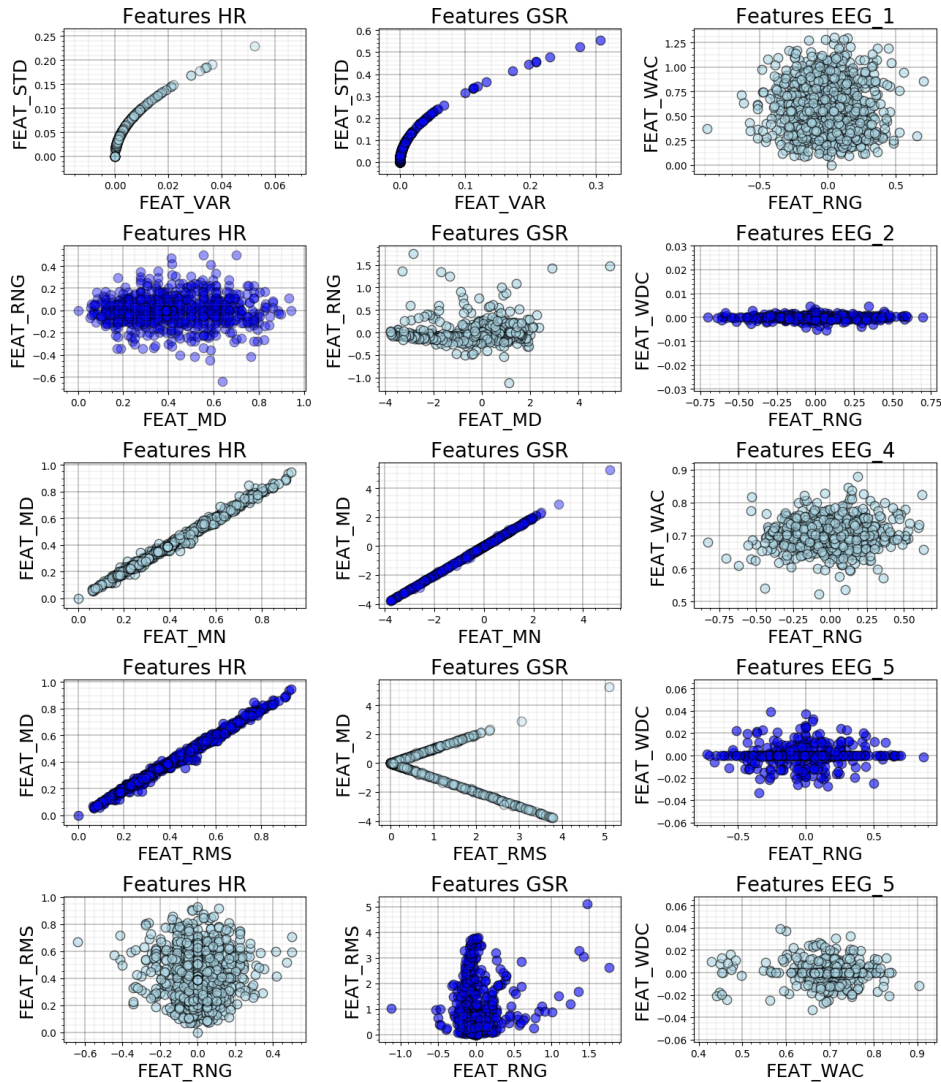


FIGURE 6.10. Scatter plot for some extracted features.

6.4.1. Pearson Correlation Coefficient - Evaluating the Features Correlations

The selection of the best features, is the process of select relevant features or remove the worst one. The best features improve and the worst degenerate the model accuracies.

In this work, the feature selection was based on correlation coefficient measurement, which it is an important method for feature analysis in machine learning models. It measures how strongly one variable or feature, depends over another variable and basically, it is defined in numerical range between -1 to +1. Variables which are uncorrelated with the analyzed objective, probably it should interfere negatively on the final model or result. In addition, if two variables

are strongly correlated to each other (i.e. very close to $[-1;-0.9]/[+0.9;+1]$), is recommended to eliminate one of these variables because seems to be same. A good correlation can merge between $[-0.7;-0.5]/[+0.5;+0.7]$.

There are three types of features correlations: positive correlation, negative correlation and no correlation (null correlation).

The most used correlation coefficient method, is the statistical method called Pearson Correlation Coefficient (PCC), also called as R-correlation, and it is defined by Equation 6.19.

$$R = \frac{\sum_{n=1}^N (y(n) - \bar{y})(\hat{y}(n) - \bar{y})}{\sqrt{\sum_{n=1}^N (y(n) - \bar{y})^2 \sum_{n=1}^N (\hat{y}(n) - \bar{y})^2}} \quad (6.19)$$

Simplifying this, we can find the Equation below.

$$R = \frac{\sqrt{\sum_{n=1}^N (\hat{y}(n) - \bar{y})^2}}{\sqrt{\sum_{n=1}^N (y(n) - \bar{y})^2}} \quad (6.20)$$

There are also methods called, determination coefficient, which it is mainly used as regression metrics method e.g., the square of PCC (R^2).

The prior sections shown the extracted features used to recognize emotions. It were features based on statistics, peaks detection, RR dispersion and wavelets. In general, the features extraction stage isn't sufficient to aim totally the next stage of an emotion recognition. Thus, all of them needed to be analyzed before going forward, since some of them can have low representativity on the recognition process. For this reason, SVD and other normalization were also applied.

Emotion Recognition

Emotion recognition is the process of identifying human emotions through the attribution of emotional states based on the observation of visual and auditory nonverbal cues. It includes facial, vocal, postural, and gestural cues displayed by a sender, that is, a person displaying an emotional reaction (Bänziger, 2014).

The proposed emotion recognition was based on Artificial Neural Networks (ANN) and Deep Learning techniques (DL). It was implemented with Python3 Toolkits (standard and data processing libraries), PyBrain, Keras and TensorFlow. This last, having also execution support of the Graphics Processing Unit (GPU).

7.1. Artificial Neural Network

The ANN is a supervised technique, inspired by the human's brain behaviours, which it can process several instructions in short periods of time, taking fast decisions and reactions. Its topology architecture can be designed according to the problem to be solved being based on the number of layers and neurons. A low number of neurons is recommended to solve simpler problems. However, if the problem complexity increases, another number of neurons must be analysed as needed. Mathematically, each single neuron, represents a single function over several parameters of activation and thresholds (or biases).

The use of ANN and DL to accurately recognize emotions, was based on a couple of researches, which it was analyzed to find out which techniques are more used nowadays on this context (see the most used techniques presented in Chapter 1). These analyses show that the techniques based on neural networks e.g., ANN, CNN, RNN, DNN, are powerful tools due to their high capacity to solve complex tasks, being massively used on modern controls, dynamic systems, data mining, automatic bio-patterns identification (e.g. fingerprints or face recognition) and robotics. It is possible to cite also the high capacity of the ANN, to produce complex and parallel solutions over the field of extracted features. Each ANN layer, can present different and parallel outputs. It is also possible to use ANN combined with other techniques such as, K-Means or SVM, for instance.

7.1.1. McCulloch-Pitts Neuron Model

The McCulloch-Pitts neuron model, was proposed in 1943 by the neuroscientist Warren McCulloch and the logician Walter Pitts. They designed the artificial neurons (perceptrons) as a structure based on: inputs, activation functions, weights, thresholds and outputs. In this model, the neurons are connected by weights and biases, to control the network output. A single perceptron network is called single-layer perceptron, which it represents a single boundary line having low capacity of classification or regression i.e., very low dimensionality. If the network presents more than a single neuron layer, it is called Multi-Layer Perceptron (MLP), which it can solve

complex problems of regression and classification. Figure 7.1, shows the structure of a single neuron model proposed by McCulloch-Pitts.

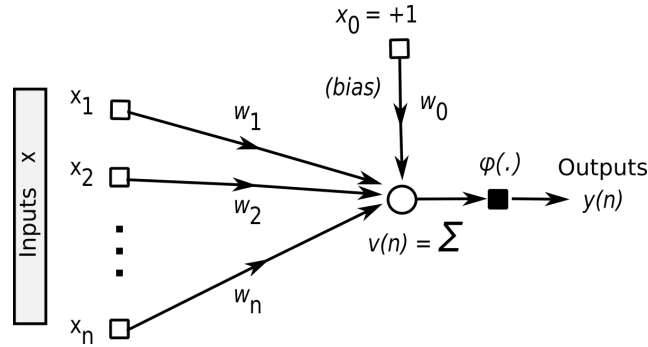


FIGURE 7.1. Perceptron model.

Several activation functions can be used to compute the neuron output, such as: identity, binary step, logistic (also called sigmoid, sigmoidal or soft step), tangentoid, Inverse Square Root Unit (ISRU), Rectified Linear Unit (ReLU), softmax, among others. In this work, three of them were considered: sigmoidal, softmax and ReLU.

7.1.2. ANN Development and Modeling

Since the ANN is a supervised method, the training must to be considered. The data training represents one fraction of the dataset and it is defined in Equation 7.1, where τ represents the training-set, $x(n)$ the input-set (or input signal features), $d(n)$ the desired output in each iteration n , and N_i that represents the number of instances of the training-set (Haykin, 2011).

$$\tau = \{x(n), d(n)\} \Big|_{n=1}^{N_i} \quad (7.1)$$

The induced local field (for forward computation), was used and can be computed by Equation 7.2, which x_i goes from input neurons i ; w_{ji} , and w_b represent the weights connections from the neuron j to i , and b_{ji} is the bias applied for each neuron, by iteration n .

$$v_j(n) = \sum_{i=1}^N w_{ji}(n)x_i(n) + b_{ji}w_b, j \geq 1 \quad (7.2)$$

For each hidden layer, two different activation functions were considered: the sigmoidal and ReLU. The sigmoidal activation function $\varphi(\cdot)$ is defined by Equation 7.3, where a determines the threshold of the function. The sigmoid function returns values between 0 and 1.

$$\varphi_j(v_j(n))_{sig} = \frac{1}{1 + e^{-av_j(n)}}, a \geq 1 \quad (7.3)$$

Another activation function applied in this work, is the ReLU or rectified linear unit. It is defined by Equation 7.4, which it returns values between 0 and $+\infty$.

$$\varphi_j(v_j(n))_{ReLU} = \begin{cases} 0 & \text{if } x < 0 \\ x & \text{if } x \geq 0 \end{cases} \quad (7.4)$$

Regarding to output layer, also two different activation functions were considered: ReLU and the softmax, which the last one is defined by Equation 7.5. It represents the prediction probability for each emotion, over all output neurons having values between 0 and 1.

$$P(y = j|X)(n) = \frac{e^{v_j(n)}}{\sum_{k=1}^{N_o} e^{v_k(n)}}. \quad (7.5)$$

The $P(y|X)$ is mainly applied in case of classification problem i.e., which the outputs return independent probabilities limited by the number of output classes in case. Otherwise, when using the $\varphi_j(v_j(n))$, the ANN output can be represented by any amount of neurons, which it must to return independent values (not probabilities), being useful when we are working with regression analysis. Since this work lies over the ANN and regression problems, the $\varphi_j(v_j(n))$ was used.

The error signal or instantaneous error produced by each neuron j forms the output layer, defined by Equation 7.6,

$$\varepsilon_j(n) = d_j(n) - y_k(n), \quad (7.6)$$

where $d_j(n)$ represents the j th element of $d(n)$ and $y_k(n)$ the k th instantaneous output. Furthermore, the $y_k(n)$ and the instantaneous error energy (ξ) of each neuron j (Equation 7.7), are both considered to reach the best network accuracy along the training epochs (iterations) (Marsland, 2015; Haykin, 2011).

$$\xi_j(n) = \frac{1}{2}\varepsilon_j^2(n) \quad (7.7)$$

The local *gradient* applied to each neuron k from the output layer, is described by Equation 7.8.

$$\delta_k(n) = \varepsilon_k(n)y_k(n)(1 - y_k(n)) \quad (7.8)$$

The ANN weights adjustments (for backward computation) applied to each output neuron, are defined by delta-rule (Equation 7.9) (Haykin, 2011),

$$\Delta w_{kj}(n) = \alpha\Delta w_{kj}(n-1) + \eta\delta_k(n)y_k(n), \quad (7.9)$$

where the momentum α ($[0;1]$) is used to avoid learning instabilities while it increases the learning rate η ($[0;1]$), to decrease the mean error; both variables are adjusted during the training phase.

7.1.3. Learning Rate Analysis

The learning rate is a fundamental variable to optimize the learning process in the recognition process. One way to find the best learning rate for such problem, is to relate the learning rate with the recognition loss or error.

For a too low learning rate, the loss function doesn't improve enough; when it is too high, the loss function i.e. the recognition begins to diverge. In the optimal learning rate range, the loss is controlled and the recognition accuracy is the most reliable, as shown in Figure 7.2-left. Figure 7.2-right, shows the *log* of the percentage of correct matches, when it intends to consider

one emotion class for each ANN output i.e., when the higher value of each neuron is taken, as the majority emotion in case (emotion classes).

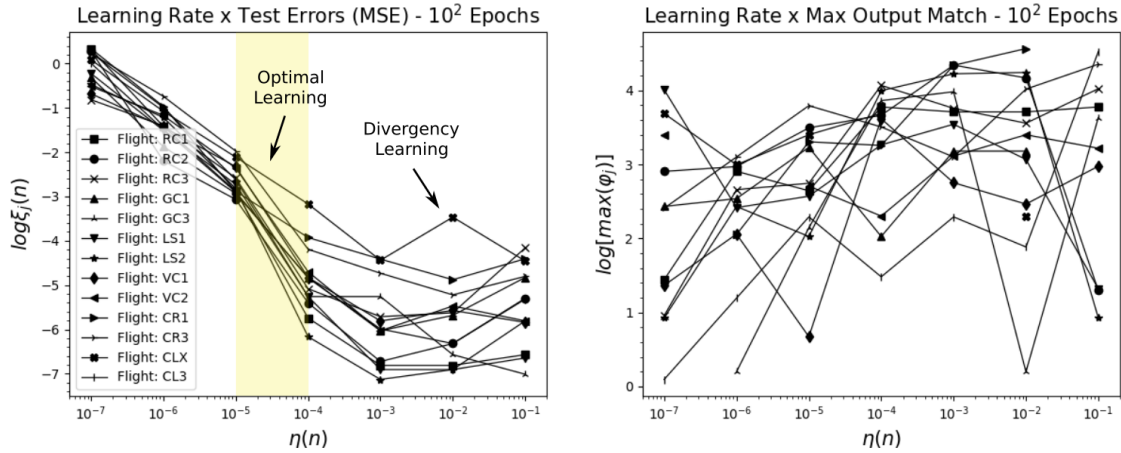


FIGURE 7.2. Learning rate $\eta(n)$ analysis by test errors $\varepsilon(n)$ for each iteration n from RC1 to CL3 (left); learning rate by correct matches (right).

The best learning rate selection used in the present work, was based on a stochastic or empirical mode, and dynamic mode.

On stochastic or empirical mode, the learning rate selection is made using a range of learning rates, testing one by one. In this case, this selection shown that the optimal learning rate range was between 10^{-5} and 10^{-4} . In this mode, the higher learning rate of this interval ($\eta = 10^{-4}$) was chosen for the recognition process.

In dynamic mode the deep learning method was used. In this case, the ‘‘Adam’’ optimization (Kingma and Ba, 2015) can be used. It is an optimization algorithm used to update network weights iteratively based on training data; it is another option instead of the classical stochastic gradient descent method.

7.1.4. Finding an Optimal Hidden Neurons

The layers placed between the input and output layers, are called hidden layers where the hidden neurons are present. A common challenger about the hidden layers, is to find an optimal number of hidden neurons inside them.

The number of the best hidden neurons to use, is found empirically according to the dataset and model to be reached. According to Hastie et al., typically the number of hidden neurons is somewhere in the range of 5 to 100, with the number changing according to the data inputs and training iteration (Hastie, Tibshirani, and Friedman, 2016); otherwise, the produced model might not have enough adaptability to figure out the nonlinearities of the input datasets. To compute the optimal number of hidden neurons avoid overfitting along the training (Equation 7.10).

$$N_h = \frac{N_s}{\rho(N_i + N_o)}, \quad (7.10)$$

where N_h , defines the number of neurons inside the hidden layers; N_s , defines the number of samples from the training dataset; ρ , defines an arbitrary scaling factor usually between 2 and 10, to indicate how general the model should be prevent overfitting; and N_i and N_o , define

respectively the number of input and output neurons. Another common approach to compute the optimal number of hidden neurons, is defined by Equation 7.11.

$$N_h = \sqrt{N_i N_o} \quad (7.11)$$

Other ways to compute the number of hidden neurons are also present by Huang and Hsu (Huang and Hsu, 2012; Tieding, Xijiang, and Shijian, 2010; Yeh, 2003).

7.1.5. Finding an Optimal Train Iterations

The increase the number of training iteration, does not mean that it increases the recognition learning along a new data as well, even if there are descend errors along the training.

Analyzing the descend errors from the train and test (validation), it is possible to detect the moment to stop training, as shown in Figure 7.3. There, it is possible to note the point of divergence between the train and test errors, where it must be used as the stop condition of the training, even if the training descend errors continue to decrease. It because the produced model can fit very well to the training dataset, but very bad at predicting new datasets. This unwanted situation is called overfitting.

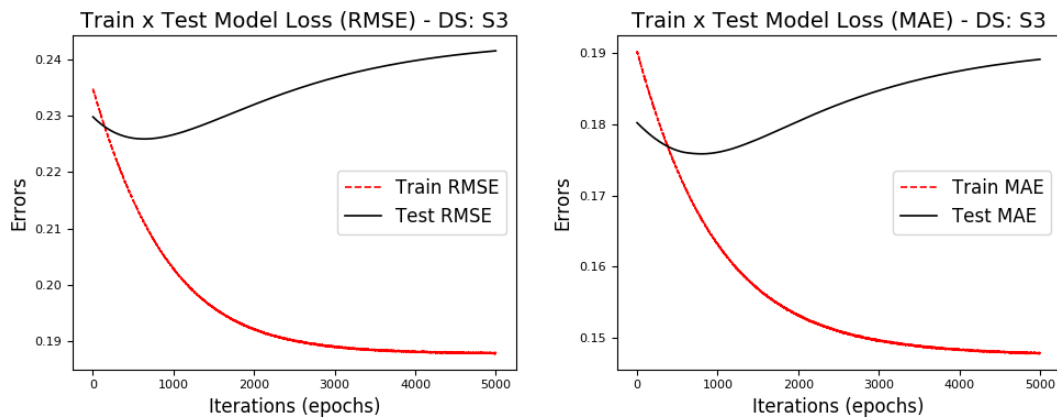


FIGURE 7.3. Descend errors and divergence descend close to 1,100 iterations.

7.2. Cross Validation - Testing Recognition Models

The emotion recognition tests, were executed based on the methodology of Leave-One-Out Cross Validation (LOOCV) (Baron and Stańczyk, 2021) because it shown to be a good methodology on the proposed multimodal system. It is based on leaving one flight dataset out (k), while it trains the ANN using the other flight datasets ($N-1$). In a practical emotion recognition, it uses the emotion datasets of the other volunteers to detect the emotions of one single volunteer (Figure 7.4).

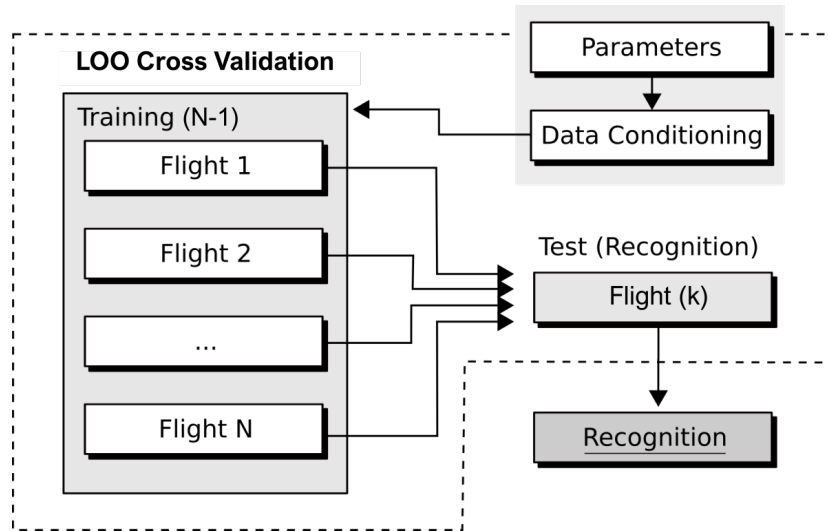


FIGURE 7.4. Cross validation applied to test the models. It trains using volunteers datasets, to detect emotions of one single volunteer k .

7.3. Realtime Outliers Removal - RTOR

In realtime regression problems, sometimes the neurons output outliers values that are very far of the optimal value; such wrong values are critical to compute correctly the evaluation metrics in realtime e.g., absolute mean errors. To correct this problem, the Realtime Outliers Removal (RTOR) method was developed in this work. The RTOR adds another layer after the ANN output, creating a batch of the outputs values $y_{1 \rightarrow n}$ to find local outliers. If it is detected, the final output will be normalized according to outliers removal methods, as shown in Figure 7.5.

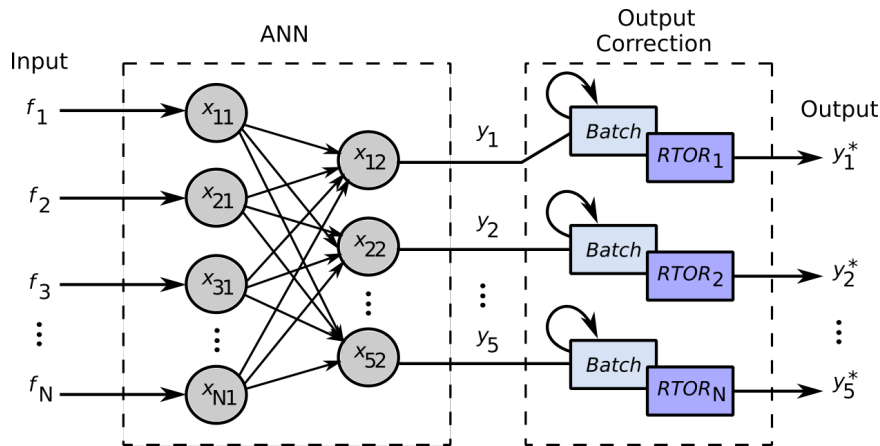


FIGURE 7.5. ANN using RTOR methodology over the output neurons $y_{1 \rightarrow n}$.

Figure 7.6, shows how it works and how its methodology is useful to produce better regression models, according to the ANN outputs. The new outputs $y_{1 \rightarrow n}^*$, are based on the batch length, which it represents the number of samples to be treated in realtime.

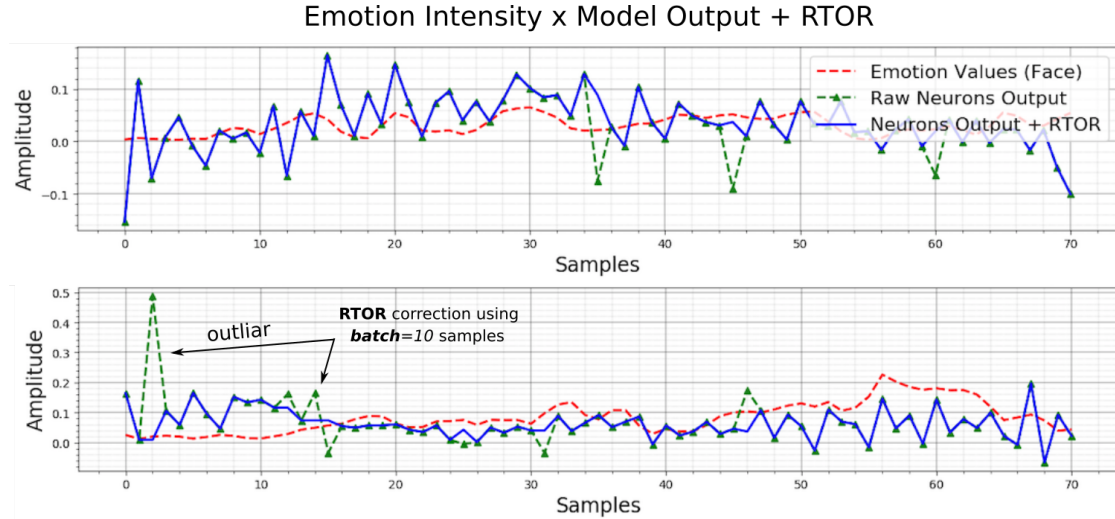


FIGURE 7.6. RTOR being applied on a neuron output. Note the corrected output y_k^* (blue) and the raw output y_k having outliers (green).

7.4. Evaluation Metrics for Emotion Output - Regression Models

Before present metrics to evaluate the emotion recognition outputs, it is extremely important to know that this work does not considers one single emotion as final output, but intensities of five emotions by time, outputted from each independent output neurons. It because, as was said in the introduction of this work, the human body can't feel one single emotion by time, but several of them, having different intensities and valence. For this reason, the presented evaluation metrics, work over all regression outputs, which it was measured separately.

Each output neuron was designed as a regression function (emotion intensities). These outputted emotions intensities are measured to define the quality of it, according to the ideal or target outputs from the training. Thus, below are presented several methods used to quantify the emotion recognition over the outputs.

7.4.1. Mean Absolute Relative Difference (MARD)

The measurement of the recognition's accuracy from each output neuron, was also based on the Mean Absolute Relative Difference (MARD). It corresponds to a direct comparison between paired measurements of a given neuron prediction and the target value.

Mathematically, it is computed as the mean value of the absolute relative difference (ARD) between the prediction outputs ($\hat{y}(n)$) and the target, as defined in Equations below (Kirchsteiger et al., 2015).

$$ARD(n) = 100\% \frac{|\hat{y}(n) - y(n)|}{y(n)} \quad (7.12)$$

$$MARD = \frac{1}{N} \sum_{n=1}^N ARD(n) \quad (7.13)$$

7.4.2. R-Squared Value (R^2)

The R^2 , is a statistical measure of coefficient determination (different of the coefficient correlation from prior chapter). It defines how well a regression line prediction, estimates the actual

regression output. In another words, it represents the proportion of the variance for an output values, that is explained by a linear model.

To calculate it, some variables must to be considered: the actual values $y(n)$, compute the mean of those values (\bar{y}) and look at the distance from the actual values to the mean ($D_{[y \rightarrow \bar{y}]}$); draw a regression line, and we come up to estimated values $\hat{y}(n)$ i.e., points from this line; compute the distance from estimated values to the mean ($D_{[\hat{y} \rightarrow \bar{y}]}$); and compare these distances values i.e, $D_{[y \rightarrow \bar{y}]}$ with $D_{[\hat{y} \rightarrow \bar{y}]}$, as defined by Equation 7.14 (Fukuyama and Goto, 2016).

$$R^2 = 1 - \frac{\sum_{n=1}^N (\hat{y}(n) - \bar{y})^2}{\sum_{n=1}^N (y(n) - \bar{y})^2} \quad (7.14)$$

It is measured between 0 to 1. When the model does not explains any of the variation in the response variable around its mean, it returns 0; otherwise, in a total fit situation, if the model represents all of the variation in the response variable around its mean, it returns 1. For larger R^2 , a better regression model is obtained.

7.4.3. Root Mean Squared Error (RMSE)

The Root Mean Squared Error (RMSE) or also called, Root Mean Squared Deviation (RMSD), computes the error distance between the estimated values $\hat{y}(n)$ and the actual values $y(n)$ and can range between 0 and ∞ , as defined below.

$$RMSE = \sqrt{\frac{\sum_{n=1}^N (\hat{y}(n) - y(n))^2}{N}} \quad (7.15)$$

7.4.4. Mean Absolute Error (MAE)

The Mean Absolute Error (MAE), represents the average of the absolute difference between the predicted values and the observed value (output or prediction). In another words, it is a linear representation, which all the single differences are weighted equally in the average, as shown in Equation 7.16. Like RMSE, it also can range between 0 and ∞ :

$$MAE = \frac{1}{N} \sum_{n=1}^N |y(n) - \hat{y}(n)| \quad (7.16)$$

This chapter presented how the emotion recognition were defined and executed in this work. ANN architecture, numbers of hidden neurons and layers were some of the information presented. In addition, several methods to analyze the obtained output models were also explained, such as outliers removal in realtime, test or validation methods i.e. LOOCV, and evaluation metrics for emotion outputs.

Result on β -Band Analysis from Simulated Flight Experiments

Considering the simulation experiment and the acquired EEG data of the volunteers, the β -band analysis was carried out based on: spectrogram analysis and statistical analysis of the brain activities, according to each proposed flight task.

8.1. β -Band Spectrogram Analysis

The developed software and spectral analysis were based on Python libraries. The spectrograms were executed by the *scipy.signal.spectrogram*. Figure 8.1, shows the EEG spectrogram referent to the flight dataset RC1, which each vertical line delimits the tasks from 1 up to 7. It was acquired of the volunteer's frontal left lobe (channel Fp1). Figure 8.1-a, shows the data already filtered (between 12 to 40Hz) correspondent to beta band (Kropotov, 2009). The raw EEG dataset (already detrended), is shown in Figure 8.1-b, where it is possible to observe a full band data before the filtering.

To try to relate the volunteer brain activities according to each flight tasks, the EEG spectrogram was considered over the β -band, presenting different magnitudes, according to each flight task. Observing the Figure 8.1-(d,e), it is possible to observe a lower magnitudes during task 3 (cruise flight), that mainly corresponds to the frequency interval between 12 and 30Hz, which it may also indicates a relaxation of the beta brain activity, thus also the volunteer, due the low complexity of the present task.

According to some safety reports, on a real aviation context (Boeing, 2017; ICAO, 2017), the safest flight phase, having the lowest number of accidents, occurs exactly in the flight phase equivalent to task 3. It shows that, the proposed experiments were able to produce similar physiological responses of a real pilot in flight. The considered spectral results can be useful to better understand why in some flight phases higher probability to occur accidents is presented. These physiological responses felt by each volunteers of these experiments, were naturally produced i.e., the experiment supervisor did not interfere on these reactions, not even he said that tasks are the most risky.

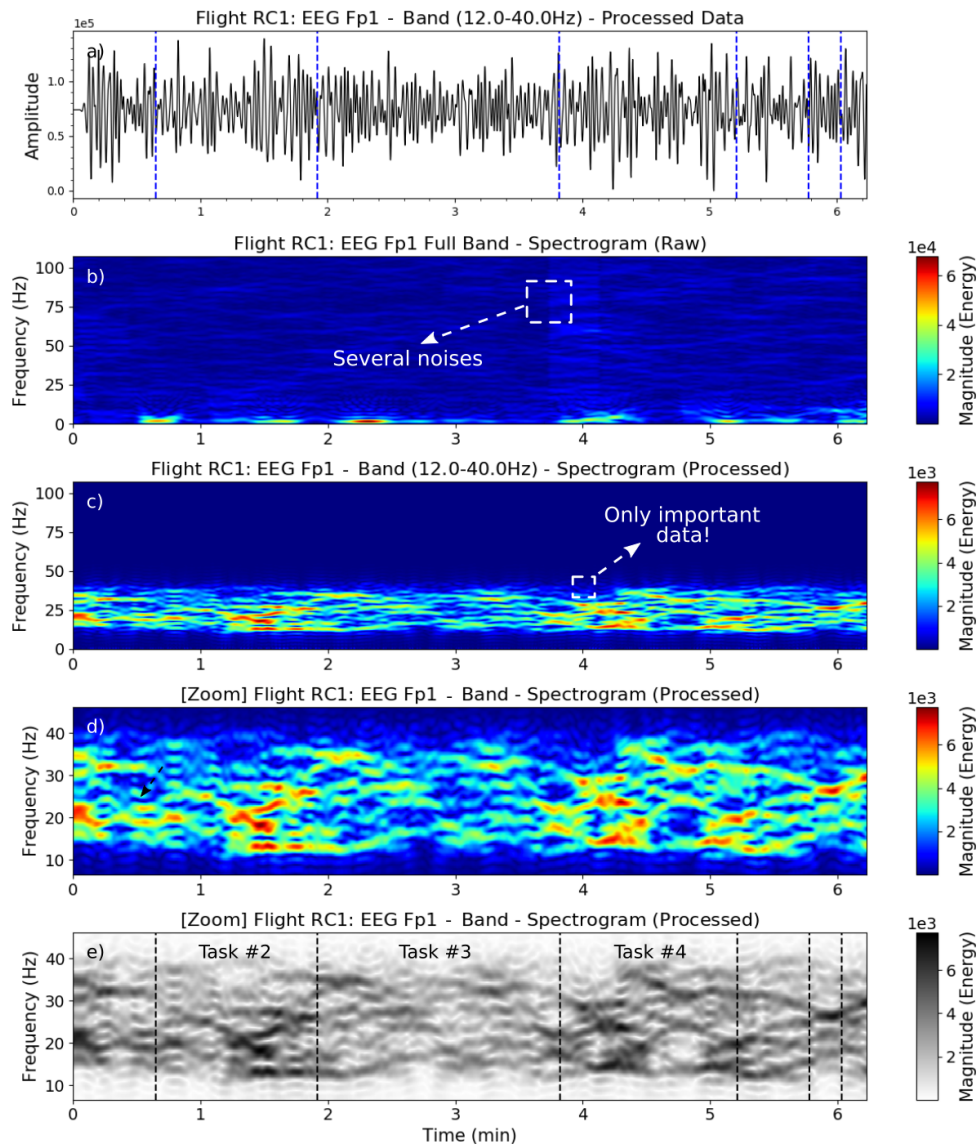


FIGURE 8.1. Spectrogram of the flight dataset RC1-frontal left lobe (Fp1). (a) Processed 12-40Hz data; (b) Raw data spectrogram; (c) Spectrogram of the processed 12-40Hz data; (d) Processed data on delimited Y-axis; (e) Grayscale spectrogram with tasks delimitation.

These higher spectra magnitudes are result of a natural complexity of some flight tasks e.g. takeoff and landing, which they require more attention and precise use of flight commands. This can explain why the beta band magnitudes increased when the landing get closer, for instance.

By observing the temporal brain area (channel T8) of the same volunteer (flight RC1), it was also possible to see the brain responses during the flight (Figure 8.2). It is interesting to analyze the feelings of the volunteers (e.g. by using questionnaires), just after starts a cruise flight (task 3), which it come after a more intense situation (high brain activity) due problems during the climb task, to a more stabilized flight; at the same way, when the volunteer felt to be close to start to descent the aircraft (task 4), the brain activity (from frontal lobe Fp1 and temporal lobe T8) shown to increase again, reflecting that the volunteer starts to be alert (or even stressed) to execute the next task.

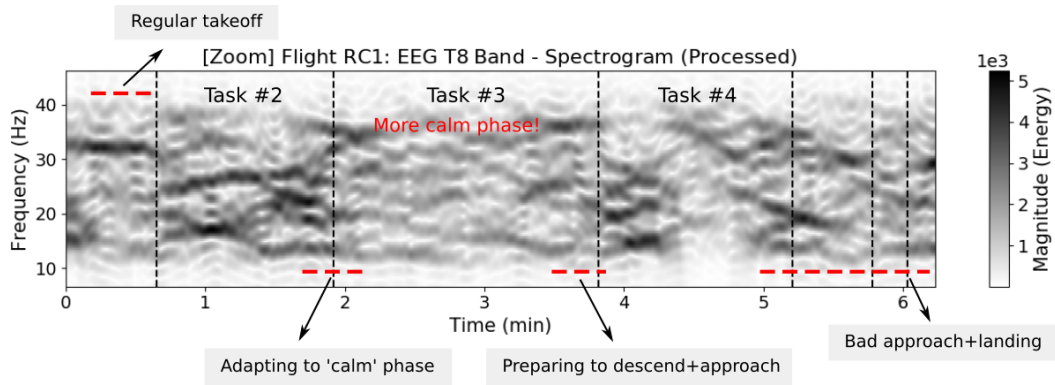


FIGURE 8.2. Spectrogram of the flight dataset RC1 - temporal right lobe (T8).

The volunteer of the flight RC1, reported feeling a little insecure, to execute the tasks climb, approaches and landing (tasks 2, 5, 6, and 7) correctly. Surely for this reason in this flight, the volunteer’s brain presented high magnitude and oscillation during those tasks, resulting in an accident on the last task i.e., landing.

A different way to represent the prior spectrogram (bottom plot), is shown in Figure 8.3. It represents the mean values of all magnitudes (on each frequency) computed by time. This representation shows the brain magnitudes along the time for each flight, of the temporal left and right lobes over positions T7 and T8.

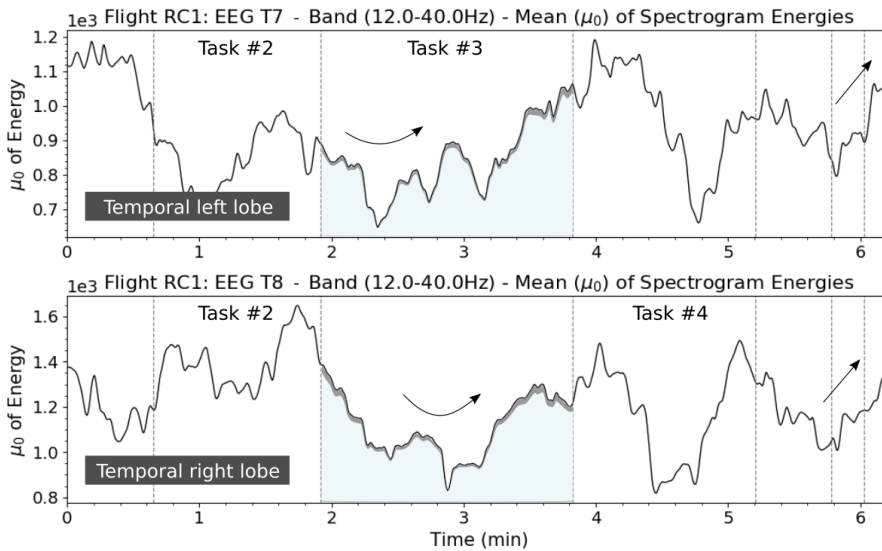


FIGURE 8.3. Mean values of spectrogram magnitudes of the flight dataset RC1 - temporal left and right lobes (T7 and T8).

By observing the temporal left lobe (channel T7), the brain signal begins high on takeoff (task 1), decreasing a little along the climb (task 2), being lower during the cruise flight (task 3); the signal starts to get high magnitudes again, when the volunteer prepared to descend (task 4), what obviously must demand more attention and alertness until the landing (task 7). Even though the volunteer of the flight RC1, was a mid-level volunteer on flight simulator, he reported to feel a little insecure on some tasks of the current flight. The opposite activity of T7 and T8, observed during the task 1, happened probably because the influence of other positions from the

brain, or due the volunteers move only one hand along the experiment reflecting these action on the other side.

Another situation of low brain activity during some flight tasks, can be found in the recorded data of the flight CR1 (frontal left lobe - F3) (Figure 8.4).

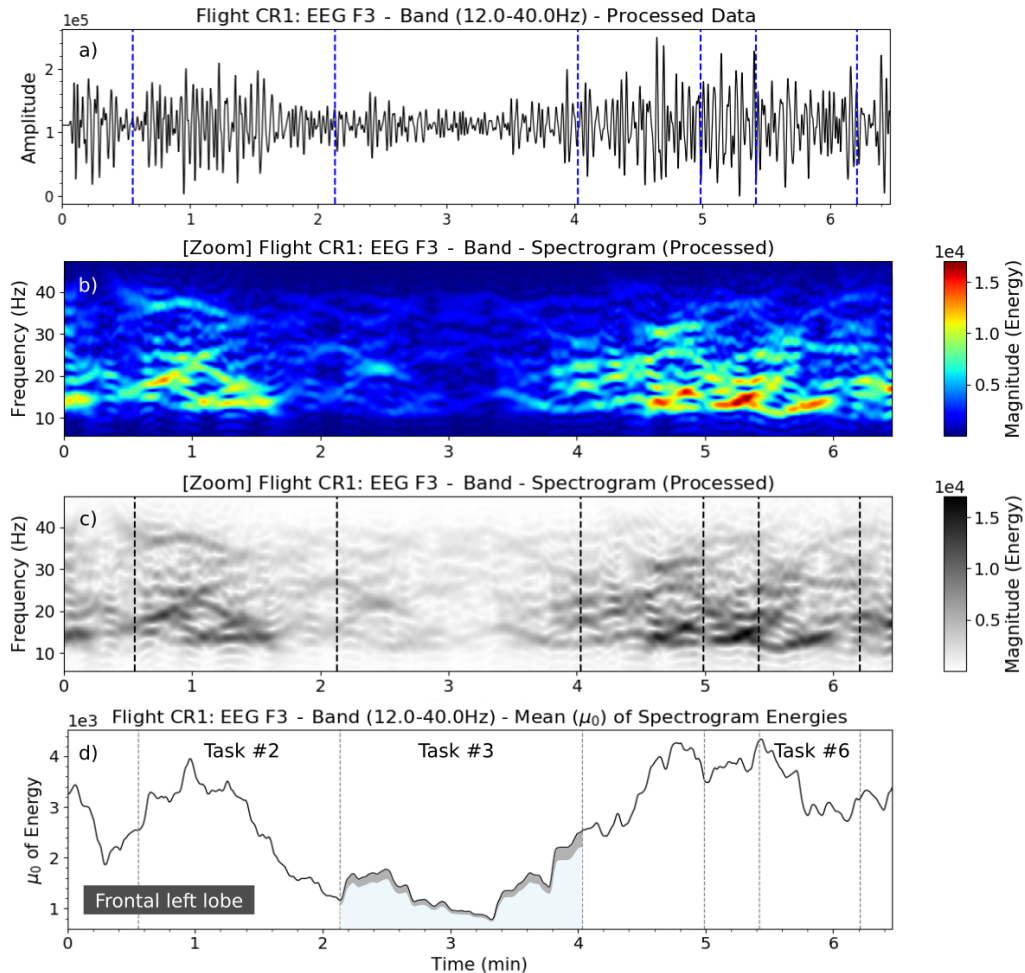


FIGURE 8.4. Spectrogram of the flight dataset CR1-frontal left lobe (F3). (a) Processed 12-40Hz data; (b) Spectrogram of the processed 12-40Hz data; (c) Grayscale spectrogram with tasks delimitation; (d) Mean values of spectrogram energies.

It shows clearly the lower levels of magnitude (mainly between 12 and 30Hz) just after takeoff (task 1) and during the cruise flight (task 3). The highest brain magnitudes were produced during the critical flight situations i.e., takeoff, approach and landing. In fact, different patterns of magnitudes were acquired on the same tasks of both flights, RC1 and CR1. The probable reason for such differences, are explained in Subsection 8.1.2.

8.1.1. Situations of Imminent Accident or Loss of Control

When the volunteers felt totally not confident about executing the tasks and/or in a situation close to an accident occurring, it was possible to see a high brain activities, as shown in Figure 8.5, with plots of the short flight experiment CR3, in which the volunteer lost the control of the airplane during the beginning of the climb (task 2), going off of the runway (runway

excursion) and not reaching the ideal velocity for takeoff. For that reason, the airplane did not reach an ideal altitude and vertical speed, colliding with the ground a few seconds later.

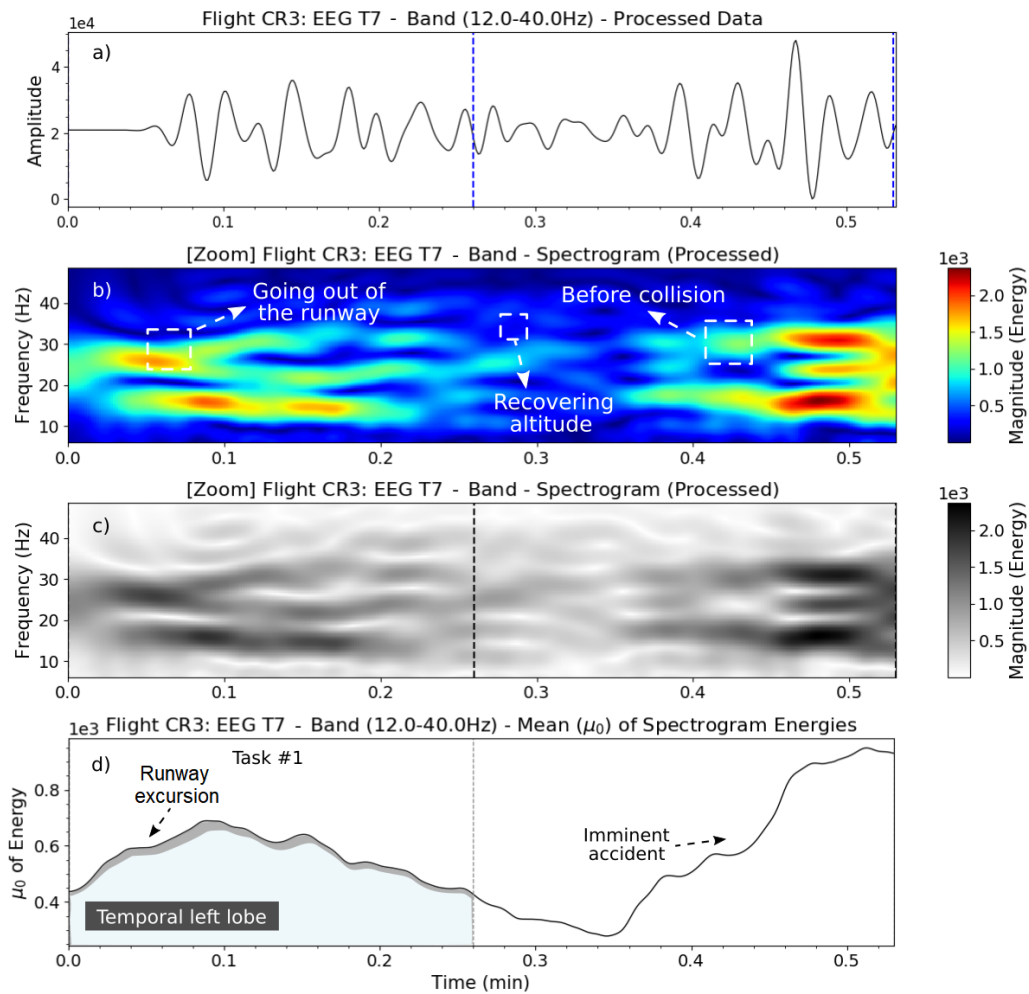


FIGURE 8.5. Spectrogram of the flight dataset CR3-temporal left lobe (T7). (a) Processed 12-40Hz data; (b) Spectrogram of the processed 12-40Hz data; (c) Grayscale spectrogram with tasks delimitation; (d) Mean values of spectrogram energies.

Regarding to the temporal left lobe (channel T7), the spectrogram of this flight clearly shows the brain activity just after the volunteer lost the aircraft controls and before the collision, with some trees over the airport area. For almost 8 s, the volunteer thought to get the airplane's controls again; probably for this reason, we can see a short period of lower brain magnitudes at the middle of the spectrogram (Figure 8.5b-d). Unfortunately, the accident occurred just few seconds after.

The same patterns of brain activities were also identified in other volunteers data; however, such a brain response depends on how the volunteer reacts when facing some flight phases. These experiments show that, when the volunteers have more experience with virtual simulation or even aviation, their brain activities presented a more similar pattern of amplitudes during most of the flight. This is important information for carrying out further research.

Analyzing the recorded video of the flight CR3 to detail the accident events, it was possible to see that the volunteer pushed the joystick back (i.e., takeoff command) at 40 knots (20.57 m/s or 74.08 km/h), instead of the recommended takeoff velocity of 80 knots (flight experiment’s checklist). After that, the aircraft started to climb slowly for almost 8 seconds (period of lower brain activity–false sensation of the correct flight procedure) and suddenly experienced a stall situation, colliding with the ground at 21 seconds. Then, the aircraft dragged on the ground, until it collided with some obstacles at 32 seconds (this was the second scared moment reported by the volunteer).

8.1.2. Volunteer’s Expertise and Brain Activity

All spectrogram analysis were used to show the brain behaviour along the tasks. It were based on volunteers that stated they were healthy. Using spectrogram analysis, it is possible to give support to know, how calm were the volunteers when facing some flight situations or moments, or also how was the volunteer’s biological reactions throughout the flight.

The spectrogram analysis obtained from the acquired data, shown a direct relation between the volunteers’ expertise (or their confidence on flight simulation) and the observed amplitude and oscillation of their brain activity during the flight. The experiment also shown that a more experienced and confident volunteers in the proposed flight tasks, had presented in general, different patterns of brain activities compared to volunteers having less expertise or less familiarity with flight simulations and/or electronic games. The volunteers informed their levels of expertise on the proposed experiment.

Figure 8.6, shows the mean values of spectrogram magnitudes of the frontal left lobe (F3) for two different volunteers: one volunteer feeling insecure to execute the proposed flight tasks, and the other volunteer feeling more confident to execute the same tasks.

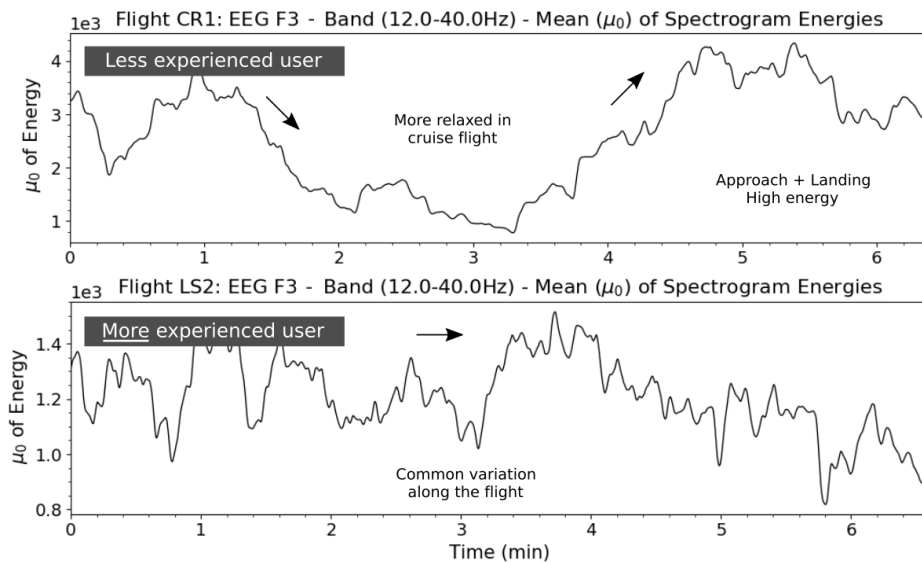


FIGURE 8.6. Mean values of spectrogram magnitudes of the flight dataset CR1 and LS2 - frontal left lobe (F3).

The brain activities of the less experienced volunteer (top plot), changed more intensely during the more calm flight phases, reaching mean values close to 4.5×10^3 units; it also presented a parabolic-shaped signal mainly between task 2 and 5, showing that the volunteer started to

feel calmer along the climb until start the descent procedure. Regarding to the more experienced and confident volunteer, it is possible to see that the brain activities, presented less intensities and less variability of magnitude along the tasks; it also reached an average amplitude close to 1.42×10^3 units i.e., 68% less, compared to the first volunteer. Such patterns were repeated along the most flights and volunteers.

The normalized mean values of the brain activities according to the volunteers' expertise, are shown in Figures 8.7-8.9, which the red line represents the beginner-level volunteers (i.e. datasets CR1, CR3, CLX and CLX), the blue line the mid-level volunteers (i.e. datasets RC1, RC2, RC3, GC1, GC3, LS1 and LS2) and the green line the mid-level and experienced-level volunteer (VC1 and VC2); it because this last datasets represents only one volunteer, which it weren't enough to reliably analyze alone. It shows clearly that a more experienced volunteers present in general, lower variations and amplitudes of the brain activities along the time; in the flight tasks which they have more complexity and risk to execute (i.e., task 1 and tasks 4-7), the beginner-level volunteers shown to be unsafe and thus reflecting in a high amplitudes of the β -band as it can be seen in Figure 8.7-Fp1, for instance.

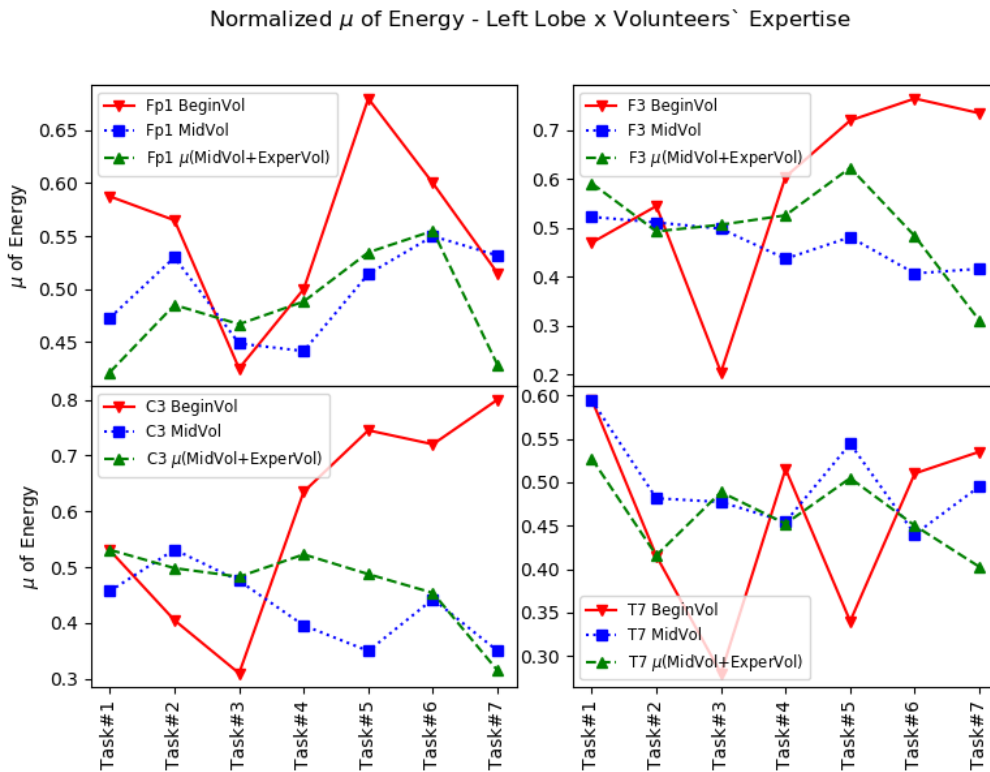


FIGURE 8.7. Normalized mean values of the brain activities for all datasets and the volunteers' expertise (left lobe).

In addition, these figures also shown that for all electrode positions, the beginner volunteers present the highest amplitudes in risky tasks and lowest amplitudes in task 3 (cruise flight), where they felt more relaxed after conclude the risky task takeoff. The same situation didn't happen with the more experienced volunteers which they shown to be more confident along most of the flight tasks as shown in Figure 8.8-Fp2 and 8.8-T8, for instance.

In every plots, the mean values of brain activities for both type of volunteers (mid-level and experienced-level), presents less oscillation between the tasks and lower amplitudes in critical

Normalized μ of Energy - Right Lobe x Volunteers' Expertise

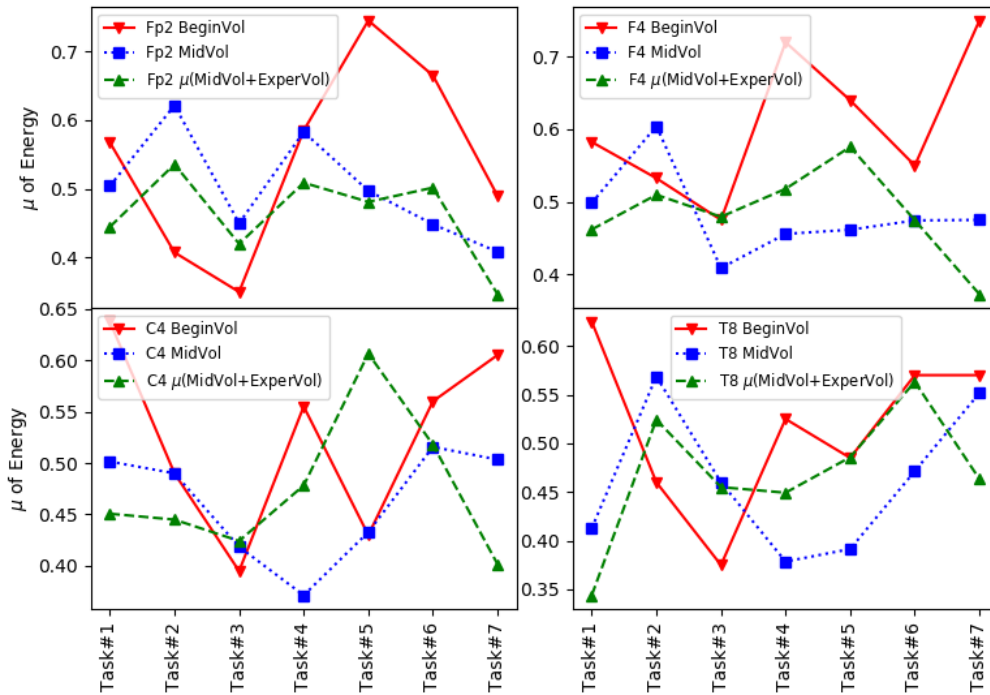


FIGURE 8.8. Normalized mean values of the brain activities for all datasets and the volunteers' expertise (right lobe).

flight phases such as, takeoff, approach and landing for instance. Another way to see that, is through the Figure 8.9, where in the takeoff, descend, approach and landing, the beginner volunteers presented higher amplitudes of brain activities compared to a more experienced volunteers on flight simulations.

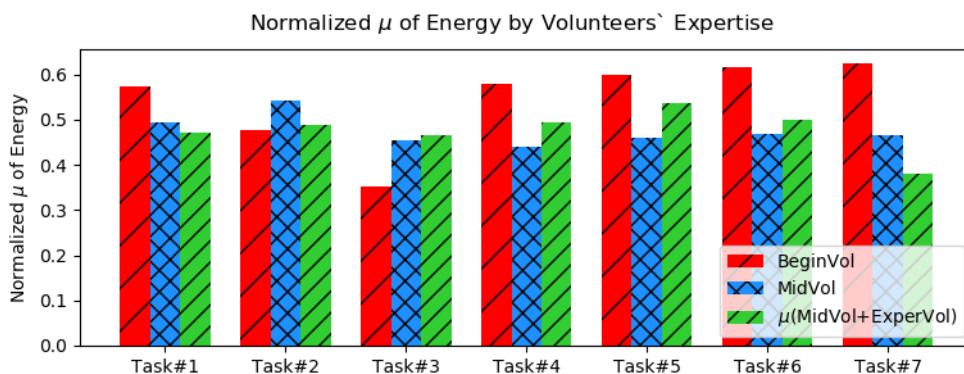


FIGURE 8.9. Normalized mean values of brain activities for all datasets over each task according to volunteers' expertise.

These last three figures reinforce the other figures and shown that indeed, a brain of a less experienced volunteers produces a more stabilized pattern of signal, being sometimes easy to identify an unsafe volunteer looking only for the data shape along the time and proposed tasks.

8.2. β -Band Analysis for Flight Tasks

A quantification of the brain responses for each flight task is described in this section, based on some statistical features.

The brain activities were analyzed according to each flight task: takeoff, climb, cruise flight (route), descent, approach, final approach and landing. It were measured based on some statistical features such as: mean value, standard deviation and variance. These information were useful to show the relation between the brain activities and those flight phases.

In less than 20% of the dataset, it is possible to observe that the signal of one lobe (e.g. left lobe), seems to have an opposite activities compared to the signal from the right lobe. One probably reasons observed for that, are based on: the brain signals coming from one lobe or position, interfering over the signal of other lobe; or due to the volunteers movements along the experiments, which they used the right hand to control the airplane, while the left hand kept immovable along each flight. Such observed motion artefacts on the beta band mainly over the motor cortex, are presented by Khanna and Carmena (Khanna and Carmena, 2017), Chung et al. (Chung et al., 2016; Chung et al., 2018).

Figure 8.10-left, shows the mean value μ_0 of the brain magnitude for each flight task, regarding to the frontal left lobe (channel Fp1). The parameter $\sigma^2[\mu_0]$ of the Figure 8.10-right, represents the variance of the mean value spectrogram μ_0 . It is important to show how the mean value spectrum μ_0 vary along the time.

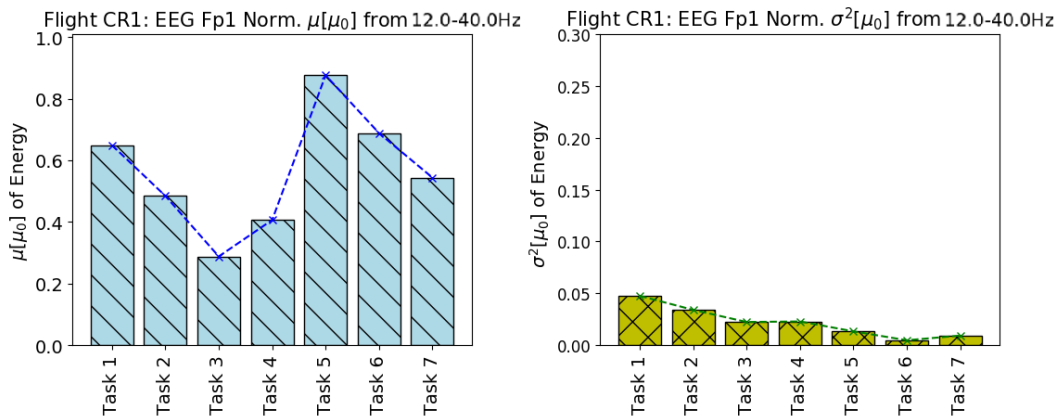


FIGURE 8.10. Mean values of brain magnitudes by tasks, of the flight dataset CR1 - frontal left lobe (Fp1), considering a total of 13 volunteers' datasets.

Table 8.1, presents the normalized mean values and standard deviation for dataset CR1. There, it is possible to see that the volunteer seemed to feel more calm or confident during the task 3; the initial approach (task 5) and final approach (task 6), presented the higher intensities.

The variance values of the brain amplitudes over the considered spectrum (12-40Hz) flight CR1, are shown in Figure 8.11. High variances between the frequencies in the same time (vertical axis), means that the spectrum magnitude of each frequency are highly different. Otherwise, it means that the brain magnitude in the same time, presented more similar intensities for each frequency. It is useful to measure which tasks presented more magnitude variances by frequencies axis, along the time.

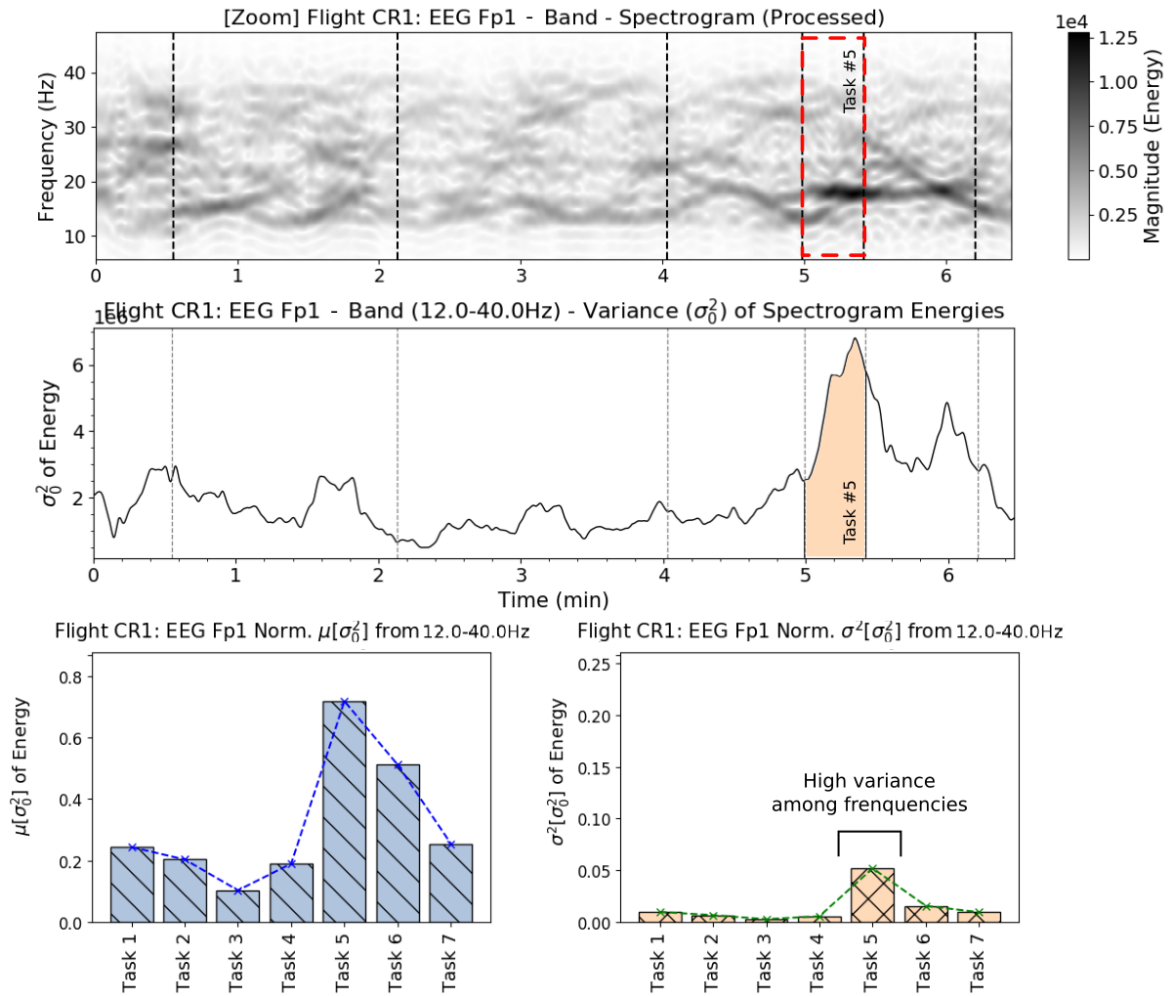


FIGURE 8.11. Mean of magnitudes by tasks, of the flight dataset CR1 - frontal left lobe (Fp1).

Tables 8.2-8.13, present the mean values, standard deviations and variances of all flight datasets.

TABLE 8.1. μ_0 , σ_0 and σ_0^2 of β -band, 31-39Hz and 40Hz of the flight dataset CR1 (beginner level volunteer).

Electrode Channel	Simulator/Flight Tasks - Flight DS:CR1 [Normalized $\mu_0 \pm \sigma_0$]						
	Task 1	Task 2	Task 3	Task 4	Task 5	Task 6	Task 7
EEG-Fp1	0.65±0.22	0.48±0.18	0.29±0.15	0.41±0.15	0.88±0.12	0.69±0.07	0.54±0.10
EEG-F3	0.51±0.13	0.52±0.23	0.18±0.12	0.72±0.19	0.85±0.05	0.72±0.14	0.68±0.03
EEG-C3	0.53±0.12	0.35±0.22	0.42±0.21	0.72±0.09	0.71±0.07	0.71±0.11	0.93±0.06
EEG-T7	0.48±0.17	0.26±0.11	0.24±0.17	0.62±0.25	0.36±0.11	0.53±0.15	0.82±0.07
EEG-Fp2	0.48±0.08	0.42±0.26	0.25±0.13	0.52±0.27	0.85±0.10	0.58±0.14	0.49±0.12
EEG-F4	0.54±0.07	0.30±0.17	0.50±0.20	0.76±0.06	0.81±0.15	0.61±0.15	0.84±0.03
EEG-C4	0.45±0.23	0.51±0.21	0.49±0.28	0.72±0.09	0.47±0.05	0.66±0.17	0.68±0.06
EEG-T8	0.43±0.17	0.34±0.14	0.48±0.23	0.77±0.11	0.61±0.03	0.50±0.08	0.56±0.14
Electrode Channel	Simulator/Flight Tasks - Flight DS:CR1 [Normalized σ_0^2]						
	Task 1	Task 2	Task 3	Task 4	Task 5	Task 6	Task 7
EEG-Fp1	0.05	0.03	0.02	0.02	0.01	0.00	0.01
EEG-F3	0.02	0.05	0.01	0.03	0.00	0.02	0.00
EEG-C3	0.01	0.05	0.05	0.01	0.01	0.01	0.00
EEG-T7	0.03	0.01	0.03	0.06	0.01	0.02	0.01
EEG-Fp2	0.01	0.07	0.02	0.08	0.01	0.02	0.01
EEG-F4	0.01	0.03	0.04	0.00	0.02	0.02	0.00
EEG-C4	0.05	0.04	0.08	0.01	0.00	0.03	0.00
EEG-T8	0.03	0.02	0.05	0.01	0.00	0.01	0.02

TABLE 8.2. μ_0 , σ_0 and σ_0^2 of β -band, 31-39Hz and 40Hz of the flight dataset RC1 (mid-level volunteer).

Electrode Channel	Simulator/Flight Tasks - Flight DS:RC1 [Normalized $\mu_0 \pm \sigma_0$]						
	Task 1	Task 2	Task 3	Task 4	Task 5	Task 6	Task 7
EEG-Fp1	0.46±0.21	0.55±0.22	0.28±0.13	0.61±0.19	0.55±0.13	0.36±0.04	0.51±0.06
EEG-F3	0.69±0.22	0.40±0.19	0.39±0.14	0.51±0.13	0.46±0.06	0.25±0.07	0.55±0.12
EEG-C3	0.60±0.15	0.49±0.17	0.32±0.11	0.33±0.15	0.11±0.07	0.37±0.16	0.69±0.21
EEG-T7	0.85±0.10	0.37±0.16	0.36±0.18	0.59±0.26	0.56±0.08	0.43±0.08	0.69±0.10
EEG-Fp2	0.36±0.32	0.60±0.23	0.49±0.22	0.68±0.16	0.65±0.07	0.65±0.08	0.59±0.06
EEG-F4	0.51±0.09	0.64±0.15	0.46±0.32	0.50±0.18	0.73±0.12	0.33±0.08	0.73±0.16
EEG-C4	0.77±0.15	0.60±0.17	0.26±0.12	0.53±0.25	0.37±0.19	0.42±0.19	0.93±0.05
EEG-T8	0.45±0.12	0.70±0.14	0.36±0.16	0.44±0.25	0.43±0.12	0.36±0.07	0.53±0.08
Electrode Channel	Simulator/Flight Tasks - Flight DS:RC1 [Normalized σ_0^2]						
	Task 1	Task 2	Task 3	Task 4	Task 5	Task 6	Task 7
EEG-Fp1	0.05	0.05	0.02	0.04	0.02	0.00	0.00
EEG-F3	0.05	0.03	0.02	0.02	0.00	0.01	0.02
EEG-C3	0.02	0.03	0.01	0.02	0.00	0.03	0.04
EEG-T7	0.01	0.02	0.03	0.07	0.01	0.01	0.01
EEG-Fp2	0.10	0.05	0.05	0.02	0.01	0.01	0.00
EEG-F4	0.01	0.02	0.10	0.03	0.01	0.01	0.03
EEG-C4	0.02	0.03	0.02	0.06	0.03	0.04	0.00
EEG-T8	0.01	0.02	0.03	0.06	0.01	0.00	0.01

TABLE 8.3. μ_0 , σ_0 and σ_0^2 of β -band, 31-39Hz and 40Hz of the flight dataset RC2 (mid-level volunteer).

Electrode Channel	Simulator/Flight Tasks - Flight DS:RC2 [Normalized $\mu_0 \pm \sigma_0$]						
	Task 1	Task 2	Task 3	Task 4	Task 5	Task 6	Task 7
EEG-Fp1	0.50±0.07	0.45±0.18	0.44±0.15	0.34±0.18	0.56±0.13	0.82±0.13	0.48±0.11
EEG-F3	0.46±0.20	0.63±0.28	0.65±0.20	0.38±0.18	0.37±0.09	0.67±0.16	0.47±0.08
EEG-C3	0.35±0.23	0.55±0.22	0.59±0.27	0.55±0.31	0.21±0.10	0.71±0.10	0.67±0.05
EEG-T7	0.52±0.13	0.52±0.22	0.42±0.18	0.33±0.21	0.63±0.10	0.70±0.18	0.45±0.05
EEG-Fp2	0.48±0.17	0.66±0.15	0.53±0.16	0.40±0.26	0.65±0.15	0.54±0.06	0.48±0.05
EEG-F4	0.47±0.06	0.55±0.18	0.28±0.11	0.47±0.22	0.31±0.08	0.61±0.07	0.56±0.09
EEG-C4	0.27±0.17	0.43±0.16	0.47±0.23	0.27±0.16	0.24±0.12	0.57±0.13	0.42±0.05
EEG-T8	0.23±0.02	0.54±0.13	0.37±0.15	0.48±0.32	0.32±0.05	0.59±0.18	0.74±0.09
Electrode Channel	Simulator/Flight Tasks - Flight DS:RC2 [Normalized σ_0^2]						
	Task 1	Task 2	Task 3	Task 4	Task 5	Task 6	Task 7
EEG-Fp1	0.00	0.03	0.02	0.03	0.02	0.02	0.01
EEG-F3	0.04	0.08	0.04	0.03	0.01	0.03	0.01
EEG-C3	0.05	0.05	0.07	0.10	0.01	0.01	0.00
EEG-T7	0.02	0.05	0.03	0.04	0.01	0.03	0.00
EEG-Fp2	0.03	0.02	0.02	0.07	0.02	0.00	0.00
EEG-F4	0.00	0.03	0.01	0.05	0.01	0.01	0.01
EEG-C4	0.03	0.02	0.05	0.03	0.01	0.02	0.00
EEG-T8	0.00	0.02	0.02	0.11	0.00	0.03	0.01

TABLE 8.4. μ_0 , σ_0 and σ_0^2 of β -band, 31-39Hz and 40Hz of the flight dataset RC3 (mid-level volunteer).

Electrode Channel	Simulator/Flight Tasks - Flight DS:RC3 [Normalized $\mu_0 \pm \sigma_0$]						
	Task 1	Task 2	Task 3	Task 4	Task 5	Task 6	Task 7
EEG-Fp1	0.27±0.20	0.31±0.09	0.39±0.11	0.10±0.09	0.23±0.17	0.66±0.08	0.86±0.09
EEG-F3	0.20±0.15	0.26±0.11	0.51±0.23	0.22±0.15	0.53±0.10	0.52±0.06	0.61±0.10
EEG-C3	0.41±0.15	0.84±0.11	0.49±0.29	0.06±0.07	0.24±0.06	0.39±0.01	0.38±0.22
EEG-T7	0.36±0.04	0.33±0.13	0.54±0.20	0.09±0.04	0.19±0.05	0.26±0.02	0.66±0.17
EEG-Fp2	0.31±0.13	0.51±0.15	0.33±0.16	0.91±0.05	0.56±0.21	0.40±0.06	0.51±0.06
EEG-F4	0.20±0.10	0.65±0.26	0.43±0.22	0.14±0.08	0.30±0.10	0.52±0.03	0.75±0.12
EEG-C4	0.33±0.15	0.36±0.06	0.49±0.21	0.05±0.05	0.58±0.16	0.91±0.10	0.78±0.12
EEG-T8	0.42±0.10	0.56±0.16	0.64±0.20	0.14±0.13	0.31±0.19	0.82±0.08	0.82±0.04
Electrode Channel	Simulator/Flight Tasks - Flight DS:RC3 [Normalized σ_0^2]						
	Task 1	Task 2	Task 3	Task 4	Task 5	Task 6	Task 7
EEG-Fp1	0.04	0.01	0.01	0.01	0.03	0.01	0.01
EEG-F3	0.02	0.01	0.05	0.02	0.01	0.00	0.01
EEG-C3	0.02	0.01	0.08	0.01	0.00	0.00	0.05
EEG-T7	0.00	0.02	0.04	0.00	0.00	0.00	0.03
EEG-Fp2	0.02	0.02	0.03	0.00	0.04	0.00	0.00
EEG-F4	0.01	0.07	0.05	0.01	0.01	0.00	0.01
EEG-C4	0.02	0.00	0.04	0.00	0.02	0.01	0.01
EEG-T8	0.01	0.02	0.04	0.02	0.04	0.01	0.00

TABLE 8.5. μ_0 , σ_0 and σ_0^2 of β -band, 31-39Hz and 40Hz of the flight dataset GC1 (mid-level volunteer).

Electrode Channel	Simulator/Flight Tasks - Flight DS:GC1 [Normalized $\mu_0 \pm \sigma_0$]						
	Task 1	Task 2	Task 3	Task 4	Task 5	Task 6	Task 7
EEG-Fp1	0.61±0.16	0.62±0.18	0.48±0.28	0.46±0.15	0.68±0.27	0.32±0.12	0.31±0.10
EEG-F3	0.65±0.15	0.68±0.24	0.43±0.28	0.43±0.15	0.40±0.13	0.22±0.13	0.13±0.10
EEG-C3	0.74±0.12	0.52±0.23	0.52±0.27	0.40±0.24	0.44±0.06	0.37±0.12	0.11±0.10
EEG-T7	0.83±0.15	0.61±0.22	0.50±0.28	0.43±0.13	0.49±0.11	0.33±0.14	0.33±0.11
EEG-Fp2	0.71±0.19	0.71±0.14	0.30±0.18	0.53±0.11	0.60±0.05	0.47±0.14	0.26±0.09
EEG-F4	0.74±0.08	0.66±0.11	0.29±0.19	0.52±0.21	0.65±0.10	0.50±0.16	0.22±0.08
EEG-C4	0.80±0.13	0.50±0.11	0.26±0.10	0.22±0.14	0.38±0.07	0.23±0.09	0.29±0.11
EEG-T8	0.80±0.14	0.63±0.19	0.48±0.23	0.42±0.10	0.49±0.11	0.31±0.09	0.31±0.09
Electrode Channel	Simulator/Flight Tasks - Flight DS:GC1 [Normalized σ_0^2]						
	Task 1	Task 2	Task 3	Task 4	Task 5	Task 6	Task 7
EEG-Fp1	0.02	0.03	0.08	0.02	0.07	0.01	0.01
EEG-F3	0.02	0.06	0.08	0.02	0.02	0.02	0.01
EEG-C3	0.01	0.06	0.07	0.06	0.00	0.01	0.01
EEG-T7	0.02	0.05	0.08	0.02	0.01	0.02	0.01
EEG-Fp2	0.04	0.02	0.03	0.01	0.00	0.02	0.01
EEG-F4	0.01	0.01	0.04	0.05	0.01	0.03	0.01
EEG-C4	0.02	0.01	0.01	0.02	0.01	0.01	0.01
EEG-T8	0.02	0.04	0.05	0.01	0.01	0.01	0.01

TABLE 8.6. μ_0 , σ_0 and σ_0^2 of β -band, 31-39Hz and 40Hz of the flight dataset GC3 (mid-level volunteer).

Electrode Channel	Simulator/Flight Tasks - Flight DS:GC3 [Normalized $\mu_0 \pm \sigma_0$]						
	Task 1	Task 2	Task 3	Task 4	Task 5	Task 6	Task 7
EEG-Fp1	0.59±0.11	0.42±0.16	0.59±0.19	0.42±0.23	0.68±0.26	0.68±0.11	0.59±0.07
EEG-F3	0.64±0.11	0.45±0.23	0.61±0.15	0.45±0.19	0.71±0.17	0.59±0.12	0.51±0.08
EEG-C3	0.30±0.05	0.29±0.09	0.38±0.10	0.30±0.13	0.61±0.27	0.61±0.30	0.20±0.11
EEG-T7	0.68±0.10	0.46±0.27	0.59±0.20	0.47±0.21	0.73±0.17	0.49±0.10	0.46±0.08
EEG-Fp2	0.74±0.22	0.48±0.23	0.59±0.25	0.49±0.19	0.43±0.12	0.48±0.07	0.28±0.20
EEG-F4	0.74±0.14	0.41±0.26	0.53±0.18	0.54±0.20	0.54±0.06	0.66±0.10	0.30±0.11
EEG-C4	0.60±0.10	0.44±0.18	0.48±0.12	0.49±0.26	0.72±0.13	0.58±0.13	0.49±0.14
EEG-T8	0.42±0.08	0.45±0.24	0.58±0.10	0.51±0.15	0.70±0.14	0.46±0.07	0.39±0.11
Electrode Channel	Simulator/Flight Tasks - Flight DS:GC3 [Normalized σ_0^2]						
	Task 1	Task 2	Task 3	Task 4	Task 5	Task 6	Task 7
EEG-Fp1	0.01	0.03	0.04	0.05	0.07	0.01	0.01
EEG-F3	0.01	0.05	0.02	0.03	0.03	0.01	0.01
EEG-C3	0.00	0.01	0.01	0.02	0.07	0.09	0.01
EEG-T7	0.01	0.07	0.04	0.04	0.03	0.01	0.01
EEG-Fp2	0.05	0.05	0.06	0.04	0.01	0.00	0.04
EEG-F4	0.02	0.07	0.03	0.04	0.00	0.01	0.01
EEG-C4	0.01	0.03	0.02	0.07	0.02	0.02	0.02
EEG-T8	0.01	0.06	0.01	0.02	0.02	0.00	0.01

TABLE 8.7. μ_0 , σ_0 and σ_0^2 of β -band, 31-39Hz and 40Hz of the flight dataset LS1 (mid-level volunteer).

Electrode Channel	Simulator/Flight Tasks - Flight DS:LS1 [Normalized $\mu_0 \pm \sigma_0$]						
	Task 1	Task 2	Task 3	Task 4	Task 5	Task 6	Task 7
EEG-Fp1	0.43±0.08	0.61±0.19	0.51±0.18	0.63±0.22	0.40±0.23	0.66±0.02	–
EEG-F3	0.39±0.06	0.52±0.25	0.32±0.12	0.42±0.09	0.39±0.09	0.29±0.03	–
EEG-C3	0.48±0.17	0.55±0.21	0.55±0.16	0.71±0.17	0.46±0.12	0.43±0.01	–
EEG-T7	0.48±0.15	0.61±0.23	0.54±0.22	0.74±0.13	0.57±0.15	0.47±0.04	–
EEG-Fp2	0.42±0.09	0.63±0.21	0.45±0.13	0.51±0.07	0.25±0.14	0.31±0.01	–
EEG-F4	0.33±0.11	0.58±0.27	0.37±0.17	0.49±0.12	0.32±0.09	0.34±0.01	–
EEG-C4	0.35±0.14	0.52±0.23	0.46±0.16	0.50±0.13	0.34±0.14	0.48±0.02	–
EEG-T8	0.31±0.13	0.51±0.23	0.40±0.22	0.29±0.10	0.26±0.11	0.31±0.02	–
Electrode Channel	Simulator/Flight Tasks - Flight DS:LS1 [Normalized σ_0^2]						
	Task 1	Task 2	Task 3	Task 4	Task 5	Task 6	Task 7
EEG-Fp1	0.01	0.04	0.03	0.05	0.05	0.00	–
EEG-F3	0.00	0.06	0.02	0.01	0.01	0.00	–
EEG-C3	0.03	0.04	0.03	0.03	0.01	0.00	–
EEG-T7	0.02	0.05	0.05	0.02	0.02	0.00	–
EEG-Fp2	0.01	0.04	0.02	0.01	0.02	0.00	–
EEG-F4	0.01	0.07	0.03	0.02	0.01	0.00	–
EEG-C4	0.02	0.05	0.03	0.02	0.02	0.00	–
EEG-T8	0.02	0.05	0.05	0.01	0.01	0.00	–

TABLE 8.8. μ_0 , σ_0 and σ_0^2 of β -band, 31-39Hz and 40Hz of the flight dataset LS2 (mid-level volunteer).

Electrode Channel	Simulator/Flight Tasks - Flight DS:LS2 [Normalized $\mu_0 \pm \sigma_0$]						
	Task 1	Task 2	Task 3	Task 4	Task 5	Task 6	Task 7
EEG-Fp1	0.45±0.22	0.75±0.16	0.45±0.23	0.53±0.22	0.50±0.09	0.35±0.13	0.44±0.10
EEG-F3	0.63±0.12	0.64±0.20	0.58±0.15	0.65±0.18	0.51±0.07	0.31±0.15	0.23±0.09
EEG-C3	0.32±0.12	0.48±0.11	0.48±0.22	0.42±0.16	0.38±0.06	0.22±0.08	0.05±0.03
EEG-T7	0.44±0.07	0.47±0.18	0.39±0.27	0.53±0.28	0.64±0.14	0.40±0.15	0.38±0.09
EEG-Fp2	0.51±0.17	0.76±0.16	0.46±0.26	0.56±0.20	0.34±0.08	0.29±0.10	0.33±0.06
EEG-F4	0.50±0.07	0.74±0.11	0.50±0.16	0.53±0.19	0.38±0.09	0.36±0.15	0.29±0.07
EEG-C4	0.39±0.10	0.58±0.13	0.51±0.19	0.54±0.20	0.40±0.08	0.42±0.11	0.11±0.08
EEG-T8	0.26±0.13	0.59±0.23	0.39±0.18	0.37±0.11	0.23±0.08	0.45±0.17	0.52±0.13
Electrode Channel	Simulator/Flight Tasks - Flight DS:LS2 [Normalized σ_0^2]						
	Task 1	Task 2	Task 3	Task 4	Task 5	Task 6	Task 7
EEG-Fp1	0.05	0.02	0.05	0.05	0.01	0.02	0.01
EEG-F3	0.01	0.04	0.02	0.03	0.00	0.02	0.01
EEG-C3	0.02	0.01	0.05	0.03	0.00	0.01	0.00
EEG-T7	0.00	0.03	0.07	0.08	0.02	0.02	0.01
EEG-Fp2	0.03	0.02	0.07	0.04	0.01	0.01	0.00
EEG-F4	0.00	0.01	0.03	0.04	0.01	0.02	0.01
EEG-C4	0.01	0.02	0.04	0.04	0.01	0.01	0.01
EEG-T8	0.02	0.05	0.03	0.01	0.01	0.03	0.02

TABLE 8.9. μ_0 , σ_0 and σ_0^2 of β -band, 31-39Hz and 40Hz of the flight dataset VC1 (experienced level volunteer).

Electrode Channel	Simulator/Flight Tasks - Flight DS:VC1 [Normalized $\mu_0 \pm \sigma_0$]						
	Task 1	Task 2	Task 3	Task 4	Task 5	Task 6	Task 7
EEG-Fp1	0.55±0.14	0.22±0.11	0.45±0.06	0.52±0.21	0.85±0.03	0.88±0.11	0.48±0.09
EEG-F3	0.77±0.14	0.31±0.13	0.42±0.09	0.42±0.30	0.92±0.07	0.67±0.18	0.31±0.11
EEG-C3	0.47±0.04	0.06±0.11	0.14±0.14	0.85±0.07	0.78±0.08	0.19±0.17	0.29±0.13
EEG-T7	0.59±0.09	0.17±0.11	0.38±0.14	0.36±0.30	0.84±0.04	0.85±0.13	0.47±0.13
EEG-Fp2	0.49±0.12	0.21±0.09	0.35±0.13	0.38±0.21	0.72±0.09	0.88±0.07	0.43±0.15
EEG-F4	0.62±0.06	0.38±0.17	0.48±0.20	0.49±0.31	0.89±0.10	0.61±0.22	0.45±0.15
EEG-C4	0.45±0.21	0.48±0.31	0.43±0.18	0.40±0.12	0.74±0.12	0.58±0.21	0.54±0.15
EEG-T8	0.34±0.02	0.29±0.13	0.41±0.07	0.45±0.23	0.69±0.03	0.80±0.10	0.59±0.14
Electrode Channel	Simulator/Flight Tasks - Flight DS:VC1 [Normalized σ_0^2]						
	Task 1	Task 2	Task 3	Task 4	Task 5	Task 6	Task 7
EEG-Fp1	0.02	0.01	0.00	0.05	0.00	0.01	0.01
EEG-F3	0.02	0.02	0.01	0.09	0.00	0.03	0.01
EEG-C3	0.00	0.01	0.02	0.01	0.01	0.03	0.02
EEG-T7	0.01	0.01	0.02	0.09	0.00	0.02	0.02
EEG-Fp2	0.01	0.01	0.02	0.04	0.01	0.00	0.02
EEG-F4	0.00	0.03	0.04	0.10	0.01	0.05	0.02
EEG-C4	0.04	0.10	0.03	0.02	0.02	0.04	0.02
EEG-T8	0.00	0.02	0.01	0.05	0.00	0.01	0.02

TABLE 8.10. μ_0 , σ_0 and σ_0^2 of β -band, 31-39Hz and 40Hz of the flight dataset VC2 (experienced level volunteer).

Electrode Channel	Simulator/Flight Tasks - Flight DS:VC2 [Normalized $\mu_0 \pm \sigma_0$]						
	Task 1	Task 2	Task 3	Task 4	Task 5	Task 6	Task 7
EEG-Fp1	0.19±0.08	0.66±0.25	0.52±0.20	0.55±0.14	0.26±0.05	0.24±0.06	0.17±0.08
EEG-F3	0.55±0.03	0.64±0.19	0.61±0.22	0.81±0.14	0.61±0.04	0.45±0.13	0.10±0.06
EEG-C3	0.74±0.05	0.87±0.07	0.84±0.09	0.45±0.13	0.47±0.21	0.74±0.03	0.27±0.22
EEG-T7	0.33±0.08	0.53±0.12	0.62±0.26	0.54±0.13	0.09±0.07	0.07±0.04	0.15±0.07
EEG-Fp2	0.28±0.02	0.69±0.24	0.43±0.17	0.49±0.21	0.21±0.05	0.23±0.04	0.14±0.05
EEG-F4	0.23±0.02	0.45±0.17	0.62±0.23	0.67±0.09	0.49±0.02	0.34±0.07	0.09±0.05
EEG-C4	0.35±0.07	0.32±0.11	0.43±0.18	0.77±0.06	0.82±0.11	0.46±0.16	0.06±0.05
EEG-T8	0.21±0.03	0.67±0.21	0.49±0.15	0.59±0.18	0.47±0.11	0.51±0.08	0.16±0.12
Electrode Channel	Simulator/Flight Tasks - Flight DS:VC2 [Normalized σ_0^2]						
	Task 1	Task 2	Task 3	Task 4	Task 5	Task 6	Task 7
EEG-Fp1	0.01	0.06	0.04	0.02	0.00	0.00	0.01
EEG-F3	0.00	0.04	0.05	0.02	0.00	0.02	0.00
EEG-C3	0.00	0.01	0.01	0.02	0.04	0.00	0.05
EEG-T7	0.01	0.02	0.07	0.02	0.00	0.00	0.00
EEG-Fp2	0.00	0.06	0.03	0.04	0.00	0.00	0.00
EEG-F4	0.00	0.03	0.05	0.01	0.00	0.00	0.00
EEG-C4	0.00	0.01	0.03	0.00	0.01	0.03	0.00
EEG-T8	0.00	0.05	0.02	0.03	0.01	0.01	0.01

TABLE 8.11. μ_0 , σ_0 and σ_0^2 of β -band, 31-39Hz and 40Hz of the flight dataset CR3 (beginner level volunteer).

Electrode Channel	Simulator/Flight Tasks - Flight DS:CR3 [Normalized $\mu_0 \pm \sigma_0$]						
	Task 1	Task 2	Task 3	Task 4	Task 5	Task 6	Task 7
EEG-Fp1	0.49±0.14	0.51±0.28	–	–	–	–	–
EEG-F3	0.28±0.17	0.54±0.36	–	–	–	–	–
EEG-C3	0.70±0.26	0.31±0.24	–	–	–	–	–
EEG-T7	0.41±0.11	0.38±0.32	–	–	–	–	–
EEG-Fp2	0.56±0.34	0.27±0.25	–	–	–	–	–
EEG-F4	0.56±0.18	0.54±0.24	–	–	–	–	–
EEG-C4	0.58±0.35	0.31±0.27	–	–	–	–	–
EEG-T8	0.62±0.28	0.39±0.23	–	–	–	–	–
Electrode Channel	Simulator/Flight Tasks - Flight DS:CR3 [Normalized σ_0^2]						
	Task 1	Task 2	Task 3	Task 4	Task 5	Task 6	Task 7
EEG-Fp1	0.02	0.08	–	–	–	–	–
EEG-F3	0.03	0.13	–	–	–	–	–
EEG-C3	0.07	0.06	–	–	–	–	–
EEG-T7	0.01	0.10	–	–	–	–	–
EEG-Fp2	0.12	0.06	–	–	–	–	–
EEG-F4	0.03	0.06	–	–	–	–	–
EEG-T8	0.08	0.05	–	–	–	–	–

TABLE 8.12. μ_0 , σ_0 and σ_0^2 of β -band, 31-39Hz and 40Hz of the flight dataset CLX (beginner level volunteer).

Electrode Channel	Simulator/Flight Tasks - Flight DS:CLX [Normalized $\mu_0 \pm \sigma_0$]						
	Task 1	Task 2	Task 3	Task 4	Task 5	Task 6	Task 7
EEG-Fp1	0.62±0.22	0.76±0.09	–	–	–	–	–
EEG-F3	0.55±0.21	0.66±0.32	–	–	–	–	–
EEG-C3	0.58±0.26	0.27±0.24	–	–	–	–	–
EEG-T7	0.61±0.29	0.48±0.23	–	–	–	–	–
EEG-Fp2	0.70±0.25	0.54±0.17	–	–	–	–	–
EEG-F4	0.43±0.29	0.73±0.26	–	–	–	–	–
EEG-C4	0.74±0.24	0.72±0.11	–	–	–	–	–
EEG-T8	0.68±0.28	0.72±0.21	–	–	–	–	–
Electrode Channel	Simulator/Flight Tasks - Flight DS:CLX [Normalized σ_0^2]						
	Task 1	Task 2	Task 3	Task 4	Task 5	Task 6	Task 7
EEG-Fp1	0.05	0.01	–	–	–	–	–
EEG-F3	0.04	0.10	–	–	–	–	–
EEG-C3	0.07	0.06	–	–	–	–	–
EEG-T7	0.08	0.05	–	–	–	–	–
EEG-Fp2	0.06	0.03	–	–	–	–	–
EEG-F4	0.08	0.07	–	–	–	–	–
EEG-C4	0.06	0.01	–	–	–	–	–
EEG-T8	0.08	0.04	–	–	–	–	–

TABLE 8.13. μ_0 , σ_0 and σ_0^2 of β -band, 31-39Hz and 40Hz of the flight dataset CL3 (beginner level volunteer).

Electrode Channel	Simulator/Flight Tasks - Flight DS:CL3 [Normalized $\mu_0 \pm \sigma_0$]						
	Task 1	Task 2	Task 3	Task 4	Task 5	Task 6	Task 7
EEG-Fp1	0.59±0.05	0.51±0.20	0.56±0.23	0.59±0.20	0.48±0.08	0.51±0.06	0.49±0.06
EEG-F3	0.54±0.10	0.46±0.22	0.23±0.10	0.49±0.17	0.59±0.06	0.81±0.11	0.79±0.13
EEG-C3	0.31±0.24	0.69±0.18	0.20±0.10	0.55±0.19	0.78±0.16	0.73±0.15	0.67±0.20
EEG-T7	0.88±0.08	0.54±0.25	0.32±0.16	0.41±0.15	0.32±0.11	0.49±0.10	0.25±0.06
EEG-Fp2	0.53±0.09	0.40±0.21	0.45±0.27	0.65±0.10	0.64±0.23	0.75±0.10	0.49±0.26
EEG-F4	0.80±0.10	0.56±0.21	0.45±0.16	0.68±0.09	0.47±0.09	0.49±0.16	0.66±0.09
EEG-C4	0.78±0.12	0.42±0.19	0.30±0.09	0.39±0.10	0.39±0.09	0.46±0.13	0.53±0.08
EEG-T8	0.77±0.18	0.39±0.25	0.27±0.12	0.28±0.15	0.36±0.11	0.64±0.17	0.58±0.15
Electrode Channel	Simulator/Flight Tasks - Flight DS:CL3 [Normalized σ_0^2]						
	Task 1	Task 2	Task 3	Task 4	Task 5	Task 6	Task 7
EEG-Fp1	0.00	0.04	0.05	0.04	0.01	0.00	0.00
EEG-F3	0.01	0.05	0.01	0.03	0.00	0.01	0.02
EEG-C3	0.06	0.03	0.01	0.04	0.03	0.02	0.04
EEG-T7	0.01	0.06	0.03	0.02	0.01	0.01	0.00
EEG-Fp2	0.01	0.04	0.07	0.01	0.05	0.01	0.07
EEG-F4	0.01	0.04	0.03	0.01	0.01	0.03	0.01
EEG-C4	0.01	0.04	0.01	0.01	0.01	0.02	0.01
EEG-T8	0.03	0.06	0.01	0.02	0.01	0.03	0.02

Result Analysis on Emotion Recognition

This work presented a multimodal solution to recognize emotions from several physiological inputs, based on the bio-reactions of volunteers and flight simulation tasks. It is proposed as one way to contribute on emotion studies over the aviation context i.e., inside of the scope of aviation accidents caused by human failures.

The achieved results shown to be able to recognize emotions felt by each volunteer acting like pilots along the simulated flights, using the datasets of other volunteers, as reference. Several tests were executed in this work to try to find the better recognition results for each volunteer i.e., the best model possible to recognize these emotions. In datamining context, the test represents a portion of the used dataset, used to validate the produced model. The cross-validation was the method used to aim the emotions recognition process for each volunteer dataset obtained during each flight experiment.

The emotion recognition tasks were initially based on two different tests: tests without use of feature extraction (i.e. raw data applied directly over the ANN inputs, with some few treatment or preprocessing), and tests with the processed data based on feature extraction. Other aspects were also considered: different ANN architectures, number of training iteration, number of inputs and hidden neurons, and different flight datasets.

In every tests of emotion recognition, the cross validation was applied to support the emotion recognition felt by one volunteer in a single flight, according to the emotions already detected from another flights. In another words, in a total of 13 flights, the training was based on 12 flight datasets ($N - 1$ flights) to try to recognize the emotions of one single flight. The dataset having intensities of facial emotions (5 different emotions), was the reference or target of the ANN training.

The facial emotion reader software, presented several mistakes, detecting wrongly several emotions which some of them were not possible to be avoided; the consequence of these wrong matches was some errors under the regression models, outputted from each output neuron.

9.1. What Has Been Done So Far

The preprocessing was the first data treatment executed over the raw datasets. It was based on signal detrend, abrupt signal corrections, normalization, outliers removals, resampling (sampling rate equalization) and so on (Figure 9.1).

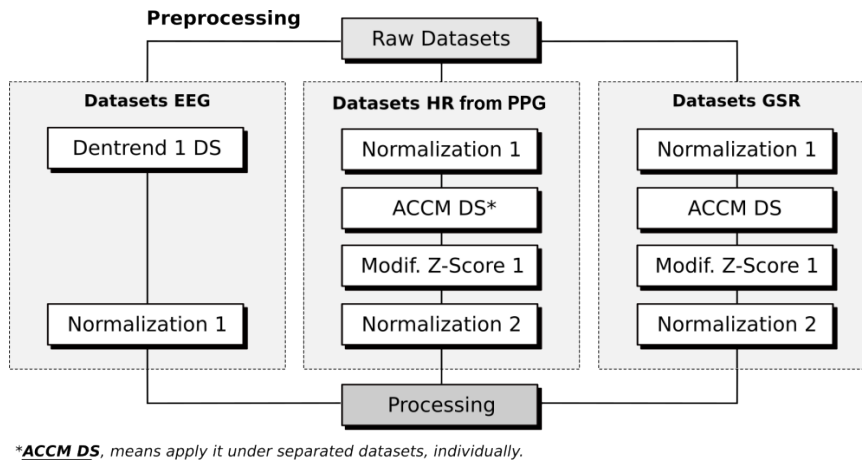


FIGURE 9.1. Preprocessing executed before the processing, feature extraction and tests.

Then, a data processing was executed, which it included a deeper analysis over the acquired datasets. It was based on drift removal (second detrend), frequency analysis, abrupt peaks detections, additional normalization and outlier removal, filtering and so on (Figure 9.2).

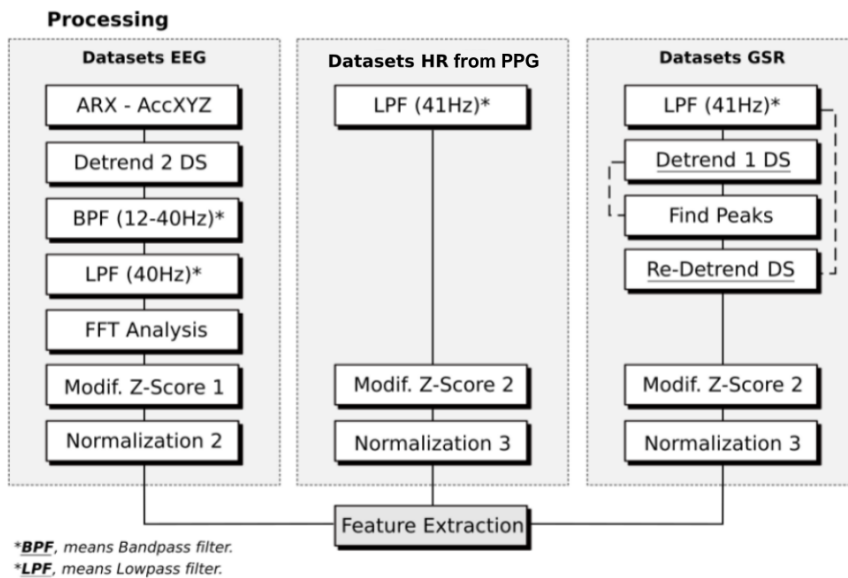


FIGURE 9.2. Processing executed before the feature extraction.

The feature extractions used on emotion recognition process, were executed over the processed datasets. Several features were considered such as: poincaré plots, statistical features, frequency-based features (e.g. wavelets), entropy, peaks detection among others. Some of these features were applied for one single type of biosignal as for instance, the peaks positions and wavelets, applied only over GSR and EEG datasets respectively.

This work based its emotion recognition process over the extracted features. Then, the ANN and deep learning techniques were used to recognize emotions of each volunteer applying these features on to input neurons, 2 hidden layers and 5 output neurons (each neuron outputting a regression model i.e, one emotion intensity). Realtime outliers removal was also applied in this process. The errors from the emotion recognition process were analyzed and computed based on RMSE and MAE.

9.2. Description of the Recognition Tests

The main procedures applied on preprocessing, processing and feature extraction are shown in the tests sequence below. It were based on the features selection and data treatment. At least the data normalization and abrupt data correction were used, for the most of the tests.

In these tests (Table 9.1), all features were considered for each biosignal i.e., 11 features of HR, 7 features of GSR and 72 features of EEG (9× 8Ch). The best and worst features were applied on these recognition inputs.

TABLE 9.1. Description of each execution test according to preprocessing, processing and feature extraction.

Tests	Preprocessing		Processing, Feature Extraction and Recognition					Biosignals		
	Detrend	Outliers	FE^*	SVD	CC^*	$\varphi_j(v_j(n))$	Optimization	HR	GSR	EEG
Test 1	–	–	–	–	–	sigmoid	'sgd'	×	×	×
Test 2	–	–	–	–	–	sigmoid	'adam'	×	×	×
Test 3	×	×	×	–	×	ReLU	'adam'	×	×	×
Test 4	×	×	×	–	×	sigmoid	'sgd'	×	×	×
Test 5	×	×	×	–	×	sigmoid	'adam'	×	×	×
Test 6	×	×	×	–	×	ReLU	'sgd'	×	×	×
Test 7	×	×	×	–	×	ReLU	'adam'	–	×	×
Test 8	×	×	×	–	×	sigmoid	'sgd'	–	×	×
Test 9	×	×	×	–	×	sigmoid	'adam'	–	×	×
Test 10	×	×	×	–	×	ReLU	'sgd'	–	×	×
Test 11	×	×	×	–	×	ReLU	'adam'	×	–	×
Test 12	×	×	×	–	×	sigmoid	'sgd'	×	–	×
Test 13	×	×	×	–	×	sigmoid	'adam'	×	–	×
Test 14	×	×	×	–	×	ReLU	'sgd'	×	–	×
Test 15	×	×	×	–	×	ReLU	'adam'	×	×	–
Test 16	×	×	×	–	×	sigmoid	'sgd'	×	×	–
Test 17	×	×	×	–	×	sigmoid	'adam'	×	×	–
Test 18	×	×	×	–	×	ReLU	'sgd'	×	×	–

CC^* : Column Centering - Data centering for each biosignal.
 FE^* : Feature Extraction - Selected all features for each biosignal.

In the next tests, was considered the features selection based on SVD (i.e. the features are selected in order of its importance). It were 6 features of HR, 4 features of GSR and 40 (5×8 Channels) features of EEG, as shown in Table 9.2.

TABLE 9.2. Description of each execution test according to preprocessing, processing and feature selection.

Tests	Preprocessing		Processing, Feature Extraction and Recognition					Biosignals		
	Detrend	Outliers	FE	SVD	CC	$\varphi_j(v_j(n))$	Optimization	HR	GSR	EEG
Test 19	×	×	×	×	×	ReLU	'adam'	×	×	×
Test 20	×	×	×	×	×	sigmoid	'sgd'	×	×	×
Test 21	×	×	×	×	×	sigmoid	'adam'	×	×	×
Test 22	×	×	×	×	×	ReLU	'sgd'	×	×	×
Test 23	×	×	×	×	×	ReLU	'adam'	—	×	×
Test 24	×	×	×	×	×	sigmoid	'sgd'	—	×	×
Test 25	×	×	×	×	×	sigmoid	'adam'	—	×	×
Test 26	×	×	×	×	×	ReLU	'sgd'	—	×	×
Test 27	×	×	×	×	×	ReLU	'adam'	×	—	×
Test 28	×	×	×	×	×	sigmoid	'sgd'	×	—	×
Test 29	×	×	×	×	×	sigmoid	'adam'	×	—	×
Test 30	×	×	×	×	×	ReLU	'sgd'	×	—	×
Test 31	×	×	×	×	×	ReLU	'adam'	×	×	—
Test 32	×	×	×	×	×	sigmoid	'sgd'	×	×	—
Test 33	×	×	×	×	×	sigmoid	'adam'	×	×	—
Test 34	×	×	×	×	×	ReLU	'sgd'	×	×	—

9.2.1. Emotion Recognition Tests based on Raw Data - Test 1 and Test 2

In these tests of emotion recognition, no feature extractions and preprocessing were considered; all raw data were directly applied on the ANN input layer. The ANN activation function was the sigmoid and two different optimization algorithms: stochastic gradient descend ('sgd') and 'adam'. Its inputs were based on HR (1 input channel), GSR (1 input channel) and EEG (8 inputs channels).

Each of the 13 flights was tested individually based on 13-fold cross-validation; it was also considered a total of 6×10^3 training iterations (epochs), adaptive learning rate and momentum, 10 neurons applied in input layer ($N_i = 10$), 2 hidden layers having 10 neurons each one ($N_h = 10 \times 2$), and 5 output neurons ($N_o = 5$) on the last ANN layer. This was one perspective of ANN architecture which a regression model was produced for each output neuron, i.e. for each output emotion.

Table 9.3, presents a emotion recognition results using a raw data approach and no feature extraction. Its results show the importance of a feature extraction in a multimodal sensing system in which on the other hand, the recognition will get undesirable results and high execution time. The MARD, RMSE and MAE were used to compare the output regression models with the emotions from the flight datasets.

9.2.2. Emotion Recognition Tests based on Feature Extraction - Test 3 to 34

All tests between 3 to 34, considered the feature extraction over the raw input data. In details, between the tests 3 to 18, 90 features were extracted, in including good and bad quality features. Between the tests 19 to 34, the SVD was applied to select the best features to be used.

The accuracy of the major match procedure, i.e. the correct match in each sample regarding to the higher emotion amplitude (between 5 emotions), presented worst values on recognition from flight dataset CLX, having no matches on the most recognition.

Table 9.4 to Table 9.19 present the tests results, based on feature extraction and also feature selection. The analysis of all these tests are presented on the next section, comparing each one and describing the achievements after some improvements.

9.3. Emotion Recognition Analysis

Figure 9.3, presents the barplots correspondent to the errors results from tests 3 to 6, with feature extraction but without feature selection and considering all three biosignals; these tests were executed according to the Table 9.1, presented before. It is also important to inform, that these tests were executed over all 13 datasets, as defined in Chapter 3.

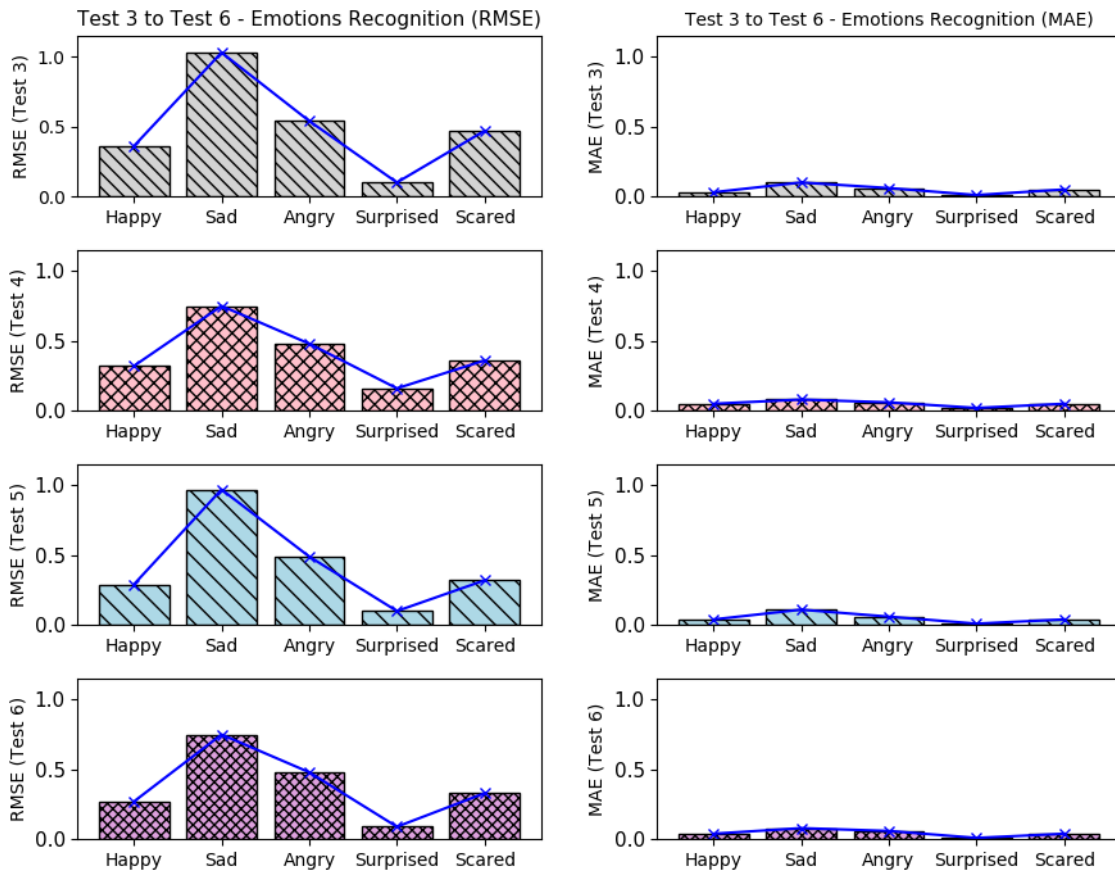


FIGURE 9.3. Errors results (RMSE+MAE) from tests 3 to 6 (with feature extraction).

It is possible to see that in the tests 3 to 6, the emotion *surprised*, presented a better recognition accuracy, having the smallest error level. The *happy* and *scared* were the emotions which also presented low errors. Nevertheless, these errors levels can be improved if the train datasets are more coherent. The emotions *sad* and *angry*, presented the worst error levels; it is probably due the misclassifications from the face emotion detection software, which sometimes confused situations of angry and disappointed rather than sadness.

If we compare all tests (from test 3 to 34), it is possible to note that again, the *surprised* emotion kept with best recognition values (low errors), as shown in Figures 9.4 and 9.5, which it presents all considered errors along the tests.

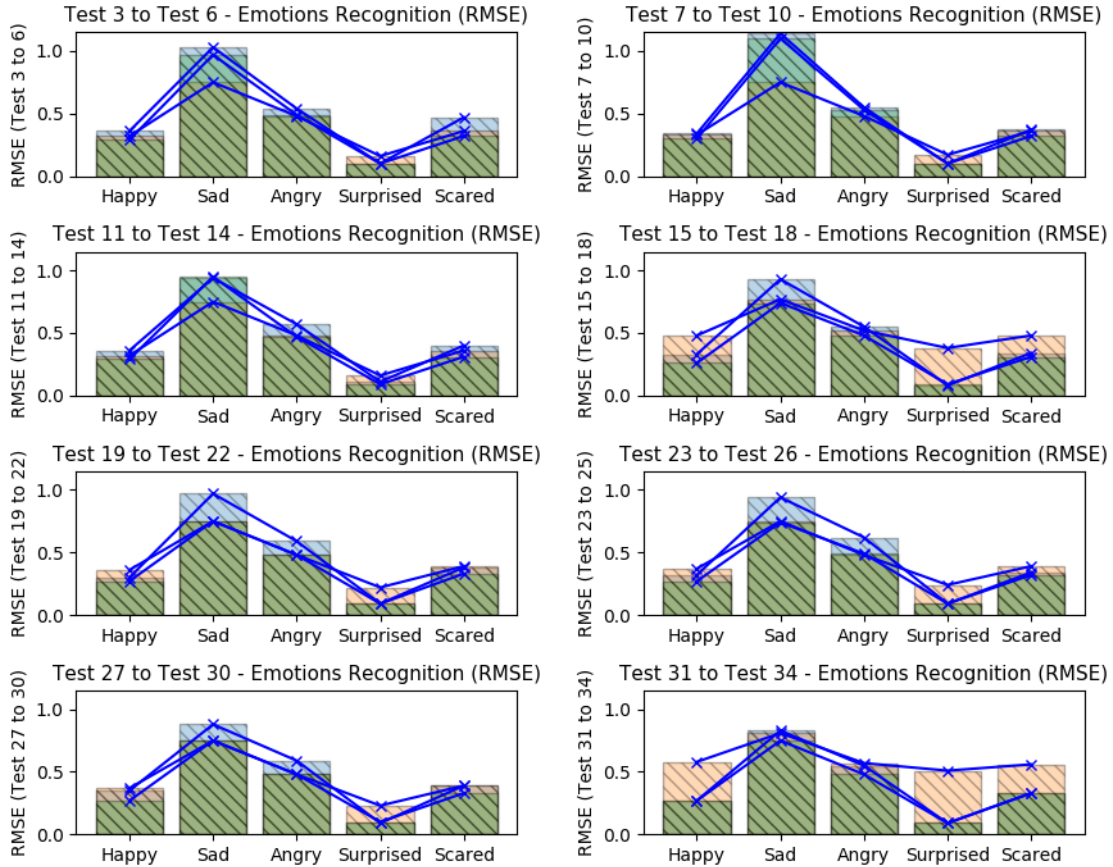


FIGURE 9.4. Errors results (RMSE) comparison from tests 3 to 34 (with feature extraction).

The worst recognition results were reached when the EEG datasets were omitted in different tests (tests 15 to 18 and tests 31 to 34), showing that in these tests, the recognition results were better when all biosignals were considered; when GSR datasets were omitted, the results presented good recognition levels too (tests 11 to 14 and tests 27 to 30). The application of feature selection based on SVD and the omission of GSR datasets, returned the less recognition errors (tests 27 to 30). The *sad* emotion got the worst error levels when HR datasets were omitted (tests 7 to 10), as like as the *happy* emotion got the worst error levels when the EEG datasets were omitted.

In resume, all tests shown that the lowest recognition errors were reached when all biosignal datasets were considered or when the GSR dataset were omitted of the model training. It also shown that the emotion *surprised* was easier to recognize, having a mean value of RMSE of 0.13 and mean value of MAE of 0.01; the worst recognition levels were found to emotion *sad*, having a mean value of RMSE of 0.82 and mean value of MAE of 0.08.

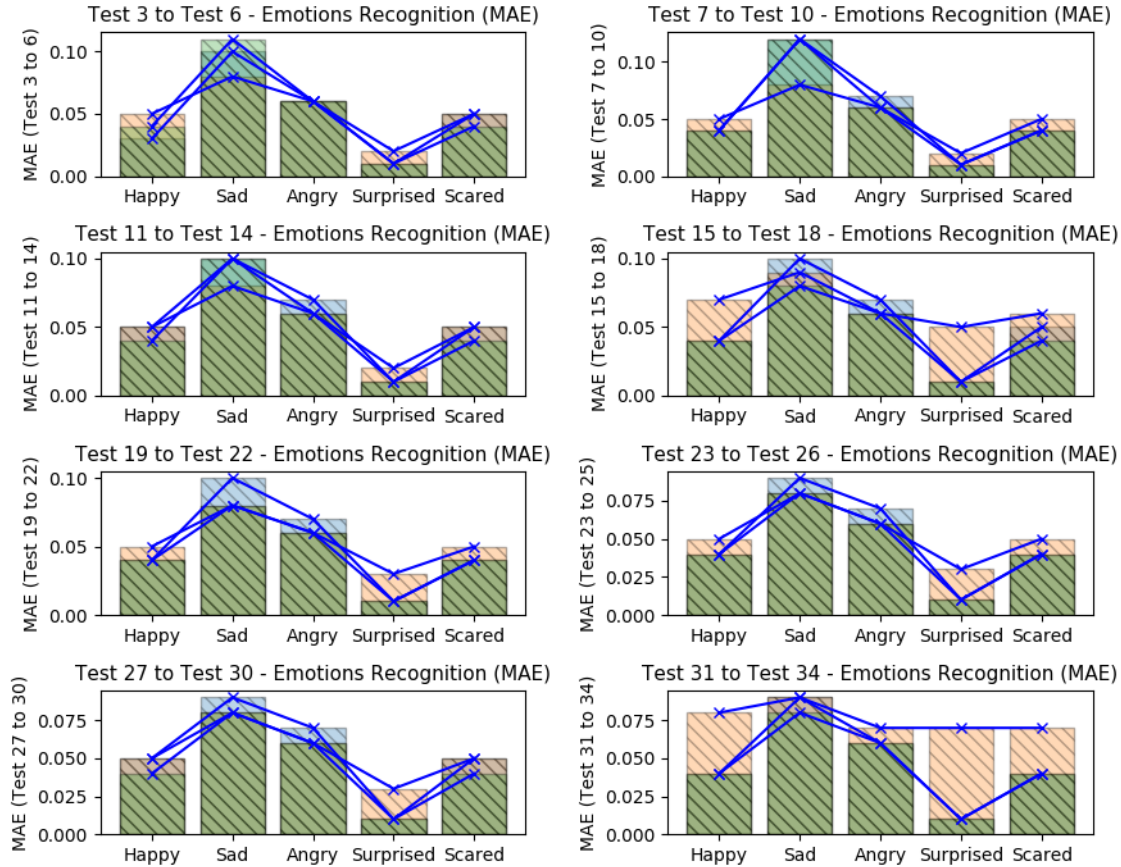


FIGURE 9.5. Errors results (MAE) comparison from tests 3 to 34 (with feature extraction).

9.3.1. Improvements Coming from the Feature Extraction

In prior discussion, was presented the need to use features extraction in a very dense or huge datasets. One direct benefit of it is the execution time. Obviously, with the feature extraction, the dataset is sampled to fractions of data which it must to continue to represent all raw data with more or equal meaning. For this reason, a featured dataset is smaller if compared to its raw dataset. Another benefit of feature extraction, is that it can bring hide information from a dataset, in statistical or frequency context, e.g. data variances and other tiny patterns of frequency domain.

Figure 9.6, shows the errors levels between the use of raw datasets (tests 1 and 2) and featured datasets (tests 3 to 34). Analyzing the RMSE values (left barplot), it is possible to see that the improvements were considerable over all emotions when feature extraction was used. The emotion *happy* presented an improvement of 89.66% (prior 3.06/actual 0.31); *sad* of 84.58% (5.38/0.82); *angry* of 86.75% (3.84/0.50); *surprised* of 93.89% (2.19/0.13); and *scared* of 88.67% (3.18/0.36). Analyzing the MAE values (right barplot), it is possible to see that the improvements were good over 4 emotions of 5 (emotion *sad* wasn't improved on MAE values), when feature extraction was used. The emotion *happy* presented an improvement of 26.04% (prior 0.06/actual 0.04); *angry* of 4.32% (0.065/0.062); *surprised* of 60.15% (0.04/0.01); and *scared* of 18.75% (0.05/0.04).

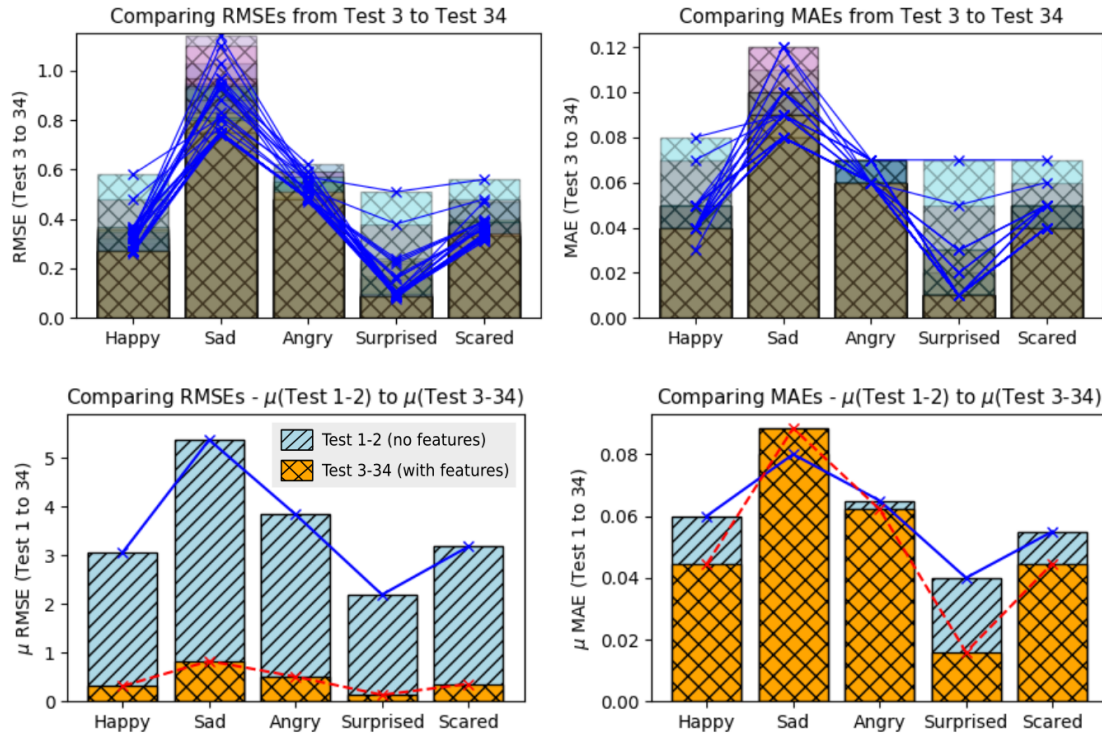


FIGURE 9.6. Errors results comparison between RMSE and MAE from tests 1 to 34 (with feature extraction).

9.3.2. Considering the Higher Emotion Intensities

The higher intensities of facial emotions by time (between 5 emotion intensities), were also computed and its number of matches were also analyzed, comparing the correct matches between its higher emotion (from the face dataset) with the higher output from the 5 neurons (output layer), as shown in Chapter 4 (Section 4.5).

The benefit to also consider these major values, is to understand if the regression models from each output neuron, is following correctively the original emotions intensities related to the other emotions. In case of some output major values present wrong label, it does not mean that it is a critical error. The high fluctuations of emotions intensities are common to happen presenting, in several times, very close intensities values between them which it is hard to separate perfectly. On the other hand, if an outputted regression model of each neuron fits perfectly with the neuron output, both error levels (RMSA and MAE) and major emotion values will converge or improve together.

The corrected number of matches between these emotions and its relations, are shown in Figure 9.7, presenting the case of tests 3 to 6. Some datasets presented a very low number of matches during all tests as for instance, GC1, LS1, VC1, CLX and CL3. These low accuracies are probably due the high misclassification of emotions from the pilots' faces as also presented on prior errors values based o RMSE and MAE. However, if considers the possibility to improve these results, the next tests can omit these datasets with low accuracies, to get better general results.

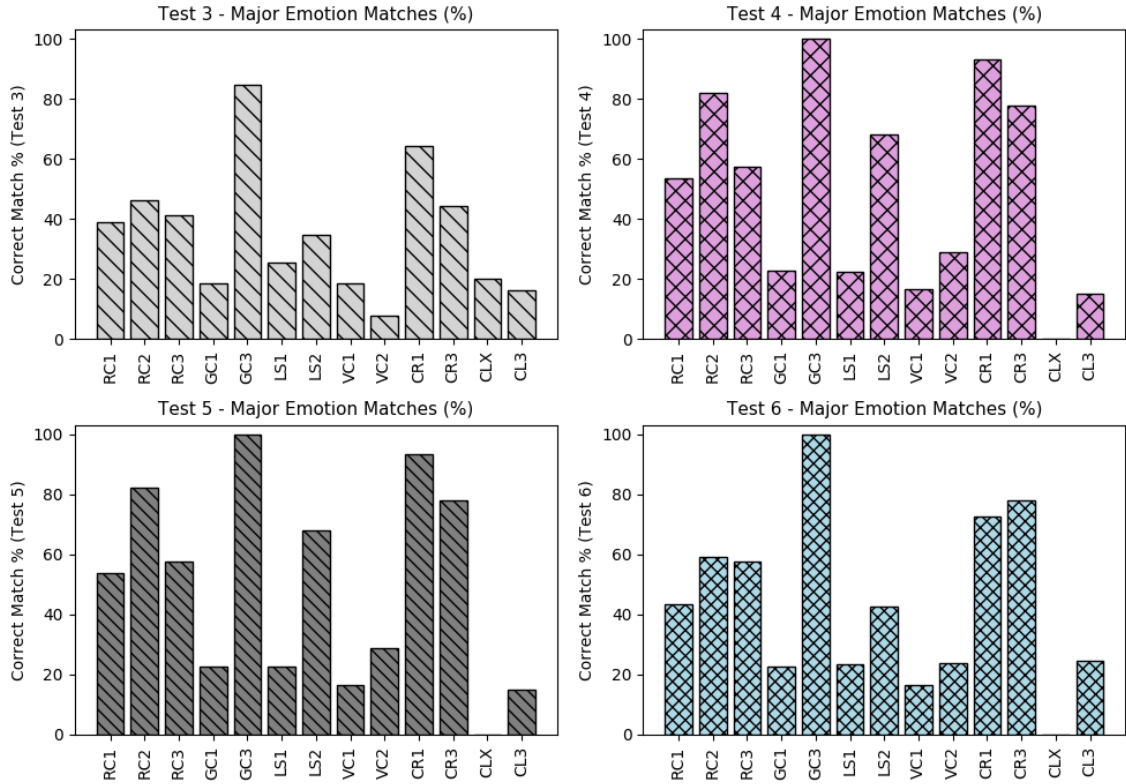


FIGURE 9.7. Major emotion accuracies from the tests 3 to 6 (with feature extraction).

When comparing all the matches (from test 3 to 34) regarding to the major emotion values, it is possible to see that the accuracy of the dataset CLX continues to present the worst accuracies and the dataset GC3 the best accuracies values.

Figure 9.8, shows a comparison of all accuracies, regarding to the major emotions from the tests 3 to 34 (top plots) and from tests 1 to 34 (bottom plot). Note that on the top plot, shows that six datasets kept the major emotion accuracies less than 50%.

The top-left plot, presents the relation between the mean of the raw dataset accuracies (tests 1 and 2) over the featured datasets accuracies (tests 3 to 34), which the raw data tests seems to have better accuracies over the featured dataset. It not necessarily means that the emotion recognition based on raw datasets was the best solution in this proposed work; going back to Section 9.3.1 and observe the error levels during the tests based on raw datasets, it is possible to see that it was extremely bad compared to the others tests based on featured dataset; this way, it can easily note that actually, a good regression models, must be based on a combination of low error levels and good major emotions accuracies.

Analyzing the bottom plot, it is possible to note that when the activation function was the sigmoid together with the gradient descend optimization, the general accuracies presented a constant behaviour along the executed tests. The activation function rectified unit, presented the worst major emotion accuracies in this work.

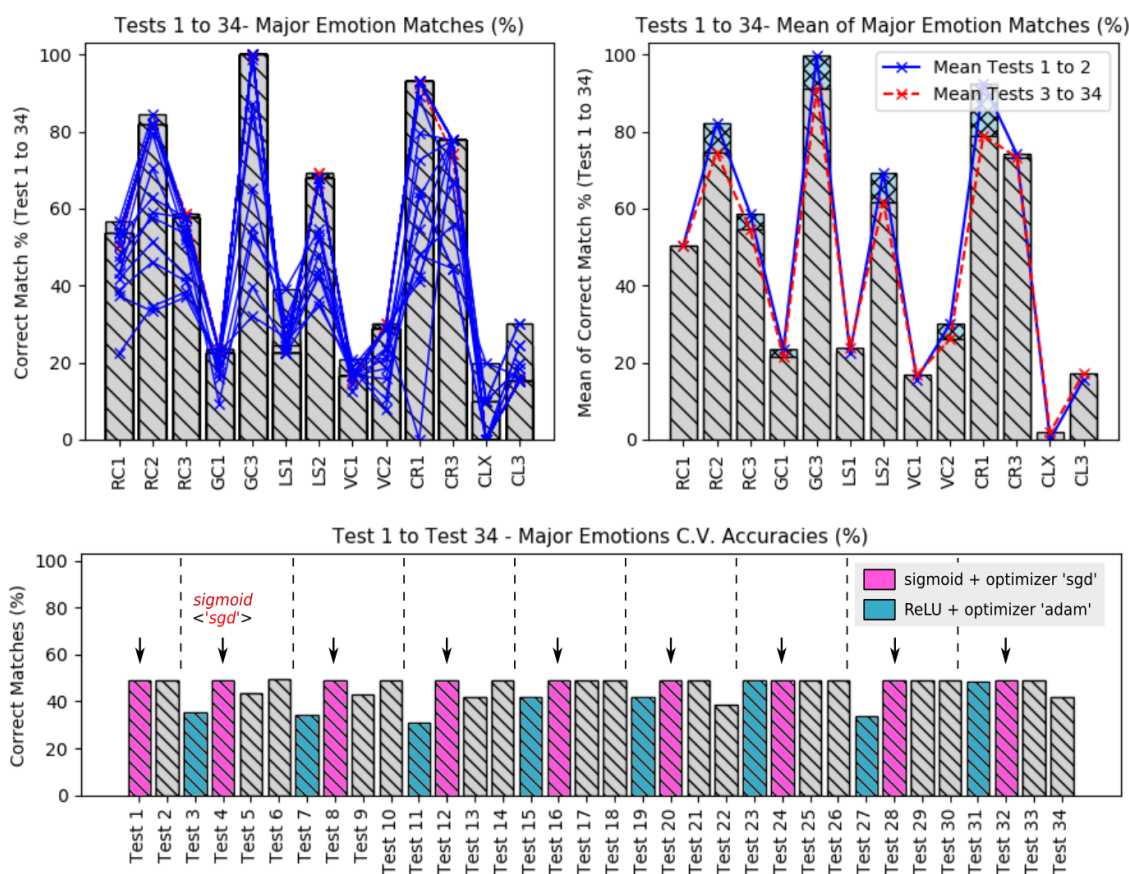


FIGURE 9.8. All major emotion accuracies from the tests 1 to 34. All accuracies (left); mean of all accuracies (right).

9.3.3. Results Improvements

To improve these results, these work shows that is strongly recommended, to first, to optimize the emotions detection from the face. It were undoubtedly, the main reason for several undesirable recognition error levels. Another way to improve it, is to omit some datasets which presented not good recognition levels; it surely will improve the general predicstions or emotion recognition.

However, some results were already improved during this work. For instance, when looking to the learning tasks, absolute improvements, were applied, changing the traditional learning techniques by the deep learning techniques. These last improvements optimized the recognition results in accuracies of recognition and in execution time.

Figure 9.9, shows the improvement due the use of deep learning techniques, regarding to the number of correct matches of the major emotions values, between all emotions considered in this work. It is possible to see, that the dataset CLX kept with worst accuracy also on traditional learning.

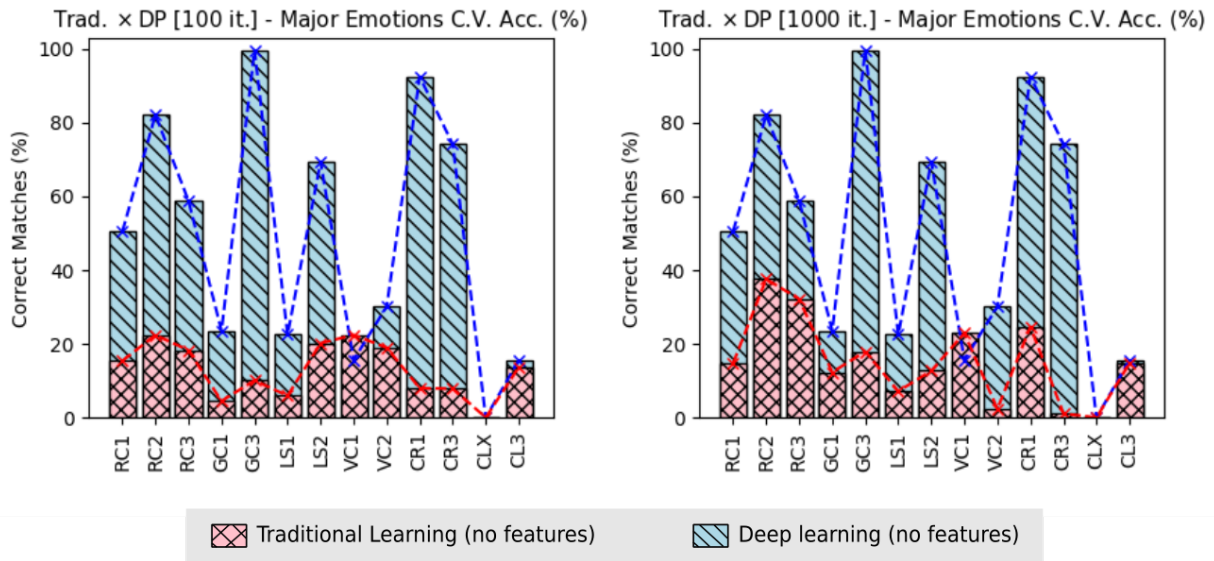


FIGURE 9.9. Traditional learning versus deep learning (DP). Improvement applied in this work, regarding to the major value emotions when applying the traditional learning and deep learning (no feature extraction).

Regarding the the accuracies of the major value emotions based on 100 training iteration of the traditional learning, the improvement happened in 11 flight datasets from 13: RC1 was improved in 69.52% (prior 15.39/actual 50.50); RC2 72.71% (22.41/82.13); RC3 of 68.97% (18.25/58.83); GC1 of 80.97% (4.48/23.55); GC3 of 89.88% (10.08/99.65); LS1 of 73.63% (5.93/22.49); LS2 of 70.96% (20.16/69.43); VC2 of 37.08% (18.95/30.12); CR1 of 91.40% (7.95/92.47); CR3 of 89.39% (7.87/74.18); and CL3 of 12.13% (13.68/15.57). The higher and lower improvements happened for dataset CR1 and CL3 respectively.

Considering the traditional learning using 1,000 training iteration, the improvement happened in 11 flight datasets from 13, as in prior situation: RC1 was improved in 70.77% (14.76/50.50); RC2 of 54.25% (37.57/82.13); RC3 of 45.31% (32.17/58.83); GC1 of 47.77% (12.30/23.55); GC3 of 82.00% (17.93/99.65); LS1 of 68.25% (7.14/22.49); LS2 of 81.17% (12.69/69.43); VC2 of 92.19% (2.35/30.12); CR1 of 73.36% (24.63/92.47); CR3 of 98.53% (1.09/74.18); and CL3 of 5.20% (14.76/15.57). The higher and lower improvements happened for dataset CR3 and CL3 respectively.

The improvement of accuracies over the major emotion values at 100 training iterations were higher, because the execution with 1,000 training iterations presented better accuracies (i.e. less difference from deep learning); however, due the very high exponential execution time of the tradition learning, it discouraged the execution of it traditional manner, using the same training iteration used with the deep learning (6,000 training iterations), which it can takes days or weeks.

Considering the improvements over the execution time, the use of deep learning instead the traditional methods, it produced an optimization of 92.17%, having 4,406.32 seconds (mean of the deep learning applied on tests 1 and 2) instead of 56,321.40 seconds (traditional learning), even when the number of training iteration was 60 times less, i.e. 100 over 6,000 from deep learning. When the training interaction of the traditional learning was increased to 1,000, the

improvement with the use of deep learning was 99.09%, having 4,406.32 seconds (deep learning) instead of 484,586.47 seconds from traditional learning, even using 6 times less training iterations.

Another way to improve the final results, is to execute more flight tests, increasing the amount of data in the dataset. Also, applying personal dataset concept, which the emotion recognition should also be based on personal characteristics of each pilot.

TABLE 9.3. Emotion recognition results tests 1 and 2. ANN with 6×10^3 train epochs and raw data (no features).

Flight Dataset	Test 1 - Emotion Recognition + RTOR - $\varphi_j(v_j(n)) = \text{sigmoid}$, $\text{opt}=\text{'sgd'}$, $N_h = 10 \times 2$, $N_o = 5$ - [Exec. Time: 4325.28s]															
	Happy			Sad			Angry			Surprised			Scared			Match Accuracy (%)
	MARD	RMSE	MAE	MARD	RMSE	MAE	MARD	RMSE	MAE	MARD	RMSE	MAE	MARD	RMSE	MAE	
DS:RC1	*	3.64	0.06	*	4.14	0.06	*	3.83	0.05	*	3.43	0.06	*	5.08	0.08	50.50 (1854/3671)
DS:RC2	*	4.34	0.06	49.35%	5.72	0.07	*	3.59	0.05	*	3.84	0.06	*	5.88	0.09	82.13 (3488/4247)
DS:RC3	*	3.88	0.05	*	9.58	0.11	*	3.78	0.06	*	3.62	0.06	*	5.57	0.09	58.83 (2342/3981)
DS:GC1	*	5.68	0.09	*	8.46	0.13	*	7.34	0.11	*	4.58	0.07	*	5.79	0.09	23.55 (961/4081)
DS:GC3	*	5.63	0.09	*	7.45	0.11	*	7.41	0.11	*	5.42	0.08	*	5.84	0.09	99.65 (4240/4255)
DS:LS1	*	5.70	0.08	*	6.22	0.08	52.55%	3.46	0.04	*	5.18	0.07	*	6.20	0.08	22.49 (1250/5558)
DS:LS2	*	5.52	0.09	84.69%	3.68	0.05	85.52%	2.93	0.04	*	5.04	0.08	*	5.42	0.08	69.43 (2844/4096)
DS:VC1	*	3.98	0.08	*	3.38	0.06	*	4.40	0.08	*	3.43	0.07	70.25%	4.79	0.08	15.63 (408/2611)
DS:VC2	*	3.76	0.08	*	3.89	0.08	*	4.27	0.09	*	2.78	0.06	*	2.53	0.05	30.12 (615/2042)
DS:CR1	*	4.46	0.07	76.31%	17.54	0.24	68.30%	5.00	0.06	*	3.58	0.06	41.14%	1.64	0.02	92.47 (3697/3998)
DS:CR3	*	1.69	0.08	53.28%	3.66	0.15	*	1.16	0.04	*	1.39	0.07	47.65%	1.28	0.05	74.18 (339/457)
DS:CLX	58.25%	4.45	0.16	48.35%	1.00	0.04	49.14%	1.73	0.07	*	1.47	0.06	33.47%	0.54	0.02	0.00 (0/518)
DS:CL3	*	3.27	0.04	40.49%	3.07	0.04	37.38%	5.58	0.07	*	5.39	0.08	*	3.76	0.05	15.57 (735/4722)
		4.31±1.11	0.08±0.02		5.98±4.05	0.09±0.05		4.19±1.77	0.07±0.02		3.78±1.29	0.07±0.00		4.18±1.92	0.07±0.02	48.81±31.67
Flight Dataset	Test 2 - Emotion Recognition + RTOR - $\varphi_j(v_j(n)) = \text{sigmoid}$, $\text{opt}=\text{'adam'}$, $N_h = 10 \times 2$, $N_o = 5$ - [Exec. Time: 4487.36s]															
	Happy			Sad			Angry			Surprised			Scared			Match Accuracy (%)
	MARD	RMSE	MAE	MARD	RMSE	MAE	MARD	RMSE	MAE	MARD	RMSE	MAE	MARD	RMSE	MAE	
DS:RC1	*	1.19	0.02	*	5.44	0.08	*	3.63	0.05	34.50%	0.79	0.01	*	1.76	0.03	50.50 (1854/3671)
DS:RC2	*	1.26	0.02	47.39%	5.77	0.07	94.12%	2.41	0.03	45.23%	1.02	0.01	*	1.73	0.03	82.13 (3488/4247)
DS:RC3	*	4.96	0.06	*	9.14	0.12	*	4.81	0.07	38.65%	0.73	0.01	*	3.44	0.05	58.83 (2342/3981)
DS:GC1	*	0.64	0.01	*	3.97	0.06	*	2.96	0.05	46.72%	0.64	0.01	*	0.74	0.01	23.55 (961/4081)
DS:GC3	*	0.63	0.01	*	3.69	0.06	*	3.34	0.05	*	0.34	0.01	*	0.84	0.01	99.65 (4240/4255)
DS:LS1	*	0.69	0.01	56.03%	1.71	0.02	37.75%	3.47	0.04	60.65%	0.97	0.01	79.73%	0.35	0.00	22.49 (1250/5558)
DS:LS2	*	0.49	0.01	44.02%	3.63	0.04	52.61%	2.99	0.04	*	0.44	0.01	*	0.27	0.00	69.43 (2844/4096)
DS:VC1	*	0.81	0.01	80.20%	2.20	0.04	*	2.39	0.04	25.78%	0.39	0.01	84.33%	7.67	0.13	15.63 (408/2611)
DS:VC2	*	0.28	0.01	*	1.76	0.03	*	1.07	0.02	77.69%	0.96	0.02	84.13%	4.68	0.09	30.12 (615/2042)
DS:CR1	*	2.48	0.04	76.79%	16.56	0.23	68.04%	5.05	0.07	41.52%	0.67	0.01	34.39%	1.93	0.03	92.47 (3697/3998)
DS:CR3	*	1.03	0.05	55.34%	2.83	0.12	*	1.34	0.05	*	0.48	0.02	46.39%	1.75	0.06	74.18 (339/457)
DS:CLX	85.26%	5.66	0.22	44.11%	0.92	0.04	59.82%	2.27	0.09	*	0.32	0.01	62.98%	1.08	0.05	0.00 (0/518)
DS:CL3	80.35%	3.49	0.04	39.31%	4.57	0.05	77.21%	9.82	0.13	23.79%	0.20	0.00	71.54%	2.24	0.03	15.57 (735/4722)
		1.82±1.71	0.04±0.05		4.78±3.98	0.07±0.05		3.50±2.13	0.06±0.02		0.61±0.26	0.01±0.00		2.19±1.97	0.04±0.03	48.81±31.67

TABLE 9.4. Emotion recognition results tests 3 and 4. ANN with 6×10^3 train epochs and input data with feature extraction.

Flight Dataset	Test 3 - Emotion Recognition + RTOR - $\varphi_j(v_j(n)) = ReLU$, $opt='adam'$, $N_h = 90 \times 2$, $N_o = 5$															
	Happy			Sad			Angry			Surprised			Scared			Match Accuracy (%)
	MARD	RMSE	MAE	MARD	RMSE	MAE	MARD	RMSE	MAE	MARD	RMSE	MAE	MARD	RMSE	MAE	
DS:RC1	*	0.23	0.02	*	0.98	0.10	*	0.63	0.06	37.63%	0.11	0.01	*	0.82	0.09	38.80 (26/67)
DS:RC2	*	0.36	0.03	76.88%	0.97	0.09	*	0.50	0.05	45.63%	0.14	0.01	*	0.31	0.02	46.15 (36/78)
DS:RC3	37.72%	0.79	0.07	*	1.66	0.14	72.50%	0.42	0.04	3.55%	0.10	0.01	*	0.56	0.05	41.09 (30/73)
DS:GC1	*	0.73	0.07	*	1.71	0.18	*	0.88	0.10	*	0.11	0.01	*	0.35	0.03	18.66 (14/75)
DS:GC3	*	0.29	0.02	*	1.05	0.10	*	0.36	0.03	*	0.19	0.02	*	0.48	0.04	84.61 (66/78)
DS:LS1	*	0.16	0.01	*	1.21	0.10	*	0.46	0.03	76.55%	0.10	0.01	*	0.30	0.02	25.49 (26/102)
DS:LS2	*	0.36	0.04	47.68%	0.45	0.04	56.47%	0.36	0.03	*	0.14	0.02	*	0.19	0.02	34.66 (26/75)
DS:VC1	*	0.13	0.01	69.21%	0.33	0.03	*	0.39	0.05	46.04%	0.06	0.01	97.80%	1.11	0.14	18.75 (9/48)
DS:VC2	*	0.26	0.04	*	0.68	0.08	*	0.57	0.08	33.75%	0.06	0.01	79.71%	0.60	0.08	7.89 (3/38)
DS:CR1	*	0.16	0.01	74.01%	2.45	0.25	62.22%	0.80	0.07	38.10%	0.12	0.01	94.20%	0.57	0.06	64.38 (47/73)
DS:CR3	*	0.07	0.02	75.32%	0.64	0.18	*	0.26	0.07	29.12%	0.02	0.01	60.91%	0.30	0.08	44.44 (4/9)
DS:CLX	84.30%	0.73	0.20	57.03%	0.18	0.05	81.75%	0.47	0.14	*	0.04	0.01	73.93%	0.19	0.05	20.00 (2/10)
DS:CL3	68.59%	0.40	0.03	88.37%	1.06	0.08	43.26%	0.87	0.08	*	0.17	0.02	66.09%	0.28	0.02	16.27 (14/86)
		0.36±0.23	0.04±0.04		1.03±0.60	0.11±0.06		0.54±0.19	0.06±0.03		0.10±0.04	0.01±0.00		0.47±0.25	0.05±0.03	35.48±20.60
Flight Dataset	Test 4 - Emotion Recognition + RTOR - $\varphi_j(v_j(n)) = sigmoid$, $opt='sgd'$, $N_h = 90 \times 2$, $N_o = 5$															
	Happy			Sad			Angry			Surprised			Scared			Match Accuracy (%)
	MARD	RMSE	MAE	MARD	RMSE	MAE	MARD	RMSE	MAE	MARD	RMSE	MAE	MARD	RMSE	MAE	
DS:RC1	*	0.17	0.02	*	0.42	0.04	79.81%	0.50	0.04	49.75%	0.10	0.01	*	0.30	0.04	53.73 (36/67)
DS:RC2	*	0.22	0.02	81.50%	0.82	0.07	71.64%	0.29	0.03	63.83%	0.12	0.01	*	0.38	0.04	82.05 (64/78)
DS:RC3	*	0.67	0.06	91.27%	1.37	0.11	63.93%	0.29	0.03	47.90%	0.11	0.01	*	0.35	0.04	57.53 (42/73)
DS:GC1	*	0.35	0.04	*	0.96	0.11	*	0.69	0.08	*	0.20	0.02	*	0.37	0.04	22.66 (17/75)
DS:GC3	*	0.35	0.04	*	0.82	0.09	*	0.70	0.08	*	0.31	0.04	*	0.38	0.04	100.00 (78/78)
DS:LS1	*	0.30	0.03	*	0.64	0.06	*	0.30	0.02	*	0.22	0.02	*	0.36	0.04	22.54 (23/102)
DS:LS2	*	0.33	0.04	59.57%	0.38	0.04	40.52%	0.22	0.02	*	0.26	0.03	*	0.32	0.04	68.00 (51/75)
DS:VC1	*	0.21	0.03	81.08%	0.31	0.04	*	0.35	0.05	*	0.13	0.02	68.24%	0.90	0.11	16.66 (8/48)
DS:VC2	*	0.22	0.04	*	0.42	0.06	*	0.36	0.06	80.59%	0.10	0.01	63.14%	0.48	0.06	28.94 (11/38)
DS:CR1	*	0.22	0.02	75.30%	2.58	0.26	66.07%	0.90	0.09	44.30%	0.10	0.01	38.14%	0.28	0.03	93.15 (68/73)
DS:CR3	*	0.09	0.03	52.57%	0.55	0.15	*	0.17	0.05	86.42%	0.05	0.02	51.41%	0.26	0.07	77.77 (7/9)
DS:CLX	76.07%	0.72	0.20	19.94%	0.06	0.02	55.09%	0.36	0.10	*	0.06	0.02	39.71%	0.10	0.03	0.00 (0/10)
DS:CL3	95.58%	0.29	0.03	28.61%	0.39	0.03	58.28%	1.07	0.10	*	0.28	0.03	45.08%	0.16	0.01	15.11 (13/86)
		0.32±0.17	0.05±0.04		0.75±0.61	0.08±0.06		0.48±0.26	0.06±0.02		0.16±0.08	0.02±0.00		0.36±0.18	0.05±0.02	49.09±32.00

TABLE 9.5. Emotion recognition results tests 5 and 6. ANN with 6×10^3 train epochs and input data with feature extraction.

Test 5 - Emotion Recognition + RTOR - $\varphi_j(v_j(n)) = \text{sigmoid}$, $\text{opt}=\text{'sgd'}$, $N_h = 90 \times 2$, $N_o = 5$																
Flight Dataset	Happy			Sad			Angry			Surprised			Scared			Match Accuracy (%)
	MARD	RMSE	MAE	MARD	RMSE	MAE	MARD	RMSE	MAE	MARD	RMSE	MAE	MARD	RMSE	MAE	
DS:RC1	*	0.17	0.02	*	0.91	0.08	*	0.61	0.07	34.72%	0.11	0.01	*	0.23	0.03	43.28 (29/67)
DS:RC2	*	0.20	0.02	83.83%	0.88	0.08	*	0.42	0.04	42.18%	0.12	0.01	*	0.23	0.02	58.97 (46/78)
DS:RC3	*	0.84	0.08	87.21%	1.52	0.13	54.73%	0.32	0.03	2.95%	0.15	0.02	*	0.14	0.02	57.53 (42/73)
DS:GC1	*	0.19	0.02	*	2.25	0.23	*	0.71	0.08	85.11%	0.09	0.01	*	0.29	0.03	22.66 (17/75)
DS:GC3	*	0.14	0.02	*	0.30	0.03	*	0.28	0.03	*	0.12	0.01	*	0.23	0.03	100.00 (78/78)
DS:LS1	*	0.22	0.02	*	1.41	0.12	*	0.41	0.03	76.14%	0.10	0.01	*	0.20	0.02	23.53 (24/102)
DS:LS2	*	0.33	0.04	53.61%	0.42	0.04	76.71%	0.41	0.04	*	0.13	0.01	*	0.23	0.02	42.66 (32/75)
DS:VC1	*	0.12	0.01	51.96%	0.28	0.03	*	0.21	0.03	25.42%	0.05	0.01	84.89%	1.04	0.13	16.66 (8/48)
DS:VC2	*	0.17	0.03	*	0.77	0.09	*	0.48	0.07	27.10%	0.06	0.01	65.38%	0.54	0.07	23.68 (9/38)
DS:CR1	*	0.23	0.02	74.46%	2.48	0.25	62.64%	0.84	0.08	39.67%	0.13	0.01	75.12%	0.47	0.05	72.60 (53/73)
DS:CR3	*	0.05	0.02	75.77%	0.65	0.19	*	0.21	0.06	17.65%	0.01	0.00	61.55%	0.26	0.07	77.77 (7/9)
DS:CLX	89.24%	0.77	0.22	48.67%	0.17	0.05	76.34%	0.48	0.14	*	0.05	0.01	54.28%	0.14	0.04	0.00 (0/10)
DS:CL3	82.20%	0.33	0.03	43.10%	0.61	0.05	49.66%	0.96	0.09	*	0.15	0.02	34.29%	0.18	0.01	24.41 (21/86)
		0.29 ± 0.23	0.04 ± 0.05		0.97 ± 0.71	0.11 ± 0.07		0.49 ± 0.22	0.06 ± 0.03		0.10 ± 0.04	0.01 ± 0.00		0.32 ± 0.23	0.04 ± 0.03	43.37 ± 27.53
Test 6 - Emotion Recognition + RTOR - $\varphi_j(v_j(n)) = \text{sigmoid}$, $\text{opt}=\text{'sgd'}$, $N_h = 90 \times 2$, $N_o = 5$																
Flight Dataset	Happy			Sad			Angry			Surprised			Scared			Match Accuracy (%)
	MARD	RMSE	MAE	MARD	RMSE	MAE	MARD	RMSE	MAE	MARD	RMSE	MAE	MARD	RMSE	MAE	
DS:RC1	*	0.16	0.02	*	0.42	0.04	78.23%	0.50	0.04	41.28%	0.13	0.01	*	0.19	0.02	53.73 (36/67)
DS:RC2	*	0.17	0.02	81.48%	0.82	0.07	69.36%	0.29	0.03	39.53%	0.12	0.01	*	0.26	0.03	82.05 (64/78)
DS:RC3	*	0.78	0.07	91.16%	1.37	0.11	62.17%	0.28	0.03	7.70%	0.12	0.01	*	0.24	0.03	57.53 (42/73)
DS:GC1	*	0.24	0.03	*	0.96	0.11	*	0.68	0.08	56.74%	0.06	0.01	*	0.26	0.03	22.66 (17/75)
DS:GC3	*	0.22	0.03	*	0.82	0.09	*	0.69	0.08	*	0.15	0.02	*	0.27	0.03	100.00 (78/78)
DS:LS1	*	0.17	0.02	*	0.65	0.06	*	0.30	0.02	50.40%	0.07	0.01	*	0.24	0.02	22.54 (23/102)
DS:LS2	*	0.23	0.03	60.13%	0.38	0.04	40.01%	0.21	0.02	*	0.11	0.01	*	0.21	0.02	68.00 (51/75)
DS:VC1	*	0.13	0.02	81.00%	0.31	0.04	*	0.35	0.05	23.69%	0.04	0.00	79.10%	1.01	0.13	16.66 (8/48)
DS:VC2	*	0.13	0.02	*	0.42	0.06	*	0.36	0.06	28.17%	0.07	0.01	66.67%	0.55	0.07	28.94 (11/38)
DS:CR1	*	0.12	0.01	75.42%	2.58	0.26	66.39%	0.92	0.09	37.37%	0.12	0.01	63.46%	0.40	0.04	93.15 (68/73)
DS:CR3	*	0.05	0.02	52.77%	0.55	0.15	*	0.17	0.05	12.71%	0.01	0.00	67.57%	0.30	0.08	77.77 (7/9)
DS:CLX	85.19%	0.76	0.21	20.16%	0.06	0.02	56.26%	0.36	0.11	*	0.04	0.01	60.20%	0.14	0.04	0.00 (0/10)
DS:CL3	73.83%	0.36	0.03	29.04%	0.39	0.03	60.25%	1.10	0.11	*	0.12	0.01	29.13%	0.18	0.01	24.41 (13/86)
		0.27 ± 0.22	0.04 ± 0.05		0.75 ± 0.61	0.08 ± 0.06		0.48 ± 0.27	0.06 ± 0.03		0.09 ± 0.04	0.01 ± 0.00		0.33 ± 0.22	0.04 ± 0.03	49.80 ± 31.33

TABLE 9.6. Emotion recognition results tests 7 and 8. ANN with 6×10^3 train epochs and input data with feature extraction.

Flight Dataset	Test 7 - Emotion Recognition + RTOR [GSR+EEG] - $\varphi_j(v_j(n)) = ReLU, \text{opt}='adam', N_h = 79 \times 2, N_o = 5$															
	Happy			Sad			Angry			Surprised			Scared			Match Accuracy (%)
	MARD	RMSE	MAE	MARD	RMSE	MAE	MARD	RMSE	MAE	MARD	RMSE	MAE	MARD	RMSE	MAE	
DS:RC1	*	0.18	0.02	*	0.76	0.08	*	0.56	0.05	34.16%	0.10	0.01	*	0.60	0.06	37.31 (25/67)
DS:RC2	*	0.29	0.03	77.74%	0.91	0.08	*	0.73	0.07	35.38%	0.11	0.01	*	0.21	0.02	33.33 (26/78)
DS:RC3	*	0.82	0.08	*	1.71	0.15	87.95%	0.48	0.05	16.05%	0.12	0.01	*	0.29	0.02	36.98 (27/73)
DS:GC1	*	0.85	0.08	*	3.25	0.33	*	0.81	0.09	*	0.11	0.01	*	0.13	0.00	20.00 (15/75)
DS:GC3	*	0.13	0.01	*	0.58	0.05	*	0.32	0.03	*	0.15	0.02	*	0.23	0.02	87.17 (68/78)
DS:LS1	*	0.14	0.01	*	1.29	0.11	*	0.41	0.03	63.89%	0.09	0.01	*	0.25	0.02	29.41 (30/102)
DS:LS2	*	0.33	0.03	63.41%	0.46	0.04	88.44%	0.53	0.05	*	0.13	0.01	*	0.20	0.02	44.00 (33/75)
DS:VC1	*	0.11	0.01	72.93%	0.38	0.05	*	0.22	0.02	42.45%	0.06	0.01	91.94%	1.04	0.13	18.75 (9/48)
DS:VC2	*	0.20	0.03	*	0.66	0.08	*	0.75	0.12	44.57%	0.09	0.01	66.76%	0.49	0.06	10.52 (4/38)
DS:CR1	*	0.16	0.01	71.86%	2.54	0.26	67.40%	0.88	0.08	45.50%	0.14	0.01	97.09%	0.58	0.07	64.38 (47/73)
DS:CR3	*	0.06	0.02	53.37%	0.60	0.16	*	0.26	0.08	24.87%	0.02	0.00	59.82%	0.28	0.07	44.44 (4/9)
DS:CLX	90.21%	0.78	0.22	90.16%	0.35	0.08	61.72%	0.41	0.11	*	0.04	0.01	69.64%	0.18	0.05	0.00 (0/10)
DS:CL3	72.18%	0.38	0.03	*	1.35	0.12	40.10%	0.81	0.07	*	0.19	0.02	98.84%	0.31	0.03	19.76 (17/86)
		0.34±0.27	0.04±0.05		1.14±0.85	0.12±0.08		0.55±0.21	0.07±0.02		0.10±0.04	0.01±0.00		0.37±0.24	0.04±0.03	34.31±22.07
Flight Dataset	Test 8 - Emotion Recognition + RTOR [GSR+EEG] - $\varphi_j(v_j(n)) = sigmoid, \text{opt}='sgd', N_h = 79 \times 2, N_o = 5$															
	Happy			Sad			Angry			Surprised			Scared			Match Accuracy (%)
	MARD	RMSE	MAE	MARD	RMSE	MAE	MARD	RMSE	MAE	MARD	RMSE	MAE	MARD	RMSE	MAE	
DS:RC1	*	0.18	0.02	*	0.42	0.04	80.56%	0.50	0.04	55.39%	0.11	0.01	*	0.31	0.04	53.73 (36/67)
DS:RC2	*	0.23	0.02	81.53%	0.81	0.07	72.44%	0.29	0.03	70.48%	0.13	0.01	*	0.39	0.04	82.05 (64/78)
DS:RC3	*	0.67	0.06	91.31%	1.37	0.11	64.92%	0.29	0.03	46.61%	0.12	0.01	*	0.36	0.04	57.53 (42/73)
DS:GC1	*	0.37	0.04	*	0.96	0.11	*	0.69	0.08	*	0.21	0.02	*	0.38	0.04	22.66 (17/75)
DS:GC3	*	0.36	0.04	*	0.82	0.09	*	0.71	0.08	*	0.33	0.04	*	0.40	0.05	100.00 (78/78)
DS:LS1	*	0.31	0.03	*	0.64	0.06	*	0.30	0.02	*	0.24	0.02	*	0.38	0.04	22.54 (23/102)
DS:LS2	*	0.35	0.04	59.58%	0.38	0.04	40.88%	0.22	0.02	*	0.27	0.03	*	0.34	0.04	68.00 (51/75)
DS:VC1	*	0.23	0.03	81.10%	0.31	0.04	*	0.36	0.05	*	0.15	0.02	67.70%	0.89	0.11	16.66 (8/48)
DS:VC2	*	0.23	0.04	*	0.42	0.06	*	0.37	0.06	88.83%	0.11	0.02	63.39%	0.47	0.06	28.94 (11/38)
DS:CR1	*	0.23	0.02	75.27%	2.58	0.26	65.93%	0.90	0.09	50.40%	0.11	0.01	35.43%	0.27	0.03	93.15 (68/73)
DS:CR3	*	0.10	0.03	52.57%	0.55	0.15	*	0.17	0.05	96.66%	0.06	0.02	50.22%	0.26	0.07	77.77 (7/9)
DS:CLX	74.99%	0.71	0.20	19.96%	0.06	0.02	54.65%	0.36	0.10	*	0.06	0.02	37.13%	0.10	0.03	0.00 (0/10)
DS:CL3	98.45%	0.28	0.02	28.62%	0.39	0.03	57.69%	1.07	0.10	*	0.30	0.03	48.72%	0.16	0.01	15.11 (13/86)
		0.33±0.17	0.05±0.04		0.75±0.61	0.08±0.06		0.48±0.26	0.06±0.02		0.17±0.08	0.02±0.00		0.36±0.18	0.05±0.02	49.09±32.00

TABLE 9.7. Emotion recognition results tests 9 and 10. ANN with 6×10^3 train epochs and input data with feature extraction.

Flight Dataset	Test 9 - Emotion Recognition + RTOR [GSR+EEG] - $\varphi_j(v_j(n)) = \text{sigmoid}$, $\text{opt}='adam'$, $N_h = 79 \times 2$, $N_o = 5$															
	Happy			Sad			Angry			Surprised			Scared			Match Accuracy (%)
	MARD	RMSE	MAE	MARD	RMSE	MAE	MARD	RMSE	MAE	MARD	RMSE	MAE	MARD	RMSE	MAE	
DS:RC1	*	0.16	0.02	*	1.31	0.13	*	0.60	0.06	31.39%	0.10	0.01	*	0.26	0.03	52.23 (35/67)
DS:RC2	*	0.20	0.02	88.69%	0.87	0.08	*	0.49	0.04	35.23%	0.10	0.01	*	0.27	0.03	62.82 (49/78)
DS:RC3	*	0.84	0.08	93.30%	1.69	0.14	62.05%	0.42	0.04	12.18%	0.17	0.02	*	0.16	0.02	57.53 (42/73)
DS:GC1	*	0.24	0.03	*	3.01	0.32	*	0.88	0.10	*	0.11	0.01	*	0.33	0.04	22.66 (17/75)
DS:GC3	*	0.14	0.02	*	0.32	0.03	*	0.28	0.03	*	0.10	0.01	*	0.21	0.02	100.00 (78/78)
DS:LS1	*	0.23	0.02	*	1.47	0.13	*	0.33	0.02	79.83%	0.11	0.01	*	0.21	0.02	22.54 (23/102)
DS:LS2	*	0.36	0.04	84.79%	0.58	0.05	99.04%	0.49	0.05	*	0.14	0.02	*	0.21	0.02	36.00 (27/75)
DS:VC1	*	0.12	0.01	42.80%	0.18	0.02	*	0.24	0.03	24.38%	0.05	0.01	84.03%	1.04	0.13	16.66 (8/48)
DS:VC2	*	0.21	0.03	*	0.85	0.11	*	0.61	0.09	32.68%	0.06	0.01	62.24%	0.53	0.07	18.42 (7/38)
DS:CR1	*	0.20	0.02	74.10%	2.54	0.26	69.06%	0.92	0.09	44.69%	0.14	0.01	62.81%	0.41	0.04	79.45 (58/73)
DS:CR3	*	0.05	0.02	67.86%	0.64	0.18	*	0.20	0.06	16.17%	0.01	0.00	59.43%	0.27	0.07	77.77 (7/9)
DS:CLX	87.93%	0.78	0.22	34.85%	0.12	0.03	75.06%	0.47	0.14	*	0.05	0.01	56.94%	0.15	0.04	0.00 (0/10)
DS:CL3	85.57%	0.32	0.03	55.74%	0.73	0.06	49.75%	0.96	0.09	*	0.16	0.02	31.13%	0.17	0.01	15.11 (13/86)
		0.30±0.23	0.04±0.05		1.10±0.85	0.12±0.08		0.53±0.24	0.06±0.03		0.10±0.04	0.01±0.00		0.32±0.23	0.04±0.03	43.17±29.45
Flight Dataset	Test 10 - Emotion Recognition + RTOR [GSR+EEG] - $\varphi_j(v_j(n)) = \text{ReLU}$, $\text{opt}='sgd'$, $N_h = 79 \times 2$, $N_o = 5$															
	Happy			Sad			Angry			Surprised			Scared			Match Accuracy (%)
	MARD	RMSE	MAE	MARD	RMSE	MAE	MARD	RMSE	MAE	MARD	RMSE	MAE	MARD	RMSE	MAE	
DS:RC1	*	0.16	0.02	*	0.42	0.04	78.20%	0.50	0.04	41.10%	0.13	0.01	*	0.19	0.02	53.73 (36/67)
DS:RC2	*	0.17	0.02	81.69%	0.81	0.07	70.00%	0.29	0.03	38.88%	0.12	0.01	*	0.26	0.03	82.05 (64/78)
DS:RC3	*	0.78	0.07	91.04%	1.38	0.11	61.69%	0.28	0.03	7.16%	0.13	0.01	*	0.24	0.03	57.53 (42/73)
DS:GC1	*	0.24	0.03	*	0.96	0.11	*	0.68	0.08	54.86%	0.06	0.01	*	0.26	0.03	22.66 (17/75)
DS:GC3	*	0.22	0.03	*	0.82	0.09	*	0.69	0.08	*	0.15	0.02	*	0.26	0.03	100 (78/78)
DS:LS1	*	0.17	0.02	*	0.65	0.06	*	0.30	0.02	48.01%	0.07	0.01	*	0.23	0.02	22.54 (23/102)
DS:LS2	*	0.22	0.03	59.91%	0.38	0.04	40.08%	0.22	0.02	*	0.11	0.01	*	0.21	0.02	68.00 (51/75)
DS:VC1	*	0.13	0.02	81.57%	0.32	0.04	*	0.35	0.05	23.35%	0.04	0.00	79.08%	1.01	0.13	16.66 (8/48)
DS:VC2	*	0.14	0.02	*	0.42	0.06	*	0.36	0.06	28.57%	0.07	0.01	66.92%	0.55	0.07	28.94 (11/38)
DS:CR1	*	0.12	0.01	75.32%	2.58	0.26	66.51%	0.92	0.09	36.94%	0.12	0.01	62.86%	0.40	0.04	93.15 (68/73)
DS:CR3	*	0.05	0.02	52.55%	0.55	0.15	*	0.17	0.05	10.35%	0.01	0.00	99.99%	0.36	0.11	77.77 (7/9)
DS:CLX	85.40%	0.76	0.21	20.48%	0.06	0.02	56.19%	0.36	0.11	*	0.04	0.01	60.31%	0.14	0.04	0.00 (0/10)
DS:CL3	73.77%	0.36	0.03	28.75%	0.39	0.03	60.22%	1.10	0.11	*	0.11	0.01	29.13%	0.18	0.01	15.11 (13/86)
		0.27±0.22	0.04±0.05		0.75±0.61	0.08±0.06		0.48±0.27	0.06±0.03		0.09±0.04	0.01±0.00		0.33±0.22	0.04±0.03	49.09±32.00

TABLE 9.8. Emotion recognition results tests 11 and 12. ANN with 6×10^3 train epochs and input data with feature extraction.

Flight Dataset	Test 11 - Emotion Recognition + RTOR [HR+EEG] - $\varphi_j(v_j(n)) = ReLU, \text{opt}='adam', N_h = 83 \times 2, N_o = 5$															
	Happy			Sad			Angry			Surprised			Scared			Match Accuracy (%)
	MARD	RMSE	MAE	MARD	RMSE	MAE	MARD	RMSE	MAE	MARD	RMSE	MAE	MARD	RMSE	MAE	
DS:RC1	*	0.25	0.02	90.11%	0.46	0.04	*	0.60	0.06	37.45%	0.12	0.01	*	0.82	0.09	22.38 (15/67)
DS:RC2	*	0.34	0.03	85.34%	0.90	0.08	*	0.81	0.08	53.12%	0.14	0.01	*	0.30	0.03	34.61 (27/78)
DS:RC3	91.62%	0.83	0.08	*	1.67	0.14	69.43%	0.43	0.04	4.61%	0.12	0.01	*	0.51	0.04	38.35 (28/73)
DS:GC1	*	0.71	0.07	*	1.28	0.13	*	0.74	0.08	*	0.14	0.01	*	0.22	0.02	21.33 (16/75)
DS:GC3	*	0.29	0.03	*	0.64	0.05	*	0.42	0.04	*	0.18	0.02	*	0.04	0.00	65.38 (51/78)
DS:LS1	*	0.19	0.01	*	1.26	0.11	*	0.43	0.03	84.13%	0.11	0.01	*	0.16	0.01	25.54 (26/102)
DS:LS2	*	0.32	0.03	46.34%	0.43	0.04	54.16%	0.35	0.03	*	0.16	0.02	*	0.23	0.02	42.66 (32/75)
DS:VC1	*	0.09	0.01	70.92%	0.35	0.04	*	0.42	0.05	32.74%	0.05	0.01	92.36%	1.09	0.14	16.66 (8/48)
DS:VC2	*	0.20	0.03	*	0.61	0.08	*	0.65	0.10	33.18%	0.08	0.01	76.57%	0.57	0.08	21.05 (8/38)
DS:CR1	*	0.15	0.01	74.95%	2.53	0.26	56.14%	0.76	0.07	37.97%	0.12	0.01	83.27%	0.51	0.06	47.94 (35/73)
DS:CR3	*	0.10	0.02	97.93%	0.65	0.20	*	0.40	0.12	38.89%	0.03	0.01	62.29%	0.27	0.07	44.44 (4/9)
DS:CLX	86.23%	0.76	0.21	91.45%	0.31	0.08	66.50%	0.43	0.12	*	0.05	0.01	67.72%	0.18	0.05	0.00 (0/10)
DS:CL3	83.46%	0.40	0.04	85.33%	1.10	0.09	48.68%	0.96	0.09	*	0.19	0.02	73.32%	0.26	0.02	19.76 (17/86)
		0.36±0.24	0.05±0.05		0.94±0.60	0.10±0.06		0.57±0.18	0.07±0.03		0.11±0.04	0.01±0.00		0.40±0.28	0.05±0.03	30.78±16.27
Flight Dataset	Test 12 - Emotion Recognition + RTOR [HR+EEG] - $\varphi_j(v_j(n)) = sigmoid, \text{opt}='sgd', N_h = 83 \times 2, N_o = 5$															
	Happy			Sad			Angry			Surprised			Scared			Match Accuracy (%)
	MARD	RMSE	MAE	MARD	RMSE	MAE	MARD	RMSE	MAE	MARD	RMSE	MAE	MARD	RMSE	MAE	
DS:RC1	*	0.17	0.02	*	0.42	0.04	80.26%	0.50	0.04	53.17%	0.11	0.01	*	0.31	0.04	53.73 (36/67)
DS:RC2	*	0.23	0.02	81.51%	0.82	0.07	72.14%	0.29	0.03	68.08%	0.13	0.01	*	0.39	0.04	82.05 (64/78)
DS:RC3	*	0.67	0.06	91.29%	1.37	0.11	64.47%	0.29	0.03	47.20%	0.11	0.01	*	0.35	0.04	57.53 (42/73)
DS:GC1	*	0.36	0.04	*	0.96	0.11	*	0.69	0.08	*	0.21	0.02	*	0.38	0.04	22.66 (17/75)
DS:GC3	*	0.35	0.04	*	0.82	0.09	*	0.70	0.08	*	0.32	0.04	*	0.39	0.04	100.00 (78/78)
DS:LS1	*	0.31	0.03	*	0.64	0.06	*	0.30	0.02	*	0.23	0.02	*	0.37	0.04	22.54 (23/102)
DS:LS2	*	0.34	0.04	59.57%	0.38	0.04	40.72%	0.22	0.02	*	0.27	0.03	*	0.33	0.04	68.00 (51/75)
DS:VC1	*	0.22	0.03	81.09%	0.31	0.04	*	0.35	0.05	*	0.14	0.02	67.95%	0.90	0.11	16.66 (8/48)
DS:VC2	*	0.23	0.04	*	0.42	0.06	*	0.37	0.06	85.55%	0.10	0.02	63.29%	0.47	0.06	28.94 (11/38)
DS:CR1	*	0.22	0.02	75.29%	2.58	0.26	65.98%	0.90	0.09	47.93%	0.10	0.01	36.52%	0.27	0.03	93.15 (68/73)
DS:CR3	*	0.10	0.03	52.57%	0.55	0.15	*	0.17	0.05	92.57%	0.05	0.02	50.69%	0.26	0.07	77.77 (7/9)
DS:CLX	75.40%	0.71	0.20	19.93%	0.06	0.02	54.83%	0.36	0.10	*	0.06	0.02	38.10%	0.10	0.03	0.00 (0/10)
DS:CL3	97.44%	0.28	0.02	28.61%	0.39	0.03	57.90%	1.07	0.10	*	0.29	0.03	47.40%	0.16	0.01	15.11 (13/86)
		0.32±0.17	0.05±0.04		0.75±0.61	0.08±0.06		0.48±0.26	0.06±0.02		0.16±0.08	0.02±0.00		0.36±0.18	0.05±0.02	49.09±32.00

TABLE 9.9. Emotion recognition results tests 13 and 14. ANN with 6×10^3 train epochs and input data with feature extraction.

Flight Dataset	Test 13 - Emotion Recognition + RTOR [HR+EEG] - $\varphi_j(v_j(n)) = \text{sigmoid}$, $\text{opt}=\text{'adam'}$, $N_h = 83 \times 2$, $N_o = 5$															
	Happy			Sad			Angry			Surprised			Scared			Match Accuracy (%)
	MARD	RMSE	MAE	MARD	RMSE	MAE	MARD	RMSE	MAE	MARD	RMSE	MAE	MARD	RMSE	MAE	
DS:RC1	*	0.16	0.02	*	0.81	0.08	*	0.56	0.06	35.43%	0.11	0.01	*	0.20	0.02	47.76 (32/67)
DS:RC2	*	0.20	0.02	81.09%	0.87	0.08	*	0.46	0.04	38.61%	0.12	0.01	*	0.22	0.02	57.69 (45/78)
DS:RC3	*	0.84	0.08	77.38%	1.58	0.13	51.85%	0.34	0.03	1.65%	0.14	0.01	*	0.21	0.02	53.42 (39/73)
DS:GC1	*	0.20	0.02	*	1.82	0.18	*	0.65	0.07	67.62%	0.07	0.01	*	0.23	0.03	22.66 (17/75)
DS:GC3	*	0.11	0.01	96.73%	0.24	0.02	*	0.23	0.02	*	0.10	0.01	*	0.21	0.02	100.00 (78/78)
DS:LS1	*	0.22	0.02	*	1.14	0.10	*	0.40	0.03	66.70%	0.09	0.01	*	0.15	0.01	22.54 (23/102)
DS:LS2	*	0.34	0.04	63.24%	0.45	0.04	80.18%	0.41	0.04	*	0.14	0.01	*	0.23	0.02	53.33 (40/75)
DS:VC1	*	0.13	0.02	41.49%	0.21	0.03	*	0.26	0.03	23.76%	0.05	0.01	84.91%	1.04	0.13	12.50 (6/48)
DS:VC2	*	0.19	0.03	*	0.76	0.09	*	0.50	0.08	27.03%	0.06	0.01	63.35%	0.53	0.07	23.68 (9/38)
DS:CR1	*	0.23	0.02	72.54%	2.47	0.25	55.38%	0.76	0.07	38.66%	0.12	0.01	60.34%	0.40	0.04	54.79 (40/73)
DS:CR3	*	0.05	0.02	84.43%	0.65	0.20	*	0.18	0.05	16.66%	0.01	0.00	61.17%	0.27	0.08	77.77 (7/9)
DS:CLX	89.97%	0.77	0.22	70.03%	0.22	0.06	74.87%	0.48	0.14	*	0.05	0.01	65.55%	0.16	0.05	0.00 (0/10)
DS:CL3	81.74%	0.33	0.03	86.35%	1.08	0.09	44.15%	0.87	0.08	*	0.16	0.02	34.68%	0.16	0.01	15.11 (13/86)
		0.29±0.23	0.04±0.05		0.95±0.65	0.10±0.06		0.47±0.19	0.06±0.03		0.09±0.04	0.01±0.00		0.31±0.23	0.04±0.03	41.63±27.44
Flight Dataset	Test 14 - Emotion Recognition + RTOR [HR+EEG] - $\varphi_j(v_j(n)) = \text{ReLU}$, $\text{opt}=\text{'sgd'}$, $N_h = 83 \times 2$, $N_o = 5$															
	Happy			Sad			Angry			Surprised			Scared			Match Accuracy (%)
	MARD	RMSE	MAE	MARD	RMSE	MAE	MARD	RMSE	MAE	MARD	RMSE	MAE	MARD	RMSE	MAE	
DS:RC1	*	0.16	0.02	*	0.42	0.04	77.85%	0.50	0.04	40.86%	0.13	0.01	*	0.19	0.02	53.73 (36/67)
DS:RC2	*	0.17	0.02	81.44%	0.82	0.07	69.82%	0.29	0.03	40.09%	0.12	0.01	*	0.26	0.03	82.05 (64/78)
DS:RC3	*	0.78	0.07	91.25%	1.37	0.11	61.95%	0.28	0.03	6.42%	0.12	0.01	*	0.24	0.03	57.53 (42/73)
DS:GC1	*	0.24	0.03	*	0.96	0.11	*	0.68	0.08	56.91%	0.06	0.01	*	0.25	0.03	22.66 (17/75)
DS:GC3	*	0.22	0.03	*	0.82	0.09	*	0.69	0.08	*	0.15	0.02	*	0.27	0.03	100.00 (78/78)
DS:LS1	*	0.17	0.02	*	0.65	0.06	*	0.30	0.02	53.04%	0.07	0.01	*	0.23	0.02	22.54 (23/102)
DS:LS2	*	0.22	0.03	59.94%	0.38	0.04	39.85%	0.21	0.02	*	0.11	0.01	99.66%	0.06	0.01	68.00 (51/75)
DS:VC1	*	0.13	0.02	82.02%	0.32	0.04	*	0.35	0.05	23.70%	0.04	0.00	78.94%	1.01	0.13	16.66 (8/48)
DS:VC2	*	0.14	0.02	*	0.42	0.06	*	0.36	0.06	28.62%	0.07	0.01	66.87%	0.55	0.07	28.94 (11/38)
DS:CR1	*	0.12	0.01	75.35%	2.58	0.26	66.63%	0.92	0.09	38.25%	0.12	0.01	62.94%	0.40	0.04	93.15 (68/73)
DS:CR3	*	0.05	0.02	52.41%	0.55	0.15	*	0.17	0.05	12.21%	0.01	0.00	67.04%	0.29	0.08	77.77 (7/9)
DS:CLX	85.36%	0.76	0.21	20.67%	0.06	0.02	56.01%	0.36	0.11	*	0.04	0.01	60.48%	0.14	0.04	0.00 (0/10)
DS:CL3	73.83%	0.36	0.03	28.76%	0.39	0.03	60.11%	1.10	0.11	*	0.11	0.01	28.65%	0.18	0.01	15.11 (13/86)
		0.27±0.22	0.04±0.05		0.75±0.61	0.08±0.06		0.48±0.27	0.06±0.03		0.09±0.04	0.01±0.00		0.31±0.23	0.04±0.03	49.09±32.00

TABLE 9.10. Emotion recognition results tests 15 and 16. ANN with 6×10^3 train epochs and input data with feature extraction.

Test 15 - Emotion Recognition + RTOR [HR+GSR] - $\varphi_j(v_j(n)) = ReLU$, $opt='adam'$, $N_h = 18 \times 2$, $N_o = 5$																
Flight Dataset	Happy			Sad			Angry			Surprised			Scared			Match
	MARD	RMSE	MAE	MARD	RMSE	MAE	MARD	RMSE	MAE	MARD	RMSE	MAE	MARD	RMSE	MAE	Accuracy (%)
DS:RC1	*	0.25	0.02	*	1.54	0.15	*	0.67	0.07	38.40%	0.09	0.01	*	0.31	0.04	50.75 (34/67)
DS:RC2	*	0.21	0.02	65.65%	1.07	0.09	55.46%	0.39	0.04	45.73%	0.14	0.01	*	0.23	0.03	82.05 (64/78)
DS:RC3	*	0.82	0.08	75.87%	1.57	0.13	30.77%	0.28	0.02	1.20%	0.13	0.01	*	0.19	0.02	54.79 (40/73)
DS:GC1	*	0.22	0.02	*	0.73	0.08	*	0.51	0.06	59.59%	0.06	0.01	*	0.23	0.03	22.67 (17/75)
DS:GC3	*	0.50	0.06	*	0.85	0.09	*	1.13	0.12	*	0.13	0.01	*	0.29	0.03	32.05 (25/78)
DS:LS1	*	0.13	0.01	43.02%	0.31	0.02	45.99%	0.56	0.05	38.62%	0.07	0.01	*	0.18	0.02	26.47 (27/102)
DS:LS2	*	0.10	0.01	48.43%	0.51	0.05	60.50%	0.46	0.05	*	0.08	0.01	*	0.22	0.03	66.67 (50/75)
DS:VC1	*	0.19	0.02	*	0.88	0.08	*	0.54	0.06	42.03%	0.06	0.01	81.53%	0.99	0.13	18.75 (9/48)
DS:VC2	*	0.20	0.03	*	0.59	0.07	*	0.32	0.05	27.24%	0.06	0.01	99.98%	0.67	0.09	28.95 (11/38)
DS:CR1	*	0.25	0.03	74.29%	2.45	0.25	84.93%	0.67	0.07	38.20%	0.12	0.01	62.07%	0.41	0.04	41.10 (30/73)
DS:CR3	51.71%	0.02	0.00	67.73%	0.65	0.19	*	0.21	0.06	20.81%	0.01	0.00	77.24%	0.32	0.09	77.78 (7/9)
DS:CLX	87.40%	0.76	0.21	70.18%	0.33	0.06	61.44%	0.38	0.11	*	0.05	0.01	59.79%	0.16	0.04	10.00 (1/10)
DS:CL3	*	0.58	0.05	42.02%	0.62	0.05	58.21%	1.07	0.10	*	0.10	0.01	53.55%	0.22	0.02	30.23 (26/86)
		0.33±0.24	0.04±0.05		0.93±0.57	0.10±0.06		0.55±0.26	0.07±0.02		0.08±0.03	0.01±0.00		0.34±0.22	0.05±0.03	41.71±22.04
Test 16 - Emotion Recognition + RTOR [HR+GSR] - $\varphi_j(v_j(n)) = sigmoid$, $opt='sgd'$, $N_h = 18 \times 2$, $N_o = 5$																
Flight Dataset	Happy			Sad			Angry			Surprised			Scared			Match
	MARD	RMSE	MAE	MARD	RMSE	MAE	MARD	RMSE	MAE	MARD	RMSE	MAE	MARD	RMSE	MAE	Accuracy (%)
DS:RC1	*	0.36	0.04	*	0.47	0.05	*	0.48	0.05	*	0.32	0.04	*	0.55	0.07	53.73 (36/67)
DS:RC2	*	0.45	0.05	89.10%	0.78	0.07	*	0.38	0.04	*	0.37	0.04	*	0.65	0.07	82.05 (64/78)
DS:RC3	*	0.54	0.05	99.06%	1.33	0.11	*	0.40	0.04	11.28%	0.35	0.04	*	0.60	0.07	57.53 (42/73)
DS:GC1	*	0.63	0.07	*	1.04	0.12	*	0.86	0.10	*	0.47	0.05	*	0.64	0.07	22.67 (17/75)
DS:GC3	*	0.62	0.07	*	0.90	0.10	*	0.87	0.10	*	0.59	0.07	*	0.65	0.07	100.00 (78/78)
DS:LS1	*	0.60	0.06	*	0.73	0.07	*	0.37	0.03	*	0.53	0.05	*	0.66	0.07	22.55 (23/102)
DS:LS2	*	0.59	0.07	70.43%	0.42	0.04	60.37%	0.28	0.03	*	0.52	0.06	*	0.59	0.07	68.00 (51/75)
DS:VC1	*	0.42	0.06	97.66%	0.38	0.05	*	0.49	0.07	*	0.35	0.05	63.25%	0.73	0.09	16.67 (8/48)
DS:VC2	*	0.41	0.07	*	0.47	0.07	*	0.49	0.08	*	0.28	0.04	81.42%	0.37	0.05	28.95 (11/38)
DS:CR1	*	0.46	0.05	73.98%	2.46	0.25	63.97%	0.76	0.07	*	0.34	0.04	22.85%	0.15	0.01	93.15 (68/73)
DS:CR3	*	0.19	0.06	52.27%	0.52	0.15	*	0.16	0.05	*	0.15	0.05	43.72%	0.20	0.05	77.78 (7/9)
DS:CLX	63.30%	0.63	0.17	31.81%	0.09	0.03	43.29%	0.30	0.08	*	0.15	0.05	18.07%	0.04	0.01	0.00 (0/10)
DS:CL3	*	0.33	0.03	32.52%	0.38	0.03	43.68%	0.87	0.08	*	0.57	0.06	*	0.35	0.04	15.12 (13/86)
		0.48±0.13	0.07±0.03		0.77±0.58	0.09±0.05		0.52±0.23	0.06±0.02		0.38±0.13	0.05±0.00		0.48±0.21	0.06±0.02	49.09±32.00

TABLE 9.11. Emotion recognition results tests 17 and 18. ANN with 6×10^3 train epochs and input data with feature extraction.

Flight Dataset	Test 17 - Emotion Recognition + RTOR [HR+GSR] - $\varphi_j(v_j(n)) = \text{sigmoid}$, $\text{opt}=\text{'adam'}$, $N_h = 18 \times 2$, $N_o = 5$															
	Happy			Sad			Angry			Surprised			Scared			Match
	MARD	RMSE	MAE	MARD	RMSE	MAE	MARD	RMSE	MAE	MARD	RMSE	MAE	MARD	RMSE	MAE	Accuracy (%)
DS:RC1	89.18%	0.16	0.02	95.43%	0.41	0.04	72.83%	0.52	0.05	44.25%	0.14	0.01	*	0.19	0.02	53.73 (36/67)
DS:RC2	*	0.19	0.02	83.59%	0.85	0.08	70.13%	0.30	0.03	47.99%	0.13	0.01	*	0.24	0.03	82.05 (64/78)
DS:RC3	*	0.80	0.08	90.09%	1.41	0.12	49.78%	0.26	0.02	17.21%	0.15	0.02	*	0.21	0.02	57.53 (42/73)
DS:GC1	*	0.23	0.03	*	0.95	0.11	*	0.67	0.08	65.26%	0.08	0.01	*	0.26	0.03	22.67 (17/75)
DS:GC3	*	0.18	0.02	*	0.72	0.08	*	0.61	0.07	*	0.12	0.01	*	0.23	0.03	100.00 (78/78)
DS:LS1	*	0.14	0.01	*	0.57	0.05	*	0.35	0.03	32.60%	0.08	0.01	*	0.18	0.02	22.55 (23/102)
DS:LS2	*	0.19	0.02	50.82%	0.34	0.03	36.44%	0.23	0.02	*	0.09	0.01	*	0.19	0.02	68.00 (51/75)
DS:VC1	*	0.16	0.02	89.02%	0.36	0.05	*	0.40	0.05	43.75%	0.06	0.01	77.37%	0.98	0.12	16.67 (8/48)
DS:VC2	*	0.10	0.02	*	0.36	0.05	*	0.30	0.05	34.69%	0.08	0.01	69.00%	0.57	0.08	28.95 (11/38)
DS:CR1	*	0.12	0.01	75.34%	2.58	0.26	66.53%	0.92	0.09	38.42%	0.12	0.01	63.33%	0.40	0.04	93.15 (68/73)
DS:CR3	*	0.05	0.02	49.08%	0.54	0.15	*	0.16	0.05	8.85%	0.01	0.00	67.53%	0.29	0.08	77.78 (7/9)
DS:CLX	86.01%	0.74	0.21	34.87%	0.12	0.03	52.43%	0.37	0.10	*	0.04	0.01	53.00%	0.14	0.04	0.00 (0/10)
DS:CL3	74.84%	0.36	0.03	32.35%	0.41	0.04	58.97%	1.09	0.11	*	0.13	0.01	32.20%	0.17	0.01	15.12 (13/86)
		0.26±0.22	0.04±0.05		0.74±0.62	0.08±0.06		0.48±0.26	0.06±0.02		0.09±0.04	0.01±0.00		0.31±0.22	0.04±0.03	49.09±32.00
Flight Dataset	Test 18 - Emotion Recognition + RTOR [HR+GSR] - $\varphi_j(v_j(n)) = \text{ReLU}$, $\text{opt}=\text{'sgd'}$, $N_h = 18 \times 2$, $N_o = 5$															
	Happy			Sad			Angry			Surprised			Scared			Match
	MARD	RMSE	MAE	MARD	RMSE	MAE	MARD	RMSE	MAE	MARD	RMSE	MAE	MARD	RMSE	MAE	Accuracy (%)
DS:RC1	*	0.16	0.02	*	0.42	0.04	78.23%	0.50	0.04	41.33%	0.13	0.01	*	0.19	0.02	53.73 (36/67)
DS:RC2	*	0.17	0.02	81.63%	0.81	0.07	70.02%	0.29	0.03	39.41%	0.12	0.01	*	0.26	0.03	82.05 (64/78)
DS:RC3	*	0.78	0.07	91.36%	1.37	0.11	61.92%	0.28	0.03	7.02%	0.12	0.01	*	0.24	0.03	57.53 (42/73)
DS:GC1	*	0.24	0.03	*	0.96	0.11	*	0.68	0.08	56.94%	0.06	0.01	*	0.26	0.03	22.67 (17/75)
DS:GC3	*	0.22	0.03	*	0.82	0.09	*	0.69	0.08	754.16%	0.15	0.02	*	0.27	0.03	100.00 (78/78)
DS:LS1	*	0.17	0.02	*	0.64	0.06	*	0.30	0.02	49.92%	0.07	0.01	*	0.23	0.02	22.55 (23/102)
DS:LS2	*	0.22	0.03	59.79%	0.38	0.04	39.79%	0.22	0.02	*	0.11	0.01	*	0.21	0.02	68.00 (51/75)
DS:VC1	*	0.13	0.02	81.48%	0.31	0.04	*	0.34	0.05	24.00%	0.04	0.00	78.96%	1.01	0.13	16.67 (8/48)
DS:VC2	*	0.14	0.02	*	0.42	0.06	*	0.36	0.06	28.36%	0.07	0.01	99.98%	0.67	0.09	28.95 (11/38)
DS:CR1	*	0.12	0.01	75.31%	2.58	0.26	66.51%	0.92	0.09	37.92%	0.12	0.01	62.94%	0.40	0.04	93.15 (68/73)
DS:CR3	*	0.05	0.02	52.57%	0.55	0.15	*	0.17	0.05	11.58%	0.01	0.00	67.73%	0.30	0.08	77.78 (7/9)
DS:CLX	85.49%	0.76	0.21	20.21%	0.06	0.02	56.07%	0.36	0.11	*	0.04	0.01	60.50%	0.14	0.04	0.00 (0/10)
DS:CL3	73.78%	0.36	0.03	28.68%	0.39	0.03	60.20%	1.10	0.11	*	0.12	0.01	28.93%	0.18	0.01	15.12 (13/86)
		0.27±0.22	0.04±0.05		0.75±0.61	0.08±0.06		0.48±0.27	0.06±0.03		0.09±0.04	0.01±0.00		0.34±0.23	0.04±0.03	49.09±32.00

TABLE 9.12. Emotion recognition results tests 19 and 20. ANN with 6×10^3 train epochs and input data with feature extraction.

Flight Dataset	Test 19 - Emotion Recognition + RTOR - $\varphi_j(v_j(n)) = ReLU$, $opt='adam'$, $N_h = 50 \times 2$, $N_o = 5$															
	Happy			Sad			Angry			Surprised			Scared			Match
	MARD	RMSE	MAE	MARD	RMSE	MAE	MARD	RMSE	MAE	MARD	RMSE	MAE	MARD	RMSE	MAE	Accuracy (%)
DS:RC1	*	0.23	0.02	*	1.41	0.13	111.92%	0.60	0.06	34.33%	0.10	0.01	*	0.30	0.03	46.27 (31/67)
DS:RC2	*	0.23	0.02	76.07%	1.04	0.09	62.81%	0.43	0.04	39.64%	0.12	0.01	*	0.12	0.01	79.49 (62/78)
DS:RC3	78.92%	0.79	0.07	*	1.87	0.17	*	0.75	0.07	9.39%	0.10	0.01	*	0.45	0.04	52.05 (38/73)
DS:GC1	*	0.18	0.02	*	0.63	0.07	*	0.70	0.07	47.64%	0.06	0.01	*	0.08	0.01	16.00 (12/75)
DS:GC3	*	0.36	0.03	*	0.53	0.06	*	0.76	0.08	*	0.17	0.02	*	0.33	0.02	55.13 (43/78)
DS:LS1	*	0.16	0.01	*	0.83	0.06	*	0.60	0.05	56.62%	0.09	0.01	*	0.20	0.01	31.37 (32/102)
DS:LS2	*	0.16	0.02	46.08%	0.45	0.04	51.09%	0.37	0.04	*	0.12	0.01	*	0.43	0.03	52.00 (39/75)
DS:VC1	*	0.27	0.03	*	0.62	0.07	*	0.56	0.07	41.08%	0.06	0.01	76.99%	1.00	0.12	20.83 (10/48)
DS:VC2	*	0.22	0.03	*	0.95	0.10	*	0.32	0.05	34.99%	0.06	0.01	75.78%	0.59	0.08	21.05 (8/38)
DS:CR1	*	0.19	0.02	67.72%	2.43	0.24	57.93%	0.89	0.08	34.98%	0.10	0.01	89.92%	0.55	0.06	63.01 (46/73)
DS:CR3	*	0.07	0.02	51.63%	0.39	0.11	*	0.20	0.05	26.57%	0.02	0.01	61.88%	0.29	0.08	77.78 (7/9)
DS:CLX	81.52%	0.72	0.20	94.39%	0.41	0.08	66.44%	0.41	0.12	*	0.06	0.01	72.31%	0.19	0.05	10.00 (1/10)
DS:CL3	81.79%	0.36	0.03	76.16%	0.99	0.08	56.92%	1.08	0.10	*	0.15	0.01	*	0.38	0.03	18.60 (16/86)
		0.30±0.20	0.04±0.04		0.97±0.58	0.10±0.05		0.59±0.23	0.07±0.02		0.09±0.03	0.01±0.00		0.38±0.23	0.04±0.03	41.81±22.81
Flight Dataset	Test 20 - Emotion Recognition + RTOR - $\varphi_j(v_j(n)) = sigmoid$, $opt='sgd'$, $N_h = 50 \times 2$, $N_o = 5$															
	Happy			Sad			Angry			Surprised			Scared			Match
	MARD	RMSE	MAE	MARD	RMSE	MAE	MARD	RMSE	MAE	MARD	RMSE	MAE	MARD	RMSE	MAE	Accuracy (%)
DS:RC1	*	0.21	0.02	*	0.42	0.04	84.78%	0.49	0.04	79.91%	0.15	0.02	*	0.37	0.04	53.73 (36/67)
DS:RC2	*	0.28	0.03	82.12%	0.81	0.07	77.49%	0.30	0.03	*	0.19	0.02	*	0.45	0.05	82.05 (64/78)
DS:RC3	*	0.63	0.06	91.97%	1.37	0.11	71.00%	0.30	0.03	39.93%	0.17	0.02	*	0.42	0.05	57.53 (42/73)
DS:GC1	*	0.43	0.05	*	0.96	0.11	*	0.72	0.08	*	0.28	0.03	*	0.45	0.05	22.67 (17/75)
DS:GC3	*	0.42	0.05	*	0.82	0.09	*	0.73	0.08	*	0.39	0.04	*	0.46	0.05	100.00 (78/78)
DS:LS1	*	0.38	0.04	*	0.64	0.06	*	0.30	0.02	*	0.31	0.03	*	0.45	0.04	22.55 (23/102)
DS:LS2	*	0.41	0.05	60.17%	0.38	0.04	43.47%	0.22	0.02	*	0.33	0.04	*	0.40	0.05	68.00 (51/75)
DS:VC1	*	0.27	0.04	82.11%	0.32	0.04	*	0.38	0.05	*	0.20	0.03	66.16%	0.85	0.10	16.67 (8/48)
DS:VC2	*	0.27	0.04	*	0.42	0.06	*	0.39	0.06	*	0.15	0.02	65.65%	0.44	0.06	28.95 (11/38)
DS:CR1	*	0.29	0.03	75.05%	2.56	0.26	65.40%	0.87	0.09	76.95%	0.16	0.02	26.21%	0.22	0.02	93.15 (68/73)
DS:CR3	*	0.12	0.04	52.55%	0.55	0.15	*	0.16	0.05	*	0.08	0.03	45.65%	0.24	0.06	77.78 (7/9)
DS:CLX	70.67%	0.69	0.19	20.69%	0.06	0.02	52.26%	0.35	0.10	*	0.08	0.02	27.11%	0.08	0.02	0.00 (0/10)
DS:CL3	*	0.27	0.02	28.84%	0.39	0.03	54.35%	1.02	0.10	*	0.37	0.04	67.15%	0.19	0.02	15.12 (13/86)
		0.36±0.15	0.05±0.04		0.75±0.61	0.08±0.06		0.48±0.25	0.06±0.02		0.22±0.10	0.03±0.00		0.39±0.17	0.05±0.02	49.09±32.00

TABLE 9.13. Emotion recognition results tests 21 and 22. ANN with 6×10^3 train epochs and input data with feature extraction.

Test 21 - Emotion Recognition + RTOR - $\varphi_j(v_j(n)) = \text{sigmoid}$, $\text{opt}=\text{'adam'}$, $N_h = 50 \times 2$, $N_o = 5$																
Flight Dataset	Happy			Sad			Angry			Surprised			Scared			Match
	MARD	RMSE	MAE	MARD	RMSE	MAE	MARD	RMSE	MAE	MARD	RMSE	MAE	MARD	RMSE	MAE	Accuracy (%)
DS:RC1	*	0.16	0.02	*	0.79	0.08	85.96%	0.50	0.05	42.72%	0.12	0.01	*	0.24	0.03	53.73 (36/67)
DS:RC2	*	0.18	0.02	78.38%	1.00	0.09	71.81%	0.31	0.03	44.98%	0.14	0.01	*	0.26	0.03	82.05 (64/78)
DS:RC3	*	0.79	0.08	*	1.56	0.14	78.75%	0.40	0.03	19.89%	0.15	0.02	*	0.29	0.03	57.53 (42/73)
DS:GC1	*	0.18	0.02	*	0.61	0.07	*	0.56	0.06	43.09%	0.05	0.01	*	0.21	0.02	22.67 (17/75)
DS:GC3	*	0.22	0.02	*	0.76	0.07	*	0.67	0.07	*	0.14	0.01	*	0.25	0.03	100.00 (78/78)
DS:LS1	*	0.17	0.01	56.53%	0.31	0.02	*	0.36	0.03	41.72%	0.08	0.01	*	0.22	0.02	22.55 (23/102)
DS:LS2	*	0.21	0.02	41.88%	0.42	0.04	37.51%	0.24	0.02	*	0.10	0.01	*	0.20	0.02	68.00 (51/75)
DS:VC1	*	0.13	0.02	64.26%	0.33	0.04	*	0.34	0.04	34.90%	0.06	0.01	83.66%	1.02	0.13	16.67 (8/48)
DS:VC2	*	0.12	0.02	*	0.30	0.04	*	0.30	0.05	33.94%	0.08	0.01	68.82%	0.57	0.08	28.95 (11/38)
DS:CR1	*	0.16	0.02	72.85%	2.53	0.26	61.33%	0.88	0.09	39.49%	0.12	0.01	60.34%	0.40	0.04	93.15 (68/73)
DS:CR3	*	0.08	0.02	33.57%	0.39	0.09	*	0.12	0.03	45.90%	0.03	0.01	62.16%	0.29	0.08	77.78 (7/9)
DS:CLX	87.78%	0.76	0.21	55.36%	0.20	0.05	57.29%	0.39	0.11	96.88%	0.05	0.01	62.19%	0.16	0.05	0.00 (0/10)
DS:CL3	79.33%	0.38	0.03	37.55%	0.56	0.05	63.14%	1.15	0.11	*	0.11	0.01	35.10%	0.19	0.01	15.12 (13/86)
		0.27±0.22	0.04±0.05		0.75±0.62	0.08±0.05		0.48±0.27	0.06±0.02		0.09±0.03	0.01±0.00		0.33±0.22	0.04±0.03	49.09±32.00
Test 22 - Emotion Recognition + RTOR - $\varphi_j(v_j(n)) = \text{ReLU}$, $\text{opt}=\text{'sgd'}$, $N_h = 50 \times 2$, $N_o = 5$																
Flight Dataset	Happy			Sad			Angry			Surprised			Scared			Match
	MARD	RMSE	MAE	MARD	RMSE	MAE	MARD	RMSE	MAE	MARD	RMSE	MAE	MARD	RMSE	MAE	Accuracy (%)
DS:RC1	*	0.16	0.02	*	0.42	0.04	78.30%	0.50	0.04	41.39%	0.13	0.01	*	0.19	0.02	53.73 (36/67)
DS:RC2	*	0.17	0.02	81.59%	0.81	0.07	69.99%	0.29	0.03	39.55%	0.12	0.01	*	0.26	0.03	82.05 (64/78)
DS:RC3	*	0.78	0.07	91.40%	1.37	0.11	61.98%	0.28	0.03	7.21%	0.12	0.01	*	0.24	0.03	57.53 (42/73)
DS:GC1	*	0.24	0.03	*	0.96	0.11	*	0.68	0.08	56.91%	0.06	0.01	*	0.26	0.03	22.67 (17/75)
DS:GC3	*	0.23	0.03	*	0.82	0.09	*	0.69	0.08	*	0.15	0.02	*	0.27	0.03	100.00 (78/78)
DS:LS1	*	0.17	0.02	*	0.64	0.06	*	0.30	0.02	50.14%	0.07	0.01	*	0.23	0.02	22.55 (23/102)
DS:LS2	*	0.22	0.03	59.83%	0.38	0.04	39.81%	0.22	0.02	*	0.11	0.01	*	0.21	0.02	68.00 (51/75)
DS:VC1	*	0.13	0.02	81.52%	0.31	0.04	*	0.34	0.05	23.83%	0.04	0.00	79.01%	1.01	0.13	16.67 (8/48)
DS:VC2	*	0.14	0.02	*	0.42	0.06	*	0.36	0.06	28.44%	0.07	0.01	66.77%	0.55	0.07	28.95 (11/38)
DS:CR1	*	0.12	0.01	75.33%	2.58	0.26	66.48%	0.92	0.09	37.57%	0.12	0.01	63.12%	0.40	0.04	93.15 (68/73)
DS:CR3	*	0.05	0.02	52.58%	0.55	0.15	*	0.17	0.05	12.02%	0.01	0.00	67.68%	0.30	0.08	77.78 (7/9)
DS:CLX	85.55%	0.76	0.21	20.33%	0.06	0.02	56.02%	0.36	0.11	*	0.04	0.01	60.56%	0.14	0.04	0.00 (0/10)
DS:CL3	73.73%	0.36	0.03	28.65%	0.39	0.03	60.20%	1.10	0.11	*	0.12	0.01	28.81%	0.18	0.01	15.12 (13/86)
		0.27±0.22	0.04±0.05		0.75±0.61	0.08±0.06		0.48±0.27	0.06±0.03		0.09±0.04	0.01±0.00		0.33±0.22	0.04±0.03	49.09±32.00

TABLE 9.14. Emotion recognition results tests 23 and 24. ANN with 6×10^3 train epochs and input data with feature extraction.

Flight Dataset	Test 23 - Emotion Recognition + RTOR [GSR+EEG] - $\varphi_j(v_j(n)) = ReLU$, $opt='adam'$, $N_h = 44 \times 2$, $N_o = 5$															
	Happy			Sad			Angry			Surprised			Scared			Match
	MARD	RMSE	MAE	MARD	RMSE	MAE	MARD	RMSE	MAE	MARD	RMSE	MAE	MARD	RMSE	MAE	Accuracy (%)
DS:RC1	95.54%	0.22	0.02	*	1.25	0.11	*	0.61	0.06	37.79%	0.11	0.01	*	0.26	0.02	43.28 (29/67)
DS:RC2	*	0.33	0.03	72.65%	0.99	0.09	61.52%	0.35	0.03	38.64%	0.11	0.01	*	0.08	0.01	70.51 (55/78)
DS:RC3	*	0.78	0.08	*	1.80	0.16	*	0.75	0.07	39.27%	0.11	0.01	*	0.38	0.03	50.68 (37/73)
DS:GC1	*	0.19	0.02	*	0.59	0.06	*	0.75	0.07	49.65%	0.06	0.01	*	0.07	0.01	9.33 (7/75)
DS:GC3	*	0.27	0.02	*	0.92	0.08	*	0.82	0.08	*	0.16	0.02	*	0.25	0.02	52.56 (41/78)
DS:LS1	*	0.42	0.02	*	0.74	0.06	*	0.66	0.06	56.57%	0.08	0.01	*	0.30	0.02	39.22 (40/102)
DS:LS2	*	0.16	0.01	54.67%	0.57	0.05	74.21%	0.54	0.05	*	0.10	0.01	*	0.07	0.01	54.67 (41/75)
DS:VC1	*	0.19	0.02	*	0.64	0.06	*	0.49	0.06	49.41%	0.07	0.01	86.96%	1.02	0.13	14.58 (7/48)
DS:VC2	*	0.19	0.03	*	0.94	0.10	*	0.49	0.06	30.19%	0.06	0.01	81.65%	0.54	0.07	28.95 (11/38)
DS:CR1	*	0.19	0.02	85.30%	2.59	0.27	59.73%	0.86	0.08	36.10%	0.11	0.01	79.43%	0.50	0.05	42.47 (31/73)
DS:CR3	*	0.05	0.01	57.15%	0.36	0.09	*	0.12	0.03	26.85%	0.02	0.01	57.71%	0.29	0.07	66.67 (6/9)
DS:CLX	92.12%	0.78	0.22	60.90%	0.21	0.05	76.76%	0.45	0.13	*	0.05	0.01	60.97%	0.17	0.04	10.00 (1/10)
DS:CL3	90.09%	0.42	0.04	40.79%	0.59	0.05	58.72%	1.12	0.10	*	0.15	0.01	*	0.47	0.04	18.60 (16/86)
		0.32±0.21	0.04±0.05		0.94±0.61	0.09±0.05		0.62±0.24	0.07±0.02		0.09±0.03	0.01±0.00		0.34±0.24	0.04±0.03	38.58±19.97
Flight Dataset	Test 24 - Emotion Recognition + RTOR [GSR+EEG] - $\varphi_j(v_j(n)) = sigmoid$, $opt='sgd'$, $N_h = 44 \times 2$, $N_o = 5$															
	Happy			Sad			Angry			Surprised			Scared			Match
	MARD	RMSE	MAE	MARD	RMSE	MAE	MARD	RMSE	MAE	MARD	RMSE	MAE	MARD	RMSE	MAE	Accuracy (%)
DS:RC1	*	0.22	0.02	*	0.42	0.04	86.46%	0.49	0.04	87.95%	0.17	0.02	*	0.39	0.05	53.73 (36/67)
DS:RC2	*	0.30	0.03	82.50%	0.81	0.07	79.64%	0.31	0.03	*	0.21	0.02	*	0.47	0.05	82.05 (64/78)
DS:RC3	*	0.62	0.06	92.38%	1.37	0.11	73.33%	0.31	0.03	37.28%	0.19	0.02	*	0.44	0.05	57.53 (42/73)
DS:GC1	*	0.45	0.05	*	0.96	0.11	*	0.73	0.08	*	0.30	0.03	*	0.46	0.05	22.67 (17/75)
DS:GC3	*	0.44	0.05	*	0.82	0.09	*	0.75	0.08	*	0.41	0.05	*	0.48	0.05	100.00 (78/78)
DS:LS1	*	0.40	0.04	*	0.65	0.06	*	0.31	0.02	*	0.33	0.03	*	0.47	0.05	22.55 (23/102)
DS:LS2	*	0.43	0.05	60.64%	0.38	0.04	44.59%	0.22	0.02	*	0.35	0.04	*	0.42	0.05	68.00 (51/75)
DS:VC1	*	0.29	0.04	82.84%	0.32	0.04	*	0.39	0.05	*	0.21	0.03	65.74%	0.84	0.10	16.67 (8/48)
DS:VC2	*	0.29	0.05	*	0.42	0.06	*	0.40	0.06	*	0.16	0.02	66.99%	0.43	0.06	28.95 (11/38)
DS:CR1	*	0.31	0.03	74.95%	2.55	0.26	65.22%	0.86	0.09	86.30%	0.18	0.02	24.24%	0.20	0.02	93.15 (68/73)
DS:CR3	*	0.13	0.04	52.54%	0.55	0.15	*	0.16	0.05	*	0.09	0.03	44.83%	0.24	0.06	77.78 (7/9)
DS:CLX	69.27%	0.69	0.19	21.23%	0.07	0.02	51.35%	0.34	0.10	366.15%	0.09	0.02	24.71%	0.07	0.02	0.00 (0/10)
DS:CL3	*	0.27	0.02	28.98%	0.38	0.03	53.37%	1.01	0.10	*	0.39	0.04	72.59%	0.21	0.02	15.12 (13/86)
		0.37±0.14	0.04±0.05		0.75±0.61	0.08±0.06		0.48±0.25	0.06±0.02		0.24±0.10	0.03±0.00		0.39±0.18	0.05±0.02	49.09±32.00

TABLE 9.15. Emotion recognition results tests 25 and 26. ANN with 6×10^3 train epochs and input data with feature extraction.

Flight Dataset	Test 25 - Emotion Recognition + RTOR [GSR+EEG] - $\varphi_j(v_j(n)) = \text{sigmoid}$, $\text{opt}=\text{'adam'}$, $N_h = 44 \times 2$, $N_o = 5$															
	Happy			Sad			Angry			Surprised			Scared			Match Accuracy (%)
	MARD	RMSE	MAE	MARD	RMSE	MAE	MARD	RMSE	MAE	MARD	RMSE	MAE	MARD	RMSE	MAE	
DS:RC1	98.41%	0.16	0.02	*	0.61	0.06	93.84%	0.53	0.05	45.62%	0.14	0.01	*	0.21	0.02	53.73 (36/67)
DS:RC2	*	0.17	0.02	79.98%	0.94	0.08	66.82%	0.29	0.03	49.97%	0.15	0.01	*	0.24	0.03	82.05 (64/78)
DS:RC3	*	0.79	0.08	*	1.42	0.13	84.15%	0.40	0.04	28.38%	0.15	0.02	*	0.28	0.03	57.53 (42/73)
DS:GC1	*	0.17	0.02	*	0.68	0.08	*	0.57	0.07	40.48%	0.06	0.01	*	0.21	0.02	22.67 (17/75)
DS:GC3	*	0.21	0.02	*	0.74	0.08	*	0.68	0.08	*	0.13	0.01	*	0.25	0.03	100.00 (78/78)
DS:LS1	*	0.14	0.01	83.83%	0.43	0.04	*	0.34	0.03	37.43%	0.08	0.01	*	0.18	0.02	22.55 (23/102)
DS:LS2	*	0.18	0.02	38.04%	0.37	0.03	38.28%	0.24	0.02	*	0.07	0.01	*	0.17	0.02	68.00 (51/75)
DS:VC1	*	0.12	0.01	67.57%	0.34	0.04	256.68%	0.33	0.04	41.18%	0.07	0.01	85.41%	1.03	0.13	16.67 (8/48)
DS:VC2	*	0.12	0.02	*	0.41	0.06	*	0.33	0.05	41.52%	0.09	0.01	70.05%	0.58	0.08	28.95 (11/38)
DS:CR1	*	0.13	0.01	75.01%	2.58	0.26	65.95%	0.92	0.09	37.43%	0.12	0.01	62.48%	0.40	0.04	93.15 (68/73)
DS:CR3	*	0.09	0.02	43.56%	0.42	0.12	*	0.13	0.03	50.69%	0.03	0.01	63.11%	0.29	0.08	77.78 (7/9)
DS:CLX	88.78%	0.77	0.22	42.48%	0.19	0.04	60.72%	0.39	0.11	88.54%	0.05	0.01	66.68%	0.16	0.05	0.00 (0/10)
DS:CL3	71.68%	0.40	0.04	35.00%	0.55	0.05	66.75%	1.19	0.12	*	0.07	0.01	40.19%	0.22	0.02	15.12 (13/86)
		0.27±0.23	0.04±0.05		0.74±0.05	0.08±0.05		0.49±0.28	0.06±0.03		0.09±0.03	0.01±0.00		0.32±0.23	0.04±0.03	49.09±32.00
Flight Dataset	Test 26 - Emotion Recognition + RTOR [GSR+EEG] - $\varphi_j(v_j(n)) = \text{ReLU}$, $\text{opt}=\text{'sgd'}$, $N_h = 44 \times 2$, $N_o = 5$															
	Happy			Sad			Angry			Surprised			Scared			Match Accuracy (%)
	MARD	RMSE	MAE	MARD	RMSE	MAE	MARD	RMSE	MAE	MARD	RMSE	MAE	MARD	RMSE	MAE	
DS:RC1	*	0.16	0.02	*	0.42	0.04	78.20%	0.50	0.04	41.41%	0.13	0.01	*	0.19	0.02	53.73 (36/67)
DS:RC2	*	0.17	0.02	81.68%	0.81	0.07	70.03%	0.29	0.03	39.32%	0.12	0.01	*	0.26	0.03	82.05 (64/78)
DS:RC3	*	0.78	0.07	91.37%	1.37	0.11	61.98%	0.28	0.03	6.68%	0.12	0.01	*	0.24	0.03	57.53 (42/73)
DS:GC1	*	0.24	0.03	*	0.96	0.11	*	0.68	0.08	56.95%	0.06	0.01	*	0.26	0.03	22.67 (17/75)
DS:GC3	*	0.23	0.03	*	0.82	0.09	*	0.69	0.08	*	0.15	0.02	*	0.27	0.03	100.00 (78/78)
DS:LS1	*	0.17	0.02	*	0.64	0.06	*	0.30	0.02	49.67%	0.07	0.01	*	0.23	0.02	22.55 (23/102)
DS:LS2	*	0.22	0.03	59.82%	0.38	0.04	39.84%	0.22	0.02	*	0.11	0.01	*	0.21	0.02	68.00 (51/75)
DS:VC1	*	0.13	0.02	81.50%	0.31	0.04	*	0.34	0.05	23.76%	0.04	0.00	78.98%	1.01	0.13	16.67 (8/48)
DS:VC2	*	0.14	0.02	*	0.42	0.06	*	0.36	0.06	28.43%	0.07	0.01	66.84%	0.55	0.07	28.95 (11/38)
DS:CR1	*	0.12	0.01	75.32%	2.58	0.26	66.50%	0.92	0.09	37.87%	0.12	0.01	63.05%	0.40	0.04	93.15 (68/73)
DS:CR3	*	0.05	0.02	52.50%	0.55	0.15	*	0.17	0.05	12.21%	0.01	0.00	67.63%	0.30	0.08	77.78 (7/9)
DS:CLX	85.52%	0.76	0.21	20.24%	0.06	0.02	56.04%	0.36	0.11	123.90%	0.04	0.01	60.63%	0.15	0.04	0.00 (0/10)
DS:CL3	73.83%	0.36	0.03	28.70%	0.39	0.03	60.14%	1.10	0.11	202.72%	0.12	0.01	28.91%	0.18	0.01	15.12 (13/86)
		0.27±0.22	0.04±0.05		0.75±0.61	0.08±0.06		0.48±0.27	0.06±0.03		0.09±0.04	0.01±0.00		0.33±0.22	0.04±0.03	49.09±32.00

TABLE 9.16. Emotion recognition results tests 27 and 28. ANN with 6×10^3 train epochs and input data with feature extraction.

Flight Dataset	Test 27 - Emotion Recognition + RTOR [HR+EEG] - $\varphi_j(v_j(n)) = ReLU, \text{opt}='adam', N_h = 46 \times 2, N_o = 5$															
	Happy			Sad			Angry			Surprised			Scared			Match Accuracy (%)
	MARD	RMSE	MAE	MARD	RMSE	MAE	MARD	RMSE	MAE	MARD	RMSE	MAE	MARD	RMSE	MAE	
DS:RC1	*	0.24	0.02	*	1.23	0.12	87.90%	0.50	0.05	40.78%	0.12	0.01	*	0.42	0.04	41.79 (28/67)
DS:RC2	*	0.22	0.02	76.24%	0.94	0.08	*	0.52	0.05	37.74%	0.12	0.01	*	0.15	0.01	51.28 (40/78)
DS:RC3	*	0.79	0.07	*	1.74	0.15	*	0.54	0.05	13.44%	0.10	0.01	*	0.45	0.04	42.47 (31/73)
DS:GC1	*	0.23	0.02	*	0.63	0.06	*	0.58	0.06	66.90%	0.07	0.01	*	0.07	0.00	17.33 (13/75)
DS:GC3	*	0.29	0.02	*	0.37	0.03	*	0.57	0.05	*	0.15	0.02	*	0.31	0.02	39.74 (31/78)
DS:LS1	*	0.24	0.02	*	1.46	0.11	*	0.54	0.04	67.00%	0.10	0.01	*	0.15	0.01	24.51 (25/102)
DS:LS2	*	0.28	0.03	69.12%	0.61	0.05	83.28%	0.50	0.05	*	0.12	0.01	*	0.42	0.04	48.00 (36/75)
DS:VC1	*	0.25	0.03	78.97%	0.36	0.04	*	0.67	0.08	36.61%	0.05	0.01	78.34%	0.96	0.12	16.67 (8/48)
DS:VC2	*	0.50	0.06	*	0.30	0.04	*	0.62	0.08	39.09%	0.06	0.01	79.43%	0.58	0.08	15.79 (6/38)
DS:CR1	*	0.20	0.02	76.89%	2.53	0.26	73.04%	0.89	0.09	32.84%	0.10	0.01	92.75%	0.56	0.06	47.95 (35/73)
DS:CR3	*	0.08	0.02	36.77%	0.37	0.09	91.51%	0.15	0.04	37.64%	0.03	0.01	72.44%	0.28	0.08	55.56 (5/9)
DS:CLX	*	0.78	0.22	64.09%	0.22	0.06	76.70%	0.48	0.14	*	0.05	0.01	95.76%	0.24	0.07	10.00 (1/10)
DS:CL3	*	0.41	0.04	43.03%	0.63	0.05	56.57%	1.07	0.10	*	0.15	0.01	*	0.44	0.03	30.23 (26/86)
		0.35±0.21	0.05±0.05		0.88±0.66	0.09±0.06		0.59±0.20	0.07±0.02		0.09±0.03	0.01±0.00		0.39±0.22	0.05±0.03	33.95±14.96
Flight Dataset	Test 28 - Emotion Recognition + RTOR [HR+EEG] - $\varphi_j(v_j(n)) = sigmoid, \text{opt}='sgd', N_h = 46 \times 2, N_o = 5$															
	Happy			Sad			Angry			Surprised			Scared			Match Accuracy (%)
	MARD	RMSE	MAE	MARD	RMSE	MAE	MARD	RMSE	MAE	MARD	RMSE	MAE	MARD	RMSE	MAE	
DS:RC1	*	0.22	0.02	*	0.42	0.04	85.85%	0.49	0.04	85.06%	0.16	0.02	*	0.38	0.05	53.73 (36/67)
DS:RC2	*	0.29	0.03	82.33%	0.81	0.07	78.82%	0.31	0.03	*	0.20	0.02	*	0.46	0.05	82.05 (64/78)
DS:RC3	*	0.62	0.06	92.22%	1.37	0.11	72.42%	0.31	0.03	38.35%	0.18	0.02	*	0.43	0.05	57.53 (42/73)
DS:GC1	*	0.44	0.05	*	0.96	0.11	*	0.72	0.08	*	0.29	0.03	*	0.46	0.05	22.67 (17/75)
DS:GC3	*	0.44	0.05	*	0.82	0.09	*	0.74	0.08	*	0.41	0.05	*	0.47	0.05	100.00 (78/78)
DS:LS1	*	0.40	0.04	*	0.65	0.06	*	0.30	0.02	*	0.32	0.03	*	0.46	0.05	22.55 (23/102)
DS:LS2	*	0.42	0.05	60.48%	0.38	0.04	44.22%	0.22	0.02	*	0.35	0.04	*	0.41	0.05	68.00 (51/75)
DS:VC1	*	0.28	0.04	82.52%	0.32	0.04	*	0.38	0.05	*	0.21	0.03	65.91%	0.84	0.10	16.67 (8/48)
DS:VC2	*	0.28	0.05	*	0.42	0.06	*	0.39	0.06	*	0.16	0.02	66.50%	0.44	0.06	28.95 (11/38)
DS:CR1	*	0.30	0.03	74.98%	2.55	0.26	65.28%	0.86	0.09	83.16%	0.17	0.02	24.83%	0.21	0.02	93.15 (68/73)
DS:CR3	*	0.13	0.04	52.54%	0.55	0.15	*	0.16	0.05	*	0.08	0.03	45.02%	0.24	0.06	77.78 (7/9)
DS:CLX	69.77%	0.69	0.19	21.01%	0.06	0.02	51.68%	0.34	0.10	*	0.09	0.02	25.58%	0.07	0.02	0.00 (0/10)
DS:CL3	*	0.27	0.02	28.92%	0.39	0.03	53.74%	1.02	0.10	*	0.38	0.04	70.50%	0.20	0.02	15.12 (13/86)
		0.37±0.15	0.05±0.04		0.75±0.61	0.08±0.06		0.48±0.25	0.06±0.02		0.23±0.10	0.03±0.00		0.39±0.18	0.05±0.02	49.09±32.00

TABLE 9.17. Emotion recognition results tests 29 and 30. ANN with 6×10^3 train epochs and input data with feature extraction.

Flight Dataset	Test 29 - Emotion Recognition + RTOR [HR+EEG] - $\varphi_j(v_j(n)) = \text{sigmoid}$, $\text{opt}=\text{'adam'}$, $N_h = 46 \times 2$, $N_o = 5$															
	Happy			Sad			Angry			Surprised			Scared			Match
	MARD	RMSE	MAE	MARD	RMSE	MAE	MARD	RMSE	MAE	MARD	RMSE	MAE	MARD	RMSE	MAE	Accuracy (%)
DS:RC1	97.63%	0.16	0.02	*	0.58	0.06	74.59%	0.50	0.05	45.69%	0.14	0.01	*	0.21	0.02	53.73 (36/67)
DS:RC2	*	0.19	0.02	*	1.02	0.09	82.16%	0.34	0.03	45.10%	0.13	0.01	*	0.28	0.03	82.05 (64/78)
DS:RC3	*	0.80	0.08	*	1.47	0.13	79.64%	0.41	0.04	30.39%	0.16	0.02	*	0.28	0.03	57.53 (42/73)
DS:GC1	*	0.17	0.02	*	0.63	0.07	*	0.54	0.06	39.86%	0.06	0.01	*	0.20	0.02	22.67 (17/75)
DS:GC3	*	0.21	0.02	*	0.69	0.07	*	0.66	0.07	628.24%	0.13	0.01	*	0.25	0.03	100.00 (78/78)
DS:LS1	*	0.13	0.01	60.50%	0.34	0.03	*	0.37	0.03	36.71%	0.08	0.01	*	0.18	0.02	22.55 (23/102)
DS:LS2	*	0.21	0.02	43.36%	0.40	0.03	38.57%	0.25	0.02	*	0.09	0.01	*	0.20	0.02	68.00 (51/75)
DS:VC1	*	0.12	0.01	70.11%	0.35	0.04	*	0.34	0.04	36.74%	0.06	0.01	84.05%	1.02	0.13	16.67 (8/48)
DS:VC2	*	0.12	0.02	*	0.46	0.06	*	0.35	0.05	41.74%	0.08	0.01	71.57%	0.57	0.08	28.95 (11/38)
DS:CR1	*	0.13	0.01	74.47%	2.57	0.26	64.81%	0.91	0.09	36.97%	0.12	0.01	61.72%	0.40	0.04	93.15 (68/73)
DS:CR3		0.09	0.02	38.12%	0.41	0.10	*	0.14	0.04	45.03%	0.03	0.01	62.83%	0.28	0.08	77.78 (7/9)
DS:CLX	88.77%	0.77	0.22	48.73%	0.20	0.04	60.12%	0.39	0.11	93.84%	0.05	0.01	65.16%	0.16	0.05	0.00 (0/10)
DS:CL3	80.86%	0.37	0.03	50.39%	0.67	0.06	57.89%	1.09	0.10	*	0.14	0.01	41.89%	0.20	0.02	15.12 (13/86)
		0.27±0.04	0.04±0.05		0.75±0.61	0.08±0.05		0.48±0.25	0.06±0.02		0.10±0.03	0.01±0.00		0.33±0.22	0.04±0.03	49.09±32.00
Flight Dataset	Test 30 - Emotion Recognition + RTOR [HR+EEG] - $\varphi_j(v_j(n)) = \text{ReLU}$, $\text{opt}=\text{'sgd'}$, $N_h = 46 \times 2$, $N_o = 5$															
	Happy			Sad			Angry			Surprised			Scared			Match
	MARD	RMSE	MAE	MARD	RMSE	MAE	MARD	RMSE	MAE	MARD	RMSE	MAE	MARD	RMSE	MAE	Accuracy (%)
DS:RC1	*	0.16	0.02	*	0.42	0.04	78.23%	0.50	0.04	41.37%	0.13	0.01	*	0.19	0.02	53.73 (36/67)
DS:RC2	*	0.17	0.02	81.63%	0.81	0.07	69.96%	0.29	0.03	39.24%	0.12	0.01	*	0.26	0.03	82.05 (64/78)
DS:RC3	*	0.78	0.07	91.43%	1.37	0.11	61.86%	0.28	0.03	6.92%	0.12	0.01	*	0.24	0.03	57.53 (42/73)
DS:GC1	*	0.24	0.03	*	0.96	0.11	*	0.68	0.08	56.80%	0.06	0.01	*	0.26	0.03	22.67 (17/75)
DS:GC3	*	0.23	0.03	*	0.82	0.09	*	0.69	0.08	*	0.15	0.02	*	0.27	0.03	100.00 (78/78)
DS:LS1	*	0.17	0.02	*	0.64	0.06	*	0.30	0.02	49.69%	0.07	0.01	*	0.23	0.02	22.55 (23/102)
DS:LS2	*	0.22	0.03	59.85%	0.38	0.04	39.78%	0.21	0.02	*	0.11	0.01	*	0.21	0.02	68.00 (51/75)
DS:VC1	*	0.13	0.02	81.66%	0.32	0.04	*	0.34	0.05	23.64%	0.04	0.00	78.86%	1.01	0.13	16.67 (8/48)
DS:VC2	*	0.14	0.02	*	0.42	0.06	*	0.36	0.06	28.42%	0.07	0.01	66.83%	0.55	0.07	28.95 (11/38)
DS:CR1	*	0.12	0.01	75.32%	2.58	0.26	66.46%	0.92	0.09	37.85%	0.12	0.01	63.04%	0.40	0.04	93.15 (68/73)
DS:CR3	*	0.05	0.02	52.57%	0.55	0.15	*	0.17	0.05	12.08%	0.01	0.00	67.65%	0.30	0.08	77.78 (7/9)
DS:CLX	85.57%	0.76	0.21	20.34%	0.06	0.02	56.07%	0.36	0.11	*	0.04	0.01	60.58%	0.15	0.04	0.00 (0/10)
DS:CL3	73.84%	0.36	0.03	28.69%	0.39	0.03	60.20%	1.10	0.11	*	0.12	0.01	28.87%	0.18	0.01	15.12 (13/86)
		0.27±0.22	0.04±0.05		0.75±0.61	0.08±0.06		0.48±0.27	0.06±0.03		0.09±0.04	0.01±0.00		0.33±0.22	0.04±0.03	49.09±32.00

TABLE 9.18. Emotion recognition results tests 31 and 32. ANN with 6×10^3 train epochs and input data with feature extraction.

Flight Dataset	Test 31 - Emotion Recognition + RTOR [HR+GSR] - $\varphi_j(v_j(n)) = ReLU, \text{opt}='adam', N_h = 10 \times 2, N_o = 5$															
	Happy			Sad			Angry			Surprised			Scared			Match Accuracy (%)
	MARD	RMSE	MAE	MARD	RMSE	MAE	MARD	RMSE	MAE	MARD	RMSE	MAE	MARD	RMSE	MAE	
DS:RC1	*	0.17	0.02	*	0.97	0.09	71.83%	0.44	0.04	43.44%	0.12	0.01	*	0.28	0.03	56.72 (38/67)
DS:RC2	*	0.20	0.02	84.17%	1.07	0.10	65.80%	0.39	0.04	42.08%	0.13	0.01	*	0.22	0.02	84.62 (66/78)
DS:RC3	*	0.78	0.07	*	1.57	0.14	*	0.66	0.07	7.33%	0.11	0.01	*	0.31	0.03	57.53 (42/73)
DS:GC1	*	0.21	0.02	*	0.99	0.10	*	0.67	0.07	60.19%	0.07	0.01	*	0.20	0.02	22.67 (17/75)
DS:GC3	*	0.21	0.02	*	0.71	0.07	*	0.64	0.07	*	0.14	0.02	*	0.26	0.03	98.72 (77/78)
DS:LS1	*	0.11	0.01	75.08%	0.56	0.03	93.22%	0.48	0.04	35.46%	0.07	0.01	*	0.18	0.02	22.55 (23/102)
DS:LS2	*	0.18	0.02	46.21%	0.44	0.04	99.98%	0.67	0.07	*	0.09	0.01	*	0.17	0.02	68.00 (51/75)
DS:VC1	*	0.12	0.02	74.40%	0.36	0.04	*	0.33	0.04	28.15%	0.04	0.00	81.74%	1.01	0.13	16.67 (8/48)
DS:VC2	*	0.09	0.01	*	0.36	0.04	*	0.29	0.04	28.21%	0.07	0.01	67.86%	0.58	0.08	28.95 (11/38)
DS:CR1	*	0.20	0.02	73.21%	2.53	0.25	66.33%	0.98	0.10	35.28%	0.12	0.01	67.98%	0.44	0.05	89.04 (65/73)
DS:CR3	*	0.07	0.02	53.17%	0.51	0.14	*	0.13	0.03	18.44%	0.01	0.00	66.41%	0.31	0.08	66.67 (6/9)
DS:CLX	89.29%	0.78	0.22	19.56%	0.07	0.02	67.79%	0.42	0.12	*	0.04	0.01	58.11%	0.15	0.04	0.00 (0/10)
DS:CL3	70.88%	0.35	0.03	48.22%	0.65	0.05	58.59%	1.09	0.10	*	0.12	0.01	48.23%	0.23	0.02	15.12 (13/86)
		0.27±0.22	0.04±0.05		0.83±0.61	0.09±0.06		0.55±0.25	0.06±0.02		0.09±0.03	0.01±0.00		0.33±0.22	0.04±0.03	48.25±31.04
Flight Dataset	Test 32 - Emotion Recognition + RTOR [HR+GSR] - $\varphi_j(v_j(n)) = sigmoid, \text{opt}='sgd', N_h = 10 \times 2, N_o = 5$															
	Happy			Sad			Angry			Surprised			Scared			Match Accuracy (%)
	MARD	RMSE	MAE	MARD	RMSE	MAE	MARD	RMSE	MAE	MARD	RMSE	MAE	MARD	RMSE	MAE	
DS:RC1	*	0.49	0.06	*	0.55	0.06	*	0.51	0.05	*	0.46	0.06	*	0.69	0.08	53.73 (36/67)
DS:RC2	*	0.59	0.06	98.61%	0.76	0.07	*	0.49	0.05	*	0.52	0.06	*	0.80	0.09	82.05 (64/78)
DS:RC3	*	0.52	0.05	*	1.28	0.11	*	0.51	0.06	11.46%	0.50	0.06	*	0.75	0.09	57.53 (42/73)
DS:GC1	*	0.77	0.09	*	1.14	0.13	*	0.99	0.11	*	0.62	0.07	*	0.79	0.09	22.67 (17/75)
DS:GC3	*	0.76	0.09	*	1.00	0.11	*	1.01	0.11	*	0.74	0.08	*	0.80	0.09	100.00 (78/78)
DS:LS1	*	0.77	0.08	*	0.85	0.08	*	0.48	0.04	*	0.70	0.07	*	0.83	0.08	22.55 (23/102)
DS:LS2	*	0.74	0.09	85.15%	0.50	0.05	81.89%	0.38	0.04	*	0.67	0.08	*	0.73	0.08	68.00 (51/75)
DS:VC1	*	0.54	0.08	*	0.46	0.06	*	0.59	0.08	*	0.46	0.07	64.98%	0.65	0.08	16.67 (8/48)
DS:VC2	*	0.51	0.08	*	0.54	0.08	*	0.58	0.09	*	0.38	0.06	96.56%	0.34	0.05	28.95 (11/38)
DS:CR1	*	0.60	0.07	73.29%	2.36	0.24	65.32%	0.67	0.06	*	0.48	0.06	39.30%	0.22	0.02	93.15 (68/73)
DS:CR3	*	0.24	0.08	52.05%	0.50	0.14	*	0.18	0.05	*	0.20	0.07	49.44%	0.17	0.05	77.78 (7/9)
DS:CLX	59.30%	0.59	0.16	46.41%	0.13	0.04	37.11%	0.25	0.07	*	0.20	0.06	30.36%	0.07	0.02	0.00 (0/10)
DS:CL3	*	0.44	0.04	39.56%	0.41	0.04	35.96%	0.75	0.07	*	0.73	0.08	*	0.50	0.05	15.12 (13/86)
		0.58±0.14	0.08±0.02		0.81±0.54	0.09±0.05		0.57±0.23	0.07±0.02		0.51±0.17	0.07±0.00		0.56±0.26	0.07±0.02	49.09±32.00

TABLE 9.19. Emotion recognition results tests 33 and 34. ANN with 6×10^3 train epochs and input data with feature extraction.

Flight Dataset	Test 33 - Emotion Recognition + RTOR [HR+GSR] - $\varphi_j(v_j(n)) = \text{sigmoid}$, $\text{opt}=\text{'adam'}$, $N_h = 10 \times 2$, $N_o = 5$															
	Happy			Sad			Angry			Surprised			Scared			Match Accuracy (%)
	MARD	RMSE	MAE	MARD	RMSE	MAE	MARD	RMSE	MAE	MARD	RMSE	MAE	MARD	RMSE	MAE	
DS:RC1	*	0.16	0.02	*	0.42	0.04	77.53%	0.50	0.04	42.25%	0.13	0.01	*	0.19	0.02	53.73 (36/67)
DS:RC2	*	0.17	0.02	81.11%	0.82	0.07	69.26%	0.29	0.03	40.21%	0.12	0.01	*	0.26	0.03	82.05 (64/78)
DS:RC3	*	0.78	0.07	90.95%	1.38	0.11	60.86%	0.28	0.03	5.41%	0.13	0.01	*	0.23	0.03	57.53 (42/73)
DS:GC1	*	0.23	0.03	*	0.95	0.11	*	0.67	0.08	54.81%	0.06	0.01	*	0.25	0.03	22.67 (17/75)
DS:GC3	*	0.22	0.02	*	0.81	0.09	*	0.69	0.08	*	0.15	0.02	*	0.26	0.03	100.00 (78/78)
DS:LS1	*	0.17	0.01	*	0.64	0.06	*	0.30	0.02	48.14%	0.07	0.01	*	0.23	0.02	22.55 (23/102)
DS:LS2	*	0.22	0.02	58.96%	0.37	0.04	39.43%	0.22	0.02	*	0.10	0.01	*	0.21	0.02	68.00 (51/75)
DS:VC1	*	0.13	0.02	80.27%	0.31	0.04	*	0.34	0.05	23.41%	0.04	0.00	79.31%	1.01	0.13	16.67 (8/48)
DS:VC2	*	0.13	0.02	*	0.41	0.06	*	0.35	0.06	28.61%	0.07	0.01	67.06%	0.55	0.07	28.95 (11/38)
DS:CR1	*	0.12	0.01	75.39%	2.59	0.26	66.63%	0.92	0.09	38.77%	0.12	0.01	63.67%	0.41	0.04	93.15 (68/73)
DS:CR3	*	0.05	0.02	52.59%	0.55	0.15	*	0.17	0.05	12.88%	0.01	0.00	68.26%	0.30	0.08	77.78 (7/9)
DS:CLX	85.75%	0.76	0.21	19.38%	0.06	0.02	56.48%	0.37	0.11	*	0.04	0.01	61.16%	0.15	0.04	0.00 (0/10)
DS:CL3	73.24%	0.36	0.03	28.45%	0.39	0.03	60.65%	1.10	0.11	*	0.11	0.01	29.36%	0.18	0.01	15.12 (13/86)
		0.27±0.22	0.04±0.05		0.75±0.62	0.08±0.06		0.48±0.27	0.06±0.03		0.09±0.04	0.01±0.00		0.33±0.22	0.04±0.03	49.09±32.00
Flight Dataset	Test 34 - Emotion Recognition + RTOR [HR+GSR] - $\varphi_j(v_j(n)) = \text{ReLU}$, $\text{opt}=\text{'sgd'}$, $N_h = 10 \times 2$, $N_o = 5$															
	Happy			Sad			Angry			Surprised			Scared			Match Accuracy (%)
	MARD	RMSE	MAE	MARD	RMSE	MAE	MARD	RMSE	MAE	MARD	RMSE	MAE	MARD	RMSE	MAE	
DS:RC1	*	0.16	0.02	*	0.42	0.04	78.20%	0.50	0.04	41.37%	0.13	0.01	*	0.19	0.02	53.73 (36/67)
DS:RC2	*	0.17	0.02	81.62%	0.81	0.07	70.03%	0.29	0.03	39.42%	0.12	0.01	*	0.26	0.03	82.05 (64/78)
DS:RC3	*	0.78	0.07	91.38%	1.37	0.11	61.93%	0.28	0.03	6.98%	0.12	0.01	*	0.24	0.03	57.53 (42/73)
DS:GC1	*	0.24	0.03	*	0.96	0.11	*	0.68	0.08	56.95%	0.06	0.01	*	0.26	0.03	22.67 (17/75)
DS:GC3	*	0.22	0.03	*	0.82	0.09	*	0.69	0.08	*	0.15	0.02	*	0.27	0.03	100.00 (78/78)
DS:LS1	*	0.17	0.02	*	0.64	0.06	*	0.30	0.02	49.93%	0.07	0.01	*	0.23	0.02	22.55 (23/102)
DS:LS2	*	0.22	0.03	59.79%	0.38	0.04	99.98%	0.67	0.07	*	0.11	0.01	*	0.21	0.02	68.00 (51/75)
DS:VC1	*	0.13	0.02	81.47%	0.31	0.04	*	0.34	0.05	23.94%	0.04	0.00	78.96%	1.01	0.13	16.67 (8/48)
DS:VC2	*	0.14	0.02	*	0.42	0.06	*	0.36	0.06	28.42%	0.07	0.01	99.98%	0.67	0.09	28.95 (11/38)
DS:CR1	*	0.12	0.01	99.99%	3.24	0.34	66.50%	0.92	0.09	37.91%	0.12	0.01	62.94%	0.40	0.04	0.00 (0/73)
DS:CR3	*	0.05	0.02	52.57%	0.55	0.15	*	0.17	0.05	11.56%	0.01	0.00	67.74%	0.30	0.08	77.78 (7/9)
DS:CLX	85.50%	0.76	0.21	20.20%	0.06	0.02	56.06%	0.36	0.11	*	0.04	0.01	60.50%	0.14	0.04	0.00 (0/10)
DS:CL3	73.78%	0.36	0.03	28.68%	0.39	0.03	60.21%	1.10	0.11	*	0.12	0.01	28.93%	0.18	0.01	15.12 (13/86)
		0.27±0.22	0.04±0.05		0.80±0.77	0.09±0.08		0.51±0.26	0.06±0.02		0.09±0.04	0.01±0.00		0.34±0.23	0.04±0.03	41.93±31.76

Findings, Limitations and Conclusions

This work presents a multimodal solution to give support in the avoidance of aviation accidents caused by human failures. In this context, the aviation was applied through the use of simulated flights and several tasks executed by volunteers having different expertise.

The experiment's scope was based on physiologic sensing approach to recognize emotions and to analyze β -band signals of several volunteers that acted like pilots in flight. All simulated flights were executed using the Microsoft Flight Simulator-Steam Edition (FSX-SE) and the aircraft Cessna 172SP. Cameras, execution checklists, questionnaires, and devices to acquire data based on GSR, HR and EEG were also used. The simulated flight plan, departed from Lisbon to Alverca, Portugal and it was executed by 8 volunteers which 13 datasets were obtained on the present analysis, having data of both genders.

The present experiment was executed looking for the volunteers side, which they acted like aircraft pilots. A total of 3 different biosignals of the volunteers' body were acquired: HR, GSR, EEG and also an additional data was considered based on face recordings, to identify emotions to give support on the offline analysis. Several sensors were used: Enobio-NE8, Shimmer3+GSR/HR, MedLab Pearl 100 and Arduino Uno. In addition, some emotional questionnaires were also applied before, during and after each flight experiment.

10.1. Findings

Regarding to the β -band analysis, several results were obtained on this experiment. In the β -band spectrogram analysis were possible to visualize the brain's behaviour during the quietest moments of the flight (reported by the volunteers through the use of questionnaires) which the spectrograms shown to have less amplitude and signal oscillation along the time, compared to the most stressful or critical flight moments. The opposite situations were also identified i.e., in flight moments which it require more attention (takeoff, approach and landing), the brain signal presented higher amplitude and oscillation. It mainly, due the level of attention and alertness that these tasks required.

Spectrograms of the EEG data were acquired from the frontal and temporal lobes, and it shown to reflect better the flight phases, according to the feelings reported by each volunteer. When the volunteers' expertise and confidence on the proposed flight simulation were considered, it showed that the highest brain magnitudes and oscillations observed of more experienced and confident volunteers, were on average close to 68.44% less compared to less experienced and unsure volunteers. Moreover, more experienced and confident volunteers in general presented different patterns of brain activities compared to volunteers having less expertise or less familiarity with flight simulations and/or electronic games. In addition, the mean of the volunteer's brain activity presented the highest amplitudes during the the takeoff, approach, final approach and landing, having values close to 37.06–67.33% higher compared to other flight moments. Additional plots of normalized mean values of brain activities for each lobe position also confirmed

that the less experienced and unsure volunteers presented higher amplitudes of β -band mainly during critical flight tasks, which it demand more attention and self-control.

Regarding to the developed emotion recognition system, the results reached different levels of accuracy. In this recognition, several features were extracted together with datamining and ANN techniques. The tests of the produced output models, showed that the lowest recognition errors were reached when all biosignal datasets were considered or when the GSR dataset were omitted of the model training. It also showed that the emotion *surprised* was the easiest to recognize, having a mean value of RMSE of 0.13 and mean value of MAE of 0.01; the emotion *sad*, presented the worst recognition levels, having a mean value of RMSE of 0.82 and mean value of MAE of 0.08. It can be partially explained by the number of emotion instances detected by the Face Reader software, which the emotions *happy*, *surprised* and *scared* presented more instances along the experiments. When only the major emotion values along the time were considered, the mean of the best classification accuracies was close of 76.42%.

10.2. Limitations

Few limitations were faced along the present work, however, the present work has managed to get round that quite well.

Some limitations were detected on the recognition of facial emotions by the Face Reader software in real time, which it presented some undetected emotions, resulting sometimes in such decrease of facial dataset and outputted model quality. Most part of these mismatches were minimized along the preprocessing and processing, but some of them continued to affect the regression models and accuracies of the emotion recognition. Other practical limitation faced during the development of this work, was the lack of support from aviation schools and pilots from Portugal, to bring the present work to a more realistic context.

10.3. Final Remarks and Future Works

To better understand the achievements of the proposed work, further studies should be performed to show the potential and applicability of emotion recognition and β -band analysis on aviation context. Thus, more emotion recognition tests need to be executed, omitting the datasets which it presented the lowest accuracies, to optimize the total mean accuracies; also, improvements to optimize the quality of the face emotion dataset, processed by the Face Reader software, to obtain better accuracies and lower error levels; to improve the facial emotions, the use of Tensorflow, YOLO+Darknet, can be used to replace the Face Reader software in real time. Also, the number of volunteers and flight experiments must to be increased to improve the models.

Further researches intend to apply these proposed experiments on real context, storing biosignals of real pilots in real time, also processing acquired data after each flight, to produce diagnosis of pilot emotions and brain activities along the real flights; execute experiments also within corporative environments and other places; apply and compare our ANN and deep learning architectures, over another methods of automatic emotion recognition; and develop other methods to optimize noisy dataset.

Therefore, the presented experiments and results, succeeded and shown that proposed theoretical and practical experiment architecture are scalable and feasible enough to apply in real

life context, whatever the emotional context and work environment, such as aviation, industry, corporative institution and so on.

References

- Abdelwahab, M. and C. Busso (2017). “Incremental adaptation using active learning for acoustic emotion recognition.” In: pp. 5160–5164. DOI: 10.1109/ICASSP.2017.7953140.
- Adhikari, S. and H. Haddad Khodaparast (2021). “A multimodal approach for simultaneous mass and rotary inertia sensing from vibrating cantilevers.” In: *Physica E: Low-dimensional Systems and Nanostructures* 125, pp. 1–10. ISSN: 1386-9477. DOI: <https://doi.org/10.1016/j.physe.2020.114366>. URL: <https://www.sciencedirect.com/science/article/pii/S1386947720304434>.
- Agrafioti, Foteini, Dimitrios Hatzinakos, and Adam K. Anderson (2012). “ECG pattern analysis for emotion detection.” In: *IEEE Transactions on Affective Computing* 3, pp. 102–115.
- al., Mikels J.A. et (2005). “Emotional Category Data on Images from the International Affective Picture System.” In: 37 (4), pp. 626–630.
- Al-Fahoum, Amjed and Ausilah A Al-Fraihat (Feb. 2014). “Methods of EEG Signal Features Extraction Using Linear Analysis in Frequency and Time-Frequency Domains.” In: 2014, p. 730218.
- Al-Qazzaz, NK et al. (2015). “Selection of Mother Wavelet Functions for Multi-Channel EEG Signal Analysis during a Working Memory Task.” In: *Sensors (Basel)* 15.11, pp. 29015–29035. DOI: <https://doi.org/10.3390/s151129015>.
- Alberdi, Ane, Asier Aztiria, and Adrian Basarab (2016). “Towards an automatic early stress recognition system for office environments based on multimodal measurements: A review.” In: *Journal of Biomedical Informatics* 59, pp. 49–75. ISSN: 1532-0464. DOI: <https://doi.org/10.1016/j.jbi.2015.11.007>. URL: <http://www.sciencedirect.com/science/article/pii/S1532046415002750>.
- Alhouseini, Amjad M.R. Alzeer et al. (2016). “Emotion Detection Using Physiological Signals EEG & ECG.” In: 8.3, pp. 103–112.
- Alonso, Jesús B. et al. (2015). “New approach in quantification of emotional intensity from the speech signal: emotional temperature.” In: *Expert Systems with Applications* 42.24, pp. 9554–9564. ISSN: 0957-4174. DOI: <https://doi.org/10.1016/j.eswa.2015.07.062>. URL: <http://www.sciencedirect.com/science/article/pii/S0957417415005229>.
- ANAC (2019). *Stabilised Approach Report - Aproximação Estabilizada*, pp. 1–2. URL: <https://www.anac.gov.br>.

- Ancel, Ersin and Ann T. Shih (2012). “The Analysis of the Contribution of Human Factors to the In-flight Loss of Control Accidents.” In: *12th AIAA Aviation Technology, Integration and Operations (ATIO) Conference*, pp. 1–13. URL: <https://ntrs.nasa.gov/search.jsp?R=20120015461>.
- Bahreini, Kiavash, Rob Nadolski, and Wim Westera (2016). “Towards real-time speech emotion recognition for affective e-learning.” In: *Education and Information Technologies* 21.5, pp. 1367–1386. ISSN: 1573-7608. DOI: 10.1007/s10639-015-9388-2. URL: <https://doi.org/10.1007/s10639-015-9388-2>.
- Bänziger, Tanja (2014). “Measuring Emotion Recognition Ability.” In: *Encyclopedia of Quality of Life and Well-Being Research*. Ed. by Alex C. Michalos. Dordrecht: Springer Netherlands, pp. 3934–3941. ISBN: 978-94-007-0753-5. DOI: 10.1007/978-94-007-0753-5_4188. URL: https://doi.org/10.1007/978-94-007-0753-5_4188.
- Barkhof, Emile et al. (2015). “Specificity of facial emotion recognition impairments in patients with multi-episode schizophrenia.” In: 2 (1), pp. 12–19.
- Baron, Grzegorz and Urszula Stańczyk (2021). “Standard vs. non-standard cross-validation: evaluation of performance in a space with structured distribution of datapoints.” In: *Procedia Computer Science* 192. Knowledge-Based and Intelligent Information & Engineering Systems: Proceedings of the 25th International Conference KES2021, pp. 1245–1254. ISSN: 1877-0509. DOI: <https://doi.org/10.1016/j.procs.2021.08.128>. URL: <https://www.sciencedirect.com/science/article/pii/S1877050921016173>.
- Barret, Lisa F., Michael Lewis, and Jeannette M Haviland-Jones (2016). “Chapter 9 - Emotion and the Autonomic Nervous System.” In: ed. by Lisa F. Barret, Michael Lewis, and Jeannette M Haviland-Jones, pp. 166 –181.
- Barrett, L.F. (2006). “Solving the emotion paradox: categorization and the experience of emotion.” In: *Pers. Soc. Psychol. Rev.* 10 (1), pp. 20–46.
- Barros, P. et al. (2017). “Emotion-modulated attention improves expression recognition: A deep learning model.” In: 253 (1), pp. 104–114.
- Beblo, Thomas et al. (2018). “Breath Versus Emotions: The Impact of Different Foci of Attention During Mindfulness Meditation on the Experience of Negative and Positive Emotions.” In: *Behavior Therapy* 49.5, pp. 702 –714. ISSN: 0005-7894. DOI: <https://doi.org/10.1016/j.beth.2017.12.006>. URL: <http://www.sciencedirect.com/science/article/pii/S0005789417301363>.
- Bendak, Salaheddine and Hamad S.J. Rashid (2020). “Fatigue in aviation: A systematic review of the literature.” In: *International Journal of Industrial Ergonomics* 76, p. 102928. ISSN: 0169-8141. DOI: <https://doi.org/10.1016/j.ergon.2020.102928>. URL: <http://www.sciencedirect.com/science/article/pii/S0169814118305535>.
- Benoit, Alexandre et al. (Aug. 2006). In: *Multimodal Focus Attention and Stress Detection and Feedback in an Augmented Driver Simulator*. Vol. 204, pp. 337–344. DOI: 10.1007/0-387-34224-9_38.

- Berle, D. and M.L. Moulds (2013). “Emotional reasoning processes and dysphoric mood: Cross-sectional and prospective relationships.” In: 8 (6), pp. 1–9. DOI: [10.1371/journal.pone.0067359](https://doi.org/10.1371/journal.pone.0067359).
- Berridge, Kent C. (2018). “Evolving Concepts of Emotion and Motivation.” In: *Frontiers in Psychology* 9.1647, pp. 1–20. DOI: <https://dx.doi.org/10.3389/fpsyg.2018.01647>. URL: <https://www.ncbi.nlm.nih.gov/pmc/articles/PMC6137142/>.
- Bertero, D. and P. Fung (2017). “A first look into a Convolutional Neural Network for speech emotion detection.” In: pp. 5115–5119. DOI: [10.1109/ICASSP.2017.7953131](https://doi.org/10.1109/ICASSP.2017.7953131).
- Boeing (2017). “Statistical Summary of Commercial Jet Airplane Accidents - Boeing Aerospace Company.” In: *Worldwide Operations — 1959–2016*, pp. 1–26. URL: https://www.boeing.com/resources/boeingdotcom/company/about_bca/pdf/statsum.pdf.
- (2023). “Statistical Summary of Commercial Jet Airplane Accidents – Boeing Aerospace Company.” In: *Worldwide Operations — 1959–2022*, pp. 1–26. URL: <https://www.boeing.com/content/dam/boeing/boeingdotcom/company/aboutbca/pdf/statsum.pdf>.
- Bozhkov, Lachezar et al. (2015). “EEG-based Subject Independent Affective Computing Models.” In: *Procedia Computer Science* 53. INNS Conference on Big Data 2015 Program San Francisco, CA, USA 8-10 August 2015, pp. 375–382. ISSN: 1877-0509. DOI: <https://doi.org/10.1016/j.procs.2015.07.314>. URL: <http://www.sciencedirect.com/science/article/pii/S1877050915018177>.
- Breakwell, G.M. (2014). “The Psychology of Risk.” In: *Landscape and Urban Planning*.
- Brester, Christina et al. (2016). “Multi-Objective Heuristic Feature Selection for Speech-based Multilingual Emotion Recognition.” In: 6.4, pp. 243–253. DOI: [10.1515/jaiscr-2016-0018](https://doi.org/10.1515/jaiscr-2016-0018).
- Cannon, W.B. (1927). “The James–Lange theory of emotion: a critical examination and an alternative theory.” In: *Am. Jour. Psyc.* 39, pp. 106–124.
- Cao, Houwei, Ragini Verma, and Ani Nenkova (2015). “Speaker-sensitive emotion recognition via ranking: Studies on acted and spontaneous speech.” In: *Computer Speech & Language* 29.1, pp. 186–202. ISSN: 0885-2308. DOI: <https://doi.org/10.1016/j.csl.2014.01.003>. URL: <http://www.sciencedirect.com/science/article/pii/S0885230814000138>.
- Capuano, A. Suchocka et al. (2017). “Interoceptive exposure at the heart of emotional identification work in psychotherapy.” In: *European Psychiatry* 41. Abstract of the 25th European Congress of Psychiatry, S783. ISSN: 0924-9338. DOI: <https://doi.org/10.1016/j.eurpsy.2017.01.1493>. URL: <http://www.sciencedirect.com/science/article/pii/S0924933817315080>.
- Cespedes-Guevara, Julian and Tuomas Eerola (2018). “Music Communicates Affects, Not Basic Emotions – A Constructionist Account of Attribution of Emotional Meanings

- to Music.” In: 9.215, pp. 1–19. DOI: <https://dx.doi.org/10.3389%2Ffpsyg.2018.00215>. URL: <https://www.ncbi.nlm.nih.gov/pmc/articles/PMC5811634/>.
- Chenchah, Farah and Zied Lachiri (2017). “A bio-inspired emotion recognition system under real-life conditions.” In: *Applied Acoustics* 115, pp. 6 –14. ISSN: 0003-682X. DOI: <https://doi.org/10.1016/j.apacoust.2016.06.020>. URL: <http://www.sciencedirect.com/science/article/pii/S0003682X16301773>.
- Chepin, Eugene V. et al. (2016). “The improved method for robotic devices control with operator’s emotions detection.” In: *IEEE Procedia Computer Science*, pp. 173–176.
- Chi, Fengfeng et al. (2019). “Multimodal temperature sensing using Zn₂GeO₄:Mn²⁺+ phosphor as highly sensitive luminescent thermometer.” In: *Sensors and Actuators B: Chemical* 296, p. 126640. ISSN: 0925-4005. DOI: <https://doi.org/10.1016/j.snb.2019.126640>. URL: <https://www.sciencedirect.com/science/article/pii/S0925400519308408>.
- Choi, Kwang-Ho et al. (2017). “Is heart rate variability (HRV) an adequate tool for evaluating human emotions? – A focus on the use of the International Affective Picture System (IAPS).” In: *Psychiatry Research* 251, pp. 192 –196. ISSN: 0165-1781. DOI: <https://doi.org/10.1016/j.psychres.2017.02.025>. URL: <http://www.sciencedirect.com/science/article/pii/S0165178116312550>.
- Chung, Jae W. et al. (2016). “Beta-band Activity and Connectivity in Sensorimotor and Parietal Cortex are Important for Accurate Motor Performance.” In: *Neuroimage* 144, 164–173. DOI: [10.1016/j.neuroimage.2016.10.008](https://doi.org/10.1016/j.neuroimage.2016.10.008).
- Chung, Jae W. et al. (2018). “Beta-band oscillations in the supplementary motor cortex are modulated by levodopa and associated with functional activity in the basal ganglia.” In: *Neuroimage Clin.* 19, 559–571. DOI: [10.1016/j.nicl.2018.05.021](https://doi.org/10.1016/j.nicl.2018.05.021).
- Clark, Caron A.C. et al. (2016). “Intersections between cardiac physiology, emotion regulation and interpersonal warmth in preschoolers: Implications for drug abuse prevention from translational neuroscience.” In: *Drug and Alcohol Dependence* 163. Emotion Regulation and Drug Abuse: Implications for Prevention and Treatment, S60 –S69. ISSN: 0376-8716. DOI: <https://doi.org/10.1016/j.drugalcdep.2016.01.033>. URL: <http://www.sciencedirect.com/science/article/pii/S0376871616001125>.
- Conneau, Anne-Claire et al. (2017). “EMOEEG: a New Multimodal Dataset for Dynamic EEG-based Emotion Recognition with Audiovisual Elicitation.” In: *25th European Signal Processing Conference (EUSIPCO)*, pp. 768 –772. ISSN: 978-0-9928626-7-1.
- Critchley, Hugo D and Sarah N Garfinkel (2017). “Interoception and emotion.” In: *Current Opinion in Psychology* 17. Emotion, pp. 7 –14. ISSN: 2352-250X. DOI: <https://doi.org/10.1016/j.copsyc.2017.04.020>. URL: <http://www.sciencedirect.com/science/article/pii/S2352250X17300106>.
- C.Rodriguez-Guerrero et al. (2017). “Improving Challenge/Skill Ratio in a Multimodal Interface by Simultaneously Adapting Game Difficulty and Haptic Assistance through

- Psychophysiological and Performance Feedback.” In: *Frontiers in Neuroscience* 11, pp. 1–242. ISSN: 1534-4320. DOI: 10.3389/fnins.2017.00242.
- Cruz, Aniana et al. (2015). “Facial Expression Recognition Based on EOG Toward Emotion Detection for Human-Robot Interaction.” In: pp. 31–37. DOI: 10.5220/0005187200310037. URL: <https://doi.org/10.5220/0005187200310037>.
- Damásio, A.R. (2001). “Emotion, cognition and the human brain.” In: *Unity of knowledge: The convergence of natural and human science* 935, pp. 101–106.
- Davletcharova, Assel et al. (2015). “Detection and Analysis of Emotion from Speech Signals.” In: *Procedia Computer Science* 58. Second International Symposium on Computer Vision and the Internet (VisionNet 2015), pp. 91–96. ISSN: 1877-0509. DOI: <https://doi.org/10.1016/j.procs.2015.08.032>. URL: <http://www.sciencedirect.com/science/article/pii/S1877050915021432>.
- De, Anurag, Ashim Saha, and M.C. Pal (2015). “A Human Facial Expression Recognition Model Based on Eigen Face Approach.” In: *Procedia Computer Science* 45. International Conference on Advanced Computing Technologies and Applications (ICACTA), pp. 282–289. ISSN: 1877-0509. DOI: <https://doi.org/10.1016/j.procs.2015.03.142>. URL: <http://www.sciencedirect.com/science/article/pii/S1877050915003786>.
- Deb, S. and S. Dandapat (2015). “A novel breathiness feature for analysis and classification of speech under stress.” In: pp. 1–5. DOI: 10.1109/NCC.2015.7084826.
- Desmet, Bart and Véronique Hoste (2013). “Emotion detection in suicide notes.” In: *Expert Systems with Applications* 40.16, pp. 6351–6358. ISSN: 957-4174. DOI: <https://doi.org/10.1016/j.eswa.2013.05.050>. URL: <http://www.sciencedirect.com/science/article/pii/S0957417413003485>.
- Devore, Jay L. (2000). *Probability and Statistics for Engineering and the Sciences*. 5th ed. Duxbury Thomson Learning.
- Dixon, Matthew L. et al. (2020). “Emotion Regulation in Social Anxiety Disorder: Reappraisal and Acceptance of Negative Self-beliefs.” In: *Biological Psychiatry: Cognitive Neuroscience and Neuroimaging* 5.1, pp. 119–129. ISSN: 2451-9022. DOI: <https://doi.org/10.1016/j.bpsc.2019.07.009>. URL: <http://www.sciencedirect.com/science/article/pii/S2451902219302022>.
- Ekman, Paul (1992). “Are There Basic Emotions?” In: *Psychological Review - American Psychological Association, Inc.* 99.3, pp. 1–4.
- (1999). “Chapter 3: Basic Emotions.” In: *John Wiley & Sons Ltd.*, pp. 45–60.
- (2016). “What Scientists Who Study Emotion Agree About.” In: *Association for Psychological Science - Perspective on Psychological Science* 11.1, pp. 31–34. DOI: 10.1177/1745691615596992. URL: <https://1ammce38pkj41n8xkpliocwe-wpengine.netdna-ssl.com/wp-content/uploads/2013/07/What-Scientists-Who-Study-Emotion-Agree-About.pdf>.
- Ekman, Paul and W.V. Friesen (1978). “Facial Action Coding System: Investigator’s Guide.” In: 1, pp. 1–15.

- Elefteriou, Florent and Preston Campbell (2015). “Chapter 49 - Involvement of sympathetic nerves in bone metastasis.” In: ed. by Heymann and Dominique, pp. 591–597. DOI: <https://doi.org/10.1016/B978-0-12-416721-6.00049-2>. URL: <https://www.sciencedirect.com/science/article/pii/B9780124167216000492>.
- Ezhilarasi, R. and R.I. Minu (2012). “Automatic Emotion Recognition and Classification.” In: *Procedia Engineering* 38. INTERNATIONAL CONFERENCE ON MODELLING OPTIMIZATION AND COMPUTING, pp. 21–26. ISSN: 1877-7058. DOI: <https://doi.org/10.1016/j.proeng.2012.06.004>. URL: <http://www.sciencedirect.com/science/article/pii/S1877705812019170>.
- Fayek, Haytham M., Margaret Lech, and Lawrence Cavedon (2017). “Evaluating deep learning architectures for Speech Emotion Recognition.” In: *Neural Networks* 92. Advances in Cognitive Engineering Using Neural Networks, pp. 60–68. ISSN: 0893-6080. DOI: <https://doi.org/10.1016/j.neunet.2017.02.013>. URL: <http://www.sciencedirect.com/science/article/pii/S089360801730059X>.
- Forgas, Joseph P. (2008). “Affect and Cognition.” In: 3 (2), pp. 94–101. DOI: 10.1111/j.1745-6916.2008.00067.x.
- Franti, Eduard et al. (2017). “Voice Based Emotion Recognition with Convolutional Neural Networks for Companion Robots.” In: *ROMANIAN JOURNAL OF INFORMATION SCIENCE AND TECHNOLOGY* 20.3, pp. 222–240.
- Fukuyama, Satoru and Masataka Goto (2016). “Music emotion recognition with adaptive aggregation of Gaussian process regressors.” In: *IEEE International Conference in Acoustics, Speech and Signal Processing (ICASSP)* 1, pp. 71–75. DOI: 10.1109/ICASSP.2016.7471639.
- Goldin, Philippe R., Hooria Jazaieri, and James J. Gross (2014). “Chapter 17 - Emotion Regulation in Social Anxiety Disorder.” In: *Social Anxiety (Third Edition)*. Ed. by Stefan G. Hofmann and Patricia M. DiBartolo. Third Edition. San Diego: Academic Press, pp. 511–529. ISBN: 978-0-12-394427-6. DOI: <https://doi.org/10.1016/B978-0-12-394427-6.00017-0>. URL: <http://www.sciencedirect.com/science/article/pii/B9780123944276000170>.
- Golinska, Agnieszka Kitlas (2013). “Poincaré Plots in Analysis of Selected Biomedical Signals.” In: *Studies in Logic, Grammar and Rhetoric* 35 (48), pp. 117–126. DOI: 10.2478/slgr-2012-0031.
- Goran, Laura and Gabriel Negoescu (2015). “Emotions at Work. The Management of Emotions in the Act of Teaching.” In: 180 (1), pp. 1605–1611.
- Goshvarpour, Atefeh, Ataollah Abbasi, and Ateke Goshvarpour (2017). “An accurate emotion recognition system using ECG and GSR signals and matching pursuit method.” In: *Biomedical Journal* 40.6, pp. 355–368. ISSN: 2319-4170. DOI: <https://doi.org/10.1016/j.bj.2017.11.001>. URL: <http://www.sciencedirect.com/science/article/pii/S2319417016301056>.

- Grinde, B. and G.G. Patil (2009a). “Biophilia: Does Visual Contact with Nature Impact on Health and Well-Being?” In: 6 (1), pp. 2332–2343.
- Grinde, Bjørn and Grete Patil (2009b). “Biophilia: Does Visual Contact with Nature Impact on Health and Well-Being?” In: 6.9, pp. 2332–2343.
- Gross, J.J. and Ross Thompson (Jan. 2007). “Emotion regulation: Conceptual foundations.” In: *Handbook of Emotion Regulation*, pp. 33–50.
- Gunes, Hatice and Hayley Hung (Apr. 2016). “Is Automatic Facial Expression Recognition of Emotions Coming to a Dead End? The Rise of The New Kids on the Block.” In: 55 (1), pp. 6–8.
- Hafen, Ryan et al. (2014). “Chapter 1 - Power Grid Data Analysis with R and Hadoop.” In: *Data Mining Applications with R*. Ed. by Yanchang Zhao and Yonghua Cen. Boston: Academic Press, pp. 1–34. ISBN: 978-0-12-411511-8. DOI: <https://doi.org/10.1016/B978-0-12-411511-8.00001-3>. URL: <http://www.sciencedirect.com/science/article/pii/B9780124115118000013>.
- Hagen, Julia, Birthe Loa Knizek, and Heidi Hjelmeland (2017). “Mental Health Nurses’ Experiences of Caring for Suicidal Patients in Psychiatric Wards: An Emotional Endeavor.” In: *Archives of Psychiatric Nursing* 31.1, pp. 31–37. ISSN: 0883-9417. DOI: <https://doi.org/10.1016/j.apnu.2016.07.018>. URL: <http://www.sciencedirect.com/science/article/pii/S0883941716301480>.
- Haiblum-Itskovitch, Shai, Johanna Czamanski-Cohen, and Giora Galili (2018). “Emotional Response and Changes in Heart Rate Variability Following Art-Making With Three Different Art Materials.” In: *Frontiers in Psychology* 9, p. 968. ISSN: 1664-1078. DOI: 10.3389/fpsyg.2018.00968. URL: <https://www.frontiersin.org/article/10.3389/fpsyg.2018.00968>.
- Harrivel, A.R. and A. Pope (2017). “Prediction of Cognitive States during Flight Simulation using Multimodal Psychophysiological Sensing.” In: *Information Systems – AIAA Infotech at Aerospace* 1, pp. 1–10.
- Hastie, Trevor, Robert Tibshirani, and Jerome Friedman (2016). “The Elements of Statistical Learning: Data Mining, Inference, and Prediction.” In: 2, pp. 0–745.
- Haykin, Simon O. (2011). “Neural Networks and Learning Machines.” In: ed. by Kindle Edition, pp. 1–936.
- He, Cheng, Yun jin Yao, and Xue song Ye (2017). “An Emotion Recognition System Based on Physiological Signals Obtained by Wearable Sensors.” In: 399, pp. 15–25. DOI: 10.1007/978-981-10-2404-7_2.
- Heuer, Kathrin et al. (2010). “Morphed emotional faces: Emotion detection and misinterpretation in social anxiety.” In: *Journal of Behavior Therapy and Experimental Psychiatry* 41.4, pp. 418–425. ISSN: 0005-7916. DOI: <https://doi.org/10.1016/j.jbtep.2010.04.005>. URL: <http://www.sciencedirect.com/science/article/pii/S0005791610000558>.

- Huang, Mei-Ling and Yung-Yan Hsu (2012). “Fetal distress prediction using discriminant analysis, decision tree, and artificial neural network.” In: *Journal of Biomedical Science and Engineering* 23, pp. 526–533. DOI: doi.org/10.4236/jbise.2012.59065.
- IATA (2016). “Environmental Factors Affecting Loss of Control In-Flight: Best Practice for Threat Recognition & Management.” In: *The International Air Transport Association (IATA)* 1, pp. 1–33.
- (2020). “IATA Releases 2019 Airline Safety Report.” In: *International Air Transport Association (IATA)* 27, pp. 1–4.
- (2022). “IATA Safety Report 2021.” In: 58, pp. 1–269. URL: https://www.iata.org/contentassets/bd3288d6f2394d9ca3b8fa23548cb8bf/iata_safety_report_2021.pdf.
- ICAO (2005). “Rules of the air – Annex 2 to the convention on international civil aviation.” In: *International Civil Aviation Organization (ICAO)*. Vol. 1, pp. 1–74.
- (2017). “Accident Statistics.” In: *Aviation Safety - International Civil Aviation Organization*. URL: <https://www.icao.int/safety/iStars/Pages/Accident-Statistics.aspx>.
- Isasi, Carmen R., Natania W. Ostrovsky, and Thomas A. Wills (2013). “The association of emotion regulation with lifestyle behaviors in inner-city adolescents.” In: *Eating Behaviors* 14.4, pp. 518–521. ISSN: 1471-0153. DOI: doi.org/10.1016/j.eatbeh.2013.07.009. URL: <http://www.sciencedirect.com/science/article/pii/S1471015313000792>.
- J., Selvaraj, Wan K. Murugappan M, and Yaacob S. (2013). “Classification of emotional states from electrocardiogram signals: a non-linear approach based on hurts.” In: *Biomedical Engineering Online* 126 (1), pp. 12–18.
- Jain, Neha et al. (2018). “Hybrid deep neural networks for face emotion recognition.” In: *Pattern Recognition Letters* 115. Multimodal Fusion for Pattern Recognition, pp. 101–106. ISSN: 0167-8655. DOI: <https://doi.org/10.1016/j.patrec.2018.04.010>. URL: <http://www.sciencedirect.com/science/article/pii/S0167865518301302>.
- James, William (1884). “What is an Emotion?” In: *Mind* 9, pp. 188–205.
- Jones, Marc V. et al. (2005). “Development and Validation of the Sport Emotion Questionnaire.” In: vol. 27. 1, pp. 407–431.
- Joutsen, Atte S. et al. (2018). “Dry electrode sizes in recording ECG and heart rate in wearable applications.” In: ed. by Hannu Eskola et al., pp. 735–738.
- Julius, O. Smith III (2008). “Introduction to Digital Filters - With Audio Applications.” In: pp. 1–460.
- Kandera, Branislav, Filip Škultéty, and Karina Mesárošová (2019). “Consequences of flight crew fatigue on the safety of civil aviation.” In: *Transportation Research Procedia* 43. INAIR 2019 - Global Trends in Aviation, pp. 278–289. ISSN: 2352-1465. DOI: <https://doi.org/10.1016/j.trpro.2019.12.043>. URL: <http://www.sciencedirect.com/science/article/pii/S2352146519306106>.

- Kaur, Barjinder, Dinesh Singh, and Partha Pratim Roy (2018). “EEG Based Emotion Classification Mechanism in BCI.” In: *Procedia Computer Science* 132. International Conference on Computational Intelligence and Data Science, pp. 752–758. ISSN: 1877-0509. DOI: <https://doi.org/10.1016/j.procs.2018.05.087>. URL: <http://www.sciencedirect.com/science/article/pii/S1877050918308196>.
- Kayaa, H., F. Gürpınar, and A.A. Salah (2017). “Video-based emotion recognition in the wild using deep transfer learning and score fusion.” In: 65, pp. 66–75.
- Khalfallah, Jihen and Jaleleddine Ben Hadj Slama (2015). “Facial Expression Recognition for Intelligent Tutoring Systems in Remote Laboratories Platform.” In: *Procedia Computer Science* 73. International Conference on Advanced Wireless Information and Communication Technologies (AWICT 2015), pp. 274–281. ISSN: 1877-0509. DOI: <https://doi.org/10.1016/j.procs.2015.12.030>. URL: <http://www.sciencedirect.com/science/article/pii/S1877050915034912>.
- Khanna, Preeya and Jose M. Carmena (2017). “Beta band oscillations in motor cortex reflect neural population signals that delay movement onset.” In: *eLife* 6, pp. 1–31. DOI: <https://doi.org/10.7554/eLife.24573>. URL: <https://www.ncbi.nlm.nih.gov/pmc/articles/PMC5468088/>.
- Kim, J. and E. André (2008). “Emotion recognition based on physiological changes in music listening.” In: *IEEE Transactions on Pattern Analysis and Machine Intelligence* 30.12, pp. 2067–2083. ISSN: 0162-8828. DOI: 10.1109/TPAMI.2008.26.
- Kima, Seung Kyung, and Meghan Sumner (2017). “Beyond lexical meaning: The effect of emotional prosody on spoken word recognition.” In: *The Journal of the Acoustical Society of America* 142.1. DOI: 10.1121/1.4991328. URL: <https://doi.org/10.1121/1.4991328>.
- Kingma, Diederik P. and Jimmy Ba (2015). “Adam: A Method for Stochastic Optimization.” In: 9, pp. 1–15.
- Kirchsteiger, H. et al. (2015). “Performance Comparison of CGM Systems: MARD Values Are Not Always a Reliable Indicator of CGM System Accuracy.” In: *Journal of Diabetes Science and Technology* 5, pp. 1030–1040. DOI: <https://doi.org/10.1177/1932296815586013>.
- Kolar, David R. et al. (2017). “Momentary emotion identification in female adolescents with and without anorexia nervosa.” In: *Psychiatry Research* 255, pp. 394–398. ISSN: 0165-1781. DOI: <https://doi.org/10.1016/j.psychres.2017.06.075>. URL: <http://www.sciencedirect.com/science/article/pii/S0165178116319916>.
- Krithika, L.B. and Lakshmi Priya G.G. (2016). “Student Emotion Recognition System (SERS) for e-learning improvement based on learner concentration metric.” In: 85, pp. 767–776.
- Kropotov, J. D. (2009). In: *Beta Rhythms. Quantitative EEG, Event-Related Potentials and Neurotherapy*, pp. 59–77. DOI: 10.1016/b978-0-12-374512-5.00003-7.

- Kucikienė, Domantė and Ruta Praninskienė (2018). “The impact of music on the bioelectrical oscillations of the brain.” In: *Acta Med Litu* 25 (2), 101–106. DOI: 10.6001/actamedica.v25i2.3763.
- Kumar, Nitin, Kaushikee Khaund, and Shyamanta M. Hazarika (2016). “Bispectral Analysis of EEG for Emotion Recognition.” In: *Procedia Computer Science* 84. Proceeding of the Seventh International Conference on Intelligent Human Computer Interaction (IHCI 2015), pp. 31–35. ISSN: 1877-0509. DOI: <https://doi.org/10.1016/j.procs.2016.04.062>. URL: <http://www.sciencedirect.com/science/article/pii/S187705091630076X>.
- L. Bruno P. Nascimento, Válber C. Cavalcanti Roza and et al. (2018). “Goal-biased probabilistic foam method for robot path planning.” In: *IEEE International Conference on Autonomous Robot Systems and Competitions (ICARSC)*, pp. 199–204.
- Lagast, S. et al. (2017). “Consumers’ emotions elicited by food: A systematic review of explicit and implicit methods.” In: *Trends in Food Science & Technology* 69, pp. 172–189. ISSN: 0924-2244. DOI: <https://doi.org/10.1016/j.tifs.2017.09.006>. URL: <http://www.sciencedirect.com/science/article/pii/S092422441730208X>.
- Lahane, Prashant and Arun Kumar Sangaiah (2015). “An Approach to EEG Based Emotion Recognition and Classification Using Kernel Density Estimation.” In: *Procedia Computer Science* 48. International Conference on Computer, Communication and Convergence (ICCC 2015), pp. 574–581. ISSN: 1877-0509. DOI: <https://doi.org/10.1016/j.procs.2015.04.138>. URL: <http://www.sciencedirect.com/science/article/pii/S187705091500647X>.
- Lan, Zirui et al. (2016). “Real-time EEG-based emotion monitoring using stable features.” In: *The Visual Computer* 32.3, 347–358. ISSN: 1432-2315. DOI: <https://doi.org/10.1007/s00371-015-1183-y>.
- Langley, J.N. (1898). “On the Union of Cranial Autonomic (Visceral) Fibres with the Nerve Cells of the Superior Cervical Ganglion.” In: *The Journal of Physiology* 23, pp. 240–270. DOI: DOI:10.1113/jphysiol.1898.sp000726.
- Lanjewar, R.B., S. Mathurkar, and N. Patel (2015). “Implementation and Comparison of Speech Emotion Recognition System using Gaussian Mixture Model (GMM) and K-Nearest Neighbor (K-NN) Techniques.” In: 49, pp. 50–57.
- Lenis, Gustavo et al. (2017). “Comparison of Baseline Wander Removal Techniques considering the Preservation of ST Changes in the Ischemic ECG: A Simulation Study.” In: *Computational and Mathematical Methods in Medicine* 2017, pp. 1–13. DOI: 10.1155/2017/9295029.
- Li, Jiaying et al. (2017). “Facial Expression Recognition with Faster R-CNN.” In: *Procedia Computer Science* 107. Advances in Information and Communication Technology: Proceedings of 7th International Congress of Information and Communication Technology (ICICT2017), pp. 135–140. ISSN: 1877-0509. DOI: <https://doi.org/10.1016/j.procs.2017.05.100>.

- 1016/j.procs.2017.03.069. URL: <http://www.sciencedirect.com/science/article/pii/S1877050917303447>.
- Lim, Nangyeon (2016). "Cultural differences in emotion: differences in emotional arousal level between the East and the West." In: *Integrative Medicine Research* 5.2, pp. 105–109. ISSN: 2213-4220. DOI: <https://doi.org/10.1016/j.imr.2016.03.004>. URL: <http://www.sciencedirect.com/science/article/pii/S2213422016300191>.
- Lopes, A.T. et al. (2017). "Facial expression recognition with Convolutional Neural Networks: Coping with few data and the training sample order." In: 61 (1), pp. 610–628.
- Mallat, Stéphane (2009). "A Wavelet Tour of Signal Processing." In: pp. 1–805.
- Mannepalli, Kasiprasad, Panyam Narahari Sastry, and Maloji Suman (2017). "A novel Adaptive Fractional Deep Belief Networks for speaker emotion recognition." In: *Alexandria Engineering Journal* 56.4, pp. 485–497. ISSN: 1110-0168. DOI: <https://doi.org/10.1016/j.aej.2016.09.002>. URL: <http://www.sciencedirect.com/science/article/pii/S1110016816302484>.
- Mao, Qi-rong et al. (2015). "Using Kinect for real-time emotion recognition via facial expressions." In: *Frontiers of Information Technology & Electronic Engineering* 16.4, pp. 272–282. ISSN: 2095-9230. DOI: 10.1631/FITEE.1400209. URL: <https://doi.org/10.1631/FITEE.1400209>.
- Marsland, Stephen (2015). "Machine Learning: An Algorithmic Perspective." In: pp. 1–457.
- Martinez, Aleix M. (2017). "Visual perception of facial expressions of emotion." In: *Current Opinion in Psychology* 17. Emotion, pp. 27–33. ISSN: 2352-250X. DOI: <https://doi.org/10.1016/j.copsyc.2017.06.009>. URL: <http://www.sciencedirect.com/science/article/pii/S2352250X17300179>.
- Mather, Mara and Julian Thayer (Feb. 2018). "How heart rate variability affects emotion regulation brain networks." In: *Current opinion in behavioral sciences* 19, pp. 98–104. DOI: 10.1016/j.cobeha.2017.12.017.
- Matiko, J.W., S. P. Beeby, and J. Tudor (2014). "Fuzzy logic based emotion classification." In: *2014 IEEE International Conference on Acoustics, Speech and Signal Processing (ICASSP)*, pp. 4389–4393. ISSN: 1520-6149. DOI: 10.1109/ICASSP.2014.6854431.
- Matlovic, T. et al. (2016). "Emotions detection using facial expressions recognition and EEG." In: pp. 18–23.
- Mayya, Veena, Radhika M. Pai, and M.M. Manohara Pai (2016). "Automatic Facial Expression Recognition Using DCNN." In: *Procedia Computer Science* 93. Proceedings of the 6th International Conference on Advances in Computing and Communications, pp. 453–461. ISSN: 1877-0509. DOI: <https://doi.org/10.1016/j.procs.2016.07.233>. URL: <http://www.sciencedirect.com/science/article/pii/S1877050916314752>.

- McKay, Mary Pat and Loren Groff (2016). “23 years of toxicology testing fatally injured pilots: Implications for aviation and other modes of transportation.” In: *Accident Analysis and Prevention* 90, pp. 108–117. ISSN: 0001-4575. DOI: <https://doi.org/10.1016/j.aap.2016.02.008>. URL: <http://www.sciencedirect.com/science/article/pii/S0001457516300410>.
- McRae, Kateri (2016). “Cognitive emotion regulation: a review of theory and scientific findings.” In: *Current Opinion in Behavioral Sciences* 10. Neuroscience of education, pp. 119–124. ISSN: 2352-1546. DOI: <https://doi.org/10.1016/j.cobeha.2016.06.004>. URL: <http://www.sciencedirect.com/science/article/pii/S2352154616301206>.
- Medlab, P100 (2017). “PEARL100L Medlab - Pulse Digital Desktop Pulse Oximeter.” In: *Medlab medizinische Diagnosegeräte GmbH*, pp. 1–2.
- Min, Yoon-Ki, Soon-Cheol Chung, and Byung-Chan Min (2005). “Physiological Evaluation on Emotional Change Induced by Imagination.” In: vol. 30, 2, pp. 137–150. DOI: [10.1007/s10484-005-4310-0](https://doi.org/10.1007/s10484-005-4310-0). URL: <https://doi.org/10.1007/s10484-005-4310-0>.
- Mishra, Badrinarayan et al. (2011). “Evaluation of work place stress in health university workers: A study from rural India.” In: *Indian Journal of Community Medicine* 36.1, pp. 39–44. DOI: [10.4103/0970-0218.80792](https://doi.org/10.4103/0970-0218.80792).
- Misky, M. (2006). “The Emotion Machine: commonsense thinking, artificial intelligence and the future of the human mind.” In: 1. ISSN: 978-0-7432-7663-4.
- Motamed, Sara, Saeed Setayeshi, and Azam Rabiee (2017). “Speech emotion recognition based on a modified brain emotional learning model.” In: *Biologically Inspired Cognitive Architectures* 19, pp. 32–38. ISSN: 2212-683X. DOI: <https://doi.org/10.1016/j.bica.2016.12.002>. URL: <http://www.sciencedirect.com/science/article/pii/S2212683X16301219>.
- Murugappan, M., R. Nagarajan, and S. Yaacob (2011). “Discrete Wavelet Transform Based Selection of Salient EEG Frequency Band for Assessing Human Emotions.” In: *Discrete Wavelet Transforms - Biomedical Applications*, pp. 33–52. DOI: [10.5772/20990](https://doi.org/10.5772/20990).
- Muthusamy, Hariharan, Kemal Polat, and Sazali Yaacob (Mar. 2015a). “Improved Emotion Recognition Using Gaussian Mixture Model and Extreme Learning Machine in Speech and Glottal Signals.” In: 2015, pp. 1–13.
- (Mar. 2015b). “Particle Swarm Optimization Based Feature Enhancement and Feature Selection for Improved Emotion Recognition in Speech and Glottal Signals.” In: *PLOS ONE* 10.3, pp. 1–20. DOI: [10.1371/journal.pone.0120344](https://doi.org/10.1371/journal.pone.0120344). URL: <https://doi.org/10.1371/journal.pone.0120344>.
- Novak, D. et al. (2011). “Psychophysiological Measurements in a Biocooperative Feedback Loop for Upper Extremity Rehabilitation.” In: *IEEE Transactions on Neural Systems*

- and Rehabilitation Engineering* 19.4, pp. 400–410. ISSN: 1534-4320. DOI: 10.1109/TNSRE.2011.2160357.
- O’Dea, Bridianne et al. (2015). “Detecting suicidality on Twitter.” In: *Internet Interventions* 2.2, pp. 183–188. ISSN: 2214-7829. DOI: <https://doi.org/10.1016/j.invent.2015.03.005>. URL: <http://www.sciencedirect.com/science/article/pii/S2214782915000160>.
- Okegbile, Samuel Dayo et al. (Apr. 2019). “A Multimodal Approach to Enhancing Automobile Security.” In: *Int. J. Comput. Vis. Image Process.* 9.2, 32–47. ISSN: 2155-6997. DOI: 10.4018/IJCVIP.2019040103. URL: <https://doi.org/10.4018/IJCVIP.2019040103>.
- Ong, D.C., J. Zaki, and N.D. Goodman (2015). “Affective cognition: Exploring lay theories of emotion.” In: pp. 143, pp. 141–162.
- Oppenheim, Alan V. and George C. Verghese (2015). *Signals, Systems and Inference*. Vol. 1. 1, pp. 1–561.
- Othman, Marini et al. (2013). “EEG Emotion Recognition Based on the Dimensional Models of Emotions.” In: *Procedia - Social and Behavioral Sciences* 97. The 9th International Conference on Cognitive Science, pp. 30–37. ISSN: 1877-0428. DOI: <https://doi.org/10.1016/j.sbspro.2013.10.201>. URL: <http://www.sciencedirect.com/science/article/pii/S187704281303646X>.
- Ozseven, Turgut (2019). “A novel feature selection method for speech emotion recognition.” In: *Applied Acoustics* 146, pp. 320–326. ISSN: 0003-682X. DOI: <https://doi.org/10.1016/j.apacoust.2018.11.028>. URL: <http://www.sciencedirect.com/science/article/pii/S0003682X18309915>.
- Patsakis, C. et al. (2014). “Personalized medical services using smart cities’ infrastructures.” In: pp. 1–5. DOI: 10.1109/MeMeA.2014.6860145.
- Patwardhan, A. S. (2017). “Multimodal mixed emotion detection.” In: pp. 139–143. DOI: 10.1109/CESYS.2017.8321250.
- Pereira, C.M.G. and S.M.M. Faria (2015). “Do you feel what I feel? Emotional development in children with ID.” In: pp. 165 (1), pp. 52–61.
- Perlovsky, Leonid I. (2020). “Higher emotions and cognition.” In: *Cognitive Systems Research* 61, pp. 45–52. ISSN: 1389-0417. DOI: <https://doi.org/10.1016/j.cogsys.2017.04.008>. URL: <https://www.sciencedirect.com/science/article/pii/S1389041719305091>.
- Petrovica, Sintija, Alla Anohina-Naumeca, and Hazım Kemal Ekenel (2017). “Emotion Recognition in Affective Tutoring Systems: Collection of Ground-truth Data.” In: *Procedia Computer Science* 104. ICTE 2016, Riga Technical University, Latvia, pp. 437–444. ISSN: 1877-0509. DOI: <https://doi.org/10.1016/j.procs.2017.01.157>. URL: <http://www.sciencedirect.com/science/article/pii/S1877050917301588>.

- Piskorski, J. and P. Guzik (2007). “Geometry of the Poincaré plot of RR intervals and its asymmetry in healthy adult.” In: *Physiology Measurement* 28, pp. 287–300. DOI: 10.1088/0967-3334/28/3/005.
- Plutchik, Robert (1980). “Theories of Emotion: Emotion Theory, Research, and Experience.” In: 1, pp. 141–162.
- Plutchik, Robert and Henry Kellerman (2013). “The Measurement of Emotions - Theories of Emotion: Emotion Theory, Research, and Experience.” In: 4, pp. 1–334.
- Poels, K. and S. Dewitte (2006). “How to capture the heart? Reviewing 20 years of emotion measurement in advertising.” In: *J. Advert. Res.* 46 (1), pp. 18–37.
- Postolache, O. Adrian (2017). “IoT for Healthcare: Smart Physiotherapy.” In: *22nd IMEKO TC4 International Symposium & 20th International Workshop on ADC Modelling and Testing*.
- Preckel, Katrin, Philipp Kanske, and Tania Singer (2018). “On the interaction of social affect and cognition: empathy, compassion and theory of mind.” In: *Current Opinion in Behavioral Sciences* 19. Emotion-cognition interactions, pp. 1–6. ISSN: 2352-1546. DOI: <https://doi.org/10.1016/j.cobeha.2017.07.010>. URL: <http://www.sciencedirect.com/science/article/pii/S2352154617300700>.
- Qamar, Saqib and Parvez Ahmad (2015). “Emotion Detection from Text using Fuzzy Logic.” In: 121.3, pp. 29–32.
- Quah, Ee Ling Sharon (2018). “Emotional reflexivity and emotion work in transnational divorce biographies.” In: *Emotion, Space and Society* 29, pp. 48–54. ISSN: 1755-4586. DOI: <https://doi.org/10.1016/j.emospa.2018.09.001>. URL: <http://www.sciencedirect.com/science/article/pii/S1755458618300197>.
- Quesada Tabares, Roylán et al. (July 2017). “Emotions Detection based on a Single-electrode EEG Device.” In: DOI: 10.5220/0006476300890095.
- Rajeswari, J. and M. Jagannath (2017). “Advances in biomedical signal and image processing – A systematic review.” In: *Informatics in Medicine Unlocked* 8, pp. 13–19. ISSN: 2352-9148. DOI: <https://doi.org/10.1016/j.imu.2017.04.002>. URL: <http://www.sciencedirect.com/science/article/pii/S2352914817300242>.
- Rajhans, Purva et al. (2016). “Putting the face in context: Body expressions impact facial emotion processing in human infants.” In: *Developmental Cognitive Neuroscience* 19, pp. 115–121. ISSN: 1878-9293. DOI: <https://doi.org/10.1016/j.dcn.2016.01.004>. URL: <http://www.sciencedirect.com/science/article/pii/S1878929315300360>.
- Randler, Christoph et al. (2017). “Anxiety, disgust and negative emotions influence food intake in humans.” In: *International Journal of Gastronomy and Food Science* 7, pp. 11–15. ISSN: 1878-450X. DOI: <https://doi.org/10.1016/j.ijgfs.2016.11.005>. URL: <http://www.sciencedirect.com/science/article/pii/S1878450X16300567>.
- Reis, E., P. Arriaga, and O. Adrian Postolache (2015). “Emotional flow monitoring for health using FLOWSENSE: An experimental study to test the impact of antismoking

- campaigns.” In: 2015 E-Health and Bioengineering Conference (EHB), pp. 1–4. DOI: 10.1109/EHB.2015.7391608.
- Reybrouck, Mark, Tuomas Eerola, and Piotr Podlipniak (2018). “Editorial: Music and the Functions of the Brain: Arousal, Emotions, and Pleasure.” In: *Frontiers in Psychology* 9.113, pp. 1–2. DOI: <https://doi.org/10.3389/fpsyg.2018.00113>. URL: <https://www.ncbi.nlm.nih.gov/pmc/articles/PMC5811634/>.
- Riaz, Amir, Shirley Gregor, and Aleck Lin (2018). “Biophilia and biophobia in website design: Improving internet information dissemination.” In: *Information and Management* 55.2, pp. 199–214. ISSN: 0378-7206. DOI: <https://doi.org/10.1016/j.im.2017.05.006>. URL: <http://www.sciencedirect.com/science/article/pii/S0378720617304640>.
- Ritter, Petra, Matthias Moosmann, and Arno Villringer (2009). “Rolandic alpha and beta EEG rhythms’ strengths are inversely related to fMRI-BOLD signal in primary somatosensory and motor cortex.” In: 30, 1168–1187. DOI: doi.org/10.1002/hbm.20585.
- Roberson, Patricia N.E. et al. (2018). “How health behaviors link romantic relationship dysfunction and physical health across 20 years for middle-aged and older adults.” In: *Social Science & Medicine* 201, pp. 18–26. DOI: <https://doi.org/10.1016/j.socscimed.2018.01.037>. URL: <https://www.sciencedirect.com/science/article/pii/S0277953618300443>.
- Rosso, I.M. et al. (2004). “Cognitive and emotional components of frontal lobe functioning in childhood and adolescence.” In: *Annals of the New York Academy of Sciences* 1021, pp. 355–362. DOI: 10.1196/annals.1308.045.
- Roza, V. César Cavalcanti and O. A. Postolache (2016). “Citizen emotion analysis in Smart City.” In: 1.1, pp. 1–6. DOI: 10.1109/IISA.2016.7785335.
- (2019). “Multimodal Approach for Emotion Recognition Based on Simulated Flight Experiments.” In: *Sensors* 19.24, p. 5516. DOI: <https://doi.org/10.3390/s19245516>.
- (2021). “ β -Band Analysis from Simulated Flight Experiments.” In: *Aerospace* 8.120, pp. 1–35. DOI: <https://doi.org/10.3390/aerospace8050120>.
- Roza, V. César Cavalcanti et al. (2019). “Emotion Assessment on Simulated Flights.” In: *14th IEEE International Symposium on Medical Measurements & Applications (MEMEA 2019)* 14.1, pp. 1–6.
- Roza, Válber C. Cavalcanti, Ana M. de Almeida, and Octavian A. Postolache (2017). “Design of an artificial neural network and feature extraction to identify arrhythmias from ECG.” In: pp. 391–396. DOI: 10.1109/MeMeA.2017.7985908.
- Roza, Válber C. Cavalcanti and Octavian A. Postolache (2017). “Design of a Multimodal Interface based on Psychophysiological Sensing to Identify Emotion.” In: *22nd IMEKO TC4 International Symposium & 20th International Workshop on ADC Modelling and Testing* 1, pp. 1–6.

- Roza, Válber C. Cavalcanti and Octavian A. Postolache (Oct. 2018). “Emotion Analysis Architecture Based on Face and Physiological Sensing Applied with Flight Simulator.” In: pp. 1036–1040. DOI: 10.1109/ICEPE.2018.8559732.
- Roza, Válber C. Cavalcanti, Regina de Souza, and Octavian A. Postolache (2017). “A multi-sensing physical therapy assessment for children with cerebral palsy.” In: *Eleventh International Conference on Sensing Technology (ICST)*, pp. 1–6.
- Roza, Válber C. Cavalcanti et al. (2018). “Performance Analysis Performance Analysis of ANN and SVM in ECG Based Arrhythmia Identification.” In: *Journal of Physics: Conference Series* 1065, p. 132004. DOI: 10.1088/1742-6596/1065/13/132004.
- Salankar, Nilima et al. (2017). “Fuzzy Logic Based Approach for Automation of Emotion Detection in Misophonia.” In: 9.1, pp. 37–55. DOI: DOI:10.5121/ijcsit.2017.9104.
- Sanchez, Alvaro et al. (2017). “Identification of emotions in mixed disgusted-happy faces as a function of depressive symptom severity.” In: *Journal of Behavior Therapy and Experimental Psychiatry* 57, pp. 96–102. ISSN: 0005-7916. DOI: <https://doi.org/10.1016/j.jbtep.2017.05.002>. URL: <http://www.sciencedirect.com/science/article/pii/S0005791616301744>.
- Sánchez-Gutiérrez, Máximo E. et al. (2014). “Deep Learning for Emotional Speech Recognition.” In: ed. by José Francisco Martínez-Trinidad et al., pp. 311–320.
- Savitzky, A. and M.J.E Golay (1964). “Smoothing and Differentiation of Data by Simplified Least Squares Procedures.” In: 36.8, pp. 1627–1639. DOI: 10.1021/ac60214a047.
- Shahin, Ismail and Mohammed Nasser Ba-Hutair (2015). “Talking condition recognition in stressful and emotional talking environments based on CSPHMM2s.” In: *International Journal of Speech Technology* 18.1, pp. 77–90. ISSN: 1572-8110. DOI: 10.1007/s10772-014-9251-7. URL: <https://doi.org/10.1007/s10772-014-9251-7>.
- Shalin, T.B. and L. Vanitha (2013). “Emotion detection in human beings using ECG signals.” In: *International Journal of Engineering Trends and Technology* 4 (5), pp. 1337–1342.
- Shimmer3 (2017). “Shimmer GSR+ Unit.” In: pp. 1–2.
- Shin, Dongmin, Dongil Shin, and Dongkyoo Shin (2017). “Development of emotion recognition interface using complex EEG/ECG bio-signal for interactive contents.” In: *Multimedia Tools and Applications* 76.9, pp. 11449–11470. ISSN: 1573-7721. DOI: 10.1007/s11042-016-4203-7. URL: <https://doi.org/10.1007/s11042-016-4203-7>.
- Shukla, Sumitra, S. Dandapat, and S. R. Mahadeva Prasanna (2016). “A Subspace Projection Approach for Analysis of Speech Under Stressed Condition.” In: *Circuits, Systems, and Signal Processing* 35.12, pp. 4486–4500. ISSN: 1531-5878. DOI: 10.1007/s00034-016-0284-9. URL: <https://doi.org/10.1007/s00034-016-0284-9>.
- Siddiquee, Masudur R. et al. (2018). “Movement artefact removal from NIRS signal using multi-channel IMU data.” In: *BioMed Eng Online* 17.120, pp. 1–16. DOI: <https://dx.doi.org/10.1186%2Fs12938-018-0554-9>.

- Sierra, A.S. (2011). “A stress-detection system based on physiological signals and fuzzy logic.” In: *IEEE Transactions on Industrial Electronics* 58 (10), pp. 4857–4865.
- Silva, Ana Patricia et al. (2017). “What’s in a name? The effect of congruent and incongruent product names on liking and emotions when consuming beer or non-alcoholic beer in a bar.” In: *Food Quality and Preference* 55, pp. 58 –66. ISSN: 0950-3293. DOI: <https://doi.org/10.1016/j.foodqual.2016.08.008>. URL: <http://www.sciencedirect.com/science/article/pii/S0950329316301707>.
- Sánchez-Porras, María José and Estrella Martínez Rodrigo (2017). “Emotional Benefits of Coca-Cola Advertising Music.” In: *Procedia - Social and Behavioral Sciences* 237. Education, Health and ICT for a Transcultural World, pp. 1444 –1448. ISSN: 1877-0428. DOI: <https://doi.org/10.1016/j.sbspro.2017.02.227>. URL: <http://www.sciencedirect.com/science/article/pii/S1877042817302276>.
- Soto-Vásquez, Marilú Roxana and Paúl Alan Arkin Alvarado-García (2017). “Aromatherapy with two essential oils from Satureja genre and mindfulness meditation to reduce anxiety in humans.” In: *Journal of Traditional and Complementary Medicine* 7.1, pp. 121 –125. ISSN: 2225-4110. DOI: <https://doi.org/10.1016/j.jtcme.2016.06.003>. URL: <http://www.sciencedirect.com/science/article/pii/S2225411016300438>.
- Steam and Microsoft (2006). *Microsoft Flight Simulator X: Steam Edition*. https://store.steampowered.com/app/314160/Microsoft_Flight_Simulator_X_Steam_Edition/.
- Subhashinia, R. and P.R. Niveditha (2015). “Analyzing and Detecting Employee’s Emotion For Amelioration Of Organizations.” In: 48 (1), pp. 530–336.
- Sun, Fangmin et al. (2017). “A wearable H-shirt for exercise ECG monitoring and individual lactate threshold computing.” In: *Computers in Industry* 92-93, pp. 1–11. ISSN: 0166-3615. DOI: <https://doi.org/10.1016/j.compind.2017.06.004>. URL: <http://www.sciencedirect.com/science/article/pii/S0166361516303116>.
- Sun, Yaxin, Guihua Wen, and Jiabing Wang (2015). “Weighted spectral features based on local Hu moments for speech emotion recognition.” In: *Biomedical Signal Processing and Control* 18, pp. 80 –90. ISSN: 1746-8094. DOI: <https://doi.org/10.1016/j.bspc.2014.10.008>. URL: <http://www.sciencedirect.com/science/article/pii/S174680941400158X>.
- Suzuki, Seigo et al. (2017). “Physio-psychological Burdens and Social Restrictions on Parents of Children With Technology Dependency are Associated With Care Coordination by Nurses.” In: *Journal of Pediatric Nursing* 36, pp. 124–131. ISSN: 0882-5963. DOI: <https://doi.org/10.1016/j.pedn.2017.06.006>. URL: <https://www.sciencedirect.com/science/article/pii/S0882596316304341>.
- Szaszák, Gyorgy, Máté Ákos Tundik, and Branislav Gerazov (2018). “Prosodic stress detection for fixed stress languages using formal atom decomposition and a statistical hidden Markov hybrid.” In: *Speech Communication* 102, pp. 14–26. ISSN: 0167-6393.

- DOI: <https://doi.org/10.1016/j.specom.2018.06.005>. URL: <http://www.sciencedirect.com/science/article/pii/S0167639317304089>.
- Takeda, R. et al. (2014). "Drift Removal for Improving the Accuracy of Gait Parameters Using Wearable Sensor Systems." In: *Sensors (Basel, Switzerland)* 14.12, pp. 23230–23247. DOI: 10.3390/s141223230.
- Tang, Yi-Yuan, Rongxiang Tang, and Michael I. Posner (2016). "Mindfulness meditation improves emotion regulation and reduces drug abuse." In: *Drug and Alcohol Dependence* 163. Emotion Regulation and Drug Abuse: Implications for Prevention and Treatment, S13–S18. ISSN: 0376-8716. DOI: <https://doi.org/10.1016/j.drugalcdep.2015.11.041>. URL: <http://www.sciencedirect.com/science/article/pii/S0376871616001174>.
- Tarnowski, Paweł et al. (2017). "Emotion recognition using facial expressions." In: *Procedia Computer Science* 108. International Conference on Computational Science, ICCS 2017, 12-14 June 2017, Zurich, Switzerland, pp. 1175–1184. ISSN: 1877-0509. DOI: <https://doi.org/10.1016/j.procs.2017.05.025>. URL: <http://www.sciencedirect.com/science/article/pii/S1877050917305264>.
- Tayel, Mazhar B. and Eslam I. AlSaba (2015). "Poincaré Plot for Heart Rate Variability." In: 9.9, pp. 708–711.
- Thomas, M.V. et al. (2013). "The effect of music on the human stress response." In: 8 (8), pp. 1–12.
- Thompson, Catharine Ward et al. (2012). "More green space is linked to less stress in deprived communities: Evidence from salivary cortisol patterns." In: *Landscape and Urban Planning* 105.3, pp. 221–229. ISSN: 0169-2046. DOI: <https://doi.org/10.1016/j.landurbplan.2011.12.015>. URL: <http://www.sciencedirect.com/science/article/pii/S0169204611003665>.
- Tieding, Lu, Chen Xijiang, and Zhou Shijian (2010). "Optimization for Impact Factors of Dam Deformation Based on BP Neural Network Model." In: 2, pp. 854–857. DOI: 10.1109/ICICTA.2010.853.
- Trigeorgis, G. et al. (2016). "Adieu features? End-to-end speech emotion recognition using a deep convolutional recurrent network." In: pp. 5200–5204. DOI: 10.1109/ICASSP.2016.7472669.
- Troy, Allison S. et al. (2018). "Cognitive Reappraisal and Acceptance: Effects on Emotion, Physiology, and Perceived Cognitive Costs." In: *Emotion* 18.1, pp. 58–74. DOI: 10.1037/emo0000371. URL: <https://www.ncbi.nlm.nih.gov/pmc/articles/PMC6188704/>.
- Umeda and Satoshi (2013). "Emotion, Personality, and the Frontal Lobe." In: *Emotions of Animals and Humans: Comparative Perspectives*. Ed. by Watanabe et al. Tokyo: Springer Japan, pp. 223–241. ISBN: 978-4-431-54123-3. DOI: 10.1007/978-4-431-54123-3_10. URL: https://doi.org/10.1007/978-4-431-54123-3_10.

- Vojtech, L. et al. (2013). “Wearable textile electrodes for ECG measurement.” In: 11 (5), pp. 410–414.
- Voznenko, Timofei I. et al. (2016). “The Research of Emotional State Influence on Quality of a Brain-Computer Interface Usage.” In: *Procedia Computer Science* 88. 7th Annual International Conference on Biologically Inspired Cognitive Architectures, BICA 2016, held July 16 to July 19, 2016 in New York City, NY, USA, pp. 391–396. ISSN: 1877-0509. DOI: <https://doi.org/10.1016/j.procs.2016.07.454>. URL: <http://www.sciencedirect.com/science/article/pii/S1877050916317100>.
- Wang, K. et al. (2015). “Speech Emotion Recognition Using Fourier Parameters.” In: *IEEE Transactions on Affective Computing* 6.1, pp. 69–75. ISSN: 1949-3045. DOI: 10.1109/TAFFC.2015.2392101.
- Wang, Xiashuang et al. (2020). “Use of multimodal physiological signals to explore pilots’ cognitive behaviour during flight strike task performance.” In: *Medicine in Novel Technology and Devices* 5, p. 100030. ISSN: 2590-0935. DOI: <https://doi.org/10.1016/j.medntd.2020.100030>. URL: <http://www.sciencedirect.com/science/article/pii/S2590093520300047>.
- Wen, Guihua et al. (2017a). “Random Deep Belief Networks for Recognizing Emotions from Speech Signals.” In: *Computational Intelligence and Neuroscience* 2017, pp. 1–9. DOI: 10.1155/2017/1945630.
- (2017b). “Random Deep Belief Networks for Recognizing Emotions from Speech Signals.” In: *Computational Intelligence and Neuroscience* 2017, pp. 1–9. DOI: 10.1155/2017/1945630.
- Woaswi, Wan et al. (Dec. 2016). “Human Emotion Detection via Brain Waves Study by Using Electroencephalogram (EEG).” In: *International Journal on Advanced Science, Engineering and Information Technology* 6, p. 1005. DOI: 10.18517/ijaseit.6.6.1072.
- Wu, S., T.H. Falk, and W.-Y. Chan (2011). “Automatic speech emotion recognition using modulation spectral features.” In: 53 (5), pp. 768–785.
- Xu, Zhicha et al. (2017). “Selecting pure-emotion materials from the International Affective Picture System (IAPS) by Chinese university students: A study based on intensity-ratings only.” In: 3 (8), pp. 83–92. DOI: 10.1016/j.heliyon.2017.e00389.
- Xue, Yawen, Yasuhiro Hamada, and Masato Akagi (2018). “Voice conversion for emotional speech: Rule-based synthesis with degree of emotion controllable in dimensional space.” In: *Speech Communication* 102, pp. 54–67. ISSN: 0167-6393. DOI: <https://doi.org/10.1016/j.specom.2018.06.006>. URL: <http://www.sciencedirect.com/science/article/pii/S0167639317303187>.
- Yang, D. et al. (2018). “An Emotion Recognition Model Based on Facial Recognition in Virtual Learning Environment.” In: *Procedia Computer Science* 125. The 6th International Conference on Smart Computing and Communications, pp. 2–10. ISSN:

- 1877-0509. DOI: <https://doi.org/10.1016/j.procs.2017.12.003>. URL: <http://www.sciencedirect.com/science/article/pii/S1877050917327679>.
- Yeh, Y.C. (2003). "Application and practice of artificial neural network." In: *Scholar Books Co. Ltd.* 1.1.
- Yin, Zhong et al. (2017a). "Physiological Feature Based Emotion Recognition via an Ensemble Deep Autoencoder with Parsimonious Structure." In: *IFAC-PapersOnLine* 50.1. 20th IFAC World Congress, pp. 6940–6945. ISSN: 2405-8963. DOI: <https://doi.org/10.1016/j.ifacol.2017.08.1220>. URL: <http://www.sciencedirect.com/science/article/pii/S2405896317317263>.
- Yin, Zhong et al. (2017b). "Recognition of emotions using multimodal physiological signals and an ensemble deep learning model." In: *Computer Methods and Programs in Biomedicine* 140, pp. 93–110. ISSN: 0169-2607. DOI: <https://doi.org/10.1016/j.cmpb.2016.12.005>. URL: <http://www.sciencedirect.com/science/article/pii/S0169260716305090>.
- Yogesh, C.K. et al. (2017a). "A new hybrid PSO assisted biogeography-based optimization for emotion and stress recognition from speech signal." In: *Expert Systems with Applications* 69, pp. 149–158. ISSN: 0957-4174. DOI: <https://doi.org/10.1016/j.eswa.2016.10.035>. URL: <http://www.sciencedirect.com/science/article/pii/S0957417416305759>.
- Yogesh, C.K. et al. (2017b). "Bispectral features and mean shift clustering for stress and emotion recognition from natural speech." In: *Computers & Electrical Engineering* 62, pp. 676–691. ISSN: 0045-7906. DOI: <https://doi.org/10.1016/j.compeleceng.2017.01.024>. URL: <http://www.sciencedirect.com/science/article/pii/S0045790617302033>.
- Zaśko-Zielińska, M. and Maciej Piasecki (2015). "Lexical Means in Communicating Emotion in Suicide Notes - on the Basis of the Polish Corpus of Suicide Notes." In: 15, pp. 237–252.
- Zha, C. et al. (2016). "Spontaneous Speech Emotion Recognition via Multiple Kernel Learning." In: pp. 621–623. DOI: 10.1109/ICMTMA.2016.152.

APPENDIX A

Publications

Along this work, several researches were developed as shown in Table A.1. The first publications tried to get more background on work needs e.g. biosignals, signal processing, feature extractions and data mining.

TABLE A.1. Publications developed during the studies of the present PhD.

PhD Context - Emotions, Biosignals, Signal Processing and Data Mining			
	Reference	Title	Published
1	Roza and Postolache, 2016	◊ Citizen emotion analysis in Smart City.	IISA
2	Roza, Almeida, and Postolache, 2017	◊ Design of an Artificial Neural Network and Feature Extraction to Identify Arrhythmias from ECG.	MeMeA
3	Roza and Postolache, 2017	◊ Design of a Multimodal Interface based on Psychophysiological Sensing to Identify Emotion.	IMEKO
4	Roza et al., 2018	◊ Performance Analysis of ANN and SVM in ECG based on Arrhythmia Identification.	IMEKO
5	Roza and Postolache, 2018	◊ Emotion Analysis Architecture based on Face and Physiological Sensing Applied with Flight Simulator.	EPE
6	Roza et al., 2019	◊ Emotions Assessment on Simulated Flights.	MeMeA
7	Roza and Postolache, 2019	◊ Multimodal Approach for Emotion Recognition based on Simulated Flight Experiments. (Journal)	Sensors
8	Roza and Postolache, 2021	◊ β -Band Analysis from Simulated Flight Experiments. (Journal)	Aerospace
Out of PhD Context - Robotics, Path Modeling and Sensing Platform			
	Reference	Title	Event
9	Roza et al., 2017	◊ Development of a Kinematic Model based on Bezier Curves for Improvement of Safe Trajectories in Active Orthosis Walking Tasks.	BAILAR
10	Roza, Souza, and Postolache, 2017	◊ A Multi-Sensing Physical Therapy Assessment for Children with Cerebral Palsy.	ICST
11	L. Bruno P. Nascimento et al., 2018	◊ Goal-Biased Probabilistic Foam Method for Robot Path Planning.	ICARSC
Not Published - Writing			
	Reference	Title	Event
12	Roza and Postolache, 2017	◊ Emotion Recognition based on Speech and ANN (main context).	-
13	Roza et al., 2018	◊ A State of the Art based on Emotion (main context).	-

In 2017, was developed the first publication on the main scope of this work i.e., multimodal sensing and emotions. Between 2018 and 2019, other publications were also developed, regarding to multimodal sensing to identify emotions and its relation with flight simulated.

A.1. Experiment with Pictures and Emotions

In 2017, the present work executed the first experiment using pictures to trigger different emotion in the user.

The IAPS dataset was applied considering 7 emotions such as: anger, boredom, disgust, anxiety/fear, happiness, sadness and normal. The emotion identification was based on ANN and Support Vector Machine (SVM).

The interface was executed with 20 healthy volunteers ($N = 20$) of both genders with age from 23-50 years old. All participants signed a consent term. For each experiment were used 14 different pictures, 2 pictures by each emotion. Each picture is presented during 15s ($t = 15s$) resulting on 280 emotions, selected by all volunteers. All sensing acquisition and questionnaires were executed in laboratory with the same conditions of light and temperature (Figure A.1).

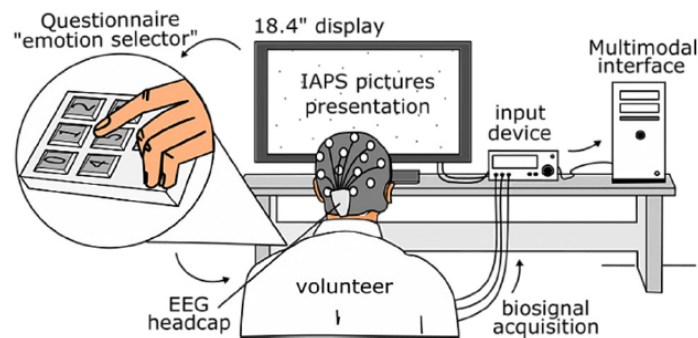


FIGURE A.1. Flow diagram of the pictures selection process from the IAPS dataset.

Considering the small "local" database used to predicts emotions (i.e. 140 emotions for training and 140 for test), the SVM prediction reached a total accuracy of 77.14%, and the best predicted emotion was happiness with 84% of accuracy.

The ANN-MLP prediction reached a total accuracy of 85.71% and the best predicted emotion was boredom with 88.20% of accuracy. Thus, the experiment shown that the prediction of emotions from psychophysiological signals reached better results when using ANN-MLP.

The electrodes used in these tasks are shown in Figure A.2, including ECG, GSR and SpO2 acquisition techniques.

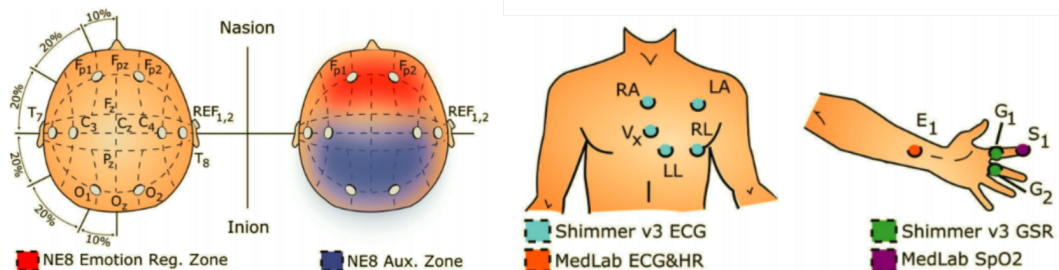


FIGURE A.2. Electrode positions for EEG (up); main and auxiliary electrodes for emotion detection (up-right); ECG, GSR and SpO2 (bottom).

A.2. Speech Emotion Recognition

Experiments including speech analysis and emotion identification were also executed in 2017 inside the context of the present work.

There, the OpenSMILE software was used to extract 88 features based on, jitters, pitches, means, standard deviations and MFCCs. To this experiment the emotion classifier was based on a light artificial neural networks using the backpropagation algorithm (Figure A.3), with 88 inputs features, 7 outputs neurons and softmax algorithm at output function. Were considered 7 different emotions in German idiom such as: anger, boredom, disgust, anxiety, happiness, sadness and normal. Each speech presented a duration time of 3 to 5 seconds.

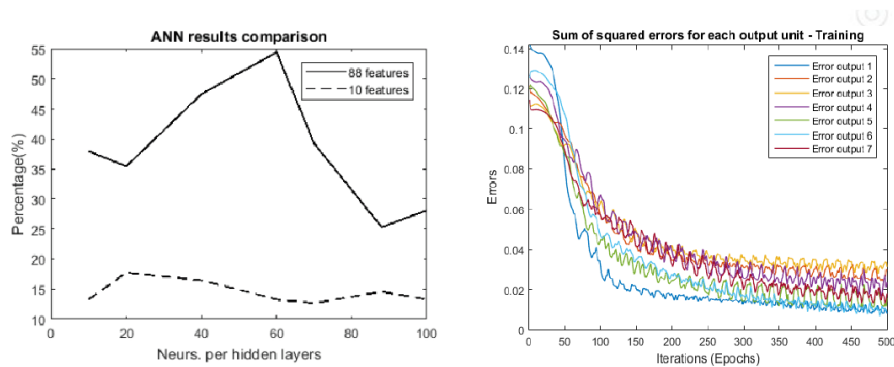


FIGURE A.3. ANN result comparison and ANN squared errors during the training.

Preliminary results shown accuracies between 47.00% to 84.40% for training, 54.43% to 93.67% for validation, giving the worst result at test (25.32% to 54.43%) phase due short dataset used in the training (Figure A.4).

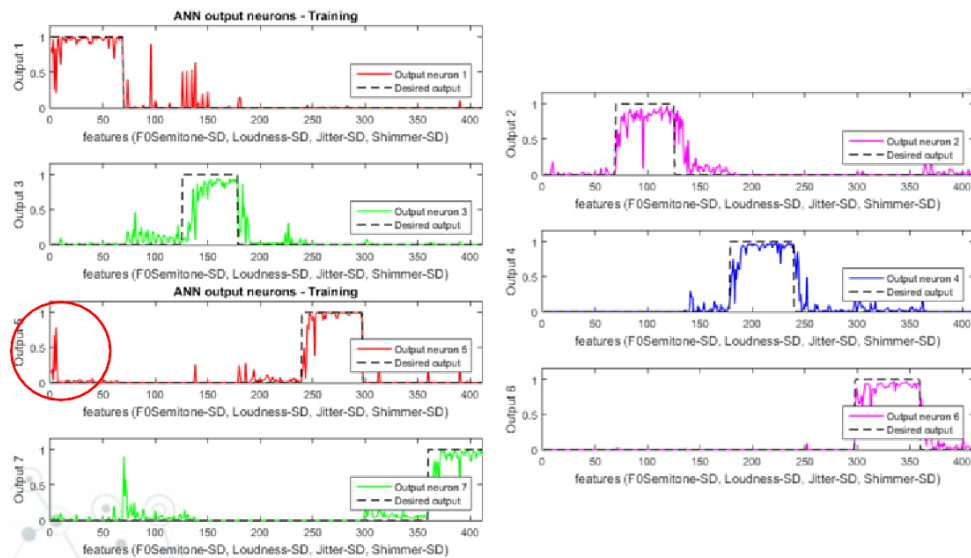


FIGURE A.4. ANN outputs during the training.

A.3. Emotion in Smart City

The initial contribution of the present work to smart city within the context of emotion identification, was initially executed in 2016.

Was proposed a design of an Android application, database and emotion identification algorithm to map specific emotions according to pictures of a city (Figure A.5), using a questionnaire to select the felt emotion when a picture was presented on screen.

The method to classify the acquired biosignals were cross-correlation (Equation ??). The Flowsense application (Reis, Arriaga, and Postolache, 2015) was used as an initial experimental parameter, considering the biosignals such as, ECG, GSR, HR and SpO2.

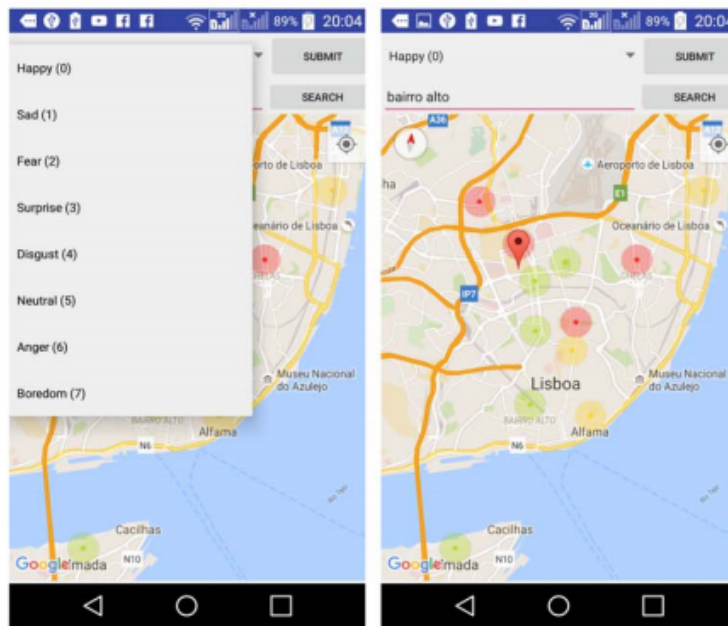


FIGURE A.5. Smart phone application screens: questionnaire and the main screen.

The initial results shown that, in 20 analyzed emotions of 18 cases, the classifier correctly match the emotion (i.e. 90% accuracy).

A.4. Main Publications

Citizen Emotion Analysis in Smart City

Válber César Cavalcanti Roza
Instituto Universitário de Lisboa/ISCTE-IUL
Universidade Federal do Rio Grande do Norte, UFRN
Lisbon, Portugal
vccra@iscte.pt

Octavian Adrian Postolache
Instituto de Telecomunicações, Instituto Universitário de
Lisboa/ISCTE-IUL
Lisbon, Portugal
octavian.adrian.postolache@iscte.pt

Abstract— Applications in Smart City context are improving the quality of life of citizens through several technological interactions. These interactions can be also used to relate the citizens' emotions to city's areas. Thus, the main objective of this work is to present a smart phone application that analyzes the citizens' emotions and the relations between these parameters and different city's areas. Daily the citizens deal with a variety of emotions due a set of factors such as, violence, street illumination or car noises, trash and pollution, for instance. The techniques used to do the acquisition of the citizens' emotions involve, heart rate (HR), heart rate variability (HRV) and galvanic skin response (GSR), measured by Shimmer3 sensors. Additionally the citizens fill an on-line questionnaire using a smart phone application. The acquired signals are also processed by a smart phone application that includes signal acquisition control, citizens' emotions analysis, emotion mapping, and data storage. Once identified and stored these citizens' emotions reported to a city's area, it can be represented by green, yellow or red color, circular icons that are plotted over the city's map, using the Google Maps API on the mobile application. Several tests for ten are presented.

Keywords— Citizens' emotion; signal analysis; smart cities; mobile application.

I. INTRODUCTION

Developments in smart city technology and the growth of embedded devices made nowadays, turn possible that their citizens receive information such as: available services in the city, alert of occurrences at different areas, information about accessibility conditions, real time traffic and road info, for instance.

Thus, there is an effort of researchers to turn the cities in a higher interactive environment, with capabilities to engage citizens in a personalized way [1], [2] and try, among other things, discover the emotions felt by its citizens, due several aspects of the city's areas such as: public transports, pollutions, street illuminations, cleaning conditions and violence, for instance.

Emotions are an important part of the human behavior and are used in several researches, such as: development of a tool of meaning detection of language to understand, classify and recognize emotions in English sentences [3]; suicide preventions [4]; detections and interpretations of emotional facial expressions in highly socially anxious individuals compared to non-anxious controls [5]; association of emotion regulation with lifestyle behaviors [6]; and a link of emotions to sustainable consumption in a big city [7].

There are also researches in detection methods based on emotion, such as: emotion-recognition from human speech [8, 9, 10]; emotion recognition, based on guidance from psychological studies of emotions, as well as from the nature of emotions and its interaction with attention [11].

This work uses electrocardiography (ECG) and galvanic skin response (GSR) to detect the citizens' emotions. These technologies are already reported in literature in several application, such as: pattern analysis for emotion detection [12]; classification of emotional states based on acquired ECG signals, as the non-linear approach based on Hurst [13] and identification of emotional states of human body [14].

Physiological reactions like stress can cause oscillation of emotions. Thus, other researches use these technologies to do also the detection and analysis of stress, such as: real time stress detection with GSR by the means of different parameter signals [15]; stress detection based on GSR and classification via Fuzzy logic [16]; production of relative diagnostic, prognostic and economic value of stress, as an initial investigation for the detection of coronary artery disease [17, 18] and use of this detection with wearable and mobile technology associated with ECG [19, 20] including via textiles [21].

Other researches report that city areas can produce positive emotions in their citizens, as the contact with natural places inside the cities. It that can promote psychological restoration, improve the mood and attention, and reduce stress and anxiety. Furthermore, this evidence is particularly important for positive associations between, experience of natural places and mental or physical health [22], what confirm the importance of the knowledge about city's areas as a good emotions agent.

To increase the level of interaction in smart city context, this work develops a smart phone application (APP) to analyze the citizens' emotions and share it to other citizens.

This APP is an important tool to improve the level of citizens' information about, what kind of emotions the citizens feel when they visit a certain city's area.

Thus, this work focuses in citizens' emotions detection, when they visit different areas of the city. Additionally, this paper refers the emotions' representation and the sharing of these emotions between citizens.

FIGURE A.6. Publication regarding to the emotional relation between city places and citizens' emotions (Roza and Postolache, 2016).

Design of a Multimodal Interface based on Psychophysiological Sensing to Identify Emotion

Válber César Cavalcanti Roza¹, Octavian Adrian Postolache²

¹*Instituto Universitário de Lisboa, ISCTE-IUL/IT&UFRN, Lisbon, Portugal, vccra@iscte-iul.pt*

²*Instituto de Telecomunicações, IT-IUL&ISCTE-IUL, Lisbon, Portugal, opostolache@lx.it.pt*

Abstract – This work proposes a design of a multimodal interface to classify or identify emotion states. Thus, 7 emotions are considered such as: anger, boredom, disgust, anxiety/fear, happiness, sadness and normal. A couple of sensing technologies to collect psychophysiological signals are used such as: galvanic skin response (GSR), heart rate (HR), electrocardiography (ECG), oxygen saturation (SpO2) and electroencephalography (EEG). The International Affective Picture System (IAPS) dataset is used to aids the classifier system. In classification task, a comparison between artificial neural networks (ANN-MLP) and support vector machine (SVM) are presented. The tests were carried out for 20 healthy volunteers ($N_p = 20$) of both genders with age from 23-50 years old. The proposed classifier presents accuracies of 85.71% when using ANN-MLP and 77.14% when using SVM.

Keywords – Multimodal interface, signal analysis, emotion classification, psychophysiological signals.

I. INTRODUCTION

Emotion is an important part of the human behavior and is organized in two primary categories – conscious and unconscious. Conscious emotion relates the emotional response based on some cognitive processes and the unconscious emotion is based on the autonomic process from nervous system [1, 2]. The interactions with pleasant places [3], hazards situations or by the judgment that it requires [4], memory bias and societal influences [2] are some situations that may determine the emotional state of an individual.

The emotions studies and its effects may be used for several purposes, researches and applications such as: detection of the relation among emotion and the regulation of lifestyle behavior [5]; analysis of its positives effects in individuals when they are in green and natural city's places [3]; analysis of suicides notes to avoid recurrent occurrences [6]; developments of tools of meaning detection of language to understand, identify and recognize emotions [7]; developments of interfaces to detect emotions from facial expressions to helps anxious

individuals [8]; also to give support in healthcare, based in smart city context and internet of things (IoT) [9].

Automatic emotion classification is a complex and important task that also can be used to improve the health and the life's quality. Different techniques may be used on the automatic emotion prediction or identification task, such as: salivary cortisol analysis [3], Hilbert-Huang transform [10], electrocardiography (ECG) [10-12], fuzzy logic, galvanic skin response (GSR) [13] and electroencephalography (EEG) [14]. Other researches present the importance of the multimodal sensing interfaces to acquire and identify emotions as for instance: identification of cognitive states of aircraft pilots while they are using flight simulators [15]; to exam of the usefulness of psychophysiological measurements in a biocooperative feedback loop to adjusts the difficulty of an upper extremity rehabilitation task [16]; and to harmonizes robotic devices and emotion states as frustration and boredom [17].

The proposed design of a multimodal sensing interface is used to gives support to emotion acquisition, processing and identification tasks using several sensing devices and identification techniques. The emotions considered are: anger, boredom, disgust, anxiety/fear, happiness, sadness and normal. Moreover, to give support to the acquisition system, the International Affective Picture System (IAPS) dataset is used, which its pictures have been rated by both male and female volunteers [18].

II. DATASET PICTURES SELECTION

The International Affective Picture System (IAPS) dataset is considered in this work to provoke emotions in the volunteers. The IAPS dataset folder "test images artphoto" with 807 pictures was initially analyzed. Its pictures are labeled as amusement, anger, awe, contentment, disgust, excitement, fear and sad.

These pictures were valued by 5 healthy volunteers (they were not part of the main experiment) to select the most representative pictures according with the emotions: anger, boredom, disgust, anxiety/fear, happiness, sadness and normal. To reduce the dataset from 807 to 14 pictures (2 pictures representing each emotion), these volunteers first selected visually a subset of 40 pictures related to the

FIGURE A.7. Publication regarding to the design of a multimodal interface based on emotion (Roza and Postolache, 2017).

Design of an Artificial Neural Network and Feature Extraction to Identify Arrhythmias from ECG

Válber César Cavalcanti Roza
ISCTE Instituto Universitário de Lisboa/IT
Universidade Federal do Rio Grande do Norte
valber_cesar_roza@iscte.pt

Ana Maria de Almeida
ISCTE Instituto Universitário de Lisboa
ana.almeida@iscte.pt

Octavian Adrian Postolache
Instituto de Telecomunicações/IT
ISCTE Instituto Universitário de Lisboa
opostolache@lx.it.pt

Abstract—This paper presents a design of an artificial neural network (ANN) and feature extraction methods to identify two types of arrhythmias in datasets obtained through electrocardiography (ECG) signals, namely arrhythmia dataset (AD) and supraventricular arrhythmia dataset (SAD). No special ANN toolkit was used; instead, each neuron and necessary calculus were modeled and individually programmed. Thus, four temporal-based features are used: heart rate (HR), R-peaks root mean square (R-RMS), RR-peaks variance (RR-VAR), and QSR-complex standard deviation (QSR-SD). The network architecture presents four neurons in the input layer, eight in hidden layer and an output layer with two neurons. The proposed classification method uses the MIT-BIH Dataset (Massachusetts Institute of Technology—Beth Israel Hospital) for training, validation and execution or test phases. Preliminary results show the high efficiency of the proposed ANN design and its classification method, reaching accuracies between 98.76% and 98.91%, when in the identification of NSRD and arrhythmic ECG; and accuracies of 86.37% (AD) and 76.35% (SAD), when analyzing only classifications between both arrhythmias.

Keywords—arrhythmia identification; pattern recognition; signal analysis; artificial neural network.

I. INTRODUCTION

Electrocardiography (ECG) is an important non-invasive technique used in medicine to observe the heart variation and abnormalities over a period of time. Continuous and typical ECG signal consists of P-waves, QRS-complexes and T-waves [1], and provides fundamental information about the electrical activity of the heart. Abnormalities in this electrical activity may represent heart diseases defined by the absence of any structural cardiac defects and are responsible for a large number of sudden, unexpected deaths, including those of young individuals [2]. Thus, several diseases may be detected through ECG analysis such as, atrial fibrillation (AF) [3,4], long QT syndrome, Brugada syndrome, catecholaminergic polymorphic ventricular tachycardia and the short QT syndrome [2] and arrhythmia [5]. Some of these diseases cannot be visually distinguished easily by a medical specialist due to its similar appearance with other signals [6]. However, a deep computational analysis may be used to detect small differences and possible diseases. To allow for such automatic detection, several features may be extracted from ECG signals such as, heart rate variability (HRV) triangular index [7], morphological features [8] through the temporal-domain analysis [7,9] and frequency-domain [1,7,10], and wavelet transform coefficients [11,12,13,14]. Furthermore, automatic methods to correctively identify diseases or patterns from these

signals may be reached through statistical Markov models [15], artificial neural networks (ANN) [1,3,6,16], linear discriminant analysis [17], and support vector machine (SVM) [18].

Arrhythmia is defined as a general term for an irregularity or rapidity of the heartbeat or an abnormal heart rhythm [4]. Arrhythmias can initiate or exacerbate acute systolic heart failure in patients with pre-existing heart disease [19]. Therefore, studies in arrhythmias characteristics, definition and consequences are explored in several works.

Leren et al., investigated early markers of arrhythmic events and improved risk stratification in early arrhythmogenic right ventricular cardiomyopathy, performing resting and signal averaged ECG [5]. Farwell et al., presents a paper review about the current clinical and molecular understanding of the electrical diseases of the heart associated with sudden cardiac death [2]. Kohno et al., presents a state-of-the-art about the relation between atrial arrhythmias and pacing-induced rhythms disorders, inside the context of cardiac implanted devices [20]. Gopinathannair et al., exposed the arrhythmia-induced cardiomyopathies (AIC) showing its definition, potential reversible condition and aspects [19].

In the arrhythmia identification context, other works present classifications and methods used. Caswell et al. used new techniques to analyze arrhythmia through morphology of the ECG waveform with success in correctly detecting fatal arrhythmias through waveform correlation analysis of intracardiac electrograms. They also defined a two-dimensional feature space with linear decision boundaries using a least squares minimum distance classifier [21]. Povinelli et al., proposed a novel, nonlinear, phase space based method to quickly and accurately identify life-threatening arrhythmias, determined for six different ECG signal lengths [22]. Artis et al. used ANNs to identify AF, using the MIT-BIH Dataset, with each AF and non-AF recordings with 15-min [3]. Shadmand and Mashoufi, developed a new personalized ECG signal classification using ANN variant named block-based neural network (BBNN) and then classify ECG heartbeats, possibly also detecting arrhythmia patterns [6]. Lin, proposed a method for heartbeat identification from ECG using ANN and grey relational analysis (GRA) to classify cardiac arrhythmias patterns [1].

This paper presents a new approach to identify two types of arrhythmias patterns from ECG signals: the arrhythmia dataset (AD) and the supraventricular arrhythmia dataset (SAD). Moreover, are used four temporal-based features: heart rate (HR), R-peaks Root Mean Square (R-RMS), RR-peaks

FIGURE A.8. Publication regarding to the design of an ANN to detect arrhythmias from ECG data (Roza, Almeida, and Postolache, 2017).

Emotion Analysis Architecture Based on Face and Physiological Sensing Applied with Flight Simulator

Válber César Cavalcanti Roza

Instituto Universitário de Lisboa, ISCTE-IUL & IT-IUL
Universidade Federal do Rio G. do Norte, UFRN
Lisboa, Portugal
valber_cesar_roza@iscte.pt

Octavian Postolache

Instituto Universitário de Lisboa, ISCTE-IUL
Instituto de Telecomunicações, IT-IUL
Lisboa, Portugal
opostolache@lx.it.pt

Abstract—This work presents an architecture as an important contribution regarding to emotional events along tasks based on flight simulations. This architecture considered eight beginner users of flight simulator ($n = 8$) while they execute a simulated flight according with the basic concepts of visual flight rules (VFR). The acquired physiological sensing were: heart rate (HR), electroencephalography (EEG) and galvanic skin response (GSR). One small camera was also used to record the users' face in order to extract, after the post-processing, the emotions of the user during the flight. The considered emotions were: happy, sad, angry, surprised, scared and disgust. Initial analysis of the GSR signals shown that the takeoff task presented 13% more variability (or emotional events) between the climb and approach tasks together; and in the same way, the landing task presented 16% more variability between the climb and approach tasks together, what shows the importance of these researches in flight safety context, mainly in these critical phases.

Keywords—emotion analysis architecture; flight simulator; physiological sensing; aviation safety; human error prevention

I. INTRODUCTION

Emotion analysis architectures arise to try to understand and classify accurately the emotional states during the execution of several tasks [1]. Computationally, several algorithms are frequently developed to reach an emotion's recognition level that be capable to be applied everywhere (e.g. stressful administrative jobs, cities' routines, critical aviation's procedures, entertainments, etc.), starting from a specific emotions sources (e.g. face, speech or physiological sensing) to a final emotion pattern recognition.

Emotion plays a critical role in human bio-regulation and survival - it is leaded by the brain, representing the result from chemical process that joins several biological (internal) and external factors as its inputs, to produce an output reflected as an emotion [2]. It can also compromise the decision-making and cognitive functioning in the aviation [3].

Its effects may result in severe aviation accidents caused by human fail as consequence of several errors that sometimes produces some hazards as for instance: failures in the analysis of flight problems and failures in the choice of a correct action that a certain situation requires [4]. Due to that, the emotional researches inside of the aviation context are getting relevance over time.

In 2017, the Boeing Aerospace Company presented a statistical summary [5], about commercial jet airplane accidents confirmed to worldwide operations for 1959 through 2016, considering airplanes that are heavier than 60,000 pounds maximum gross weight. With this summary is possible to note that each year the aviation has been safer, reaching lower levels of accidents with fatalities including hull losses or not. Although, there are no reasons to relax, because there are another problems to solve, i.e. the emotional factors that can be dangerous on the flight operations.

This work uses a proposal of emotions analysis architecture to apply on aviation context. In this study, only simulated flights were used with beginner users of flight simulator.

II. METHODOLOGY

Before the main experiment starts, each beginner user was trained to the main experiment based on: the flight maneuvers, airplane controls in the air, takeoff, climb, navigation (cruise route), descend, approach and landing. It was applied to show to the flight simulator's users how each flight control works, learning how to execute actions in an airplane such as, pitch, roll and also the tasks of the proposed experiment.

After the training, the main experiment presents a data acquisition from 8 beginner users ($n = 8$) of flight simulator during the execution of 7 different tasks while flying based on basic concepts of visual flight rules (VFR) through the air traffic rules and procedures applicable to air traffic in Lisbon FIR and Santa Maria Oceanic FIR, conform with Annex 2 and 11 to the Convention on International Civil Aviation [6].

Using the aviation context, this work is based on several data acquisition such as: face recordings, questionnaires, heart parameters, skin conductivity and electroencephalography. These data were stored to execute an initial feasibility analysis and to show that the proposed architecture can be applied in this context (Fig. 1).

A. Flight Scenario – Route of the Experiment

The experimental scenario or route used in this work was based on a real flight plan, using the same place of the real experiment, i.e. Lisbon. It was useful to give more realism to the experiment, what can produce more effective reactions being very important to this work.

FIGURE A.9. Publication regarding to the design of a multimodal architecture based on emotion and flight simulator (Roza and Postolache, 2018).

Performance Analysis of ANN and SVM in ECG Based Arrhythmia Identification

V C C Roza^{1,2}, A M Almeida¹, P M B Silva Girão^{3,4}, and O A Postolache^{1,5}

¹Instituto Universitário de Lisboa, ISCTE-IUL/IT, Lisbon, Portugal

²Universidade Federal do Rio Grande do Norte, UFRN, RD Norte, Brazil

³Instituto de Telecomunicações, Lisbon, Portugal

⁴DEEC, Instituto Superior Técnico/UL, Lisbon, Portugal

⁵Instituto de Telecomunicações, IT-IUL, Lisbon, Portugal

E-mails: valber_cesar_roza@iscte.pt, ana.almeida@iscte.pt,
psgirao@tecnico.ulisboa.pt, opostolache@lx.it.pt

Abstract. This paper presents a performance analysis of Artificial Neural Network (ANN) and Support Vector Machine (SVM) algorithms in arrhythmia identification task based on ECG signals. Six features are used for both algorithms: short signal 1-D wavelet energy (SS-WVE), short signal continuous wavelet transform mean (SS-CWTM), heart rate (HR), R-peaks root mean square (R-RMS), RR-peaks variance (RR-VAR) and QRS-complex standard deviation (QRS-SD). The identification methods use the MIT-BIH Dataset (Massachusetts Institute of Technology–Beth Israel Hospital) for training, validation and test phases. In this work, preliminary results shown that the classification obtained using SVM is marginally better than the one obtained with the ANN classifier for the same classification task (i.e. arrhythmia pattern identification).

1. Introduction

One of the most important and non-invasive techniques used in medicine is the Electrocardiography (ECG). It is used to observe the heart activities, i.e. variation and abnormalities over a period of time. This signal consists of several waves patterns such as U-waves, P-waves, T-waves and QRS-complexes and provides an important information about the electrical activity of the heart. Abnormal patterns in this electrical activity may represent heart diseases such as, atrial fibrillation (AF) [1], Brugada syndrome, long QT syndrome, short QT syndrome, and arrhythmia [2], that are defined by any structural cardiac defects, responsible for a large number of sudden, unexpected deaths. However, some of these diseases can't be visually distinguished easily by a medical specialist due to its similar appearance with other ECG signals [3]. A computational analysis may be used to detect these small abnormalities. Then, to allow an automatic detection of these abnormalities, several features may be extracted from ECG such as: heart rate variability (HRV) [4], morphological features using temporal and frequency-domain analysis [5, 6]. To identify it, Markov models, artificial neural networks (ANN) and support vector machine (SVM) [7-9] can be used.

In a general definition, arrhythmia represents an irregularity or rapidity of the heartbeat or an abnormal heart rhythm and can initiate or exacerbate acute systolic heart failure [1, 9, 10, 11]. Its analysis and patterns are explored in several works. Leren et al., investigated early markers of arrhythmic events and improved risk stratification in early arrhythmogenic right ventricular cardiomyopathy [2]. Lin, proposes a method for heartbeat identification from ECG using ANN and grey relational analysis (GRA) [1]. Shadmand and Mashoufi developed a new personalized ECG signal classification using an ANN variant named block-based neural network (BBNN) [3]. Pavinelli et al. proposed a novel nonlinear phase space based method to quickly and accurately identify life-threatening arrhythmias [12].

This paper presents a comparison analysis between the performance ANN and SVM in arrhythmia identification based on two types of arrhythmias patterns from ECG signals, considering six different features and the MIT-BIH Arrhythmia Dataset.

2. Dataset description

This work uses the MIT-BIH (Massachusetts Institute of Technology–Beth Israel Hospital) Dataset to provide the ECG signals used during training, validation, and test of both classifiers.

FIGURE A.10. Publication regarding to the performance analysis of ANN and SVM on arrhythmia identification (Roza et al., 2018).

Emotions Assessment on Simulated Flights

V. C. Roza,
Instit. de Telecomunicações
ISCTE-IUL, Lisbon
Portugal
valber_cesar_roza@iscte.pt

O. Postolache
Instit. de Telecomunicações,
ISCTE-IUL, Lisbon Portugal
opostolache@lx.it.pt,

V. Groza
University of Ottawa,
Canada
vgroza@uottawa.ca

J. M. Dias Pereira,
Instit. de Telecomunicações, EST-IPS
Setúbal, Portugal
dias.pereira@estsetubal.ips.pt

Abstract— The emotions on pilots play important role on their performance during the service. Thus, an emotion prediction methodology based on physiological parameters such as galvanic skin response and heart rate as so as the facial recognition was considered in the present work. Several tests with eight volunteers were carried out that were used flight simulator. A small camera and the Face Reader software were used to record the users' face during the fly task and to perform the video off-line processing to extract facial emotions during performed flights. The considered emotions were: happy, sad, angry, surprised, scared and disgust. To predict these emotions, the Artificial Neural Network (ANN) was applied. The experiment shows that is possible to predict emotions using these data and the best predict model was reached with 2 hidden layers, having a minimum squared error of 0.219.

Keywords— Emotion monitoring, heart rate, GSR sensing, emotion analysis, flight simulator, aviation safety.

I. INTRODUCTION

Emotion analysis and prediction are an important research field that are useful to try to understand and predict accurately several emotions inside a certain contexts and tasks [1]. Several algorithms were developed to reach the best emotional predictions which can be applied on different scenarios (e.g. entertainments, cities' routines, stressful administrative jobs, critical aviation's, procedures). The acquisition of these emotions is majority taken from physiological sensing, speech, face and body gestures.

Emotions play a critical role in human bio-regulation and survival. These emotions' characteristics are leaded by the brain as results of several chemical processes that joins several biological and external factors, which produce an output reflected as an emotion [2]. The influence of emotions can also compromise the decision- making and cognitive functioning in the aviation affecting the heart functioning [3], for instance. Its effects may result in severe aviation accidents caused by human failure as consequence of systematic errors that sometimes produces some hazards as for instance: failures in the analysis of flight problems and failures in the choice of a correct action that a certain situation requires [4]. These are some reasons that motivate the need of emotional researches inside of the aviation contexts as for instance: drugs abuse, familiar problems, suicides, alcohol consumptions, workload, stress long flights, among others.

Looking for the same problem, Antonio et al. (2018), developed a study based on flight simulator, emotion and heart rate. They confirmed the sensitivity of the HR to cognitive demand and training effects, with increased HR when the task was more difficult and decreased HR with training (time-on-task) which can be critical in many flight situations [5].

The Boeing Aerospace Company presented a statistical summary [6], about the commercial jet airplane accidents confirmed to worldwide operations for 1959 through 2016, considering airplanes that are heavier than 60,000 pounds maximum gross weight.

There was shown that each year, the amount of air accidents is getting lower (decreasing the events of accident) including fatalities with hull losses or not. Even with these data, there are other problems that need to find good solutions, as for instance, the emotional factors that can be dangerous on the flight operations when it is treated with irresponsibility.

II. METHODOLOGY

Preliminary training was carried out with the volunteers including simulation tasks such as: flight maneuvers, airplane controls in the air, takeoff, climb, navigation (cruise route), descend, approach and landing. The training focused on how each flight control works, controls that are later used to execute airplane navigation tasks during the proposed experiment.

In the present work eight volunteers (beginners on flight simulator (Fig. 1)) were performed seven different tasks based on basic concepts of visual flight rules (VFR) through the air traffic rules and procedures applicable to air traffic in Lisbon FIR and Santa Maria Oceanic FIR. The rules and procedure conform with Annex 2 and 11 from the Convention on International Civil Aviation [7][8].



Fig. 1. Simulator GUI for Aircraft Cessna-172.

FIGURE A.11. Publication regarding to the emotional assessment on simulated flight experiments (Roza et al., 2019).

Article

Multimodal Approach for Emotion Recognition Based on Simulated Flight Experiments

Válber César Cavalcanti Roza ^{1,2,*} and Octavian Adrian Postolache ¹

¹ Instituto Universitário de Lisboa (ISCTE-IUL) and Instituto de Telecomunicações (IT-IUL), Av. das Forças Armadas, 1649-026, Lisbon, Portugal; valbercesar@gmail.com (V.C.C.R.); opostolache@lx.it.pt (O.A.P.)

² Universidade Federal do Rio Grande do Norte (UFRN), Av. Sen. Salgado Filho, 3000, Candelária, 59064-741, Natal-RN, Brazil

* Correspondence: valbercesar@gmail.com

Received: 18 October 2019; Accepted: 9 December 2019; Published: date



Abstract: The present work tries to fill part of the gap regarding the pilots' emotions and their bio-reactions during some flight procedures such as, takeoff, climbing, cruising, descent, initial approach, final approach and landing. A sensing architecture and a set of experiments were developed, associating it to several simulated flights ($N_{flights} = 13$) using the Microsoft Flight Simulator Steam Edition (FSX-SE). The approach was carried out with eight beginner users on the flight simulator ($N_{pilots} = 8$). It is shown that it is possible to recognize emotions from different pilots in flight, combining their present and previous emotions. The cardiac system based on Heart Rate (HR), Galvanic Skin Response (GSR) and Electroencephalography (EEG), were used to extract emotions, as well as the intensities of emotions detected from the pilot face. We also considered five main emotions: happy, sad, angry, surprise and scared. The emotion recognition is based on Artificial Neural Networks and Deep Learning techniques. The Root Mean Squared Error (RMSE) and Mean Absolute Error (MAE) were the main methods used to measure the quality of the regression output models. The tests of the produced output models showed that the lowest recognition errors were reached when all data were considered or when the GSR datasets were omitted from the model training. It also showed that the emotion *surprised* was the easiest to recognize, having a mean RMSE of 0.13 and mean MAE of 0.01; while the emotion *sad* was the hardest to recognize, having a mean RMSE of 0.82 and mean MAE of 0.08. When we considered only the higher emotion intensities by time, the most matches accuracies were between 55% and 100%.

Keywords: emotion recognition; physiological sensing; multimodal sensing; deep learning; flight simulation

1. Introduction

With the growth of air safety and accident prevention, especially in the mechanical-structural and avionics aspects, a gap of probable cause of accidents is emerging, which can justify the occurrence of several unwanted situations. This can be referred to as the relationship between emotions and aviation accidents caused by human failure.

The development of research about the relation between emotions and aviation activities is quite new and is mainly based on preliminary and final accident reports. It was important to show the real need of improvements and strategies regarding emotion effects in risky situations of a real flight, mainly on take off, approach and landing.

To know how important are the studies of emotions over the aviation contexts, we first need to understand emotion definitions. Emotion is led by the brain and it can sometimes be the result of chemical processes that join several internal and external factors to produce an output or response

FIGURE A.12. Publication regarding to the multisensing approach to identify emotions based on simulated flight experiments (Roza and Postolache, 2019).

Article

β -Band Analysis from Simulated Flight Experiments

Válber César Cavalcanti Roza ^{1,2,*} and Octavian Postolache ¹

¹ Instituto de Telecomunicações (IT-IUL), Instituto Universitário de Lisboa (ISCTE-IUL), Av. das Forças Armadas, 1649-026 Lisbon, Portugal; opostolache@lx.it.pt

² Centro de Tecnologia (CT), Universidade Federal do Rio Grande do Norte (UFRN), Av. Sen. Salgado Filho, 3000, Candelária, Natal 59064-741, Brazil

* Correspondence: valbercesar@gmail.com

Abstract: Several safety-related improvements are applied every year to try to minimize the total number of civil aviation accidents. Fortunately, these improvements work well, reducing the number of accident occurrences. However, while the number of accidents due to mechanical failures has decreased, the number of accidents due to human errors seems to grow. On that basis, this work presents a contribution regarding the brain's β -band activities for different levels of volunteers' expertise on flight simulator, i.e., experienced, mid-level and beginner; in which they acted as pilots in command during several simulated flights. Spectrogram analysis and statistical measurements of each volunteer's brain's β -band were carried out. These were based on seven flight tasks: takeoff, climb, cruise flight, descent, approach, final approach and landing. The results of the proposed experiment showed that the takeoff, approach and landing corresponded to the highest brain activities, i.e., close to 37.06–67.33% more than the brain activity of the other flight tasks: when some accidents were about to occur, the intensities of the brain activity were similar to those of the final approach task. When the volunteers' expertise and confidence on flight simulation were considered, it was shown that the highest brain magnitudes and oscillations observed of more experienced and confident volunteers were on average close to 68.44% less, compared to less experienced and less confident volunteers. Moreover, more experienced and confident volunteers in general presented different patterns of brain activities compared to volunteers with less expertise or less familiarity with flight simulations and/or electronic games.

Keywords: electroencephalography; beta band; statistical analysis; aviation safety



Citation: Roza, V.C.C.; Postolache, O. β -Band Analysis from Simulated Flight Experiments. *Aerospace* 2021, 8, 120. <https://doi.org/10.3390/aerospace8050120>

Academic Editor: Mario Innocenti

Received: 8 March 2021

Accepted: 15 April 2021

Published: 21 April 2021

Publisher's Note: MDPI stays neutral with regard to jurisdictional claims in published maps and institutional affiliations.



Copyright: © 2021 by the authors. Licensee MDPI, Basel, Switzerland. This article is an open access article distributed under the terms and conditions of the Creative Commons Attribution (CC BY) license (<https://creativecommons.org/licenses/by/4.0/>).

1. Introduction

The present research considers the analysis of the beta band, based on electroencephalography (EEG) data in the context of simulated flight, with several flight tasks. With such analysis, it is possible to reinforce the need for studies on this field and also the development of new technologies that increase the ability of real pilots to regulate their physiological response before, during and after real flights.

Nowadays, aviation accidents continue to occur, and together with these undesirable situations come the aviation safety's improvements. Some of these improvements were presented in the airline safety report on 6 April 2020 by the International Air Transport Association (IATA). It revealed the accident rates of 2019 and showed all improvements compared to 2018–2014. In 2019, there were 53 accidents, 8 of which were fatal, including 240 deaths. In 2018, there were a total of 62 accidents, 11 of which were fatal, including 523 deaths. The represents a reduction by 9 accidents (3 fatal) and 283 deaths in 2019 compared to 2018. For the period of 2014–2018, there were an average of 63.2 accidents, including 8.2 fatal, with 303.4 deaths per year [1]. In 2017, the Boeing Aerospace Company presented a statistical summary [2] of commercial jet airplane accidents confirmed for worldwide operations for 1959 through 2016. It considered airplanes that are heavier than 60,000 pounds maximum gross weight, showing a very clear statistical analysis of

FIGURE A.13. Publication regarding to the β -band analysis (Roza and Postolache, 2021).

A.5. Publications out of Main Work Context (Parallel Publications)

At the same period, several parallel publications i.e., out of PhD context, were also developed, which most of it were published inside the context of robotics, path planning and multisensing platforms (Figures A.14 to A.16).

Development of a Kinematic Model based on Bézier Curves for Improvement of Safe Trajectories in Active Orthosis Walking Tasks

Válber C.C. Roza¹, Kassio J.S. Eugenio², Vanessa G.S. Morais³, Pablo J. Alsina⁴ and Márcio V. de Araújo⁵

Abstract—This work presents a kinematic walking model for an active orthosis with 4 degrees of freedom based on Bézier curves as foot trajectory. Moreover, the proposed model reinforces the importance of this model for crossing holes and other obstacles. Gravitational reactions and balance control are not considered in this paper, because the user is supported by a couple of crutches. The proposed method was simulated based on Ortholeg orthosis parameters with 20kg of structural weight, for users from 1,55m to 1,70m height and weight up to 65kg. Simulation experiments shown that for walking task, including crossing holes and small obstacles, the proposed model obtained good results.

Keywords: kinematics walking model; Bézier curves trajectory; orthosis modelling; assistive robotics.

I. INTRODUCTION

In recent years, the development of assistive devices is growing in the academic community. Besides of other robotic systems, the assistive technology that includes robotics systems must be based mainly on reliability, robustness and safety just as several devices around the world that tries to fill this field such as: smart wheelchair [1], active orthosis using biosignals [2] and mechanical/robotic prosthesis for arms, hands and foot [3].

There are several kinematic walking models to active orthosis or humanoid robots. Uchiyama et al., simulated a walking motion for a powered orthosis using a couple of central pattern generators (CPG) [4]. Haghghi and Nekoui, used Cubic Polynomial method as a foot trajectory generator for one humanoid robot eight joints [5]. Santos et al., proposed a new architecture for a biped robot with seven DOF per each leg and one DOF corresponding to the toe joint, dividing the walking gait into the Sagittal and Frontal planes [6]. Marques et al., presented a different method to model kinematics of humanoid robots avoiding the restriction to the frontal and sagittal planes [7]. Rameez and Khan, presented dynamic equations of motion and its Matlab simulation of joints position using equations with forward kinematics and inverse kinematics [8].

With the Bézier curves other approaches may define a geometric representation of trajectories and curves such as:

¹Válber Roza is with Dept. of Science and Technology, University Institute of Lisbon (ISCTE-IUL, Portugal) and Federal University of Rio Grande do Norte (UFRN, Brazil). valber_cesar_roza@iscte.pt

^{2,3}Kassio Eugenio and Vanessa Morais are with the Dept. of Mechatronic Engineering, UFRN, Brazil. kassioeugenio@gmail.com

⁴Pablo Alsina is with the Dept. of Computation Engineering and Mechatronic Engineering, UFRN, Brazil. pablo@dca.br

⁵Márcio Araújo is with the Dept. of Mechanical Engineering and Mechatronic Engineering, UFRN, Brazil. marcio@ct.ufrn.br

Cubic Polynomial method [5], Nelson polynomials [9] and polynomial spirals [10].

This work presents a solution for foot trajectory modeling based on Bézier curves and inverse kinematics, applied to a 4 degrees of freedom active orthosis on walking task, crossing holes and small obstacles. The gravitational reactions and balance control are not considered, since the user walking is supported by a couple of crutches.

II. THE ORTHOLEG PROTOTYPE

The proposed inverse kinematic model is based on an active orthosis parameters with 4 degrees of freedom (DoF) named Ortholeg v1.0. It has four actuators placed in the knees and hips controlled on sagittal plane, 20kg of structural weight and being applied to users within a height range between 1,55m to 1,70m and 65kg weight. It is able to perform movements such as straight walk, sit and stand up [11].

Furthermore, other Ortholeg version is being developed by the group [12] as shown in Figure 1.

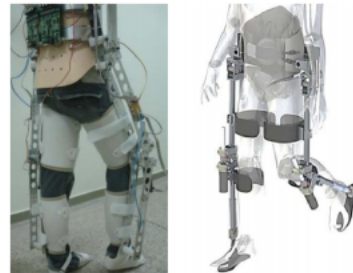


Fig. 1. Orthosis Ortholeg v1.0 (left) and v2.0 (right).

III. BÉZIER CURVES AS FOOT TRAJECTORY

Bézier curves are a powerful tool for constructing free-form curves and surface. It have a fundamental importance for computer aided geometric design (CAGD) and computer graphics (CG) [13]. In this work are used to define the foot trajectories of an active orthosis, giving support to walking and crossing obstacles tasks.

Mathematically the Bézier curves are based on the *binomial coefficients* and are defined by a set of *control points* $\{P_0, P_1, P_2, \dots, P_n\}$ where n represents the order's curve. For

FIGURE A.14. Publication regarding to the inverse kinematic applied to orthosis walking tests (Roza et al., 2017).

A Multi-sensing Physical Therapy Assessment for Children with Cerebral Palsy

Regina de Souza
Instituto Universitário de Lisboa, ISCTE-IUL
Instituto de Telecomunicações, IT-IUL
regina_souza@iscte.pt

Válber César Cavalcanti Roza
Instituto Universitário de Lisboa, ISCTE-IUL
IT-IUL&UFRN
valber_cesar_roza@iscte-iul.pt

Octavian Postolache
Instituto Universitário de Lisboa, ISCTE-IUL
Instituto de Telecomunicações, IT-IUL
opostolache@ix.it.pt

Abstract — This work presents the development of a multi-sensing interface called Palsy Thera Sense, to provide information data obtained during physical therapy of the children with cerebral palsy. It allows the monitoring the children's motor skills, and provide metrics that can be later used for proper and effective training. This interface is based on distributed force measurement system characterized by two different load cells. The signals from signals from the load cells distributed on the level of a force platform and at the level of child's body support ropes that are tied on the cerebral palsy spider cage are acquired and wireless transmitted to a client computation platform. Thus different tests can be carried out including, center of forces measurements and gait simulations. These tests can be study of children balance during different activities such as serious game playing for upper limb rehabilitation. The interface shown to be an important tool that provide support to cerebral palsy rehabilitation process, and for objective evaluation of the patients during the rehabilitation period. Several experimental results are included in the paper highlighting the capabilities of the designed and implemented multi-sensing system.

Keywords – Cerebral palsy; rehabilitation; assistive technology; signal analysis; multi-sensing devices.

I. INTRODUCTION

Physical medicine and rehabilitation (PM&R), also known as physiatry or rehabilitation medicine, aims to enhance and restore the functional ability and quality of life to those with physical impairments or disabilities affecting the brain, spinal cord, nerves, bones, joints, ligaments, muscles, and tendons [1]. Subjective and objective evaluations that are current used by physiotherapist provide information about rehabilitation process. The usage of scale physical rehabilitation outcome is a current method to extract information about motor capability of the patient under physical rehabilitation, however is highly affected by subjective elements that conduct to less accurate evaluation results. Nowadays, to increase the accuracy of the motor condition progress of the patients under physical rehabilitation, the smart sensors and advanced signal processing are used [1-2], however, there are still a lack of implementation in the field of cerebral palsy rehabilitation monitoring and physical rehabilitation outcome.

Cerebral palsy is a term generalized from the chronic non-progressive encephalopathy. It consists of a group of changes in the development of motor functions, resulting from a static lesion in the central nervous system [3]. This injury can occurs due to several factors during periods of prenatal, natal and

neonatal [4-5]. The incidence of this pathology is very high, being the most common disorder in child development [6].

The most common types of cerebral palsy are: spastic, dyskinesia, ataxia and Mixed forms (most often spasticity and ataxia, athetosis, less often and athetosis) [7]. As solution to improve physical condition of this type of children, physical therapy allows to stimulate the patient's motor development, allowing their brain to "learn" the movements performed during the sessions that can be appropriate monitored using smart sensing systems [reference].

Several multi-sensing solutions that are designed to give support to stimulation of motion and to provide the balance aid during the gait rehabilitation process, are reported in literature [8-12], however are less or not reported systems for cerebral palsy monitoring. Several metrics can be mentioned as a sensing systems associated with the postural analysis of the body and its static and dynamic balance such as, center of pressure position and trajectory pressure that were considered in different practical approaches [13-15].

In this context the work presents the development of a multi-sensing interface called Palsy Thera Sense, to give support to the physical rehabilitation for children with cerebral palsy, allowing the monitoring of static and dynamic behavior and providing accurate information about the motor skills, and to evaluate the physical rehabilitation plan effectiveness.

This paper is organized such as: Section II presents the Palsy Thera Sense description, including the hardware and software; Section III, presents the results analysis, as such as the tests executed with all developed platforms and its output signals; Section IV presents the conclusions and future works and the acknowledgements presented in Section V.

II. MULTI-SENSING FRAMEWORK DESCRIPTION

This work presents a multi-sensing interface called Palsy Thera Sense. It is a rehabilitation system composed of two platforms that includes two types of force sensors (i.e. load cells) to monitor the forces applied by a patient with cerebral palsy while he performs the gait rehabilitation under physiotherapist's supervision.

It is represented by a wireless sensor network including node with multiple force measurement channels that support the physical training monitoring for children with cerebral palsy. The signals obtained for different performed tasks such as, gait task and body equilibrium (or body balance during serious game performing) are transmitted to the wireless sensor

FIGURE A.15. Publication regarding to the development of a multisensing platform to give support to children with cerebral palsy (Roza, Souza, and Postolache, 2017).

Goal-biased Probabilistic Foam Method for robot path planning

Lufs B. P. Nascimento, Diego S. Pereira, Pablo J. Alsina, Mauricio R. Silva, Daniel H. S. Fernandes
*Department of Computing Engineering and Automation
Federal University of Rio Grande do Norte (UFRN)
Natal, RN, Brazil*

lbruno@ufrn.edu.br, dgs pereira@gmail.com, pablo@dca.ufrn.br, mauricio@bsd.com.br, eng.danielhsfernandes@gmail.com

Válber C. C. Roza
*Department of Information Science and Technology
Instituto Universitário de Lisboa (ISCTE-IUL)
Lisboa, Portugal
valber_cesar_roza@iscte.pt*

Armando S. Sanca
*Department of Technology
State University of Feira de Santana
Feira de Santana, Bahia, Brazil
armando@ecom.ufes.br*

Abstract—This paper presents an improved variation of Probabilistic Foam Method (PFM) for robot path planning. In PFM, a structure named probabilistic foam, formed by bubbles propagate through the free space from initial configuration to goal as a breadth-first search, obtaining a collision-free path. Although the method is able to obtain a navigable path, it is computationally expensive. We propose a new foam propagation approach inspired on random tree growth from RRT. Results from simulation experiments using 2D and 3D map show benefits with the new method.

Index Terms—autonomous robotics, path planning, collision-free path, probabilistic foam method, bubbles of free-space.

I. INTRODUCTION

Probabilistic path planners are interesting strategies that aim to generate a set of robot configurations on free space by its sampling in a random way until finding the goal configuration. These methods usually use few computation resources because they construct an approximate model of the configuration space [1], as opposed to some deterministic methods that construct an exact space model [2].

There are several probabilistic path planners in literature, Probabilistic Roadmaps [3] and Rapidly-Exploring Random Tree (RRT) [4], [5] are the most known, but in the last years a lot of studies have been developed in this area, including applications on autonomous vehicle navigation applications [6], in Unmanned Aerial Vehicles (UAVs) [7], in robots manipulators [8], among other relevant ones.

In [9] and [10] bubbles of free space were introduced. A bubble was defined as a circle centered at a robot configuration with radius computed using minimum distance between the robot and the set of obstacles in workspace. In this context, the bubbles were used on Elastic Bands, a finite series of bubbles that makes the collision-free path be able to deform itself when changes in the environment are detected in real time.

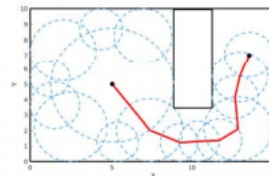


Fig. 1: Collision-free path obtained by Probabilistic Foam propagated through the free space

In [11] a new robot path planning, called Probabilistic Foam Method (PFM) was proposed. The foam propagates in free space by the expansion of connected bubbles from initial configuration to goal configuration, a method similar to wavefront propagation (strategy for several methods based on potential fields), thus forming a search tree similar to the RRT. The formed foam represents an approximate coverage of the free space, similar to methods based on approximated convex cell decomposition. An important characteristic of the PFM is that bubbles provide a safe region to robot maneuverability, just using distance information. Figure 1, shows an example of the probabilistic foam.

Although PFM has yielded good results, the method does not use strategies that minimize the computational effort in the search process, considering that the propagation of the foam executes a breadth-first search over the free space, which can be a slow process until it finds the goal. In this way, we presented the Goal-biased Probabilistic Foam (GBPM), a new approach for the foam propagation of the Probabilistic Foam Method that aims to reduce computed bubbles number, as a result minimizing the processing time. GBPM is inspired on

FIGURE A.16. Publication regarding to the improvement of a probabilistic method over path planning tasks (L. Bruno P. Nascimento et al., 2018).

APPENDIX B

Additional Plots of each Volunteer

Figures B.1-B.7, show the brain magnitudes of several lobes along each proposed flight tasks and volunteers' expertise. Figures B.6 and B.7, show smoother signals, having less abrupt variation along short window of time, comparing to the signal variation and shape of the beginner and mid-level volunteers.

However, even when the volunteers are mid-level e.g., it doesn't ensure that they will feel insecure (not confident) sometimes and consequently, reflecting similar pattern of a beginner level; it is simple to understand that, the massive training for each different flight and aircraft are the point and for this reason, different expertise of volunteers may reflect similar brain patterns if they are not confident in some situation. The training is the key of a successful flight and this work tries to bring clearly the need to train more the pilots to avoid several problems in the flight procedures.

These low amplitudes and signal variations along the time, may mean that the volunteer is more relaxed during the flight, presenting less brain oscillations over short times. It makes sense, since the volunteer of the flights VC1 and VC2 reported to be confident with the proposed flight tasks and aircraft commands, but sometimes he said to push himself to execute the tasks as well as possible.

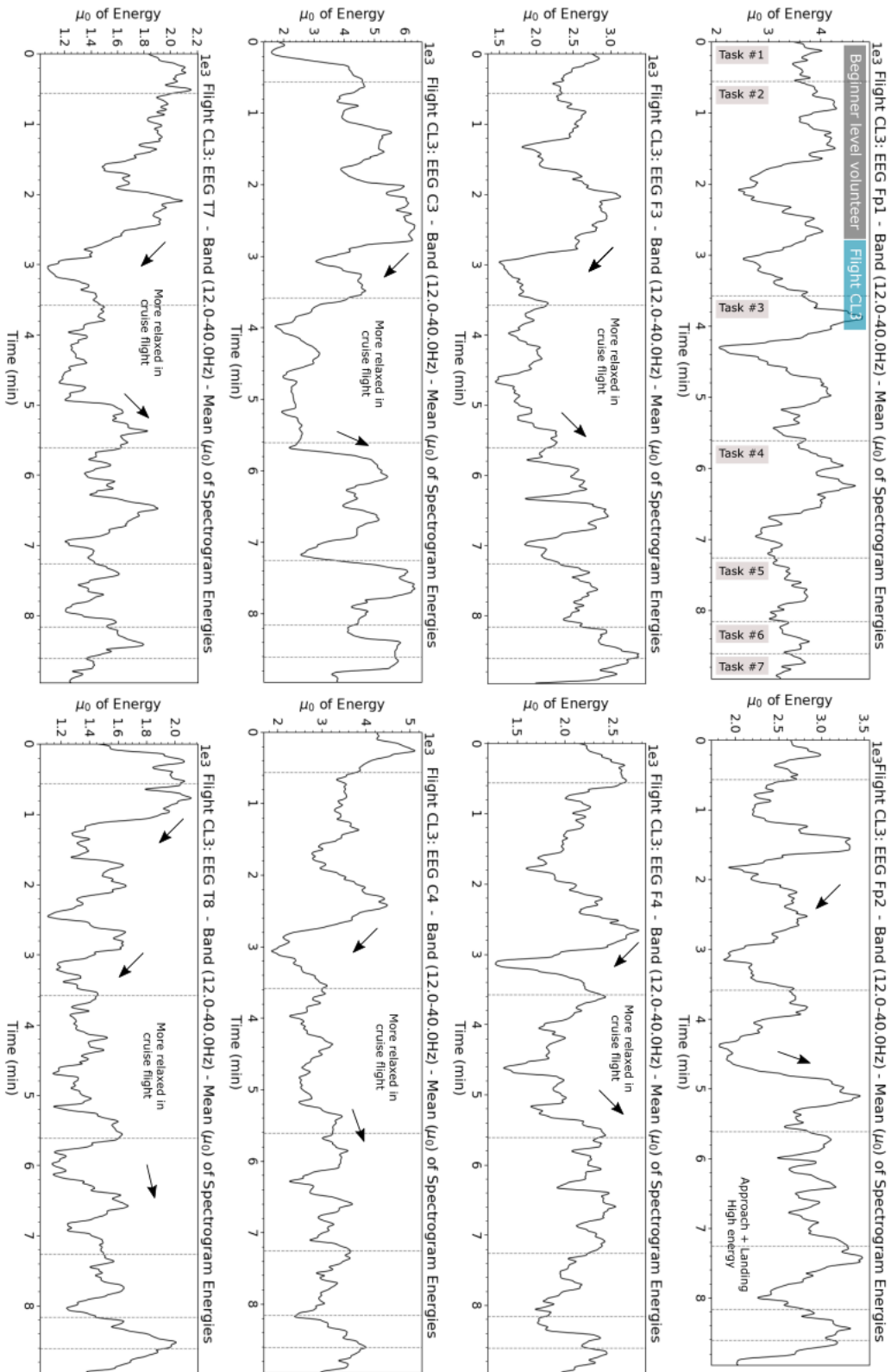


FIGURE B.1. Mean of magnitudes by tasks and lobes, of the flight dataset CL3 (beginner level volunteer).

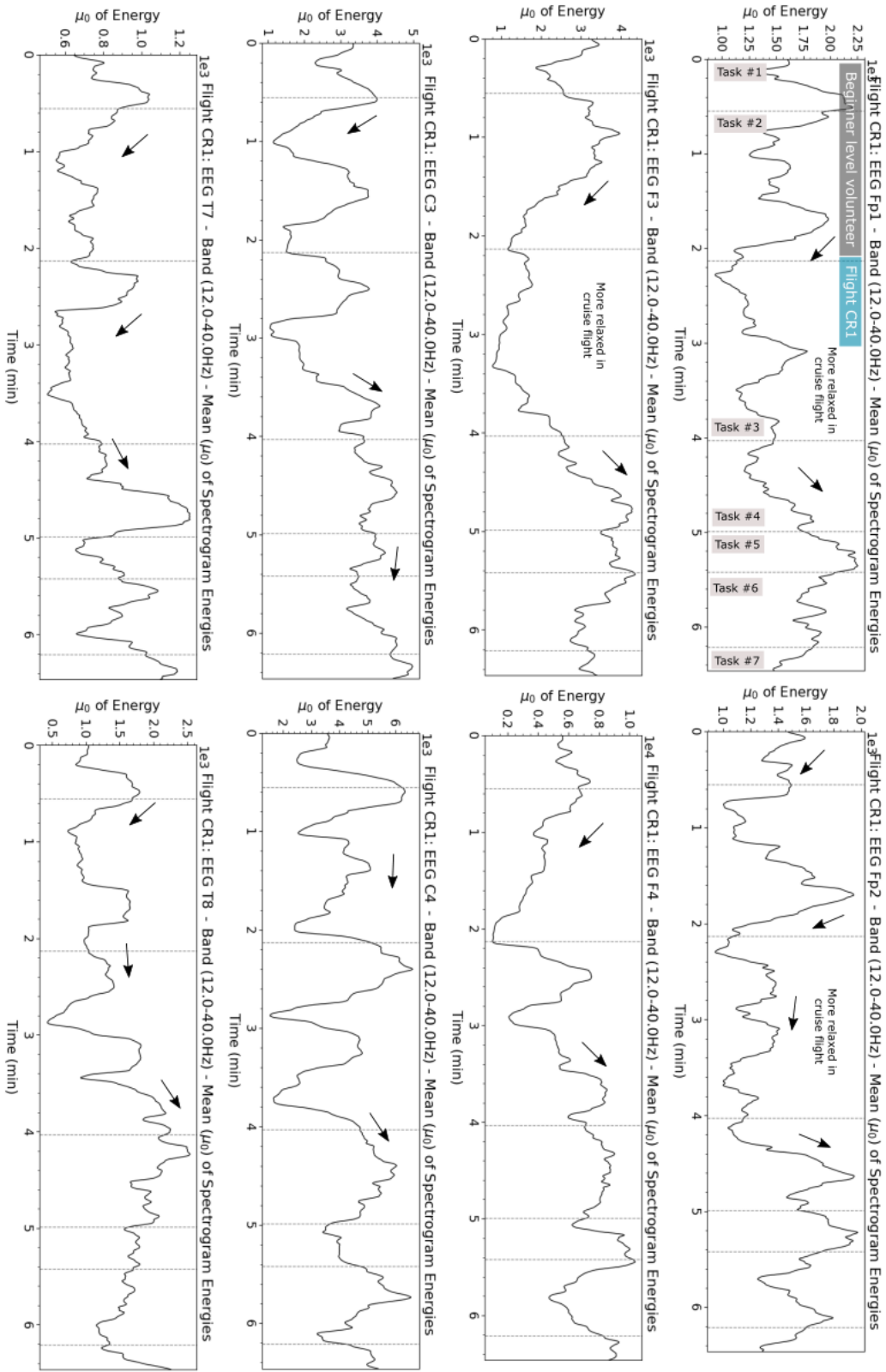


FIGURE B.2. Mean of magnitudes by tasks and lobes, of the flight dataset CR1 (beginner level volunteer).

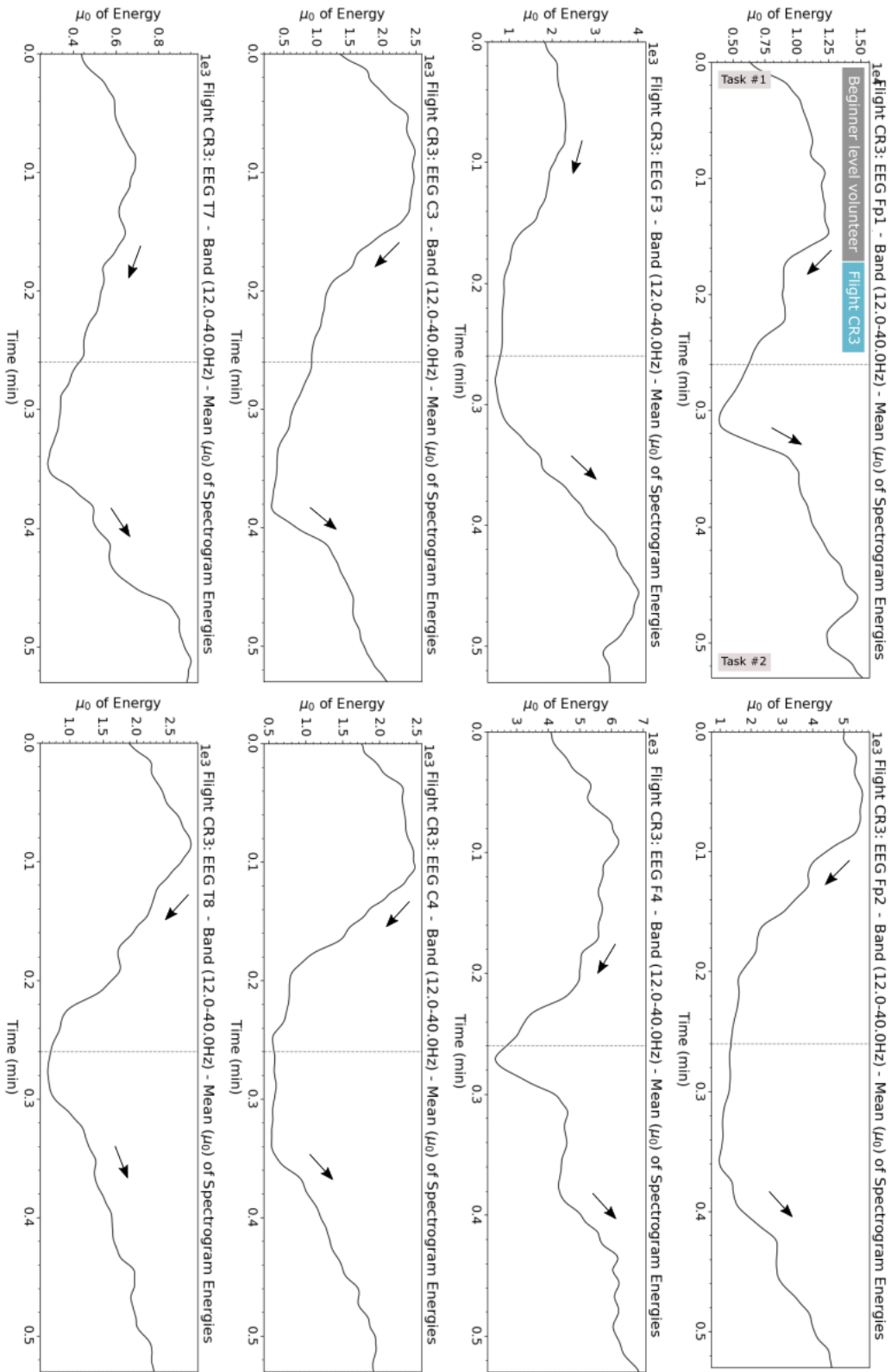


FIGURE B.3. Mean of magnitudes by tasks and lobes, of the flight dataset CR3 (beginner level volunteer).

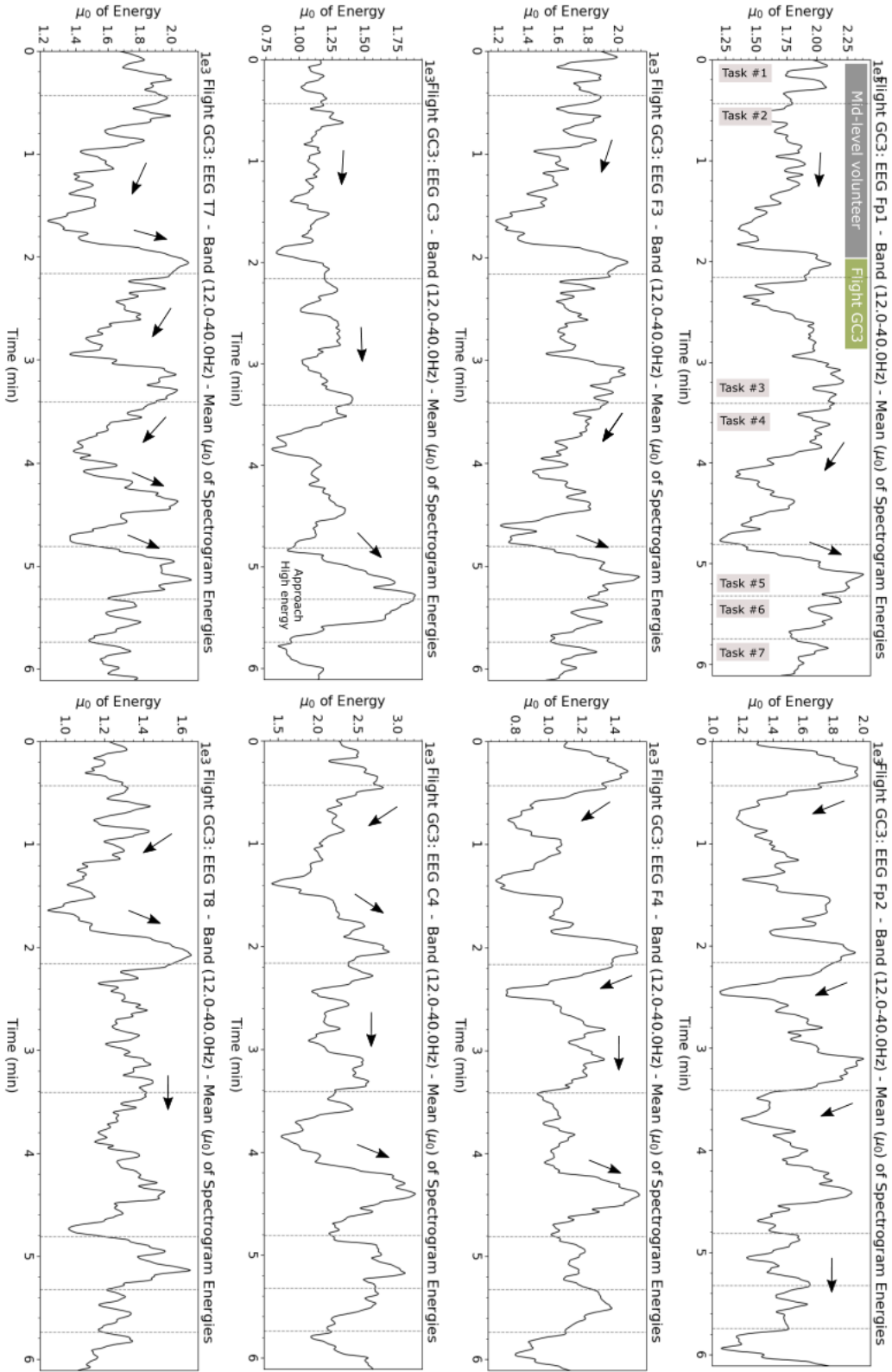


FIGURE B.4. Mean of magnitudes by tasks and lobes, of the flight dataset GC3 (mid-level volunteer).

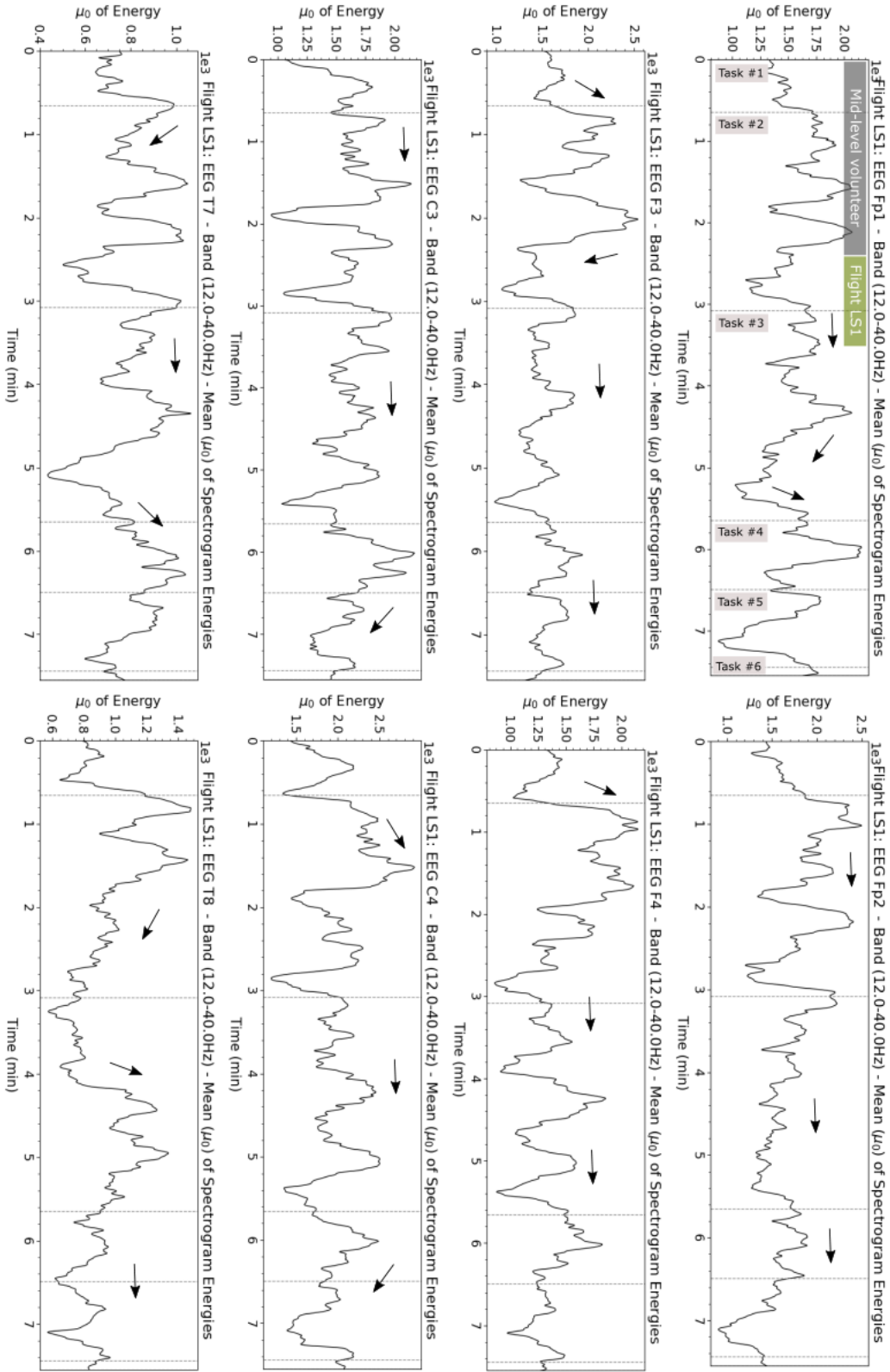


FIGURE B.5. Mean of magnitudes by tasks and lobes, of the flight dataset LS1 (mid-level volunteer).

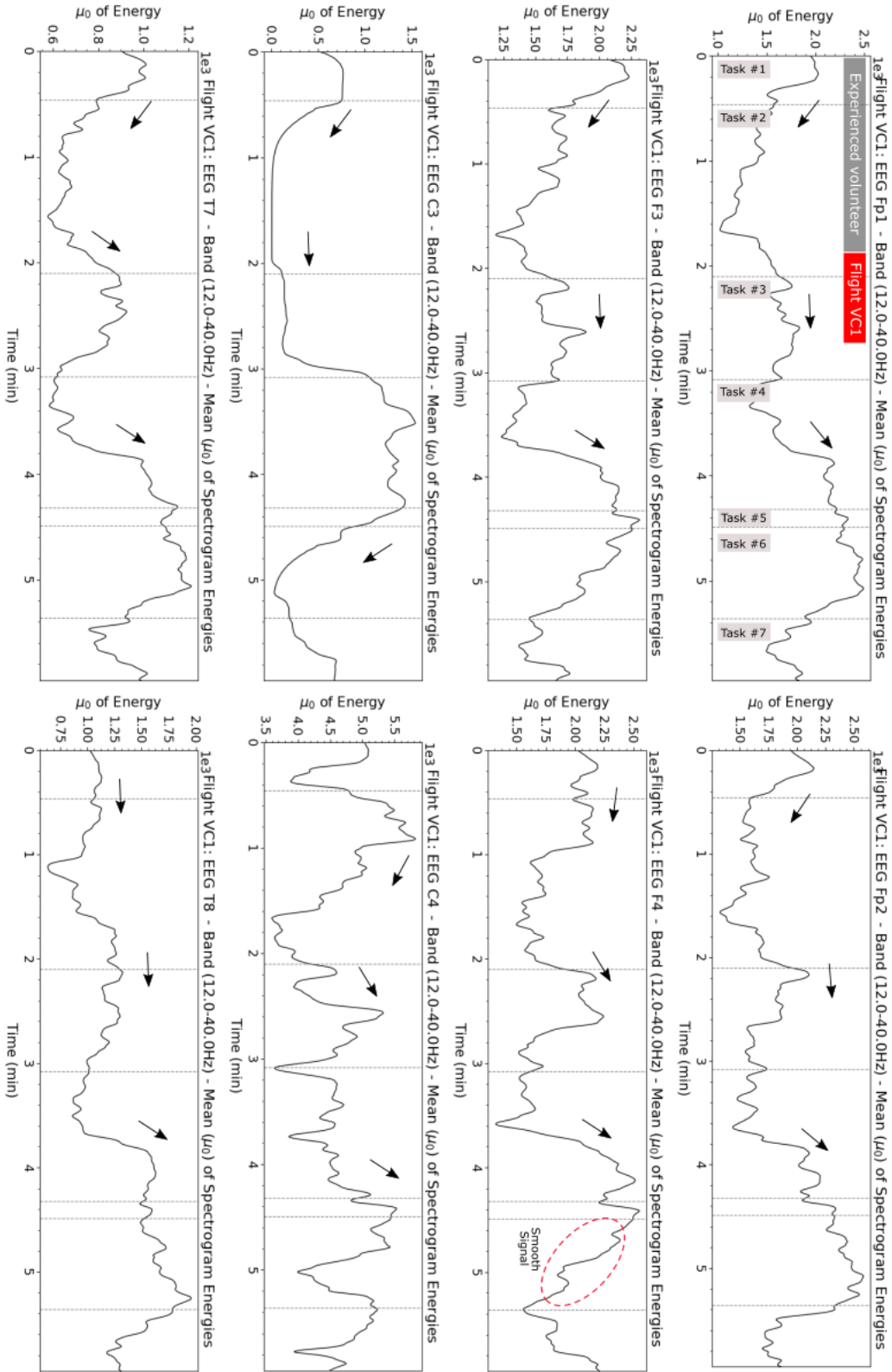


FIGURE B.6. Mean of magnitudes by tasks and lobes, of the flight dataset VC1 (experienced level volunteer).

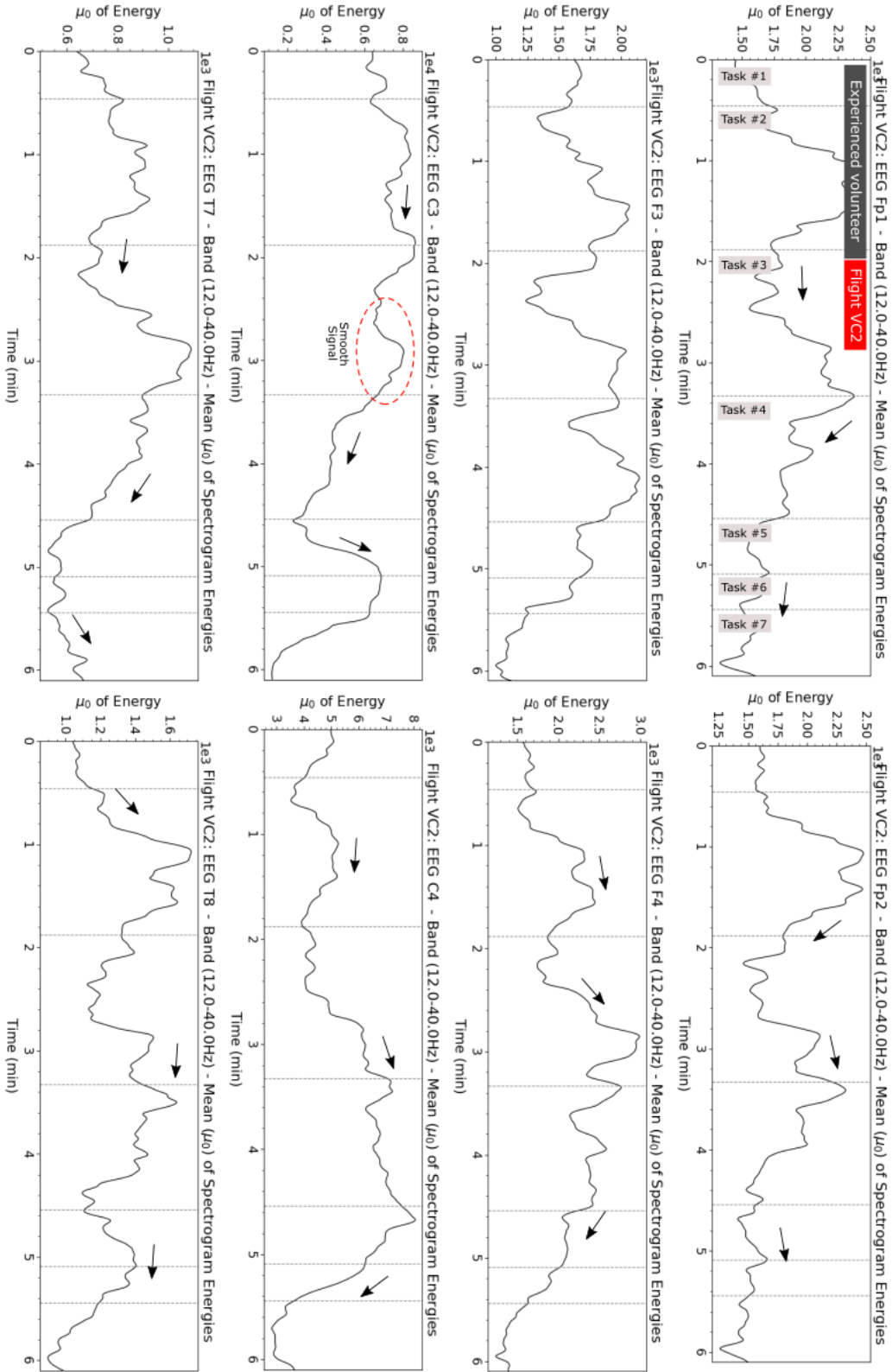


FIGURE B.7. Mean of magnitudes by tasks and lobes, of the flight dataset VC2 (experienced level volunteer).

APPENDIX C

Emosense Software - User Manual

The present work developed two software to give support to the data acquisition, processing and emotion recognition, those are: Emosense RT (real time/online version), and Emosense Processing (offline version).

C.1. Emosense Realtime/Online

Figure C.1, shows the configuration panel of the Emosense RT, which it have all parameters to be configured before the acquisition process, e.g., sensors to connect, experiment and test time, log file, real time markers, and so on.



FIGURE C.1. Configuration panel.

Figure C.2, shows three main panels: RT acquisition panel, aviation experiment setup and electrodes setup for ExG (ECG, EMG, EEG and EOG), GSR and HR. In the RT acquisition panel, 7 different signals can be acquired; serial data, bluetooth data, TCP data and accelerometers data. In the aviation experiment panel, the experiments based on aviation can be adapted, producing a final report having specific information on aviation context.

The electrodes panel, presents several electrodes selections, according to experiment in case. In addition of several signal acquisition, the face of the user in experiment, is also recorded to be analyzed in the post processing phase.



FIGURE C.2. Three main panel: RT acquisition panel, aviation experiment panel and electrodes setup panel.

C.1.1. Log File Nomenclature

The Emosense RT software, produces files of its own. A total of two data files are produced: readable data file (.emo), having a data table that permits to be processed further; and a plot file (.pdf), having images of plots of the data acquired in real time. In addition, a additional file are produced when a RT marker is used, taking a photo of the user at the same moment of the markers.

After stop the experiment, the Emosense RT, record a pair of files, data.emo and plot.pdf, following by the date and time of recording, being the ID of the finished experiment (Figure C.3). Other log files are produced also, but based on the configuration system, experiment steps and errors warnings along the acquisition.

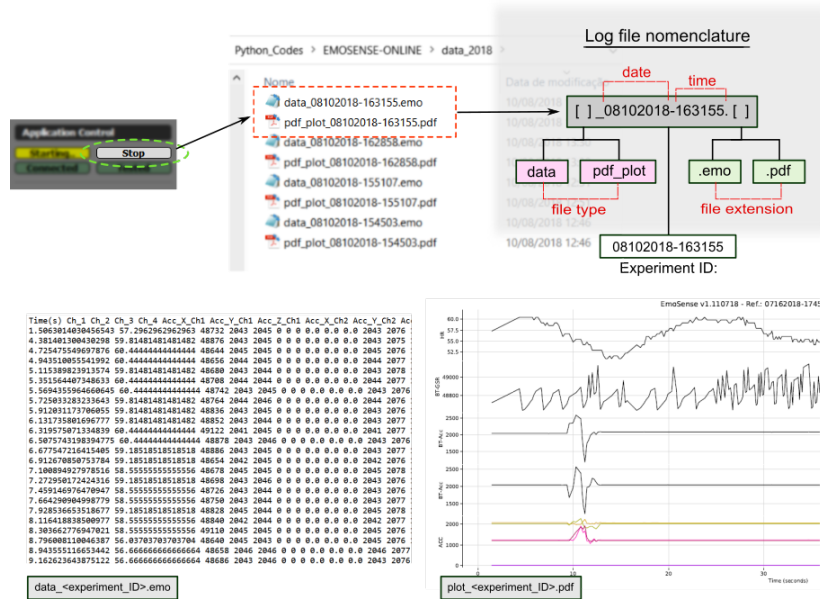


FIGURE C.3. Log storage and nomenclature.

C.2. Emosense Offline

Figure C.4, shows the Emosense Offline software that uses the recorded data by the Emosense RT, to execute processing and to find patterns to aim the regression/classification process.

Several resources are provided by it: Filtering, FFT, wavelets, auto markers, signal cutting, spectrograms, features extractions, cross correlation, Pearson's coefficient, print plots, and so on.

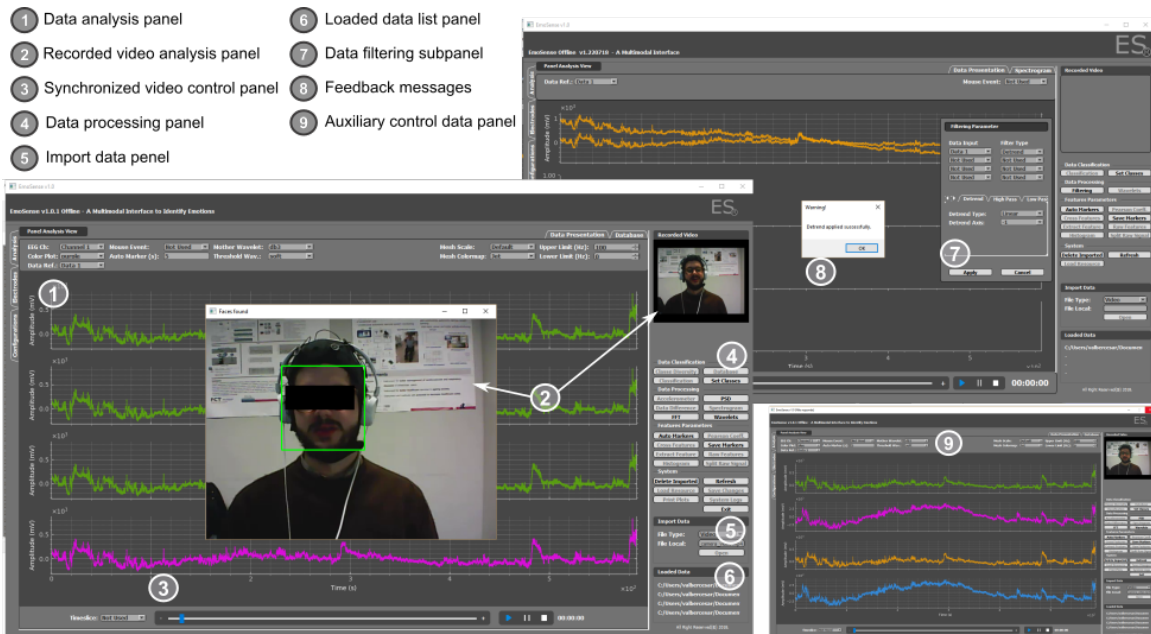


FIGURE C.4. Emosense Offline software.